Aston University

Some pages of this thesis may have been removed for copyright restrictions.

If you have discovered material in AURA which is unlawful e.g. breaches copyright, (either yours or that of a third party) or any other law, including but not limited to those relating to patent, trademark, confidentiality, data protection, obscenity, defamation, libel, then please read our Takedown Policy and contact the service immediately

THE FABRICATION OF BIODEGRADABLE NANOSPHERES FROM NOVEL HYDROXYALKANOATES FOR THE DELIVERY OF ACTIVES OF PHARMACEUTICAL AND AGRICULTURAL INTEREST

GRAHAM RICHARD CARLIN

Doctor of Philosophy

ASTON UNIVERSITY

APRIL 2001

This copy of the thesis has been supplied on condition that anyone who consults it is understood to recognise that its copyright rests with its author and that no quotation from the thesis and no information derived from it may be published without proper acknowledgement.

ASTON UNIVERSITY

THE FABRICATION OF BIODEGRADABLE NANOSPHERES FROM NOVEL HYDROXYALKANOATES FOR THE DELIVERY OF ACTIVES OF PHARMACEUTICAL AND AGRICULTURAL INTEREST

GRAHAM RICHARD CARLIN

Doctor of Philosophy

April 2001

This work describes the fabrication of nanospheres from a range of novel polyhydroxyalkanoates supplied by Monsanto, St Louis, Missouri, USA for the delivery of selected actives of both pharmaceutical and agricultural interest. Initial evaluation of established microsphere and nanosphere fabrication techniques resulted in the adoption and optimisation of a double sonication solvent evaporation method involving the synperonic surfactant F68. Nanospheres could be consistently generated with this method.

Studies on the incorporation and release of the surrogate protein Bovine Serum Albumin V demonstrated that BSA could be loaded with between 10-40% w/w BSA without nanosphere destabilisation. BSA release from nanospheres into Hanks Balanced Salts Solution, pH 7.4, could be monitored for upto 28 days at 37°C.

The incorporation and release of the Monsanto actives – the insecticide Admire® ({1-[(6-chloro-3-pyridinyl)methyl]-N-nitro-2-imidazolidinimine}) and the plant growth hormone potassium salt Gibberellic acid (GA_3K) from physico-chemically characterised polymer nanospheres was monitored for upto 37 days and 28 days respectively, at both 4°C and 23°C. Release data was subsequently fitted to established kinetic models to elaborate the possible mechanisms of release of actives from the nanospheres.

The exposure of unloaded nanospheres to a range of physiological media and rural rainwater has been used to investigate the role polymer biodegradation by enzymatic and chemical means might play in the *in vivo* release of actives and agricultural applications.

The potential environmental biodegradation of Monsanto polymers has been investigated using a composting study (International Standard ISO/FDIS 14855) in which the ultimate aerobic biodegradation of the polymers has been monitored by the analysis of evolved carbon dioxide. These studies demonstrated the potential of the polymers for use in the environment, for example as a pesticide delivery system.

KEYWORDS: Polyhydroxyalkanoates, nanospheres, polymer biodegradation, Composting, *in vitro* release.

For My Mother and Father

Thank You

DON'T LET YOUR FEARS STAND IN THE WAY OF YOUR DREAMS!

No Fear Inc, USA

IN NATURE, NOTHING IS EVER RIGHT. THEREFORE, IF EVERYTHING IS GOING RIGHT.....SOMETHING IS WRONG!

ANONYMOUS

ACKNOWLEDGEMENTS

Firstly, I would like to thank my supervisor Dr. Terry Atkins for his continuous a assistance and guidance throughout this thesis.

I would also like to express my thanks to Dr. S.R.Holding at Rapra Technology L conducting the majority of the gel permeation chromatography work in this thesis; I Tompkins in the Biochemistry Department at Birmingham University for allowir access to the SEM/TEM suite; and at Aston University, to Karen Farrow for all he and technical knowledge with GC-MS and Wendy Amass for her help and guidanc the composting study.

I am most grateful to Sue Turner and William Field for their enthusiasm, exc technical knowledge and friendship throughout my time at Aston.

I acknowledge Monsanto for the financial assistance they gave me.

A huge 'Thank You' goes to Fiona Salvage for her help, time and friendship over the years, under the most trying circumstances!

More thanks than I can express in words goes to my Mother and Father for their unri love, encouragement and support, always.

Last, and by no means least, I wish to thank my many friends, especially Ashley I Edward Wareham and Nigel Slaughter for successfully preventing me from going ins could not have done this without you guys! Thank You!

Cheers

GRAHAM RICHARD CARLIN

MARCH 2001

CONTENTS PAGE

ABBREVIATIONS

ADMIRE®	1-({6-chloro-3-pyridinyl}methyl)-N-nitro-2-imidazolidinimine
ANOVA	one way analysis of variance
ATP	adenosine triphosphate
BCA	bicinchoninic acid
BIOPOL®	poly(hydroxybutyrate-hydroxyvalerate)
BSA	bovine serum albumin
CMP	2-chloro-5-methylpyridine
CCMP	2-chloro-5-chloromethylpyridine
CO_2	carbon dioxide
Acetyl CoA	acetyl coenzyme A
DCM	dichloromethane
dGA_3	deuteriated gibberellic acid
DIBLOCK	poly(ethylene glycol)-poly(hydroxybutyrate-hydroxyvalerate)
DSC	differential scanning calorimetry
EC_{50}	effective concentration to kill/treat 50% of animals
EDTA	ethylenediaminetetraacetic acid
FDA	Food and Drug Administration
F68	Synperonic F68 surfactant
GA_3K	gibberellic acid potassium salt
GC	gas chromatography
GC-MS	gas chromatography-mass spectroscopy
GLC	gas liquid chromatography
GPC	gel permeation chromatography
HBSS	Hank's balanced salts solution (pH7.4)
3HB 3HC	poly(hydroxybutyrate-hydroxycaproic)
HC	hydroxycaproic
HCl	hydrochloric acid
HPLC	high pressure liquid chromatography
HV	hydroxyvalerate
IR	infra red
K_1	first order release constant
K_H	Higuchi release constant
KCl	potassium chloride
K_{OC}	sorption coefficient
LC_{50}	lethal concentration required to kill 50% of animals
LD_{95}	lethal dose required to kill 95% of animals
M	molarity

MACE	modified acetylcholine esterase
MC	methylcellulose
mg	milligram
ml	millilitre
Mn	number average molecular weight
MWt (Mw)	weight average molecular mass
mV	milli-Volts
n	number of samples
NADPH	nicotinamide adenine dinucleotide phosphate
NaOH	sodium hydroxide
nm	nanometre
NCS	new born calf serum (pH7.1)
O/O	oil in oil
O/W	oil in water
PCS	photon correlation spectroscopy
PCL	poly(ε-caprolactone)
PDS	pesticide delivery system
PHA	polyhydroxyalkanoate
PHB	polyhydroxybutyrate
PHBHV	polyhydroxybutyrate-hydroxyvalerate
PHBHV-Diol	polyhydroxybutyrate-hydrxyvalerate-Diol
PHBHV-Diol-PEG	polyhydroxybutyrate-hydrxyvalerate-Diol-polyethylene glycol
PHV	polyhydroxyvalerate
pg	pecogram
ppm	parts *per* million
PVA	polyvinylalcohol
PVP	polyvinylpyrrolidone
r^2	regression coefficient
RES	reticuloendothelial system
rpm	revolutions *per* minute
RP-HPLC	reverse phase high performance liquid chromatography
SDS	sodium dodecyl sulphate
SEM	standard error of the mean
SPAN40	sorbitan monopalmitate
TGA	thermogravimetric analysis
T_g	glass transition temperature
T_m	crystalline melting temperature
TRIBLOCK	poly(hydroxybutyrate-hydroxyvalerate)-Diol-polycaprolactone
μm	micrometre

UV	ultraviolet
W/O	water-in-oil
W/O/W	water-in-oil-in-water
w/w	weight *per* weight
w/v	weight *per* volume
v/v	volume *per* volume

LIST OF FIGURES

LIST OF TABLES

LIST OF EQUATIONS

CHAPTER 1

INTRODUCTION

During the last two decades there has been considerable interest and progress in the field of parenteral controlled release systems. This is largely due to the fact that protein and peptide therapeutics currently represent eight of the top one hundred prescription pharmaceuticals in the United States. In addition, biotechnology products such as cytokines and recombinant proteins are projected to account for fifteen percent of the total United States prescription drug market by 2003 (Sanders & Hendren, 1997). Of the protein and peptide based products now on the market, many are administered as daily injections and despite the success of biotechnology products to date, enormous effort continues to be focused on the development of more convenient and non-invasive means of administration for those products that require frequent but prolonged dosing (Sanders & Hendren, 1997).

The fabrication of polymer-based devices for the delivery of drugs is a common technique, where prolonged drug release is regulated either by diffusion through the polymer barrier or by erosion of the polymer matrix (Jalil & Nixon, 1990a). Early polymer-based devices for parenteral administration were prepared from silicon rubber (Folkman & Long, 1964) and polyethylene (Desai *et al*, 1965). Polymer-based drug delivery devices made from these materials have a serious drawback in that they are non-biodegradable and consequently require surgical removal after drug exhaustion. Moreover, it has been reported that even after surgical removal of a silastic implant containing contraceptive steroids, foreign material remained *in vivo*, with the potential to cause serious toxicological hazards (Tatum, 1970).

During the 1980's and 1990's considerable interest was focused (Koosha *et al*, 1989; Watts *et al*, 1990; Gangrade & Price, 1992) on the development of small biodegradable polymer based carriers as controlled release systems for the oral and parenteral delivery of therapeutic peptides and proteins in order to achieve satisfactory efficacy and increase patient compliance. The delivery of a variety of biologically active molecules from these biodegradable, sustained and controlled release devices has subsequently been utilised by many other industries in the agricultural and veterinary areas. The biodegradation of the polymers in the natural environment into non toxic products is also essential.

In vivo, following release of the bioactive materials, the exhausted delivery devices remain in the body to be completely degraded to inert, biocompatible degradation products.

To be classified as an *in vivo* biodegradable polymer suitable as a controlled release system, the synthetic or natural material must degrade, either enzymatically or non-enzymatically, to produce biocompatible, non-toxic by-products. These must be either further metabolized or excreted via normal physiological pathways (Jalil & Nixon, 1990b). Many natural and synthetic biodegradable polymers have been fabricated into implants, microcapsules and nanocapsules, containing a wide variety of drugs, for prolonged drug delivery (Deasy, 1984). Of the materials investigated there are only a few immunologically tolerable biodegradable polymers. Natural materials used in delivery systems range from virus envelopes, whole living cells such as

erythrocytes, genetically engineered fibroblasts and myoblasts (Gibbons, 1992), to cellular components such as the polysaccharides, hyaluronic acid, aluronic acid, chitin, starch (DeLuca *et al*, 1987) and proteins such as fibrogen, collagen, albumin and gelatine (Kramer *et al*, 1974). Bovine serum albumin (BSA) and Human serum albumin (HAS) have been investigated for the targeting of anticancer agents (Zolle *et al*, 1970; Widder *et al*, 1979, 1980, 1982; Fujimoto *et al*, 1981). It has been reported that the sustained release of insulin from BSA microspheres was maintained for two weeks (Goosen *et al*, 1983). Other natural polymers have also been used as microparticulate drug carriers for parenteral administration, including collagen (Bradley & Wilkes, 1977; Rubin *et al*, 1973), haemoglobin (Willmot *et al*, 1985) and gelatine (Yoshioka *et al*, 1981; Hashidu *et al*, 1977). In addition to the benefits of reduced invasive surgery, before and after administration, the incorporation of drugs into biodegradable microspheres has the advantage of slowing down the rate of the biodegradation of the drug by the host organism and also protection of host tissues from possible acute toxicological effects of the drug. Other natural materials include the polyhydroxyalkanoates (PHA), such as polyhydroxybutyrate (PHB) and polyhydroxyvalerate (PHV). These are produced by microbial synthesis. However, the cost and uncertainty of the purity of these polymers restricts their use (Jalil & Nixon, 1990c) and attention has therefore focussed on the synthetic biodegradable polymers, where the processing conditions, availability, cost and quality control can be monitored.

Some of the many synthetic materials that have been utilized in controlled release devices, such as microspheres and nanospheres, include aliphatic polyesters of polyglycolide, poly (L-lactide) (PLLA), poly (DL-lactide) (PDLLA), poly (d,l lactide-co-glycolide) (PLGA) and poly (ε-caprolactone) (Zhang *et al*, 1997), as well as poly (orthoesters) (Heller *et al*, 1990), poly (alkylcarbonate) (Kojima *et al*, 1985), poly (amino acids) (Li *et al*, 1993), polyanhydrides (Leong *et al*, 1986) and polyacrylamides (Arturson *et al*, 1983). Of these the aliphatic polyesters, such as poly(lactic acid) (PLA) and poly (lactide-co-glycolide) (PLGA) have attracted most attention because of their good biocompatibility and controllable biodegradation. Kulkarni *et al* (1971) established that poly(lactic acid) was suitable for surgical suture and vascular grafting because the material did not elicit an immunological response. Poly(lactic acid) and its copolymers with glycolic acid have been used to fabricate controlled release systems in the form of films (Yolles *et al*, 1984); Pitt *et al*, 1979), beads and rods (Scwope *et al*, 1975) and microcapsules and microspheres (Beck *et al*, 1979; Suzuki & Price, 1985). A disadvantage, however, of using synthetic polymers to fabricate drug delivery devices is that residues of polymerisation such as initiators, additives and un-reacted monomers are undesirable and toxic, especially if the device is to be administered parenterally (Wood, 1980). It is for this reason that the present study focuses on the use of some commercially modified naturally available polymers based on PHA, namely polyhydroxybutyrate-hydroxyvalerate, (PHBHV), and a number of novel, genetically produced 'natural' polymers, from Monsanto, St.Louis, Missouri, U.S.A. These include 3-hydroxybutyrate-3-hydroxycaproic (3HB-3HC), polyhydroxybutyrate-hydroxyvalerate-Diol (PHBHV-Diol) and polyhydroxybutyrate-hydroxyvalerate-Diol-polyethylene glycol (PHBHV-Diol-PEG). The present work has also investigated the use of a novel, in-house synthesised triblock-co-polymer, produced by combining PHBHV-Diol with

polycaprolactone. The addition of the polycaprolactone to the triblock-co-polymer is predicted to increase the rate of biodegradation compared with homopolymers and simple co-polymers, that have a low biodegradation rate which can be expressed in years (Yasin *et al*, 1989; Holland *et al*, 1990).

FIGURE 1 – STRUCTURE OF POLYCAPROLACTONE

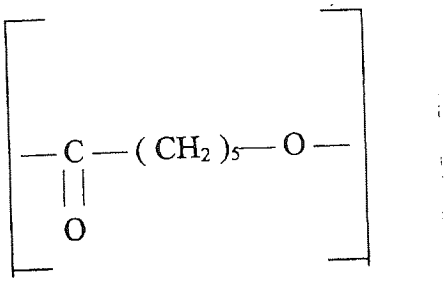

Structure of polycaprolactone

POLYCAPROLACTONE

Example of Triblock copolymer

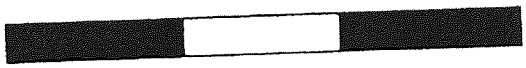

PHBHV-DIOL

FIGURE 2 – STRUCTURE OF TRIBLOCK COPOLYMER

The most notable PHA generated by fermentation was the copolymer BIOPOL® (PHBHV). This biopolymer was originally manufactured by ICI Biopolymers and sold under license by Marlborough Biopolymers, Billingham, Cleveland UK. ICI Biopolymers repurchased BIOPOL® from Marlborough Biopolymers and sold all rights and technology to Monsanto, St Louis, Missouri, USA.

FIGURE 3 – STRUCTURE OF BIOPOL®

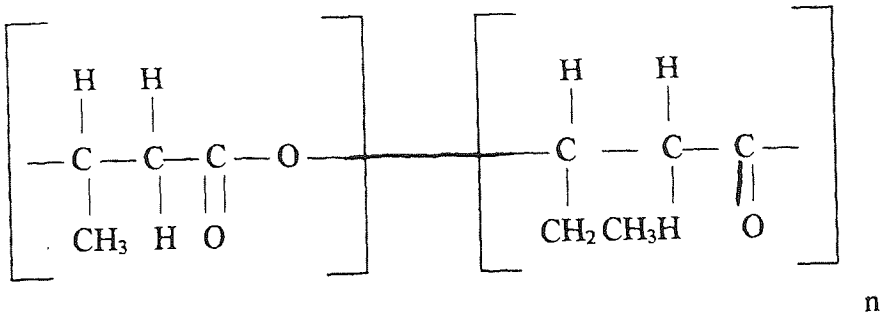

Hydroxybutyrate **Hydroxyvalerate**

Structure of BIOPOL®

BIOPOL® is a polyhydroxyalkanoic acid, that was originally produced in multi-kilogram batches through fermentation of a glucose-utilising mutation of the micro-organism, *Alcaligenes eutrophus*, although Monsanto is currently using biotechnology to produce the biopolymer in Rapeseed oil plants. BIOPOL® is ideally suited for the production of sundries capable of being disposed of in land infill sites and by composting because of its biodegradable nature. Current and potential uses of BIOPOL® include food packaging, disposable plates, cups, trays and cutlery, grocery sacks, rubbish bags, bottles and containers for food, cosmetics, shampoo, personal care products and fibres. PHB-HV is now being investigated as a candidate for the fabrication of controlled drug release devices, such as microspheres, although, at present PHB-HV is not yet licensed with either the UK or US regulatory authorities for internal use as a medical device (Peacock, 1995), and there is some evidence to suggest that at high concentrations the two monomers (HB and HV) may inhibit cellular growth (Poulton *et al*, 1988). Poly(3-hydroxybutyrate) (PHB) is but one member, albeit the most abundant, of a general class of polyhydroxyalkanoates (PHA). Other PHAs are composed of copolymers which possess properties different from PHB and hence result in a different spectrum of activity and uses. The first indication that the polymer (PHB) discovered by Lemoigne in 1926 might contain proportions of 3-hydroxyacids other than 3HB was given by Wallen and Rohwedder who, in 1974, reported heteropolymers in chloroform extracts of activated sewage sludge. They noted the presence of 3HB and 3-hydroxyvalerate (3HV) as major constituents of the heteropolymer with C_6 and possibly C_7 3-hydroxyacids as minor components (Anderson & Dawes, 1990). The heteropolymer had a lower melting point than PHB and unlike the homopolymer proved to be soluble in hot ethanol. Most of the known

polyhydroxyalkanoates are polymers of 3-hydroxyacids (Akhtar & Pouton, 1996), possessing the general formula:-

FIGURE 4 – STRUCTURE OF POLYHYDROXYALKANOATES (PHA)

Structure of polyhydroxyalkanoate. (PHA)

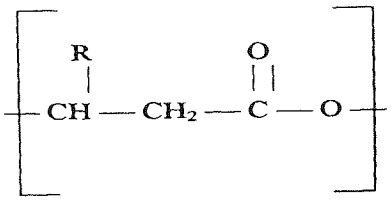

R= methyl; 3-hydroxybutyrate.

R= ethyl: 3-hydroxyvalerate.

The similarity of the chemical structure of PHB to that of polypropylene (both have a compact right-handed helix and melting points near 180°C) attracted the attention of ICI plc to the potential use of PHB for fibre and plastic applications, particularly in the biomedical field, where biocompatibility and biodegradability are important features. The homopolymer, PHB, alone is far stiffer and more brittle than polypropylene, making it an inferior material. However, when copolymer formation occurs with 3HB and 3HV monomer units, as is the case in BIOPOL®, a decrease in crystallinity and melting point occurs altering the physical properties of the material, making it less stiff and far stronger. As a consequence of this, a large range of biomaterials can be synthesised ranging from the hard brittle homopolymer to the soft and tough copolymer, simply by altering the 3HV content.

1.2 The synthesis and biodegradation of PHB

One of the most intriguing developments in polyhydroxybutyrate biochemistry has been its discovery in the plasma membranes of gram-positive and gram-negative bacteria (Bauer & Owen, 1988) and subsequently in eucaryotic cell membrane fractions, with the highest concentration in the membranes of mitochondria and microsomes (Reusch, 1989). In eucaryotic cell membranes, transmembrane channel-like structures consisting of PHB alpha helices have been shown to surround a hollow ionic cylinder of phosphate and calcium ions. These structures are thought to play a role in the regulation of intracellular calcium concentrations, calcium

signalling and possibly the transfer of genetic material (Reusch & Sadoff, 1988; Anderson and Dawes, 1990; Gursel & Hasirci, 1995). One of the major advantages accruing to an organism from the synthesis of high molecular weight PHB is the ability to store large quantities of reduced carbon. The presence of PHB retards the degradation of cellular components such as RNA and protein during nutrient starvation and it has even been suggested that PHB can act as a mechanism of survival in times of starvation in man. As well as the production of PHAs in nature, they can now be chemically synthesized by direct condensation (Bloembergen *et al*, 1986; Bloembergen *et al*, 1989). This process dramatically improves the purity and reproducibility of the product. On the other hand biosynthesis avoids the use of either chemical catalysts or initiators which could cause toxicological problems if they remained in the pharmaceutical product.

The cyclic pathway for PHB biosynthesis and degradation was elaborated in 1973. In most organisms, PHB is synthesized from acetyl coenzyme A (acetyl-S-CoA) by a sequence of three reactions controlled by 3-ketothiolase (EC 2.3.1.16), acetoacetyl CoA reductase (EC 1.1.1.36) and poly(3-hydroxybutyrate) synthase.

FIGURE 5 – CYCLIC PATHWAY FOR PHB BIOSYNTHESIS

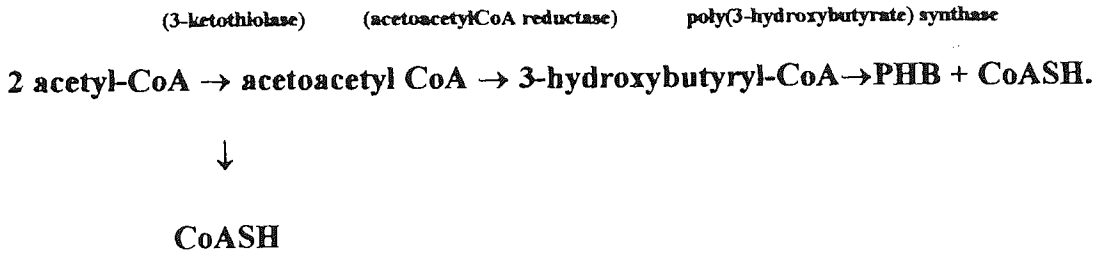

Little is known about the pathways and control mechanisms involved in the synthesis of bacterial polyesters other than PHB.

1.3 The industrial synthesis of PHAs

Most published work on the biosynthesis of polyhydroxyalkanoates, other than PHB, has involved the use of two bacteria: *Alcaligenes eutrophus* and *Pseudomonas oleovarans*. By altering the medium on which these bacteria grow, the accumulated PHAs can be altered. For example with glucose as the carbon source, *A.eutrophus* accumulates up to 80% w/w PHB (Holmes, 1985). When propionic acid is included with glucose, a random copolymer containing both 3HB and 3HV monomer units is produced (Holmes, 1988).

The 3HV content of the PHA depends on the ratio of propionic acid to glucose during the polymer accumulation stage. With valeric acid as the sole carbon source a copolymer containing 90 mol% HV units has been produced (Doi *et al*, 1987). *A.eutrophus* is also capable of producing polyhydroxyalkanoates containing 4HB and 5HV monomers, which can be incorporated into copolymers and terpolymers when *A.eutrophus* is supplied with various single or mixed carbon sources (Doi *et al*, 1987). Similar variations can also be achieved by growing *P.oleovarans* on a range of media. Other bacteria which have now been shown to produce PHAs include the photosynthetic bacteria *Rhodospirillium rubrum* and *Rhizobium meliloti*. 3HB-co-3HV copolymers have been produced by several bacteria including *Rhodococcus, Corynebacterium* and *Nocardia* strains (Anderson & Dawes, 1990). ICI produced their PHB from *A.eutrophus* in a glucose salts medium using phosphate exhaustion as the growth-limiting factor. In the process growth cessation occurred after about 60 days, by which time very little PHB had been synthesized. Glucose was then added to the culture and over the next 48 hours a massive accumulation of the polymer occurred, providing up to 75% of the total dry biomass. Copolymers of PHB and PHV are produced in a similar manner except that both glucose and propionic acid were required. The hydroxyvalerate content of the polymer was controlled by the ratio of glucose to propionate in the feedstock (Anderson & Dawes, 1990). Recovery of the polymer was by large scale solvent extraction, which although giving high recovery rates was an expensive technique which involved large volumes of solvent and hence capital investment in the solvent recovery plant. ICI used a process of hot methanol reflux to remove lipids and phospholipids followed by extraction of the PHB with either chloroform or methylene chloride. The solution was filtered hot to remove cell debris and cooled to precipitate PHB, which was then vacuum dried. Due to the high costs of this process an alternative non-solvent method was devised by ICI involving cell disintegration by shock treatment followed by the addition of a series of enzymatic and detergent digesting processes to solubilise the non-PHB components. The PHB was washed, flocculated and recovered as a white powder (Anderson & Dawes, 1990). Novel copolyesters of 3HB and 4HB with a range of compositions varying from 0 to 49% 4HB, have been obtained from *A.eutrophus,* presented with either 4-hydroxybutyric acid and 4-chlorobutyric acids or with γ-butyrolactone as substrates (Doi *et al*, 1988; Doi *et al*, 1990; Kunioka *et al*, 1989; Anderson and Dawes, 1989). Copolymers containing more then 40 mol% 4HB exhibited the mechanical properties of rubber (Kunioka *et al*, 1989).

1.4 Biodegradability of polyhydroxyalkanoates

Studies on the biodegradability of 4HB containing polymers have shown that the biodegradation rate is far greater than that of PHB or 3HB-co-3HV polymers. It has also been shown by Doi and colleagues (1987) that the inclusion of 3HV together with 3HB in the polymer had no significant effect on biodegradation compared with the biodegradation rate of the homopolymer PHB, although other studies have tended to contradict this finding. For example, a study by Holland *et al* (1987), found that PHB-HV was chemically biodegraded by an ester hydrolysis mechanism, the rate of which was dependent on the copolymer ratio and

composition, the degree of polymer crystallinity, polymer molecular weight and polymer processing conditions. In addition, an increase in the PHV content led to a decrease in polymer crystallinity and this increased the rate of polymer biodegradation. One of the major features of polyhydroxyalkanoates is their ability to biodegrade in the natural environment. Doi and colleagues (1989) found that temperature affected the rate of biodegradation of polymer in a 0.01M phosphate buffer (pH 7.4). At 37°C no polymer erosion had occurred after 180-days. However, after incubation periods of approximately 20 days for 3HB-co-4HB and around 80 days for both PHB and 3HB-co-3HV at 37°C, a reduction in molecular weight could be detected for all polymers. The greatest molecular weight loss occurred with the 4HB-containing copolymers. From their results Doi and colleagues concluded that hydrolytic degradation occurred by homogenous erosion in two stages. In the first stage, random hydrolytic chain scission of the ester groups led to a decrease in molecular weight, this was followed in the second stage by erosion and weight loss when the molecular weight had reached about 13,000 Daltons. The rate of chain scission was increased by and is proportional to the presence and number of 4HB monomer units. Hydrolytic degradation of PHB *in vitro* proceeds to the monomer D-(-)-3-hydroxybutyric acid which is a normal constituent of blood and one of 3 ketone bodies produced endogenously by ketogenesis. These properties suggest that PHB is well tolerated *in vivo* (Akhtar & Pouton, 1996). However, there is limited information in the literature on the hydrolytic degradation of PHB-HV copolymers, either *in vitro* or *in vivo* (Akhtar & Pouton, 1996) and at present no information is available on the biodegradation of either genetically produced Monsanto polymers, such as PHBHV-Diol and 3HB 3HC, or the novel triblock-co-polymers generated by the Polymer and Bio-Materials Research Group, Chemical Engineering and Applied Chemistry, Aston University, Birmingham, UK.

In recent years, due to the rapid and innovative progress in analytical and biological techniques, there has been a dramatic increase in the production of genetically engineered, biologically active, therapeutic peptides and proteins such as hormones, cytokines, monoclonal antibodies, enzymes, tissue growth factors and antibodies. The production of these materials has only served to highlight the immense difficulties associated with the delivery of such macromolecules to target tissues (Peacock, 1996). Normal administration routes, such as the oral route, are ineffective either due to high proteolytic activity in the gastro intestinal tract or poor absorption through the intestinal wall. The alternative vaginal (Hutchinson and Furr, 1987; Pitt, 1990; Okada *et al*, 1993, 1994), rectal, intranasal (Anile *et al*, 1984), and buccal routes (Andres *et al*, 1983) all give low and variable bioavailablity (Hutchinson and Furr, 1987).

It was for this reason that considerable interest (Koosha *et al*, 1989; Watt *et al*, 1990; Gangrade and Price, 1992) has focused on the development of small biodegradable polymer based carriers, as a controlled release system for the oral and parenteral delivery of these peptides and proteins, in order to achieve satisfactory efficacy and increased patient compliance. However, many problems are encountered when attempts are made to incorporate macromolecules into polymeric systems (Atkins, 1997). Most of these problems derive

from either interactions between the polymer matrix and the incorporated macromolecule, i.e. 'polymer-polymer' compatibility phenomena (Holland *et al*, 1986; Hutchinson and Furr, 1987), or the inability of biological macromolecules, unless in a stable crystalline state, to withstand the solvents and temperatures often involved in the fabrication of synthetic polymers (Atkins and Peacock, 1996). Also stability problems arise with high molecular weight species and chemically useful bioactive proteins are generally so prone to thermal and hydrolytic instability that the use of conventional blending and solution techniques to bring about polymer matrix incorporation is rarely feasible. The *in vitro* hydrolytic degradation of commercially available polyester copolymers such as poly (β-hydroxybutyrate-hydroxyvalerate), PHB-HV (Holland *et al*, 1987; Atkins and Peacock, 1996), and poly(lactide-co-glycolide) (Hutchinson and Furr, 1990; Swarbrick and Boylan, 1990; Jalil and Nixon, 1990c), in simple aqueous buffers has been well characterised. In an expanding market it is prudent to evaluate the potential of other novel polyesters. The degradation of PHB-HV and poly (L-lactide) *in vitro* by relatively simple hydrolytic chemical mechanisms has been shown to give reasonable correlation with degradation *in vivo* (Holland *et al*, 1987; Jamahidi *et al*, 1986). In addition, *in vitro* studies offer advantages such as accessibility, reproducibility and the control of physico-chemical parameters (Atkins, 1998).

1.5 AIMS

In order to develop a nanosize delivery system for pharmaceutically and agriculturally useful actives it was essential to develop a method for the reproducible fabrication of biodegradable nanospheres, not only to ensure accurate results for *in vitro* dissolution studies but also for the continuous production of the delivery devices on a commercial scale. Besides optimising the fabrication technique, physico-chemical parameters including percentage yield, particle diameter, morphology, zeta potential, changes in weight average molecular mass (as a result of the fabrication technique and the incorporation of actives), thermal characteristics (such as changes in polymer glass transition, recrystallisation and melting point temperatures), residual moisture content following freeze-drying, residual PVA content and finally residual DCM (which could be toxic *in vivo*) will be determined.

Nanosphere fabrication techniques including Oil-in-Water, Oil-in-Oil, Water-in-Oil-in-Water and the F68 synperonic surfactant double sonication solvent evaporation method will be evaluated. The technique which generates nanospheres will initially be employed to fabricate nanospheres loaded with the surrogate protein Bovine Serum Albumin. The *in vitro* release of BSA from the nanospheres will be monitored in the well characterised physiological medium Hanks Balanced Salts Solution (pH 7.4), at 37°C over 28 days. Release data will be plotted in terms of daily release and total cumulative release. Mean percentage harvest and consequent percentage weight loss of unloaded and BSA loaded nanospheres after incubation in HBSS will then be determined in order to establish the additional weight loss not associated with the release of BSA. Any changes in nanosphere diameter, zeta potential, weight average molecular mass and residual PVA occurring during incubation will then be determined.

Optimization of the fabrication technique and characterisation of the resultant nanospheres will be followed by studies on the incorporation and release of two actives supplied by Monsanto, namely the insecticide Admire® ({1-[(6-chloro-3-pyridinyl)methyl]-N-nitro-2-imidazolidinimine}) and the plant growth hormone potassium salt Gibberellic acid (GA_3K). The same physico-chemical characterisation and results analysis will be employed as used for the release of BSA from loaded nanospheres. However, the two actives will be released into rural rainwater at both 4°C and 23°C instead of physiological media at 37°C to mimic release into the environment.

Incubation of unloaded nanospheres in a range of physiological media will be performed to characterise the mechanism of polymer biodegradation and the rate of biodegradation *in vivo* at 37°C. Incubation in rural rainwater at 4°C and 23°C will be used to mimic the biodegradation of nanospheres in the external environment. Incubation in HBSS (pH 7.4) at 37°C will be used to mimic biodegradation of polymer nanospheres in a standard physiological buffer at body temperature and should provide information on the simple chemical hydrolysis of biodegradable polyesters under physiological conditions. Incubation in New-

born Calf Serum (pH 7.1) at 37°C will provide information on the potential effects serum enzymes and serum protein adsorption might have on nanosphere integrity and biodegradation in parenteral applications. Incubation in porcine pancreatin at 37°C will mimic the enzymatic biodegradation of nanospheres in the small intestine. Finally, incubation in rural rainwater at 4°C and 23°C will provide information on the biodegradation of polymer nanospheres used to deliver environmentally important compounds.

A composting study using some of the polymers employed in the fabrication of nanospheres used in biodegradation studies and the release of actives will be carried out using the International Standard ISO/FDIS 14855. This describes the internationally accepted method for the determination of the ultimate biodegradation and disintegration of plastic materials under controlled composting conditions by the monitoring of evolved carbon dioxide. This work will confirm how the polyester nanospheres act and biodegrade in the environment, when used for example as pesticide or plant growth factor delivery systems.

CHAPTER 2

MATERIALS AND METHODS

2.1 MATERIALS

2.1.1 SYNTHETIC POLYMERS USED IN FABRICATION STUDIES

The polymers used throughout this work were polyhydroxybutyrate-hydroxyvalerate-diol (PHBHV-Diol), and the Diblock copolymer, polyethylene glycol-poly hydroxybutyrate-hydroxyvalerate (PEG-b-PHBHV). The polymer polyhydroxybutyrate-hydroxycaproic (3HB 3HC) was also used in initial studies, including BSA encapsulation work, but due to limited supplies it was not possible to use this polymer throughout. A novel in-house Tri-block copolymer, poly(hydroxybutyrate-hydroxyvalerate)-diol-polycaprolactone (PHBHV-Diol-polycaprolactone) was supplied by the Speciality Materials Group at Aston University. This was used in initial fabrication and characterisation work, but was not available in sufficient quantities to enable its use in active incorporation and release studies. Initial fabrication and characterisation work was also conducted using commercially available 83.1 kDa BIOPOL® (PHBHV). The chemical structures and physical properties of all these polymers are summarised below in Table 1. They were all supplied by Monsanto, St. Louis, Missouri, USA, in the form of white, anhydrous powders, stored in a desiccator at room temperature until required.

TABLE 1 – KNOWN PHYSICAL CHARACTERISTICS OF THE FABRICATION POLYMERS

MONSANTO CODE	THESIS CODE	COMPOSITION	APPEARANCE	MONSANTO SUPPLIED MWt (Daltons)
-	BIOPOL®	88% PHB, 12% PHV	FINE WHITE POWDER	83,100
-	TRIBLOCK		CREAM, CRYSTALLINE POWDER	14,000
6,262,759	DIBLOCK	PEG-b-PHBHV	FINE WHITE POWDER	37,000
6,070,814-C	3HB 3HC	92% 3HB, 8% 3HC	FIBROUS WHITE POWDER	172,000
6,092,546-F	PHBHV-DIOL	PHBHV-DIOL	FINE WHIE POWDER	1500

2.1.2 CHEMICALS

Double distilled water was used in all experimental work unless otherwise stated and all reagents were either of analytical grade or HPLC grade. Poly(vinyl alcohol), 88% hydrolysed, MWt 13-23 kD and dichloromethane were purchased from Aldrich Chemical Company, Gillingham, UK. Bovine serum albumin (BSA), fraction V powder, 98-99% pure; bicinchoninic acid (BCA); 4% copper II sulphate pentahydrate; sodium dodecyl sulphate (SDS); potassium chloride; sodium hydroxide tablets; ammonium chloride; barium hydroxide; soda lime; iodine; potassium iodide; porcine pancreatin; phosphoric acid; 1,2 dichlorobenzene; sorbic acid; indium; gibberellic acid potassium salt (GA_3K, 95% pure); boric acid; bromcresol green; methyl red and cellulose powder (particle size<20μm) were all purchased from Sigma Aldrich Company Ltd, Poole, Dorset, UK. Hank's Balanced Salts Solution (HBSS – sterile, without phenol red, pH 7.4); amphotericin B; penicillin (10,000 IU ml^{-1})/streptomycin (10mg ml^{-1}); non heat treated New Born Calf Serum (NCS, batch number 30Q 1653 D) from New Zealand, mycoplasma and virus screened, containing low levels of protease and esterase activity, pH 7.1) and porcine pancreatin were all purchased from GIBCO Life Technologies Ltd, Paisley, Scotland, UK. Synperonic F68 was a gift from ICI, Billingham, UK. Selenium Kjeldahl tablets; propan-2-ol (isopropyl alcohol); and pH 4, 7 and 11 buffer solutions were all purchased from BDH, Poole, UK. 1-{(6-chloro-3-pyridinyl)methyl}-N-nitro-2-imidazolidinimine (Admire®) and the original batch of gibberellic acid potassium salt (GA_3K) were all supplied by Monsanto, St. Louis, Missouri, USA. Deuteriated gibberellic acid (dGA_3) was purchased from Professor Lewis Mander, Research School of Chemistry, Australia National University, Canberra, ACT 0200. HPLC water; HPLC methanol; HPLC chloroform; hydrochloric acid; sulphuric acid and alcohol were all supplied in-house. Gas chromatography grade dichloromethane, chloroform and glass mass spectroscopy vials were purchased from Fisher Scientific, UK. Nitrogen gas; hydrogen gas and air were purchased from BOC, UK. Rain water (pH 6.24) was collected from rural areas surrounding Birmingham, UK (Mr & Mrs Carlin, Tamworth, Staffordshire), and filtered (0.22μm) prior to use. Disposable syringes; 0.22μm syringe top filters and sterile screw-capped polypropylene tubes (15ml volume, conical base) were purchased from Sarstedt Ltd, Leicester, UK. Cellulose filters (3 μm pore size) and polyamide membrane filters (0.22 μm) were purchased from Whatman International Ltd, Maidstone, Kent, UK. Compost (6 month old, Green Garden Waste – M602) was supplied by J. Moody Ltd, UK. Granular PHB homopolymer and Biopol® were supplied by Monsanto, St. Louis, Missouri, USA.

2.2 METHODS

2.2.1 O/O (OIL-IN-OIL) SINGLE EMULSIFICATION WITH SOLVENT EVAPORATION METHOD FOR THE FABRICATION OF MICROSPHERES

PHB-HV microspheres were prepared by combining an organic phase containing 1gram of PHB-HV dissolved, by brief ultrasonication (100 watt ultrasonic bath for five minutes) in 30ml of dichloromethane (DCM) with a continuous oil phase consisting of 125grams of light white mineral oil containing 2% w/w SPAN 40. The organic phase was quickly combined with the continuous phase and emulsified using a high shear head (Silverson Machines Ltd, Cheshire, UK) at 4000rpm for 30 minutes at 35°C. Droplet formation was monitored by light microscopy and the final emulsion stirred using a Heidolph stirrer (Heidolph, Lab-plant Ltd, Huddersfield, UK) at 2000rpm with a three bladed propeller set in an off-centre position for a further 60 minutes at 35-37°C to facilitate solvent evaporation. The emulsion was then left for a further 30 minutes at 35°C to allow the microspheres to harden. Meanwhile, around 600ml of petroleum ether was warmed to 55°C in a clingfilm topped beaker. The microspheres were separated by vacuum filtration using solvent resistant 47mm diameter polypropylene backed PTFE filters (1μm) (Whatman, Maidstone, England) and washed three times with the pre-warmed petroleum ether to wash out the SPAN 40 and remove any oil. The microspheres were air-dried, washed, and stored desiccated at room temperature. The fabrication protocol has been summarised in Figure 6, below.

FIGURE 6 – OUTLINE PROTOCOL FOR O/O (OIL-IN-OIL) SINGLE EMULSIFICATION WITH SOLVENT EVAPORATION METHOD

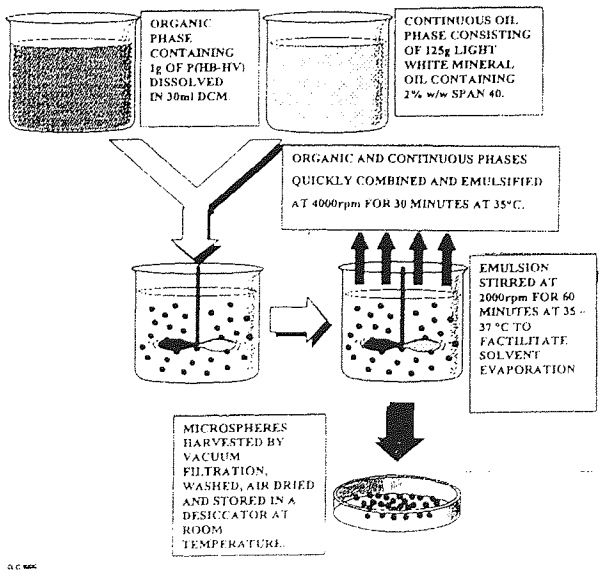

2.2.2 0/W (OIL-IN-WATER) SINGLE EMULSIFICATION WITH SOLVENT EVAPORATION METHOD FOR THE FABRICATION OF MICROSPHERES

The (O/W) single emulsification with solvent evaporation technique was originally described by Beck *et al* (1979). In the present work an organic phase was prepared by dissolving 500mg of PHB-HV in 20ml of DCM at room temperature with five minutes of ultrasonication (100watt ultrasonic bath). An aqueous phase was prepared by dissolving 2.25g (2.25 % w/v) of PVA in 100ml of double distilled water, with continuous stirring and slight warming. Both these phases were then cooled simultaneously in an ice bath for one hour, to increase the viscosity of the solution. The organic phase was then added drop by drop to the lightly stirred aqueous phase. The entire mixture was then emulsified for eight minutes at 8000rpm using a Silverson L4RT (Silverson Machines Ltd, Cheshire, UK). The final emulsion was stirred at 2000rpm with a three bladed propeller (Heidolph, Lab-plant Ltd, Huddersfield, UK) set in an off-centre position for a further two hours at room temperature to facilitate solvent evaporation. The resulting suspension was aliquoted into centrifuge tubes, and centrifuged at 4500rpm for 20 minutes. The white precipitations were re-suspended in a minimum volume of double distilled water by gentle shaking and then pooled. The suspension was aliquoted into a series of centrifuge tubes and centrifuged a second time for 20 minutes at 4500rpm. The supernatant was removed and the pellets re-suspended in double distilled water, before being centrifuged a third time. The pellets were re-suspended in a minimum volume of double distilled water and pooled. A small sample of the suspension was examined by light microscopy, and the remainder pre-frozen at -20°C in a minimal volume of double distilled water, prior to freeze-drying (Edwards Modulyo 4L, BOC Ltd, Sussex, UK). The fabrication protocol has been summarised in Figure 7.

Modifications were carried out to this technique in order to improve solvent evaporation and reduce the overall loss of polymer. To improve the speed and effectiveness of the solvent evaporation stage, the temperature of the emulsion was increased from room temperature to 39°C in a water bath (Gallenkamp, UK) and stirred with a three bladed propeller (Heidolph, Lab-plant Ltd, Huddersfield, UK) set in an off-centre position.

FIGURE 7 – OUTLINE PROTOCOL FOR 0/W (OIL-IN-WATER) SINGLE EMULSIFICATION WITH SOLVENT EVAPORATION METHOD

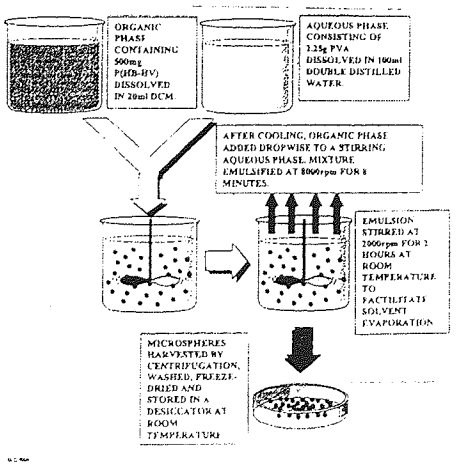

2.2.3 W/O/W (WATER-IN-OIL-IN-WATER) DOUBLE EMULSIFICATION WITH SOLVENT EVAPORATION METHOD FOR THE FABRICATION OF MICROSPHERES AND NANOSPHERES

A primary emulsion was prepared first. This consisted of an aqueous phase, composed of 0.05% w/v methylcellulose and 0.5% w/v PVA in 5ml of double distilled water. An organic phase was then prepared which consisted of 1gram of PHB-HV dissolved in 20ml of DCM and cooled for one hour in an ice bath. The aqueous and organic phases were then mixed by the drop-wise addition of the aqueous phase into the organic phase, followed by emulsification with a 3/8" mini-micro probe (Silverson Machines Ltd, Cheshire, UK) for 4 minutes at 3/4 speed. A secondary emulsion was prepared consisting of 1.5 % w/v PVA in 75ml of double distilled water. The primary emulsion was added to the secondary aqueous phase and emulsified for 8 minutes at 8000rpm using a Silverson L4RT (Silverson Machines Ltd, Cheshire, U.K.). The final emulsion was the gently warmed to 39°C, whilst being stirred with a double bladed paddle set in an off centre position to facilitate solvent evaporation, for one hour. The final emulsion was centrifuged in several aliquots at 14,000rpm for 40 minutes at room temperature. The supernatants were discarded and the pellets re-suspended in double distilled water and re-centrifuged at 14,000rpm for 40 minutes. This washing process was repeated two further times. The final pellets were re-suspended in a minimum amount of double distilled water and frozen overnight prior to freeze-drying and storage at -20°C.

In order to improve the morphology of the microspheres an extended solvent evaporation step was introduced involving low speed stirring. In addition, with the inclusion of a sonication step (14-16 μamps for 10minutes), the microsphere mean diameter could be significantly reduced. This could be carried out either by:-

a) sonication of the primary emulsion after emulsification,
b) sonication of the secondary emulsion after emulsification in the normal way,
c) sonication alone to create the primary emulsion, followed by emulsification to create the secondary emulsion or,
d) emulsification of the primary phase followed by sonication alone to produce the secondary emulsion.

The original fabrication protocol has been summarised in Figure 8, overleaf.

FIGURE 8 – OUTLINE PROTOCOL FOR W/O/W (WATER-IN-OIL-IN-WATER) DOUBLE EMULSIFICATION WITH SOLVENT EVAPORATION METHOD

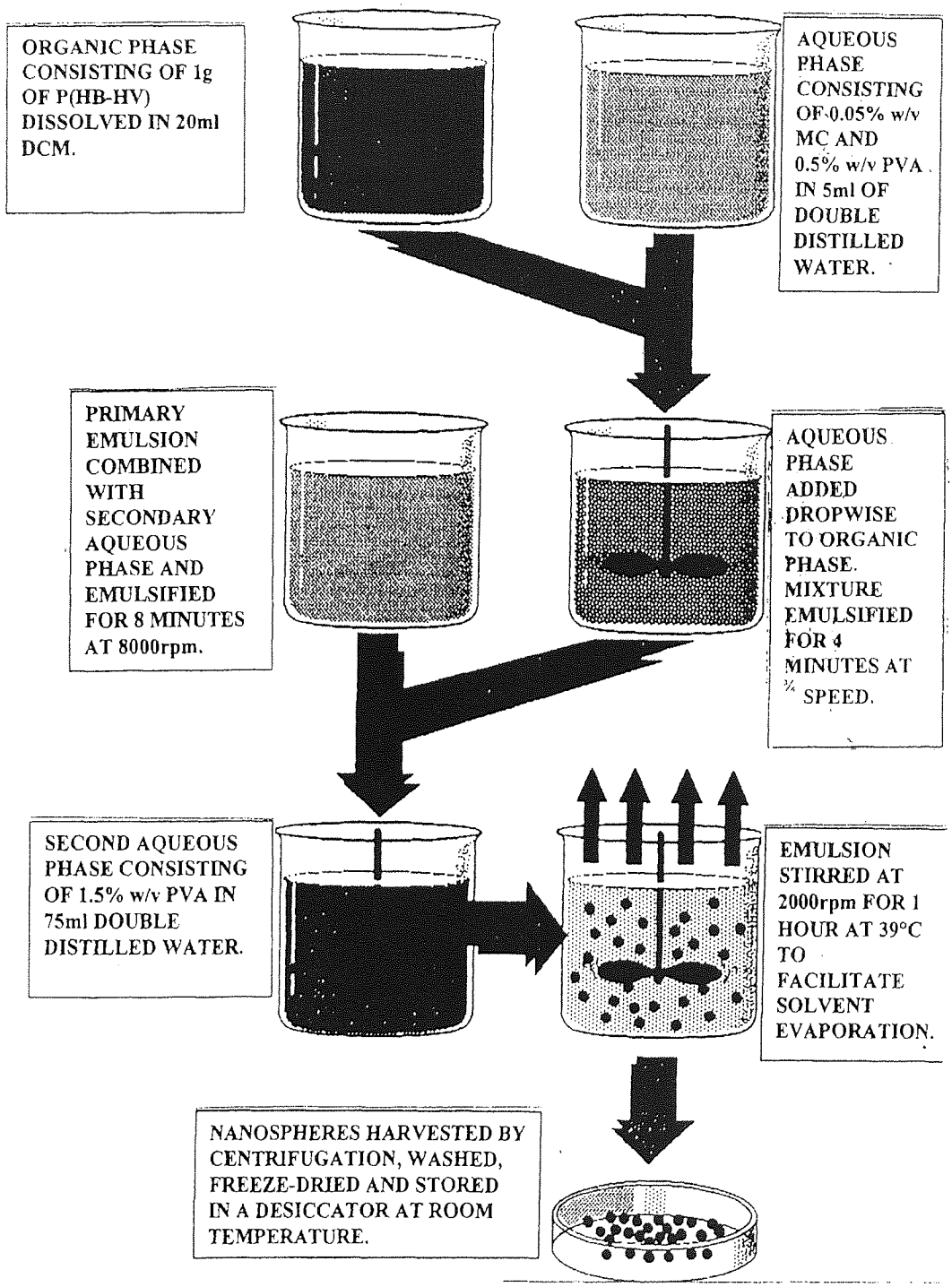

2.2.4 F68 DOUBLE SONICATION SOLVENT EVAPORATION METHOD FOR THE FABRICATION OF NANOSPHERES

A primary emulsion was prepared by mixing 250mg of PHBHV-Diol, Diblock or 3HB 3HC polymer, 5ml DCM, 0.5ml double distilled water and 10mg synperonic F68. The final solution was pre-cooled in ice for one hour and the entire mixture sonicated, over ice, for 3 minutes on full power (26μamps). This primary emulsion was then added drop-wise into a pre-cooled secondary aqueous phase, containing 625mg PVA dissolved in 25ml of double distilled water and the mixture sonicated on low power (14μamps), over ice. Once all the primary emulsion had been added, the sonication power was increased to full (26μamps) for a further 4minutes. The resulting emulsion was then stirred with the aid of a magnetic stirrer at ambient temperature overnight to allow the solvent to completely evaporate. The nanospheres were harvested by centrifugation at 31000rpm for 30minutes, washed with double distilled water, re-suspended and re-centrifuged at 31000rpm for 30minutes. This process was repeated a further two times, before the nanospheres were stored at -20°C in a minimum volume of double distilled water, prior to freeze-drying. The fabrication protocol has been summarised in Figure 9, below.

FIGURE 9 – OUTLINE PROTOCOL FOR F68 DOUBLE SONICATION SOLVENT EVAPORATION METHOD

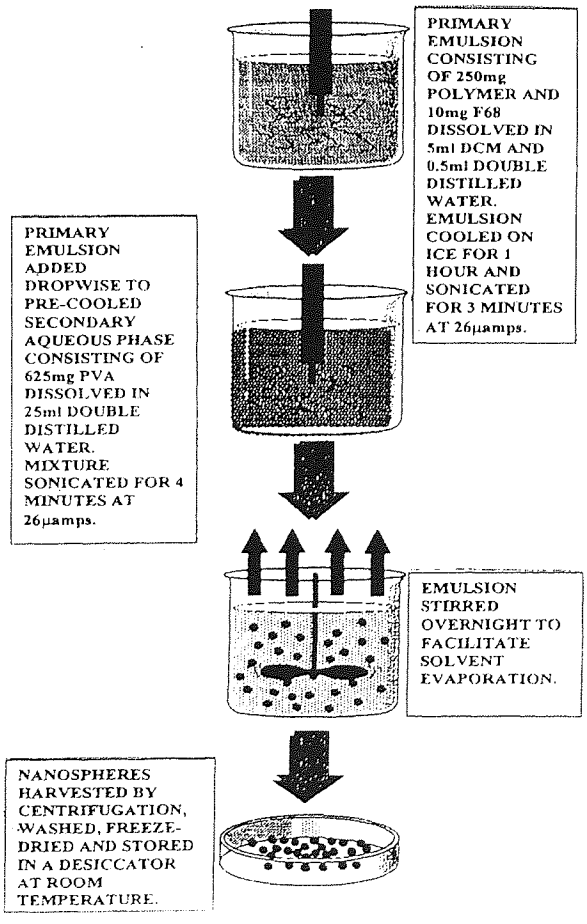

2.2.5 FREEZE DRYING

The nanosphere preparations were retained in glass vials containing a minimum volume of double distilled water and pre-frozen at -20°C. Prior to freeze drying the tops of the glass vials were covered with Parafilm® punctured with a series of holes to allow the pressures to equilibrate and retain the preparation upon decompression. The samples were then freeze-dried (Edwards Modulyo 4L Freeze-drier, BOC Ltd, Sussex, UK) at a chamber pressure of ~0.2 Torr for 48hours, to ensure removal of water and residual tightly bound solvent. The lyophilised samples were stored in sealed tubes in a desiccator at room temperature until required for use.

The percentage yield of the nanospheres was calculated from the ratio of the dry weight of nanospheres obtained to the total dry weight of polymer originally used in fabrication, using equation 1 below.

EQUATION 1 – PERCENTAGE YIELD OF UNLOADED NANOSPHERES

$$\% \text{ Yield} = \frac{\text{Final weight of freeze-dried nanospheres (gm)}}{\text{Initial weight of polymer (gm)}} \times 100$$

When nanospheres were loaded with active material the weight of active formed part of the dry weight of polymer and the yield was calculated using equation 2 below. In this work polymer was replaced with active during fabrication in order to give theoretical loadings of 10%, 20%, 30% and 40% w/w.

EQUATION 2 – PERCENTAGE YIELD OF LOADED NANOSPHERES

$$\% \text{ Yield} = \frac{\text{Nanosphere yield (gm)}}{\text{Polymer + Active (gm)}} \times 100$$

2.2.6 SCANNING ELECTRON MICROSCOPY

Scanning electron microscopy was used to assess the diameter (from bars on the micrograph), surface topography and extent of biodegradation of the nanospheres where their diminutive size permitted. Aluminium stubs were prepared by lightly sanding the surface to ensure good electrical conductivity. A thin layer of nanospheres was mounted onto an aluminium stub using an adhesive carbon disc and excess removed by gently knocking the stub. The stub was then placed into a splutter coater (Emscope SC500) and under an argon atmosphere, the surface of the stub was coated with a 20nm gold film. Nanospheres were examined using scanning electron microscope (Cambridge Instruments Stereoscan 90B, 35KV) and temporary records made using thermal prints. Work was also carried out under the supervision of Lesley Tompkins at the Department of Biochemistry, University of Birmingham, UK, using a Joel 120 CX II Temscan electron microscope, fitted with a scanning electron microscope attachment from which photographic records of the nanospheres were obtained.

2.2.7 PARTICLE SIZE ANALYSIS BY PHOTON CORRELATION SPECTROSCOPY (PCS)

Nanosphere diameter analysis was performed by Photon Correlation Spectroscopy, using a Malvern Zetasizer 1000 (Malvern Instruments Ltd, Malvern, UK). Photon correlation spectroscopy is a digital method for measuring intensity fluctuations in which the number of photons arriving at a detector at a set sampling time is repeatedly counted. The time autocorrection function of the detected intensity is then computed by a correlator. In a PCS experiment laser light of specific intensity, polarisation and wavelength are focused into the sample. The molecules in the illuminated part of the sample are subsequently subjected to an oscillating electric field. An oscillating dipole moment is thus induced and as a result light is scattered in all directions except in the direction of the dipole axis i.e. the direction of polarisation of the incident light. The main part of the scattered light will thus have the same polarisation as the incident light though generally there will also be a depolarised component due to the fact that the polarisability may change for different directions in the molecules. This machine is capable of measuring the diameter of particles in the range of 3 to 3000nm using a spectrogoniometer coupled with a computer interfaced analysis system. Information on the diameter of the nanospheres, as well as the polydispersity correlation (an estimate of the width of the distribution) measured using laser light, a scattered light detector (photomultiplier) and a correlator are provided on a printed results sheet. The particle size distribution in double distilled water was measured by quasi elastic light scattering measurements. Small particles scatter less light from a monochromatic polarised light source than larger ones. However, for a given viscosity of solvent, smaller particles undergo more rapid Brownian motion than larger ones and it is this measurement which is determined by means of the photon correlator. An example of the printout obtained from the machine can be seen in Figure 10, below.

A 250µl aliquot of nanosphere suspension in double distilled water was removed prior to freeze-drying and combined with 50ml of filter sterilised double distilled water (0.22µm filter). The sample was dispersed thoroughly by sonication in a 100 Watt ultrasonic bath for around 30 minutes to remove any aggregation. A small aliquot (2ml) of the sample was then placed in the machine and its temperature allowed to equilibrate to 25°C before being analysed. The accuracy of the determination was confirmed using a 245nm polystyrene nanosphere standard (Malvern Instruments Ltd, Malvern, UK).

FIGURE 10 – A TYPICAL PHOTON CORRELATION SPECTROSCOPY PRINTOUT FOR UNLOADED 3HB 3HC NANOSPHERES SHOWING MEAN NANOSPHERE SIZE AND SIZE DISTRIBUTION PROFILE

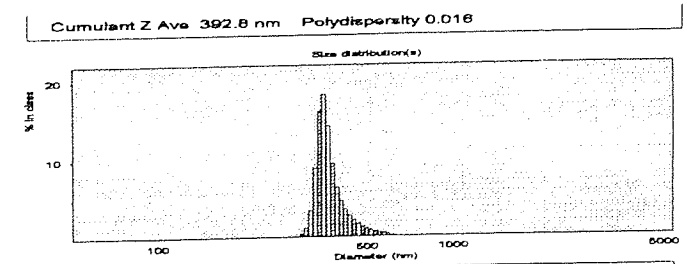

Size (nm)	% volume	Size (nm)	% volume	Size (nm)	% volume
271.2	0.1	354.1	14.2	462.2	1.4
280.4	0.2	366.1	9.5	477.9	1.1
289.9	0.4	378.5	6.5	494.1	0.9
299.7	1.2	391.3	4.7	510.8	0.7
309.9	3.4	404.6	3.6	528.1	0.6
320.4	9.0	418.2	2.8	546.0	0.6
331.2	16.1	432.4	2.2	564.5	0.5
342.5	18.2	447.1	1.6	583.6	0.3

2.2.8 MEASUREMENT OF THE SURFACE CHARGE ON NANOSPHERES – THE ZETA POTENTIAL

The relationship between particle surface charge and potential macrophage phagocytosis of nanospheres is important in parenteral and other forms of drug delivery. It is generally accepted that uncharged microspheres display a reduced uptake by the reticulo-endothelial system (Tabata and Ikada, 1990). Zeta potential is also important in agricultural applications where maximum dispersion of the active loaded nanospheres is desirable and hence the development of discrete charged units is essential. Colloidal particles will generally be dispersed by Brownian motion although many environmental stresses, such as high temperatures and freeze-thaw cycles, can have effects on dispersion. Measurement of the magnitude of the charge on the surface of microspheres and nanospheres is very important because one of the major problems with all colloidal dispersions is their innate inability to remain stable as single independent unaggregated particles for long periods of time. Systems that retain the single particle state are termed "colloidally stable", whereas unstable systems form aggregates or clumps. Colloidal particles generally have an electronegative surface charge with zeta potentials in the range of -14 to -30mV. Proteins fall into this category, but they become less electronegative with decreasing pH. Particles with highly negative zeta potentials (i.e. more electronegative than -30mV) exhibit electrostatic repulsion between the discrete charged units, preventing flocculation and stabilising the dispersion. Between -14 and -30mV there is a plateau region, marking the threshold of either coagulation or dispersion. Flocculation is often seen when the colloidal particles are more positive than -14mV. Table 2, below shows the relationship between the zeta potential and colloid stability (Riddick, 1968).

TABLE 2 - RELATIONSHIP BETWEEN ZETA POTENTIAL AND COLLOIDAL STABILITY (RIDDICK, 1968)

Aston University

Content has been removed for copyright reasons

An electropositive range of dispersion from zero to at least +70 mV is possible, but is seldom employed by either Nature or man (Riddick, 1968).

The origin of surface charge depends on the nature of the particle and its surrounding medium. For particles dispersed in liquids, two of the most important factors are the ionisation of chemical groups at

the particle surface and the differential adsorption of different charges from the solution. The development of a net charge at the particle surface affects the distribution of ions in the surrounding interfacial region, resulting in an increased concentration of counter ions, ions of opposite charge to that of the particle, close to the surface. There is a non-uniform distribution of ions of opposite charge (positively adsorbed counter-ions) in the liquid adjacent to the solid whereas co-ions of the same charge are repelled (negatively adsorbed). Thus an electrical double layer is formed around each particle. The liquid layer surrounding the particle can be considered to exist in 2 parts:- a) an inner region that includes ions bound relatively strongly to the surface at approximately one hydrated radius distance (the Stern layer), partially neutralising the charge on the colloid; and b) an outer or diffuse region in which ion distribution is determined by a balance of electrostatic forces and random thermal motion. The electrical potential close to the surface therefore decays as the distance from the surface increases, eventually reaching zero (no net charge) in the bulk solution. An individual nanosphere and its most closely associated ions move through the solution as a charged unit and the electrical potential at the boundary of this unit, i.e. at the surface of shear between the particle with its strongly bound ion atmosphere (Stern layer) and the bulk surrounding medium, is known as the zeta potential (ζ) or electrokinetic potential.

Zeta potential measurements can be used as an indirect measure of the surface charge (Müller *et al*, 1986). There are four main techniques used to measure zeta potentials, all of which rely on the electrokinetic behaviour of the nanospheres in aqueous suspension. These techniques include electrophoresis, electro-osmosis, streaming potential and sedimentation potential. In the present work, zeta potential measurements were carried out by the most widely used method of microelectrophoresis using a Malvern ZetaMaster® (Malvern Instruments Ltd, Malvern, UK). The process is fully automated and is operator-independent requiring a sample size of 1×10^6 particles, which is processed in minutes. The main advantages of the method over other electrophoretic techniques is its high speed and high resolution. It does, however, have the disadvantage of being very expensive to set-up. In the present work, a small aliquot (0.1ml) of nanosphere suspension in double distilled water was added to 10ml of 1mM KCl, and sonicated in a 100 Watt ultrasonic bath for 30 minutes. The ZetaMaster® was prepared by washing the internal cell with 10ml of 1mM KCl. A 2ml sample was then injected into the machine with a syringe and zeta potentials were automatically determined as the mean of five determinations (± S.D). These values were manually changed to mean value ± SEM. The zeta potential (mV) is not a uniquely definable parameter and is strongly pH dependent. It represents an overall measurement of surface interactions with the medium, rather than the surface charge. Therefore, it is important to define the solution in which the nanospheres were suspended. Figure 11, overleaf, shows a typical printout obtained from the Zetamaster, and shows the mean zeta potential (mV) ± standard deviation from the mean of a nanosphere sample in 1mM KCl.

FIGURE 11 – TYPICAL ZETAMASTER® PRINTOUT FOR THEORETICAL 20% w/w GA_3K LOADED PHBHV-DIOL NANOSPHERES SHOWING MEAN ZETA POTENTIAL AND ZETA POTENTIAL DISTRIBUTION PROFILE

PHB GA 20.1
Live data
Cell type Capillary cell Ref. Beam Mode

Run	Pos.	KCps	Mob.	Zeta	Width	Time
1	17.0	2986.5	-0.857	-11.0	6.2	14:01:08
2	17.0	3012.8	-0.784	-10.1	6.2	14:01:29
3	17.0	3071.9	-0.804	-10.3	6.1	14:01:50
4	17.0	2818.4	-0.781	-10.0	6.1	14:02:11
5	17.0	3125.8	-0.930	-11.9	6.1	14:02:32
Average		3003.0	-0.831	-10.6	6.2	
+/-		116.5	0.063	0.8	0.0	

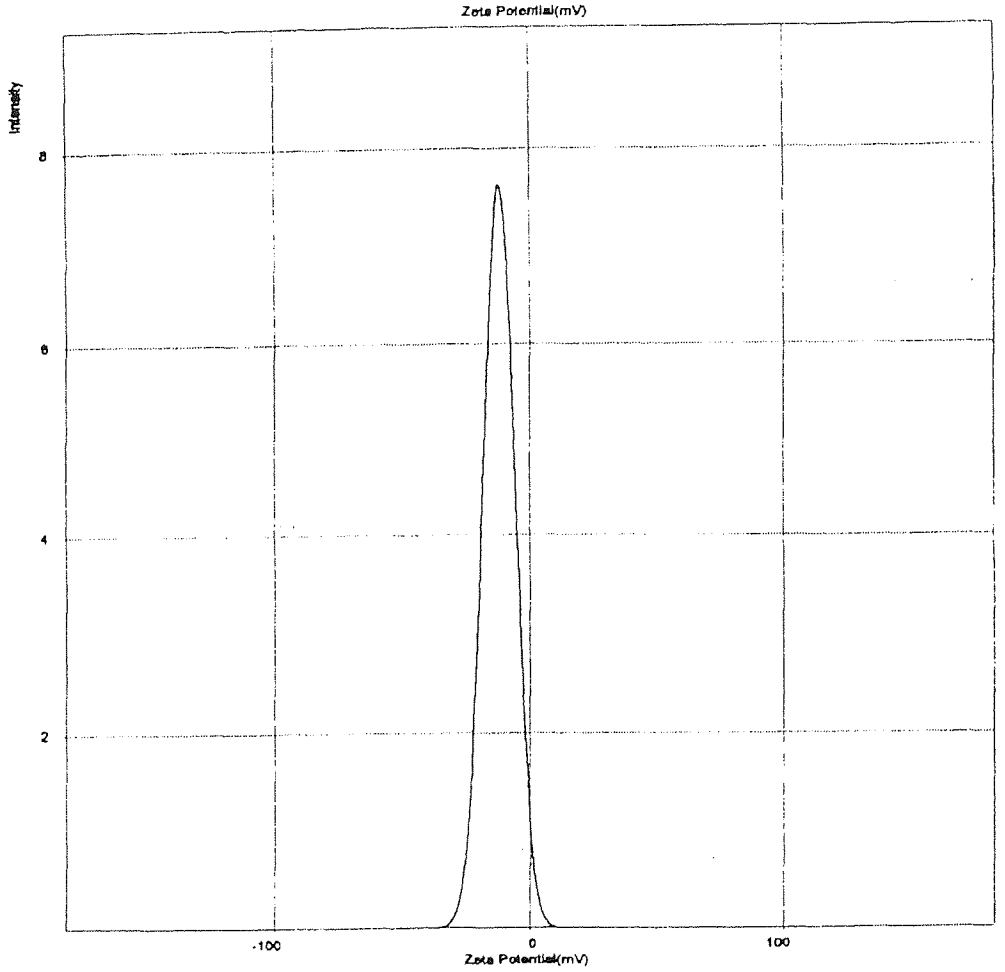

Malvern Instruments Ltd, Malvern UK +44 1684 892456

2.2.9 MOLECULAR WEIGHT DETERMINATION USING GEL PERMEATION CHROMATOGRAPHY (GPC)

Determination of the molecular weight of virgin polymers is extremely important because it can assist in predicting the rate of polymer degradation during incubation in physiological and agricultural media. Nanospheres composed of low molecular weight polymer will degrade at a faster rate than nanospheres fabricated using the same polymer with a higher molecular weight, and hence will release nanoencapsulated drug at faster rate (Ogawa *et al*, 1988). The determination of molecular weight can be used to monitor the changes in the molecular weight that may occur as a result of nanosphere fabrication. Changes in molecular weight can highlight polymer damage and help predict the potential rate of biodegradation and the rate of release of loaded active. Measurement of molecular weight of polymer nanospheres after incubation in physiological and agricultural media can give some indication of the rate and extent of biodegradation, because the shortening of polymer chains causes a reduction in polymer molecular mass and this represents the first stage of polymer de-esterification (Yates, 1998).

Gel Permeation Chromatography (GPC) is a method of solute separation with molecular size as the discriminating factor. Molecules in the sample permeate the stationary phase at different speeds and are thus retained within the column for different lengths of time, proportional to their molecular size. GPC columns are tightly packed with a gel (PL gel) and then completely filled with the mobile phase solvent. The same solvent is used to dissolve the sample before it is introduced into the column. The pore size of the gel determines the molecular size range within which separation occurs. GPC analysis of polymers in order to determine molecular weight distributions, chain lengths and the extent of cross linking within a polymer has been well rehearsed. The molecular weight averages (Mn, Mw) indicate the number and length (or weight) of the polymeric chains formed during manufacture. Mn is the number-average molecular weight, which is the molecular weight of the average chain length in a polymer sample. Mw is the molecular weight equal to the modal molecular weight of polymer chains, known as the weight average molecular weight. As Mn represents the molecular weight of the average chain length in a polymer sample, and Mw refers to the molecular weight equal to the modal molecular weight of the polymer chains, the value of Mw is always larger than Mn except in the case of a truly monodispersed system where the values are identical (Conway, 1996).

To determine the Mw of unloaded and loaded nanosphere samples, a solution of each sample was prepared by adding 25ml chloroform to 50mg of freeze dried nanospheres and refluxing gently for 20 minutes. On cooling, a small amount of 1,2-dichlorobenzene was added as an internal marker and the solutions thoroughly mixed by vortexing. All solutions were filtered through a polyamide membrane (0.22μM) prior to chromatography. The chromatographic conditions employed are summarised in Table 3, below. The acquired data was processed using Viscotek Trisec 3.0 software which produced numerical and graphical analysis of the sample data, as shown in Figure 12, below. The GPC system was calibrated with polystyrene standards. Some GPC analyses were carried out at RAPRA Technology Ltd, Shawsbury, Shrewsbury, UK, with funding from EPSRC research grant 97560183.

TABLE 3 – GPC CHROMATOGRAPHIC CONDITIONS

SYSTEM COMPONENT	CONDITION
COLUMN	PLgel 2 × MIXED BED-B, 30cm, 10 MICRONS
SOLVENT	CHLOROFORM
FLOW-RATE	1ml *per* MINUTE
TEMPERATURE	40°C
DETECTOR	REFRACTIVE INDEX

Figure 12, below, shows a typical printout obtained using Viscotek Trisec 3.0 processed GPC data for unloaded Diblock nanospheres.

FIGURE 12 – TYPICAL GEL PERMEATION CHROMATOGRAPHY PRINTOUT FOR UNLOADED DIBLOCK NANOSPHERES SHOWING MOLECULAR WEIGHT DISTRIBUTION AND CALCULATED MOLECULAR WEIGHT (produced by Rapra Technology Limited using Viscotek Trisec 3 software)

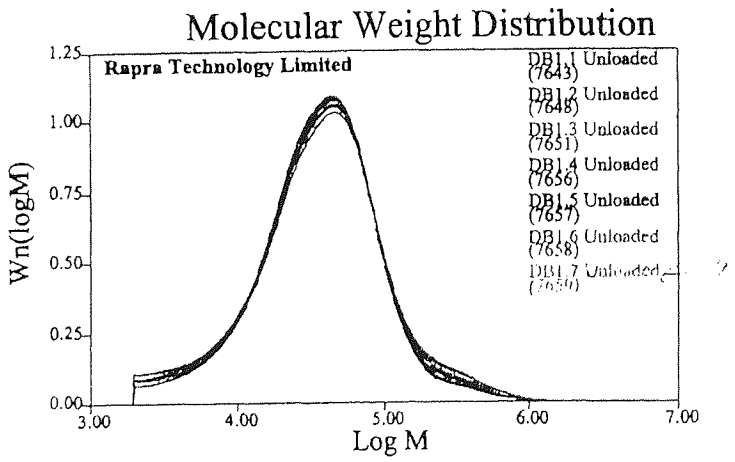

SAMPLE	RUN NUMBER	MOLECULAR WEIGHT
DB 1.1 – UNLOADED (7643)	A 2813	53, 600
DB 1.1 UNLOADED (7643)	A 2820	54, 500
DB 1.2 UNLOADED (7648)	A 2824	52, 100
DB 1.3 UNLOADED (7651)	A 2834	64, 800
DB 1.3 UNLOADED (7651)	A 2838	63, 700
DB 1.4 UNLOADED (7656)	A 2841	63, 700
DB 1.4 UNLOADED (7656)	A 2847	63, 400

2.2.10 DETERMINATION OF THE THERMAL CHARACTERISTICS OF POLYMER NANOSPHERES USING DIFFERENTIAL SCANNING CALORIMETRY

Differential scanning calorimetry (DSC) is one of the easiest of modern analytical techniques to use. The method requires minimum sample preparation, and quantitative information can be obtained from just a few milligrams of material (Richardson, 1994). Polymer colloids and lattices typically contain a large number of polymer chains, with each individual chain having a molecular weight in the region of about 10^5 to 10^7 Daltons. The arrangement of the polymer chains within the fabrication polymer of nanospheres determines whether the polymer is described as either an amorphous, crystalline, rubbery or glassy (Mathot, 1994). Residual monomer retained in the polymer particle can result in polymer swelling as a result of the polymer being soluble in the monomer. The physical state of nanosphere polymer can be important in close-range interactions and in the drying process. Soft nanospheres tend to coalesce and produce a continuous film, whereas hard nanospheres remain discrete in the dry state. In the present work, DSC analysis of virgin polymers, as well as loaded and unloaded polymer nanospheres has been performed in order to characterise the physical state of the fabrication polymer after nanoencapsulation. This information can also be used to confirm the loading of active material into nanospheres during nanoencapsulation, by observing the change in the glass transition temperature (Tg) (Theeuwees *et al*, 1974) and the extent of polymer biodegradation.

In the present work DSC thermograms were produced using a computer interfaced Perkin-Elmer system 4. An indium standard with a known endotherm of 156.9°C, corresponding to a heat of transition of $28.45 Jg^{-1}$, was used as the temperature calibrator. Samples (approximately 10mg of either virgin polymer or freeze-dried nanospheres, either unloaded or loaded with active) were sealed into aluminium pans. The latter were exposed to a thermal gradient of 20-200°C and compared with an empty aluminium pan as a control, under a constant atmosphere of nitrogen. The samples were then cooled at a rate of 320°C *per* min down to -40°C. This removed the potential influence of any previous thermal history of the polymer, such that any differences observed in thermal characteristics would be the result of the method of nanosphere fabrication. Once cooled to -40°C all thermal profiles were generated using a heating rate of 10°C *per* min under a nitrogen atmosphere. Operating functions were controlled by the computer and routine thermal analysis was carried out using the Perkin-Elmer DSC 4 computer software. The thermal profile was presented as a thermogram, from which details of melting points (Mpt) depending on the number of components in the polymer, glass transition temperature (Tg) and crystallinity were extrapolated. Figure 13 shows a typical thermogram of one of the novel Monsanto polymers, 3HB 3HC, produced by this DSC technique.

FIGURE 13 – TYPICAL DIFFERENTIAL SCANNING CALORIMETRY PROFILE FOR VIRGIN 3HB 3HC POLYMER SHOWING GLASS TRANSITION TEMPERATURE (Tg), RECRYSTALLISATION TEMPERATURE AND MELTING POINTS

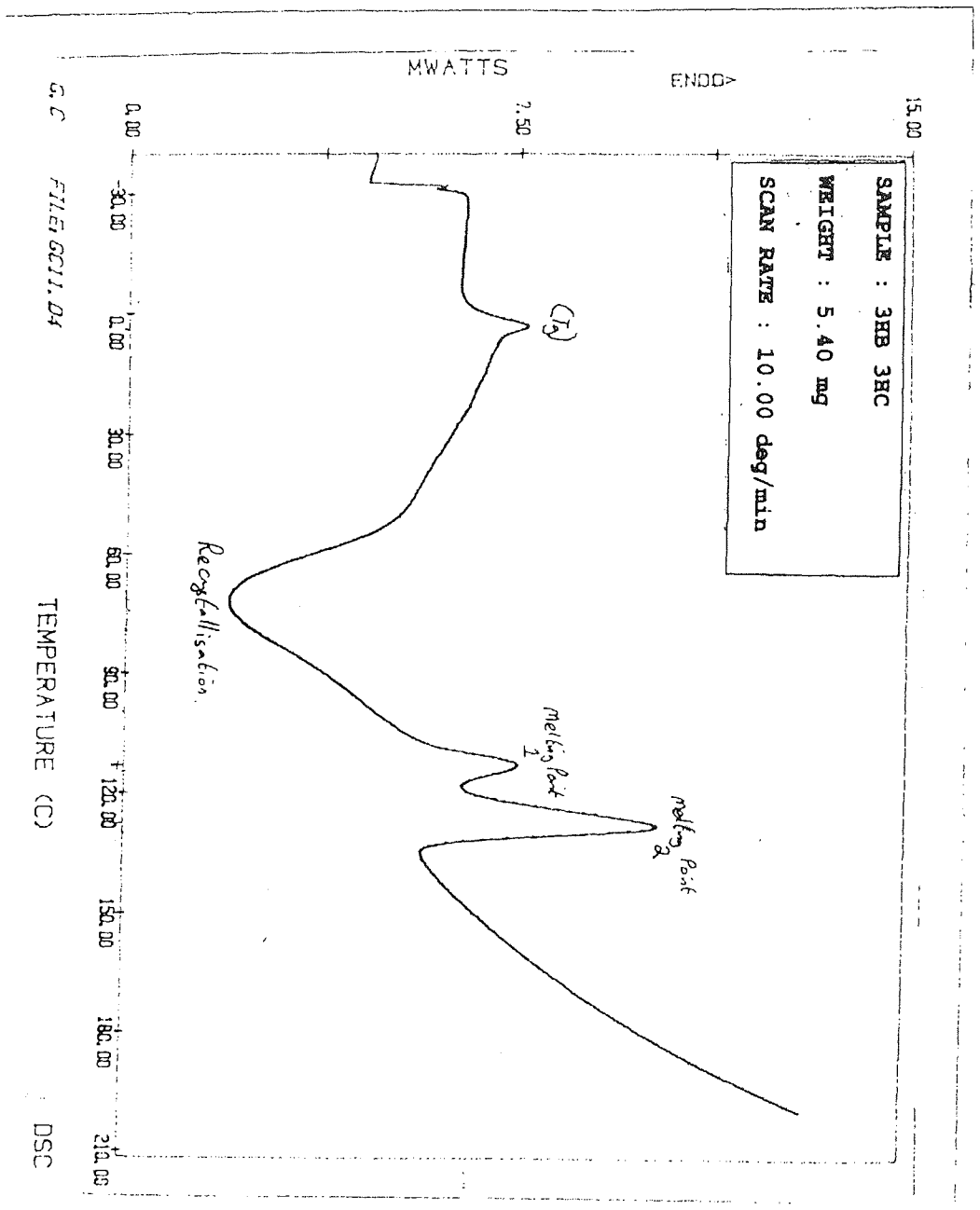

2.2.11 THERMO-GRAVIMETRIC ANALYSIS (TGA) OF WATER CONTENT

The moisture content of freeze dried nanospheres was determined by TGA. Samples of freeze dried product were heated to 130°C in a Perkin-Elmer TGS-2 TG analyser, linked to a Perkin-Elmer TADS 3600 thermal analysis data station with related software. Sample weight was plotted as a function of temperature and moisture determined using the system software package. A typical trace for theoretical 20% w/w GA_3K loaded Diblock nanospheres is shown in Figure 14, below.

FIGURE 14 – TYPICAL THERMOGRAVIMETRIC ANALYSIS PROFILE FOR THEORETICAL 20% w/w GA_3K LOADED DIBLOCK NANOSPHERES SHOWING PERCENTAGE WEIGHT LOSS AFTER HEATING

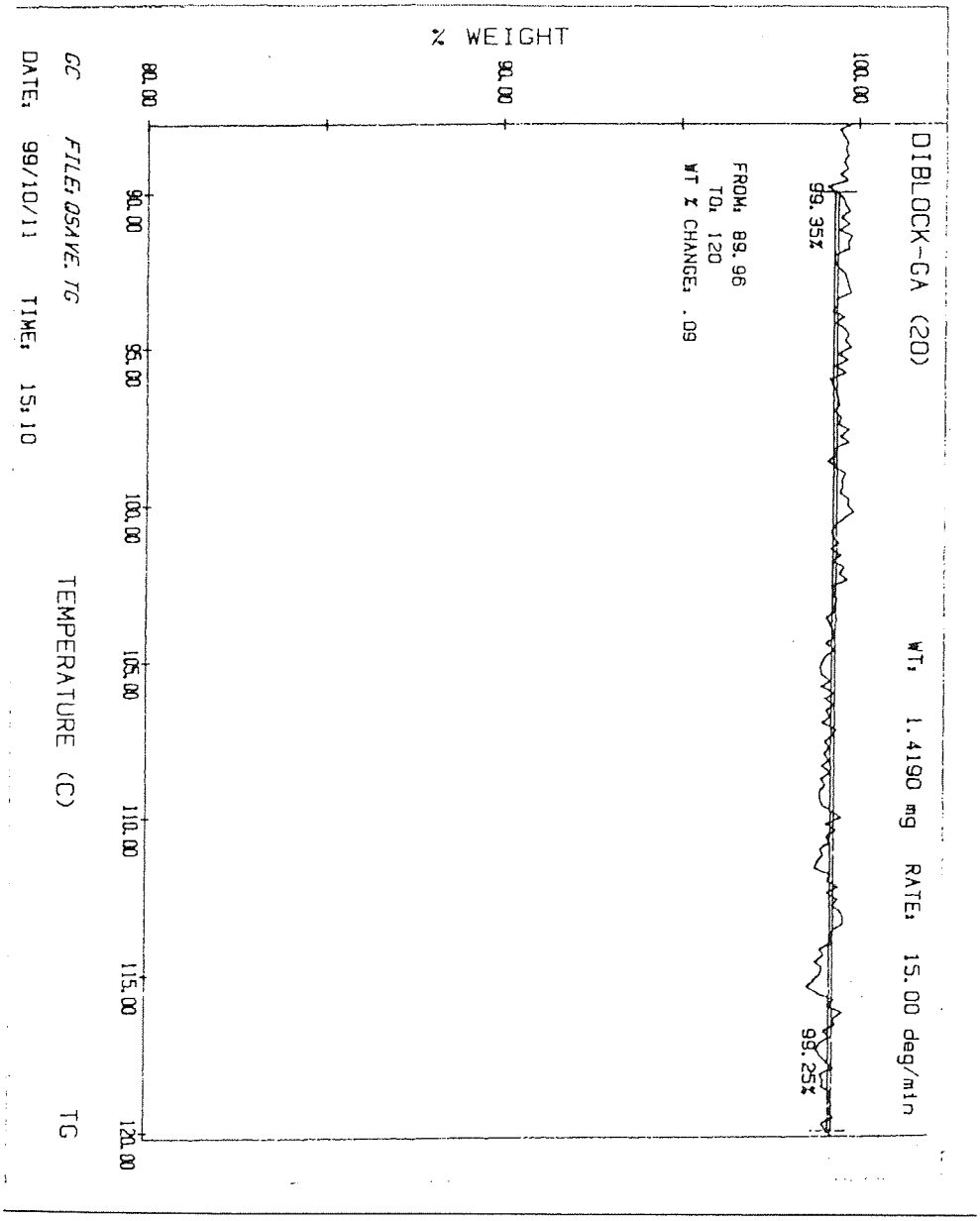

2.2.12 DETERMINATION OF RESIDUAL POLYVINYL ALCOHOL (PVA) IN NANOSPHERES

Most microsphere and nanosphere fabrication methods depend on the emulsification of aqueous and organic phases followed by the removal of the solvent by evaporation. Residual surfactants and chlorinated solvents are considered a drawback of these methods and quantification of these contaminants is therefore extremely important for pharmaceutical efficacy (Bazile *et al*, 1992). Although PVA is generally considered safe and non-toxic the emulsification process may contaminate the final product with PVA and influence final product characteristics. It has been reported that extended contact times of PVA with microspheres can lead to incorporation of the hydrocolloid into the matrix, increasing the burst release of encapsulated drug or antigen (Kwong *et al*, 1986). On the other hand, precoating microspheres with PVA has been shown to reduce the surface hydrophobicity resulting in a reduced macrophage uptake (Tabata & Ikada, 1988). Residual PVA has been reported to be approximately linearly related to the specific surface area of microspheres (Alléman *et al*, 1993). Surface associated PVA may influence the efficiency of adsorption of the active to the nanosphere surface. Furthermore, the increased wetting of freeze-dried nanospheres by residual PVA may aid the preparation of reproducible suspensions for dosing but may also alter the biodistribution and subsequent release of encapsulated active (Pepper, 1997). These detrimental effects have spurred some workers to investigate the residual levels of PVA (Alléman *et al*, 1993; Conway, 1996). Due to the extended solvent evaporation time used in the double sonication solvent evaporation method employed in the present work, the level of residual PVA in nanospheres has been determined as follows.

Exactly 40mg of nanospheres was added to 5ml of HPLC chloroform. The mixture was sonicated for 10 minutes before being filtered through a 3μm cellulose filter. The filter was further washed with 10ml of HPLC chloroform and allowed to dry. In order to dissolve the PVA attached to the membrane, the filter was boiled in 20ml of double distilled water for 1 minute. A 1ml aliquot of this PVA solution was added to 3ml of 4% w/v boric acid and 0.6ml of iodine solution (1.27% w/v iodine and 2.5% w/v potassium iodide). The total volume was adjusted to 10ml with water and the absorbance was measured spectrophotometrically at λ max of 690nm.

A standard calibration curve, Figure 15 below, was generated by preparing a series of triplicate PVA concentrations ranging from 0 to 0.1% w/v and each subjected to identical treatment as described above. The concentration of residual PVA in the nanospheres was obtained by extrapolation from the standard calibration curve.

FIGURE 15 – RESIDUAL PVA (% w/v) STANDARD CALIBRATION CURVE (mean values ± SEM, n=3)

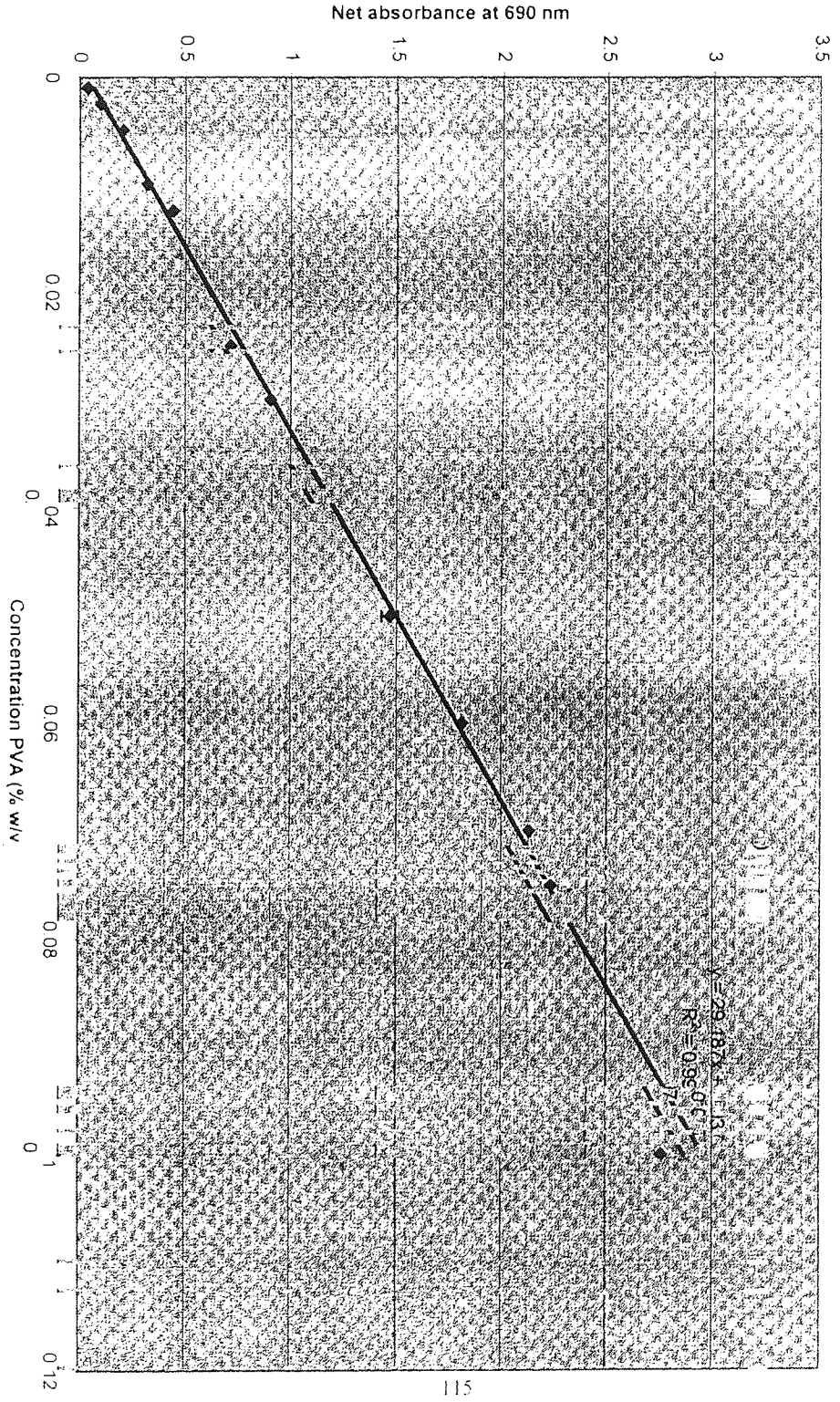

2.2.13 DETERMINATION OF RESIDUAL DICHLOROMETHANE (DCM) IN NANOSPHERE PREPARATIONS

The fabrication of polyalkanoate nanospheres using the double sonication method requires the use of the chlorinated organic solvent dichloromethane, and the amount of residual solvent in nanospheres must be determined due to its toxicity. Dichloromethane is the most suitable solvent for solvent evaporation processes, including the double sonication solvent evaporation method. This is because it has a low boiling point (42°C) and a low aqueous solubility (~2% v/v) resulting in rapid evaporation rate for nanosphere production. However, toxicity concerns limit the acceptable residual levels of DCM in parenteral drug delivery devices. Martindale (31st Edition, 1996) states that the recommended UK limits for short term exposure is < 250ppm with a maximum long term exposure level of 100ppm. The U.S limits are 500ppm and 2000ppm for long and short-term exposure, respectively. DCM is a suspected carcinogen and mutagen (Martindale, 1996). When ingested it is metabolised to carbon monoxide, causing damage to the liver and kidneys, as well as skin irritation and nervous system disorders. Excess solvent can be removed from preparations by extending drying times but this increases costs and may alter the performance of the delivery system. The excess residual solvent is bound to the polymer and the amount bound depends on the drying process and the hydrophobicity of the polymer, i.e. increased hydrophobicity leads to increased solvent binding (Conway, 1996). Also, a more compact delivery system structure, such as nanospheres, may be expected to retain more solvent. However, the nanosphere preparations used in the present work were extensively freeze-dried and consequently the amount of residual DCM was expected to be low.

In order to determine the residual DCM after fabrication, exactly 20mg of nanospheres was accurately weighed and dissolved in 1ml of GC grade chloroform. This was immediately injected into a Pye Unicam Series 304 gas chromatograph (injection temperature 70°C, column temperature 60°C, detector temperature 120°C), coupled to a Pye Unicam integrator and trace recorder. The injection volume was 2μl and the column used for DCM detection was a 1metre 0.8% THED on Carbopack C 80/100 mesh, with pressures for nitrogen (N_2, the carrier gas) of 20 mm Hg, hydrogen (H_2) of 1.1 Kg/cm^2, and air of 0.4 Kg/cm^2. At a flame ionisation amplitude of 1×10^2 attenuation, a calibration curve was constructed for standards of GC grade dichloromethane in GC grade chloroform, over the range 1:100 000 to 1: 20 000. The concentration of residual DCM liberated from the nanospheres when run under identical conditions was obtained by interpolation. A typical GLC trace is shown in Figure 16, overleaf.

FIGURE 16 – TYPICAL GAS LIQUID CHROMATOGRAPHY PROFILE FOR DCM:CHLOROFORM (1:20,000) STANDARD, COMPLETE WITH COMPUTER INTEGRATOR PRINTOUT

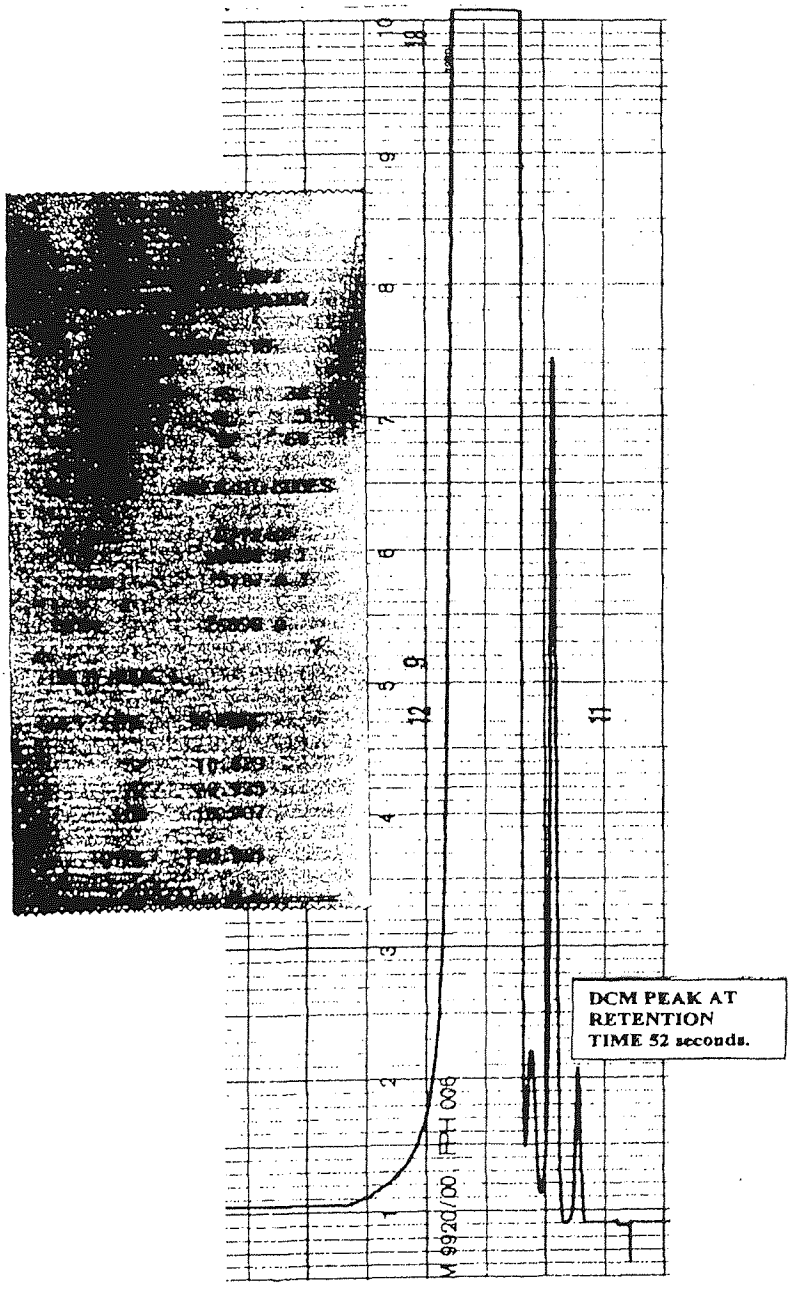

2.2.14 FABRICATION OF BSA LOADED NANOSPHERES

Nanospheres with theoretical loading of 10%, 20%, 30% and 40% w/w BSA were fabricated using the double sonication, solvent evaporation method (Section 2.2.4, Page 56), from PHBHV-Diol, 3HB 3HC and Diblock polymers. A quantity of the dry weight of polymer was replaced with BSA in proportion to the theoretical loading, so as to keep the total weight of solid material to 250mg, as shown in Table 4, below.

TABLE 4 - THE WEIGHT OF POLYMER AND THE WEIGHT OF ADDED BOVINE SERUM ALBUMIN USED TO CREATE A RANGE OF THEORETICAL LOADINGS (10 – 40 % LOADING w/w)

THEORECTICAL % LOADING (w/w)	WEIGHT OF POLYMER (mg)	WEIGHT OF BSA (mg)
0	250	0
10	225	25
20	200	50
30	175	75
40	150	100

2.2.15 DETERMINATION OF BSA CONCENTRATION USING THE BICINCHONINIC ACID PROTEIN ASSAY (BCA)

The Bicinchoninic Acid (BCA) assay is a rapid, sensitive and reproducible method of protein determination, which is extremely flexible and where both time and temperature can be varied to meet the needs of the investigator (Smith *et al*, 1985). The BCA assay allows accurate detection of low protein concentrations between 200ng to 500µg of protein per assay and consequently is ideal for the determination of the concentration of protein released from nanospheres preparation *in vitro*. The principle behind the assay is that proteins, such as the surrogate protein BSA, reduce alkaline Cu^{2+} to Cu^{1+} in a concentration dependent manner (Lowry *et al*, 1951). Bicinchoninic acid (4,4'-dicarboxy-2,2'-biquinolone) is a highly specific chromogenic reagent for Cu^{1+} forming a purple complex with an absorbance maximum at 562nm (Tikhanov and Mustafin, 1965; Mazonski *et al*, 1963). With reference to standard curves constructed using a range of protein (BSA) concentrations (0-200µg BSA *per* ml) the resultant absorbance of the sample measured at 562nm is directly proportional to the BSA concentration. Briefly the method of protein determination required that BCA reagent was freshly prepared daily by adding one part of 4% w/v copper II sulphate pentahydrate solution to fifty parts of bicinchoninic acid solution and mixed thoroughly. In the standard assay protocol 100µl of protein sample was added to 2ml of the above freshly prepared protein determination reagent in a labelled test tube and vortex mixed

thoroughly. Sample tubes were then incubated at 37°C for 30 minutes in a water bath. The tubes were cooled to room temperature and the absorbance of the solution was read at 562nm using water to zero the instrument.

Standard curves were produced using a range of BSA concentrations (0-100μg per assay) dissolved in (a) double distilled water, (b) Hanks Balanced Salts Solution (HBSS) and (c) neutralised 0.1M NaOH (a strong base used to attack ester linkages of the polymeric backbone) with 5% w/v sodium dodecyl sulphate (to aid protein solubilisation and used in encapsulation efficiency experiments). Calibration curves were constructed by plotting standard protein concentration in μg against the absorbance at 562nm and the concentration of protein in samples obtained by extrapolation. The protein concentration (mg/ml) in the unknown samples was calculated using Equation 3, below. All samples were assayed for BSA content in triplicate, and results are expressed as the mean of three determinations (± SEM).

EQUATION 3 - CALCULATION OF PROTEIN CONCENTRATION (mg/ml) IN BCA ASSAY.

$$\text{Protein concentration (mg/ml)} = \frac{\text{mg protein per assay}}{\text{ml of unknown in assay}}$$

The BCA assay has been shown to be compatible with 1M NaCl, 0.1M NaOH, 1% SDS, 0.1M HCl and 1% detergents, but is incompatible with 100mM EDTA, 1mM DTT and 20% ammonium sulphate (Smith *et al*, 1985).

2.2.16 DETERMINATION OF BSA IN SUPERNATANTS

In order to determine how much protein had been lost to the secondary aqueous phase and in centrifugation washes during nanosphere fabrication, the supernatants from the secondary aqueous phase and all the centrifugation stages were combined and the total volume recorded. Samples (200μl) from both the pooled washes and the original secondary aqueous phase were subjected to the standard BCA assay protocol. The resulting protein concentration (mg/ml), multiplied by the sum of the total volume of the washes and the secondary aqueous phase, was used to estimate the total amount of protein lost during the fabrication process.

2.2.17 DETERMINATION OF THE BSA NANOENCAPSULATION EFFICIENCY

The amount of BSA either nanoencapsulated or adsorbed *per* unit dry weight of nanospheres (% w/w) was determined by a modification of the method described by Hora *et al* (1990). Exactly 1mg of nanospheres was incubated for at least 3 hours with 1ml of 0.1M NaOH (used to hydrolyse ester linkages

of the polymeric backbone) containing 5% w/v sodium dodecyl sulphate (SDS) to aid protein solubilisation, until the solution lost all turbidity. The solution was then neutralised to pH 7 by the addition of a few drops of 1M HCl. The resultant solution was subsequently analysed for BSA using the BCA assay procedure. In this case a series of BSA standards (0-100μg/ml) was prepared in neutralised NaOH/SDS digestion buffer. All samples were assayed in triplicate and the results expressed as the mean of three determinations (± SEM).

The BSA content of nanospheres was also determined by dissolving 1mg of nanospheres in 1ml of DCM. The BSA was then extracted with two successive 3ml washes with double distilled water. The second wash was left sealed overnight to ensure maximum partitioning of the BSA into the aqueous phase. The upper aqueous layer was then removed and combined with the product of the first aqueous extraction. A BCA assay was used to determine the BSA concentration with reference to a calibration curve of absorbance versus BSA concentration in double distilled water. All samples were assayed in triplicate and results were the mean of three determinations (± SEM). From these determinations, the % w/w of BSA nanoencapsulated *per* dry weight of nanospheres was calculated and the encapsulation efficiency determined, using Equation 4, below.

EQUATION 4 – PERCENTAGE NANOENCAPSULATION EFFICIENCY

$$\text{Encapsulation efficiency \%} = \frac{\text{BSA nanoencapsulated (\% w/w)}}{\text{Theoretical loading (\% w/w)}} \times 100$$

2.2.18 RELEASE OF BSA INTO HBSS *IN VITRO*

The release of BSA from nanospheres was investigated by incubating 100mg of loaded nanospheres in 2ml of sterile Hank's buffer, pH 7.4 (HBSS - without Phenol Red) at 37°C for 28 days or until exhaustion, in sealed plastic tubes shaken twice daily. Supernatant medium was removed daily by aspiration after centrifugation (4000*rpm* for 20 minutes) and replaced with fresh medium at 37°C to provide sink conditions for release and/or biodegradation and discourage microbial growth. Supernatants were filtered through a 0.22μm filter to remove any nanospheres and assayed for BSA. Negative controls consisting of unloaded nanospheres were maintained under identical conditions throughout the study. At the end of the study, polymer nanospheres were freeze-dried, digested and assayed for residual protein.

2.2.19 FABRICATION OF ADMIRE® LOADED NANOSPHERES

Nanospheres with theoretical loadings of 10%, 20%, 30% and 40% w/w Admire® were fabricated using the double sonication, solvent evaporation method (Section 2.2.4, Page 56), from both PHBHV-Diol and Diblock polymers. A quantity of the dry weight of polymer was replaced with active in proportion to the theoretical loading, so as to keep the total weight of solid material to 250mg, as summarised in Table 5, below.

TABLE 5 - THE WEIGHT OF POLYMER AND THE WEIGHT OF ADMIRE® USED TO CREATE A RANGE OF THEORETICAL LOADINGS (10 – 40% ADMIRE® w/w)

THEORECTICAL % LOADING (w/w)	WEIGHT OF POLYMER (mg)	WEIGHT OF ADMIRE® (mg)
0	250	0
10	225	25
20	200	50
30	175	75
40	150	100

2.2.20 DETERMINATION OF ADMIRE® CONCENTRATION IN SUPERNATANTS

In order to determine how much Admire® had been lost to the secondary aqueous phase, and subsequent centrifugation washes during the fabrication process, the supernatants were analysed for Admire® spectrophotometrically at the λ max of 265nm (Unicam Heλios β U.V spectrophotometer). Admire® concentrations were calculated by extrapolation from a calibration curve.

2.2.21 DETERMINATION OF ADMIRE® NANOENCAPSULATION EFFICIENCY

The DCM method employed to determine the BSA encapsulation efficiency in nanospheres could not be used with Admire® loaded nanospheres because of the high solubility of both fabrication polymers and Admire® in the solvent. Isopropanol was therefore chosen instead of DCM because Admire® is only slightly soluble (1-2grams *per* litre) in this solvent whereas the two polymers are not.

Exactly 10mg of crushed freeze-dried nanospheres was combined with 10ml of isopropanol in a sealed glass vial. The mixture was stirred for several days at ambient temperature to encourage dissolving and release of all the Admire®. The mixture was filtered through a 0.22μm filter to remove polymer debris

and the concentration of Admire® measured spectrophotometrically by extrapolation from a calibration curve.

The encapsulation efficiency was calculated using equation 4, below.

EQUATION 4 – PERCENTAGE NANOENCAPSULATION EFFICIENCY

$$\text{Encapsulation efficiency \%} = \frac{\text{Admire® nanoencapsulated (\% w/w)}}{\text{Theoretical loading (\% w/w)}} \times 100$$

2.2.22 RELEASE OF ADMIRE® INTO RURAL RAINWATER *IN VITRO* AT 4°C AND 23°C

The release of Admire® from 10%, 20%, 30% and 40% w/w Admire® theoretically loaded nanospheres was determined by incubating 100mg of nanospheres in 2ml of filtered rural rainwater (0.22μm filter, pH 6.2) at both 23°C and 4°C for 37 days in capped plastic tubes and agitated twice daily. Supernatant medium was removed daily by aspiration after centrifugation at 4500rpm for 20 minutes (Mistral 2000, MSE) and replaced with fresh filtered rainwater at either 23°C or 4°C, to provide sink conditions for release and discourage microbial growth. The supernatants were filtered (0.22μm) to remove any contaminating nanospheres before the Admire® concentration in the samples was determined spectrophotometrically at 265nm via extrapolation from a standard calibration curve. At the end of the study the remaining nanospheres were freeze-dried, digested and analysed for residual Admire® using the method described in Section 2.2.21, page 74.

Negative controls consisting of unloaded nanospheres were also maintained and monitored under identical conditions throughout the time period of the study.

2.2.23 FABRICATION OF GIBBERELLIC ACID (GA_3K) LOADED NANOSPHERES

Nanospheres with a theoretical loading of 10%, 20%, 30%, and 40% w/w GA_3K were fabricated from both PHBHV-Diol and Diblock using the double sonication solvent evaporation method (Section 2.2.4, page 56). A quantity of the dry weight of the polymer was replaced with active in proportion to the theoretical loading, so as to keep the total weight of the material at 250mg. See Table 6, below.

TABLE 6 - THE WEIGHT OF POLYMER AND THE WEIGHT OF ADDED GA_3K TO CREATE A RANGE OF THEORETICAL LOADINGS

(10% -40% GA_3K w/w)

THEORECTICAL % LOADING (w/w)	WEIGHT OF POLYMER (mg)	WEIGHT OF GA_3K (mg)
0	250	0
10	225	25
20	200	50
30	175	75
40	150	100

2.2.24 DETERMINATION OF GA_3K IN SUPERNATANTS

In order to determine how much GA_3K had been lost into the secondary aqueous phase and in centrifugation washes during nanosphere fabrication, the supernatants from the secondary aqueous phase and all centrifugation washes were combined and the total volume recorded. Samples were subjected to the GA_3K spectrophotometric assay protocol (Section 2.2.27, page 77). GA_3K concentrations were calculated by extrapolation from a standard calibration curve.

The resulting GA_3K concentration (mg/ml) multiplied by the total volume of the supernatants was used to calculate the total amount of GA_3K lost during the fabrication process.

2.2.25 DETERMINATION OF GA_3K NANOENCAPSULATION EFFICIENCY

The nanoencapsulation efficiency was determined using method 2 described in Section 2.2.17, page 72, except that the λ max of GA_3K in water (228nm) was used and the nanoencapsulation efficiency calculated using Equation 4, below.

EQUATION 4 – PERCENTAGE NANOENCAPSULATION EFFICIENCY

$$\text{Encapsulation efficiency \%} = \frac{GA_3K \text{ nanoencapsulated (\% w/w)}}{\text{Theoretical loading (\% w/w)}} \times 100$$

2.2.26 RELEASE OF GA_3K *IN VITRO* INTO RURAL RAINWATER

The release of GA_3K from 10%, 20%, 30% and 40% w/w GA_3K loaded nanospheres was monitored by incubating 100mg of nanospheres in 2ml of filtered rural rainwater (0.22μm filter, pH 6.2) at both 4°C and 23°C for 30 days in capped plastic tubes, with twice daily agitation. Supernatant medium was aspirated daily after centrifugation at 4500rpm for 20 minutes (Mistral 2000, MSE) and replaced with fresh medium at either 4°C or 23°C, to provide sink conditions for release and discourage microbial growth. The supernatants were then filtered (0.22μm) to remove contaminating nanospheres before determination of the GA_3K concentration in the samples. After 28 days incubation the remaining nanospheres were freeze-dried, digested and analysed for residual GA_3K using the method detailed in Section 2.2.25, page 76.
Negative controls consisting of unloaded nanospheres were maintained under identical incubation conditions throughout the study and release samples processed for GA_3K like activity.

2.2.27 SPECTROPHOTOMETRIC DETERMINATION OF GA_3K CONCENTRATION IN RELEASE SAMPLES

The absorbance of 1ml release samples was determined using a Unicam Heλios β UV spectrophotometer at 228nm - the λ max of GA_3K in rainwater. Figure 17 below, shows the standard calibration curve generated for a range of GA_3K concentrations from 10μg/ml to 1300μg/ml at 228nm. The concentration of GA_3K in the samples was extrapolated from the standard curve.

FIGURE 17 – GA_3K STANDARD CALIBRATION CURVE IN RURAL RAINWATER (mean values ± SEM, n=3)

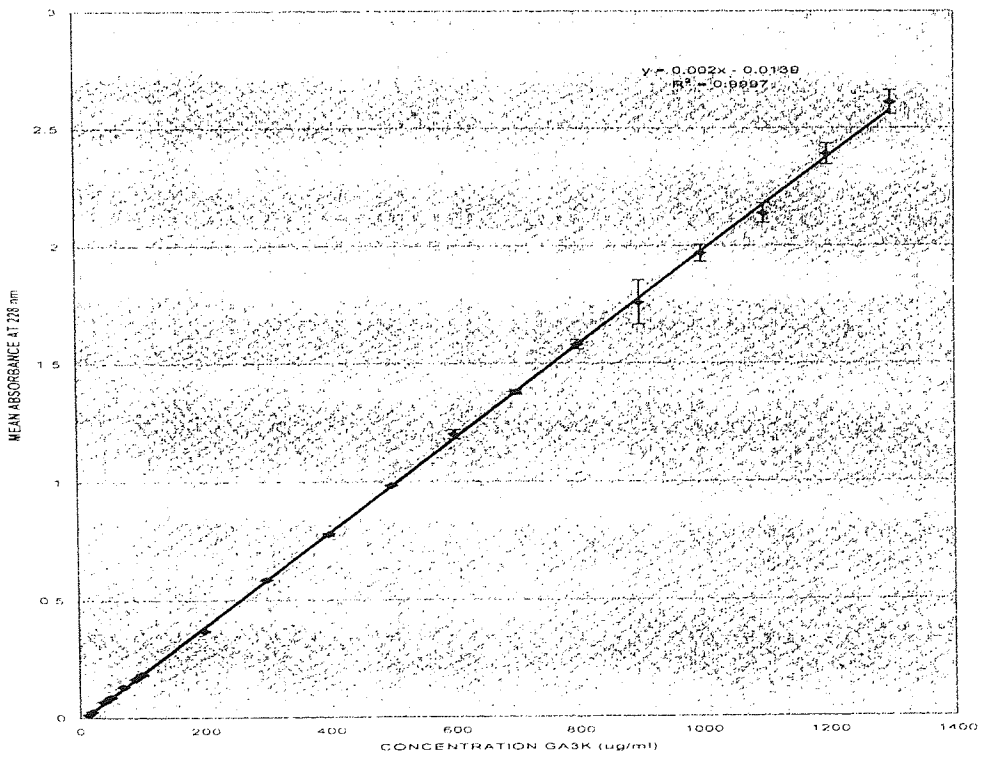

2.2.28 *IN VITRO* BIODEGRADATION OF UNLOADED NANOSPHERES IN RAINWATER AT 4°C AND 23°C, HANK'S BALANCED SALTS SOLUTION, NEW BORN CALF SERUM AND PANCREATIN AT 37°C.

100mg of unloaded nanospheres, fabricated from either PHBHV-Diol, 3HB 3HC or Diblock polymers using the double sonication solvent evaporation method detailed in Section 2.2.4, page 93, were placed into 15ml conical tipped plastic tubes. To these samples was added 2ml of either sterile heat equilibrated rural rainwater, HBSS, NCS or pancreatin. The rainwater samples were incubated at both 4°C and 23°C, and the HBSS, NCS and pancreatin samples were incubated at 37°C, over 28 days. The tubes were agitated twice daily. Supernatant was removed daily by aspiration after centrifugation at 4500*rpm* for 20 minutes (Mistral 2000, MSE, U.K) and replaced with fresh temperature matched incubation medium to provide sink conditions and discourage microbial growth. The supernatants of samples incubated in HBSS, NCS, pancreatin and rural rainwater were filtered (0.22μm) to remove any contaminating nanospheres and assayed using the same method as the release study they were shadowing.

2.2.29 DETERMINATION OF THE RATE OF BIODEGRADATION OF PHBHV-DIOL, PHB HOMOPOLYMER AND CELLULOSE TO CARBON DIOXIDE BY THE MICROBIAL CONTENT OF GREEN GARDEN WASTE COMPOST

Figure 18 below shows the set-up for a single aerobic composting reactor, as used for monitoring the evolution of carbon dioxide from the biodegradation of cellulose and synthetic polyalkanoates.

FIGURE 18 - A SINGLE AEROBIC BIODEGRADATION COMPOSTING REACTOR SYSTEM - (Extracted from "Modified version of ISO/DIS 14855"

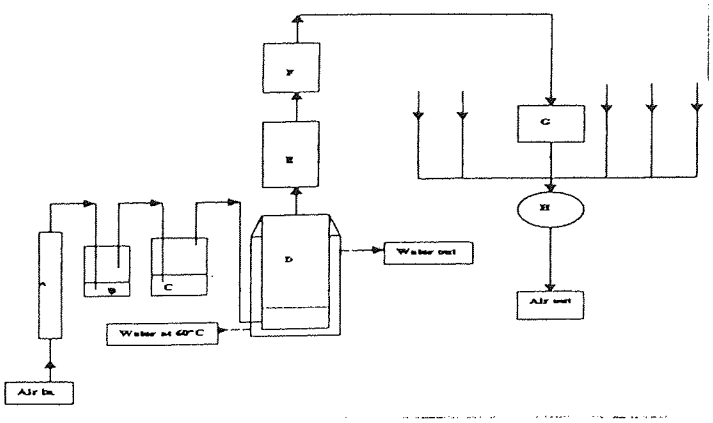

DIAGRAM CODE	DESCRIPTION
A	SODA LIME
B	BARIUM HYDROXIDE
C	DISTILLED WATER
D	SINGLE REACTION VESSEL + WATER JACKET
E	WATER CONDENSER
F	AIR CONDENSER
G	PUMP AND FLOW METER
H	IR DETECTOR

The entire aerobic biodegradation composting system can be seen in Figures 19 and 20 below and consists of a total of six reactor vessels.

FIGURE 19 – PART OF THE LABORATORY COMPOSTING SYSTEM SHOWING PUMP AND FLOW RATE METERS COUPLED TO REACTION VESSELS

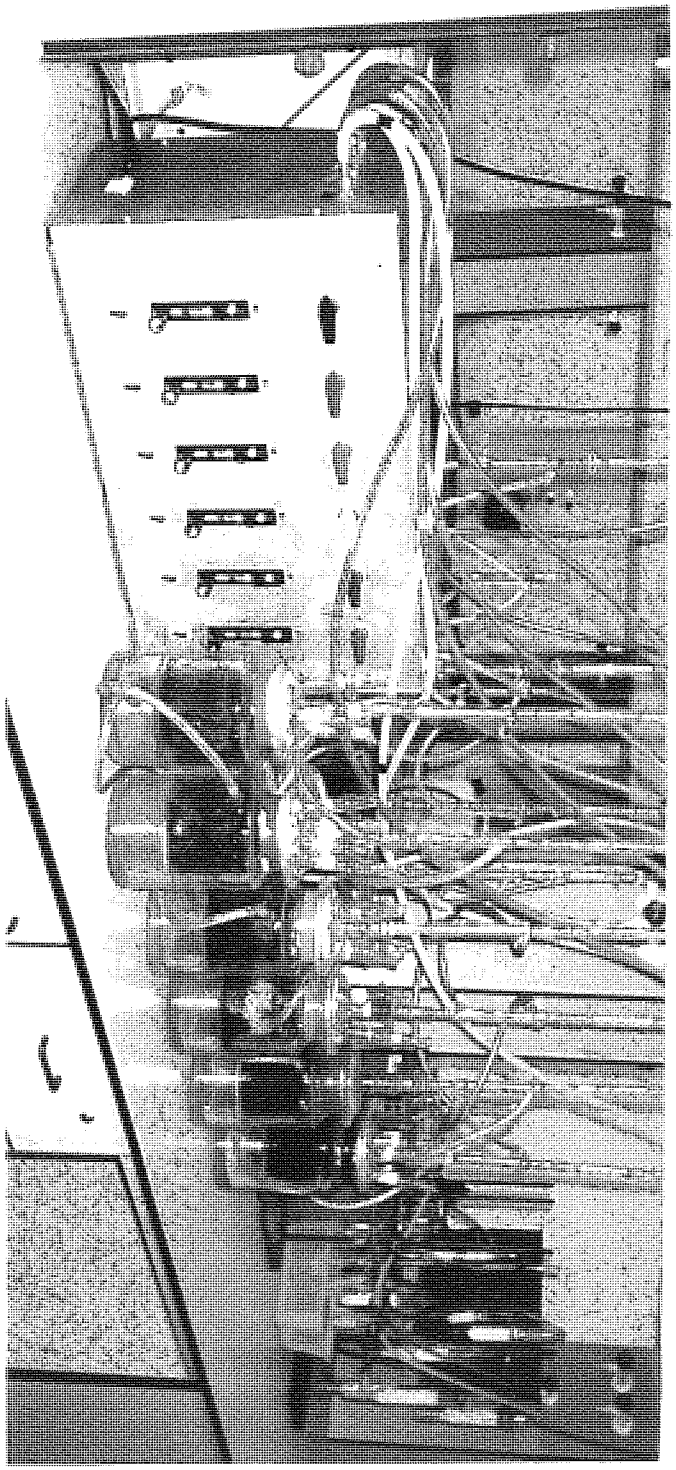

FIGURE 20 - PART OF THE LABORATORY COMPOSTING SYSTEM SHOWING AIR INTAKE THROUGH SODA LIME, BARIUM HYDROXIDE AND DISTILLED WATER

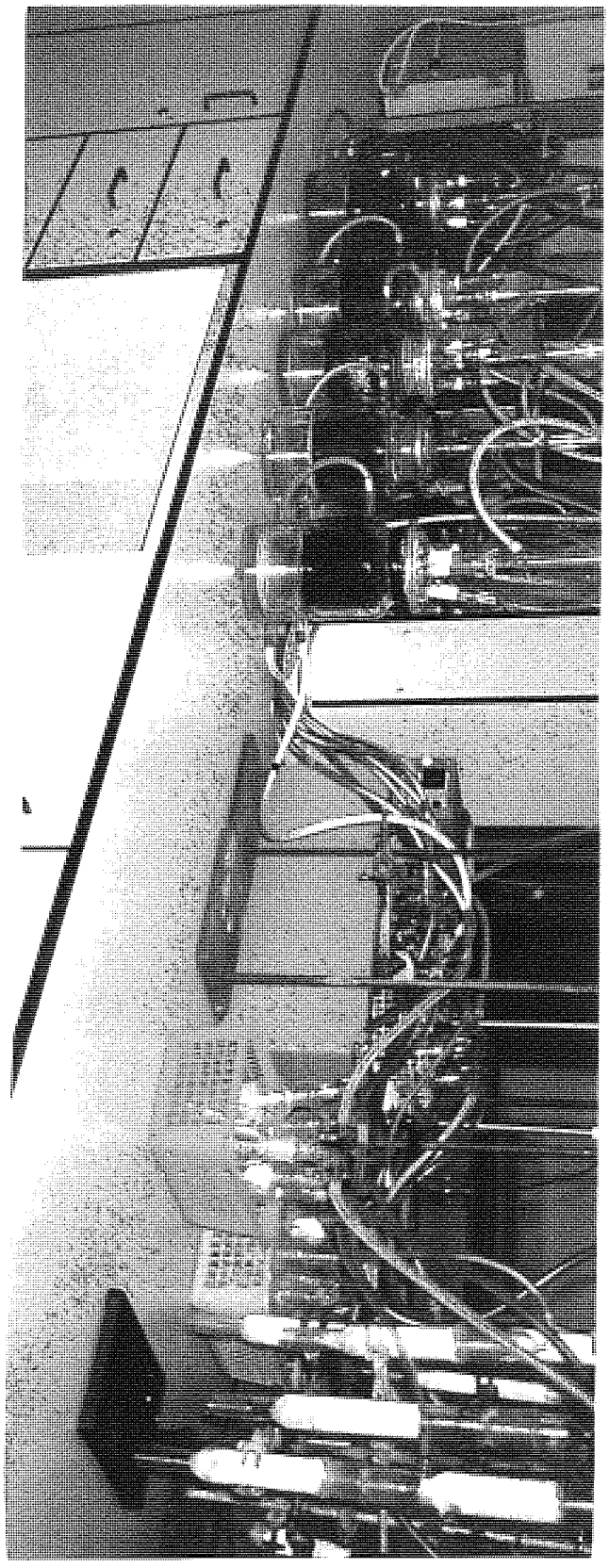

In order to verify the compost as an iso-standard compost (International Standard ISO/FDIS 14855, 1999) and hence use it in the biodegradation analysis, the 6 month old, late stage mesophilic compost had to pass a 10 day incubation test. This involved manipulation of the compost in terms of heat production and moisture content until the compost mimicked a thermophilic stage compost. For this initial 10 day incubation period test, exactly 600grams of M602 compost was added to each of the six reaction vessels (Labelled D, on Figure 18, page 78). From each vessel a small quantity (~20grams) of compost was removed for the analysis of moisture, total nitrogen, carbon and pH. The reaction vessels were then hermetically sealed and maintained at the optimum composting temperature (58°C ± 2), using a thermal water jacket. Carbon dioxide free humidified air, generated by drawing air through soda lime, barium hydroxide and distilled water, was passed continuously through the system at 100ml *per* minute. The percentage carbon dioxide in the exhausted air was determined twice daily using an infrared detector (TQ Environmental plc, UK), and the average amount of carbon dioxide (grams) evolved *per* day calculated. The vessels were opened and stirred every two days to maintain aerobic conditions. The mean mass of volatile solids in the anhydrous compost over the 10 days was computed and from the rate of carbon dioxide produced, the activity of the M602 compost, in terms of CO_2 production *per* gram of volatile solids, was calculated using Equation 5, below.

EQUATION 5 – ACTIVITY OF SOIL IN TERMS OF CO_2 EVOLUTION AFTER AN INITIAL 10 DAY INCUBATION PERIOD - (MASS CO_2 EVOLVED (mg) *PER* GRAM VOLATILE SOLIDS)

$$\text{Mass of } CO_2 \text{ produced per day (g)} = \text{Mean IR reading} \times 2.634$$

$$\text{Total mass } CO_2 \text{ over 10 days (g)} = \text{Mass } CO_2 \text{ per day (g)} \times 10$$

Mean mass of volatile solids in 600 grams of compost (mg) =

$$600 \times \frac{\text{Total anhydrous material (\% of 600 g)} \times \text{Mean volatile solids (\% of 600 g))}}{100}$$

Mass of CO_2 evolved (mg) *per* gram of volatile solids =

$$\frac{\text{Total mass } CO_2 \text{ evolved in 10 days (g)}}{\text{Mean mass of volatile solids in 600grams of compost} \times 1000}$$

In order to qualify as an iso-standard compost (International Standard ISO/FDIS 14855, 1999) that could be legitimately used in the polymer biodegradation analysis the compost had to produce between 50mg and 150mg of carbon dioxide *per* gram of volatile solids, over the 10 day period. Production of too much carbon dioxide means that the compost must be stabilised by aeration for several days before being re-tested over another 10 day period. Too little carbon dioxide production would mean that the compost is not suitable, and a fresh sample of compost must be tested.

After the 10 day incubation period, exactly 50grams of polymer powder was added to five of the six reaction vessels (two with PHBHV-Diol, two with Cellulose and one with PHB). The remaining vessel containing compost alone gave a control background CO_2 reading. The contents of the vessels were mixed thoroughly to ensure the polymers were distributed evenly throughout the compost before being hermetically sealed again. The percentage carbon dioxide in the air emitted from the vessels was recorded twice each day for a period of 75 days. The vessels were aerated every couple of days and an analysis of the compost, in terms of pH, moisture content, total nitrogen content and carbon content was performed every week. The flow rate through each vessel was maintained at 100ml *per* minute and checked once a week. Distilled water (to humidify the air) and barium hydroxide (to remove carbon dioxide from the air) levels were checked daily and topped up as and when required. The mean net volume of carbon dioxide produced *per* day was used to calculate the total mass of carbon dioxide produced *per* day. From this the total cumulative theoretical mass of carbon dioxide produced from the biodegradation of the polymers occurring in each vessel was computed using the following equations, equation 6.1 for cellulose, equation 6.2 for PHB and equation 6.3 for PHBHV-Diol, below.

EQUATION 6.1 – CALCULATION OF THE TOTAL CUMULATIVE MASS OF CO_2 PRODUCED AS A RESULT OF CELLULOSE BIODEGRADATION

50grams of cellulose will produce 81.5grams CO_2, by complete biodegradation.

The amount of CO_2 produced per day = 2.64* × Mean daily IR reading

$$\% \text{ Total theoretical mass of } CO_2 = \frac{(2.64 \times \text{Mean daily IR reading})}{81.5} \times 100$$

$$= 3.24 \times \text{Mean daily IR reading}$$

* For calculation of 2.64, see Appendix Section 1.2, page 266.

EQUATION 6.2 – CALCULATION OF THE TOTAL CUMULATIVE MASS OF CO_2 PRODUCED AS A RESULT OF PHB BIODEGRADATION

50grams of PHB will produce 102.33grams CO_2, by complete biodegradation.

$$\% \text{ Total theoretical mass } CO_2 = \frac{(2.64 \times \text{Mean daily IR reading})}{102.33} \times 100$$

$$= 2.58 \times \text{Mean daily IR reading}$$

EQUATION 6.3 – CALCULATION OF THE TOTAL CUMULATIVE MASS OF CO_2 PRODUCED AS A RESULT OF PHBHV-DIOL BIODEGRADATION

50grams of PHBHV-Diol will produce 105.56grams CO_2, by complete biodegradation.

$$\% \text{ Total theoretical mass } CO_2 = \frac{(2.64 \times \text{Mean daily IR reading})}{105.56} \times 100$$

$$= 2.5 \times \text{Mean daily IR reading}$$

2.2.30 DETERMINATION OF THE MOISTURE CONTENT OF THE GREEN GARDEN WASTE COMPOST

A small pre-weighed crucible was filled with a sample of compost from each of the six reaction vessels. This was immediately re-weighed and the combined weight recorded. The weight of the compost was found by the difference. The crucible containing the compost was then placed in an oven, pre-heated to 110°C and left for 24hours. After this time the crucible and compost was re-weighed, stirred and replaced in the oven for a further 24hours. This process was repeated until a constant weight was obtained.
The moisture content of the compost was calculated using equation 7, below.

EQUATION 7 – PERCENTAGE MOISTURE CONTENT OF THE COMPOST

Initial weight of compost (g) - Dry weight of compost (g)

= Xgrams (weight of moisture)

Percentage moisture content of compost =

$$\frac{\text{Xgrams}}{\text{Initial weight of compost (g)}} \times 100$$

2.2.31 DETERMINATION OF THE VOLATILE SOILDS CONTENT OF THE COMPOST

The pre-weighed, just dried compost from Section 2.2.29, page 78 and crucible were placed in a pre-heated oven at 560°C for 24hours. The incinerated sample was then re-weighed, stirred and re-heated for a further 24hours. The process was repeated until a constant weight was obtained.
The weight loss represented the loss of organic, volatile material. The percentage volatile solids content of the compost was determined using equation 8, below.

EQUATION 8 – THE PERCENTAGE VOLATILE SOLIDS CONTENT OF THE COMPOST

Initial weight of dry compost (g) – Weight of incinerated compost (g)

= Xgrams (weight of volatile solids)

Percentage volatile solids content of compost =

$$\frac{\text{Xgrams}}{\text{Weight of incinerated compost (g)}} \times 100$$

2.2.32 DETERMINATION OF THE COMPOST pH

Around 1gram of compost was placed in a conical flask with 25ml of distilled water. This was mixed vigorously for 5 minutes before the pH was measured using a pre-calibrated pH probe (Gallenkamp, Germany). All pH measurements were carried out in triplicate.

2.2.33 DETERMINATION OF THE TOTAL NITROGEN CONTENT OF THE COMPOST USING THE MICRO-KJELDAHL METHOD (Kjeldahl, 1883)

The determination of nitrogen content of compost by the standard Kjeldahl method provides a measure of the total nitrogen. Digestion of the compost with concentrated sulphuric acid removes carbon as carbon dioxide and converts organic nitrogen to ammonia; the presence of a selenium catalyst speeds up the conversion of organic nitrogen to ammonia. Markham Still steam distillation with excess of strong alkali

then releases the ammonia, which is trapped in boric acid and determined by titration with hydrochloric acid. The amount of ammonia so determined is a direct measure of the total nitrogen in the compost.

Exactly 0.5gram of compost was placed into a micro-Kjeldahl flask, to which was added 5ml of concentrated sulphuric acid. The contents of the flask were digested gently at first until the initial frothing had subsided, and then more vigorously for 3hours. A quarter of a Kjeldahl selenium tablet (150mg catalyst) was then added, and the flask heated for a further 3hours until the liquid turned straw coloured. The flask was removed from the rack and the contents allowed to cool to room temperature before being transferred quantitatively into a 25ml volumetric flask. The digestion flask was carefully rinsed out with several small volumes of water, which were also added to the volumetric flask and the contents mixed well.

A Markham microstill was set up and the apparatus thoroughly steamed out before use. A 5ml sample of digest was placed into the filler cup, to which was added a drop of indicator (0.1% bromcresol green with 0.01-0.02% methyl red in 95% alcohol). This was washed into the still with a few ml of tap water. The stopper was replaced, and 5ml of 40% NaOH added to the cup. The clip on the drain tube was then closed. A conical flask containing 10ml of saturated boric acid was placed under the outlet of the condenser, with a few drops of indicator, to cover the tip. The stopper was lifted slightly to let the NaOH run into the digest – a small amount of NaOH was left in the cup to act as a seal, and stop gas escaping. The contents of the still were distilled for 2 minutes. Distillation was continued for a further 2 minutes until a maximum of 10ml of distillate had been collected. The still was washed out by placing a beaker under the condenser and pinching the steam feed tube so the contents of the still were sucked back into the outer jacket. Distilled water was added through the filler cup and the steam feed tube pinched again to wash the still out. The drain clip was opened to allow the waste to run out.

The contents of the conical flask containing the ammonia absorbed by the boric acid was the titrated against 0.01M hydrochloric acid. The total nitrogen content of the compost was calculated using equation 9, below.

EQUATION 9 – TOTAL NITROGEN CONTENT OF THE COMPOST

1000ml of 0.01M HCl = 0.14gram nitrogen,

however, only W ml of 0.01M HCl was added

$$\therefore \quad \frac{1000}{W} = X$$

Taking into account the Dilution Factor

$$\frac{X}{5} \times 25\text{ml} = Y$$

$$\frac{0.14}{Y} = \mathbf{Z\ grams\ of\ nitrogen\ in\ 0.5\ grams\ of\ soil.}$$

2.2.34 STATISTICAL ANALSYIS

Data presented in this thesis are represented by the mean value ± standard error of the mean, SEM. Where relevant, mean value ± SEM were compared with each other statistically using either Student's unpaired two-tailed t-test at 95% confidence limits, or one-way analysis of variance (ANOVA), using GraphPad Instat® for the PC.

CHAPTER 3

EVALUATION OF MICROSPHERE AND NANOSPHERE FABRICATION TECHNIQUES

3.1 INTRODUCTION

The aim of this preliminary work was to establish and characterise techniques available for the fabrication of microspheres and nanospheres in the sub 1 μm range, using the commercially available polymer polyhydroxybutyrate hydroxyvalerate (PHB-HV), 83 000 Daltons, containing 12.6% HV, also known as BIOPOL®. The most promising technique, in terms of generating monodispersed nanospheres with small uniform diameters, would be used to fabricate nanospheres from a range of novel polyesters supplied by Monsanto and the Speciality Materials Group of Aston University.

As part of the CASE (Co-operative Awards in Science and Engineering) collaboration, Monsanto made 5 novel polymers available. Some of the polymers were only generated in small quantities, and so it was decided to investigate the parameters affecting nanosphere fabrication using the low molecular weight polymer, PHBHV-Diol (1500 Daltons), and for comparison, the high molecular weight polymer, 3HB 3HC (172 000 Daltons). There is evidence to suggest that low molecular weight polymers produce the smallest microspheres and that high molecular weight polymers, due to their tendency to be less soluble in organic solvent, produce larger microspheres (Jalil and Nixon, 1990). Microspheres and nanospheres were fabricated using oil-in-oil single emulsification, oil-in-water single emulsification, water-in-oil-in-water double emulsification and water-in-oil-in-water double sonication methods.

3.2 RESULTS

3.2.1 FABRICATION OF UNLOADED PHB-HV MICROSPHERES USING THE O/O SINGLE EMULSIFICATION WITH SOLVENT EVAPORATION METHOD

The first fabrication method employed was the O/O single emulsion technique, detailed in Section 2.2.1, page 52 and used to generate unloaded microspheres of polyhydroxybutyrate-hydroxyvalerate polymer, (PHB-HV), 83 000 Daltons, containing 12.6% HV. This technique was already well established in our laboratory for the production of PLGA 75:25 microspheres. Figure 21, below, shows a scanning electron micrograph of a PHB-HV microsphere fabricated using the O/O single emulsion technique. The polymer chains in the microsphere walls appeared to be loosely bound, which gave rise to the heavily structured, macroporous and rugose surfaces characteristic of PHB-HV microspheres (Embleton and Tighe, 1992).

FIGURE 21 - SCANNING ELECTRON MICROGRAPH OF A PHB-HV MICROSPHERE FABRICATED USING THE O/O SINGLE EMULSION TECHNIQUE

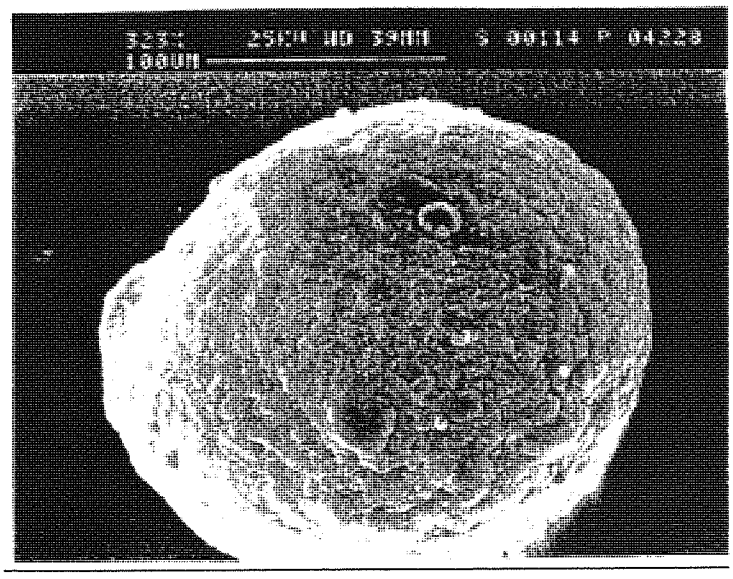

The microspheres generated were relatively large with a mean particle diameter of some 206 μm ± 51 (mean value ± SEM, n=3). The technique resulted in a very high mean microsphere yield of 88.17% ± 2.23 (mean value ± SEM, n=3) and some polymer debris.

In order to reduce the amount of polymer debris (non-patent microspheres) generated, an alternative O/O method using acetronitrile as the solvent was investigated (Tsai *et al*, 1986; Jalil and Nixon, 1990). Here the PHB-HV was dissolved in a minimum of DCM and then made up to volume with acetronitrile. This variation of the method resulted in the production of large heterogeneous microspheres, with a much narrower particle size distribution, all in the region of 100 μm (117 μm ± 14, [mean value ± SEM, n=3]) and with no polymer debris. The mean microsphere yield remained high at 91.86 %± 1.17 (mean value ± SEM, n=3).

3.2.2 EFFECT OF INCREASING THE EMULSIFICATION SPEED IN THE O/O METHOD

Ogawa *et al* (1988) and Jeffery *et al* (1993) have reported that when using poly(d,l- lactide-co-glycolide), PLGA in the O/O method, microsphere particle diameter decreases exponentially with increasing emulsification speed. This is also accompanied by a narrowing of the microsphere size distribution. Recent work by Sah *et al* (1995), found that a change in shear rate (emulsification speed) did not result in a reduction in microsphere particle diameter, but did greatly influence the internal matrix structure of the microspheres, with increasing shear rate producing an increase in the number of cavities with a small internal diameter.

In the present work, increasing the emulsification speed from 4000 rpm to 8000 rpm reduced the mean particle diameter of the resulting microspheres from 117 ± 14 μm (mean value ± SEM, n=3) to 61 ± 15 μm (mean value ± SEM, n=3). The percentage yield remained high at 91.33% ± 4 (mean value ± SEM, n=3) using the increased emulsification speed. Figure 22 below shows a scanning electron micrograph of microspheres fabricated using the increased emulsification speed in the O/O single emulsion technique. The microspheres obtained when using the increased emulsification speed still retained their rugose surface and macroporosity, characteristic of PHB-HV microspheres.

FIGURE 22 - SCANNING ELECTRON MICROGRAPH OF PHB-HV MICROSPHERES FABRICATED USING THE INCREASED EMULSIFICATION SPEED (8000 rpm) IN THE O/O SINGLE EMULSION TECHNIQUE

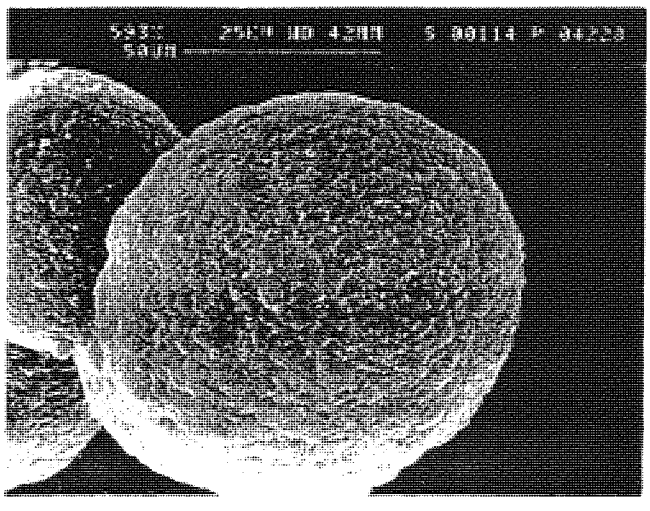

3.2.3 FABRICATION OF UNLOADED PHB-HV MICROSPHERES USING THE O/W SINGLE EMULSION WITH SOLVENT EVAPORATION METHOD

Due to the relatively large diameter (61 ± 15 μm [mean value ± SEM, n=3]) of the microspheres fabricated when using the O/O single emulsion technique an O/W single emulsion technique (Beck *et al*, 1979), as detailed in Section 2.2.2, page 53, was evaluated. The O/W method had the potential to produce microspheres with a much smaller diameter (sub 1 μm) than the O/O method (Jalil and Nixon, 1990). Figure 23 shows a scanning electron micrograph of microspheres produced by the O/W technique with a mean diameter ~3 μm. Because of their small size microspheres could not be separated discretely on the scanning electron microscope stubs and tended to appear as clusters. The limited resolution of the scanning electron microscope did not permit close examination of the surface topography of the microspheres.

FIGURE 23 - PHB-HV MICROSPHERES FABRICATED USING THE O/W SINGLE EMULSION WITH SOLVENT EVAPORATION METHOD

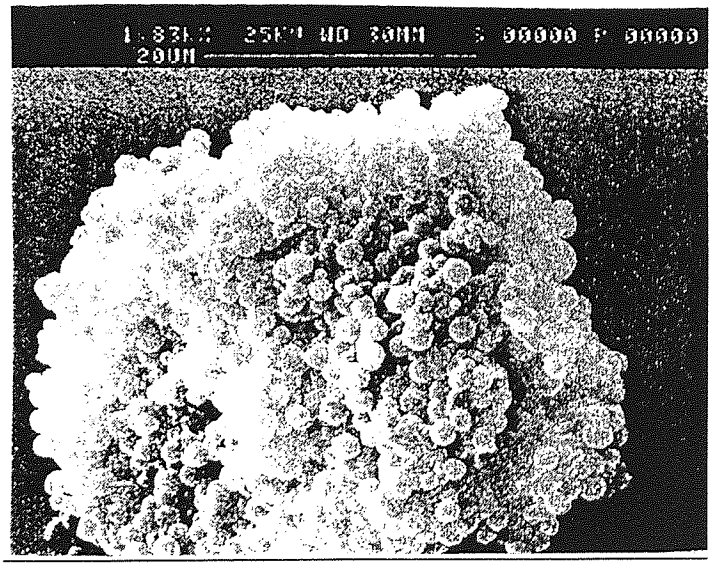

In the O/W method, whilst there was evidence to suggest that increasing the emulsification speed from 4000 rpm to 8000 rpm did result in a reduction in the mean diameter of the microspheres, there was some suspicion that the mean particle diameters obtained using the Malvern Mastersizer® were values for aggregates of microspheres rather than separated individual microspheres. The best estimate of particle diameter was probably that obtained from the scanning electron micrographs.

TABLE 7 – MALVERN MASTERSIZER® MEAN PARTICLE DIAMETER OF PHB-HV MICROSPHERES FABRICATED USING THE O/W SINGLE EMULSIFICATION METHOD WITH SOLVENT EVAPORATION AT EMULSIFICATION SPEEDS OF 4000 AND 8000 rpm (mean value ± SEM, n=3)

POLYMER	SPEED (rpm)	MEAN PARTICLE DIAMETER (μm)
PHB-HV	4000	34.87 ± 17.6
PHV-HV	8000	2.39 ± 0.89

3.2.4 FABRICATION OF UNLOADED PHB-HV MICROSPHERES USING THE W/O/W DOUBLE EMULSIFICATION WITH SOLVENT EVAPORATION METHOD

Preliminary studies also involved evaluation of the W/O/W double emulsification with solvent evaporation method for the fabrication of unloaded PHB-HV microspheres (Ogawa *et al,* 1988), as described in Section 2.2.3, page 54. This technique was reported to be particularly good for the encapsulation of drugs that are sensitive to organic solvents and have high aqueous solubility.

Preliminary work confirmed that spherical microspheres and nanospheres could be generated using this technique, but the resolution of the scanning electron microscope was not sufficient to resolve the surface topography of single nanospheres adequately. As a result the sizing of the microspheres and nanospheres could only be achieved using a Malvern MasterSizer E®, which gave mean particle diameters of 0.44 ± 0.1 μm (mean value ± SEM, n=3) after freeze-drying.

The small particle diameters obtained for nanospheres fabricated using the W/O/W double emulsification method with solvent evaporation was very attractive, and it was initially decided that this fabrication technique should be employed for the fabrication of nanospheres.

3.2.5 FABRICATION OF UNLOADED NANOSPHERES USING THE F68 DOUBLE SONICATION SOLVENT EVAPORATION METHOD

A variation on the W/O/W double emulsification method was evaluated in which sonication was used to create both the primary and secondary emulsions, instead of homogenisation, and the synperonic surfactant F68 was used as a stabiliser in the primary emulsion, instead of methylcellulose and PVA. The F68 double sonication solvent evaporation method was already well established in the drug delivery research laboratories at Aston University for the generation of sub 200nm PLGA nanospheres, and so it

was decided to evaluate the potential of this technique to generate nanospheres using PHBHV-Diol, 3HB 3HC and Triblock polymers. This method is detailed in Section 2.2.4, page 56 and the results of preliminary studies using the F68 double sonication solvent evaporation method have been summarised in Table 8, below.

TABLE 8 - MEAN PARTICLE DIAMETER AND MEAN ZETA POTENTIAL OF UNLOADED PHBHV-DIOL, 3HB 3HC AND TRIBLOCK POLYMER NANOSPHERES FABRICATED USING THE F68 DOUBLE SONICATION SOLVENT EVAPORATION METHOD (mean value ± SEM, n=3)

POLYMER	MEAN PARTICLE DIAMETER (nm)	MEAN ZETA POTENTIAL (mV)
PHBHV-DIOL	275.5 ± 2.1	-20.76 ± 0.38
3HB 3HC	396.51 ± 4.4	-10.97 ± 0.74
TRIBLOCK (PHBHV-DIOL-POLYCAPROLACTONE)	225.9 ± 1.6	-4.1 ± 0.08

The F68 double sonication solvent evaporation method produced nanospheres with the smallest diameter of any method previously investigated as shown in Table 8. The mean zeta potential of the unloaded PHBHV-Diol nanospheres at –20.76 ± 0.38 mV (mean value ± SEM, n=3), places them in the stability band known as the 'threshold of delicate dispersion' (Riddick, 1968). This was the most negative zeta potential so far achieved in the present work and indicates that the nanospheres are stable in suspension.

Although the mean particle diameter of the unloaded Triblock polymer nanospheres is very small at 225.9 nm ± 1.6 (mean value ± SEM, n=3), the mean zeta potential is considerably more positive at –4.1 ± 0.08 mV (mean value ± SEM, n=3) than that of the unloaded nanospheres fabricated from the Monsanto polymers, indicating that the nanospheres are less stable in suspension.

3.3 DISCUSSION

Preliminary evaluation of fabrication techniques has confirmed that O/W, O/O and W/O/W emulsification techniques are all capable of creating a range of microspheres and nanospheres from the commercially available copolymer PHB-HV. The acetronitrile O/O method created microspheres with the largest diameter at 117 μm ± 14 (mean value ± SEM, n=3), while the original W/O/W emulsification technique using PHB-HV created nanospheres with the smallest diameter at 440 nm ± 0.1 (mean value ± SEM, n=3).

The mean particle diameter of PHB-HV microspheres generated using both the O/W and the O/O single emulsification techniques could be decreased significantly by increasing the shear rate (emulsification speed). This observation is consistent with work carried out by Ogawa *et al* (1988), Jalil and Nixon (1990a, 1990b), Conti *et al* (1995), Benita *et al*, (1984) and Watts *et al* (1990), but not with that of Sah *et al* (1995), who found that an increase in shear rate did not result in a reduction in microsphere particle diameter, but instead produced an increase in the number of cavities, with smaller internal diameter. The relationship between the mean particle diameter of the product and the speed of emulsification is believed to be dependent upon the size of droplets produced during the emulsification process (Arshady, 1991; Julienne *et al*, 1992). Although an increase in emulsification speed has been demonstrated to cause a decrease in the mean particle diameter of the resultant microspheres, there are many other manoeuvres which can be used to reduce the mean particle diameter. These include increasing the concentration of surfactant in the oil phase (Jalil and Nixon, 1990a; Scholes *et al*, 1993; Conti *et al*, 1995); decreasing the concentration of polymer in the organic phase (Watts *et al*, 1990; Julienne *et al*, 1992; Scholes *et al*, 1993; Pavanetto *et al*, 1993); decreasing the loading of the microsphere matrix (Jalil and Nixon, 1990b) and finally, brief sonication of the microspheres either during or following the emulsification process (Jalil and Nixon, 1989; Scholes *et al*, 1993; Park, 1994).

One of the aims of the present work was to generate small nanospheres for commercial application of interest to Monsanto. For this basis, attention was turned to the evaluation of the F68 double sonication solvent evaporation method. This technique generated very small nanospheres with a mean diameter using PHBHV-Diol of 275.5 nm ± 2.1 (mean value ± SEM, n=3) and of 396.51 nm ± 4.4 (mean value ± SEM, n=3) using 3HB 3HC. The novel in-house Triblock polymer supplied by the Speciality Materials Group of Aston University was used to fabricate nanospheres with a mean diameter of 225.9 nm ± 1.6 (mean value ± SEM, n=3).

The zeta potential of the PHBHV-Diol nanospheres created using the F68 double sonication solvent evaporation method was also the most negative at –20.76 mV ± 0.38 (mean value ± SEM, n=3) suggesting that the nanospheres would be stable in suspension and less likely to aggregate. The presence of polycaprolactone in the Triblock polymer influenced the zeta potential. The zeta potential of nanospheres generated with the Triblock polymer was considerably more positive at –4.1 ± 0.08 mV

(mean value ± SEM, n=3) than that of nanospheres generated using either PHBHV-Diol at –20.76 ± 0.38 mV (mean value ± SEM, n=3) or 3HB 3HC polymers at –10.97 ± 0.74 (mean value ± SEM, n=3), placing the nanospheres in the stability band known as the 'Range of strong aggregation and precipitation' (Riddick, 1968). Since only very small quantities of the Triblock polymer were available it was not possible to use the polymer in any further work.

The high molecular weight Monsanto polymer, 3HB 3HC (172 kD), produced significantly larger nanospheres than the low molecular weight Monsanto polymer, PHBHV-Diol (1500 Daltons). This observation was consistent with work by Jalil and Nixon, 1990, who suggested that the higher the molecular weight of the fabrication polymer, the larger is the mean particle diameter of the resulting microspheres / nanospheres because of the reduced polymer solubility and dramatically increased viscosity.

The results of this preliminary work confirm that the most promising method for the fabrication of small diameter nanospheres with highly negative zeta potentials was the F68 double sonication solvent evaporation method. This method met the criteria to generate the smallest nanospheres possible and was used throughout the remainder of the work, to create both unloaded nanospheres and nanospheres loaded with actives of interest to Monsanto.

CHAPTER 4

THE INCORPORATION INTO AND RELEASE OF BSA FROM NANOSPHERES FABRICATED FROM NOVEL MONSANTO POLYALKANOATES

4.1 INTRODUCTION

The present work is based upon the nanoencapsulation and release of the surrogate protein Bovine Serum Albumin (BSA) from polymeric nanospheres fabricated with three novel polymers supplied by Monsanto, these being PHBHV-Diol, 3HB 3HC and Diblock. The use of these novel Monsanto polyesters in the fabrication of BSA loaded nanospheres provides the opportunity to establish the conditions required for the optimum loading of active materials of pharmaceutical and agricultural interest. Preliminary studies with these polymers confirmed that loaded nanospheres could be fabricated using the double sonication solvent evaporation method described in Section 2.2.4, page 56. As a consequence, this method has been employed to fabricate unloaded and BSA loaded nanospheres composed of PHBHV-Diol, 3HB 3HC and Diblock polymers. The nanoencapsulation of BSA, and its subsequent release into Hanks Balance Salts Solution, pH 7.4, at 37°C over time, was carried out to provide information on the potential of the nanosphere system for oral and parenteral delivery of pharmaceutical actives. Nanospheres offer the advantage of an extended *in vivo* half life for peptides by providing protection against extremes of pH and enzymatic degradation in the gastro-intestinal tract, and they demonstrate excellent adjuvant properties for the extended release of protein antigens (Eldridge *et al*, 1990).

BSA was used as a surrogate protein because it has well characterised stability, solubility, flexibility and charge (Peter, 1975), as well as being low cost and easily obtainable. Detection of BSA is also rapid and can be carried out using several well characterised methods including the BCA assay as detailed in Section 2.2.15, page 71. Bovine serum albumin has a molecular weight of ~66 000 Daltons, and consists of 581 amino acid residues. Although considerably larger than the Monsanto actives, albumin is characterised as being a relatively small protein, but possess good solubility and can be obtained in a range of particle sizes. In many emulsification techniques BSA interacts with the organic polymer phase to form a semi-solid interfacial film, stabilising the emulsion (Nihant *et al*, 1994), hence results using BSA cannot be directly extrapolated to other proteins with different physico-chemical properties. However, formulation studies involving the loading of BSA into microspheres and nanospheres are still useful because they provide information on potential loadings, diameters and charge characteristics.
Table 9, below, shows the basic chemical information of the BSA used in these nanoencapsulation experiments.

TABLE 9 - BASIC CHEMICAL INFORMATION ABOUT BSA FRACTION V USED IN THESE NANOENCAPSULATION EXPERIMENTS

DESCRIPTION	CHARACTERISTIC
CHEMICAL NAME	BOVINE SERUM ALBUMIN, FRACTION V
THESIS NAME	BSA
MOLECULAR WEIGHT	66 000 DALTONS
APPEARANCE	CREAM COLOURED, CRYSTALLINE POWDER

4.2 RESULTS

4.2.1 MEAN PERCENTAGE YIELD OF UNLOADED AND THEORETICAL 10%, 20%, 30% AND 40% w/w BSA LOADED PHBHV-DIOL, 3HB 3HC AND DIBLOCK NANOSPHERES

Unloaded nanospheres and nanospheres theoretically loaded with either 10%, 20%, 30%, or 40% w/w BSA were routinely fabricated from PHBHV-Diol, 3HB 3HC and Diblock polymers using the method described in Section 2.2.14, page 71. The mean total weight of nanospheres (mg) produced during fabrication was computed and can be seen in Appendix Section 2.1, page 266. The mean percentage yield of nanospheres was computed from the mean total weight of nanospheres and the results are summarised in Table 10, below.

TABLE 10 – THE EFFECT OF THEORETICAL PERCENTAGE BSA LOADING AND FABRICATION POLYMER ON THE MEAN PERCENTAGE YIELD OF NANOSPHERES

(mean values ± SEM, n=12)

THEORETICAL % LOADING	POLYMER	MEAN % YIELD
0	PHBHV-DIOL	71.76 ± 0.83
10	PHBHV-DIOL	61.3 ± 0.35[a]
20	PHBHV-DIOL	60.4 ± 1.3[a]
30	PHBHV-DIOL	59.5 ± 1.8[a]
40	PHBHV-DIOL	61.6 ± 1.4[a]
0	3HB 3HC	68.96 ± 2.2
10	3HB 3HC	68.9 ± 0.58
20	3HB 3HC	68.9 ± 1.9
30	3HB 3HC	68.27 ± 0.35
40	3HB 3HC	67.87 ± 0.87
0	DIBLOCK	66.17 ± 1.4
10	DIBLOCK	62.11 ± 2.19
20	DIBLOCK	64 ± 3.5
30	DIBLOCK	51.92 ± 1.04[b]
40	DIBLOCK	41.47 ± 1.8[b]

a, significantly reduced ($P<0.05$) compared with the mean percentage yield of unloaded nanospheres fabricated using PHBHV-Diol.

b, significantly reduced ($P<0.05$) compared with the mean percentage yield of unloaded nanospheres fabricated using Diblock polymer.

Loading PHBHV-Diol nanospheres with a theoretical percentage BSA loading of 10% w/w to 40% w/w significantly reduced the mean percentage yield of PHBHV-Diol nanospheres compared with unloaded PHBHV-Diol nanospheres.

On the other hand BSA loading had no significant effect on the mean percentage yield of 3HB 3HC nanospheres, Table 10.

Increasing the theoretical percentage BSA loading to 30% w/w and 40% w/w significantly reduced the mean percentage yield of Diblock nanospheres.

4.2.2 DETERMINATION OF THE MEAN PARTICLE DIAMETER OF UNLOADED AND THEORETICAL 10%, 20%, 30% AND 40% w/w BSA LOADED PHBHV-DIOL, 3HB 3HC AND DIBLOCK NANOSPHERES, PRIOR TO USE IN RELEASE STUDIES

Particle diameter analysis, performed using Photon Correlation Spectroscopy, was carried out on all unloaded and BSA loaded nanospheres preparations as described in Section 2.2.7, page 58. The results of the particle diameter analysis have been summarised in Table 11, below.

TABLE 11 – THE EFFECT OF THEORETICAL PERCENTAGE LOADING AND FABRICATION POLYMER ON THE MEAN PARTICLE DIAMETER OF NANOSPHERES

(mean values ± SEM, n=12)

THEORETICAL % LOADING	POLYMER	MEAN DIAMETER (nm)
0	PHBHV-DIOL	275.6 ± 1.79
10	PHBHV-DIOL	295 ± 13.73
20	PHBHV-DIOL	328.8 ± 5.4
30	PHBHV-DIOL	384.7 ± 19
40	PHBHV-DIOL	557.4 ± 19.49[a]
0	3HB 3HC	396.51 ± 4.4
10	3HB 3HC	504.2 ± 21.46
20	3HB 3HC	561.6 ± 22.19
30	3HB 3HC	615.2 ± 13.7
40	3HB 3HC	703 ± 16.8[a]
0	DIBLOCK	328 ± 7.57
10	DIBLOCK	361 ± 8.33
20	DIBLOCK	401.67 ± 8.1
30	DIBLOCK	432.3 ± 15.41
40	DIBLOCK	464.3 ± 17.46[a]

a, significantly increased ($P<0.05$) compared with unloaded nanospheres fabricated from the same polymer.

Particle diameter analysis demonstrated that there was positive correlation between the theoretical percentage BSA loading and the mean diameter of nanospheres fabricated from PHBHV-Diol, 3HB 3HC and Diblock polymers. The mean particle diameter of BSA loaded nanospheres was significantly increased, irrespective of the theoretical percentage loading, compared with the mean particle diameter of unloaded nanospheres. Of the three fabrication polymers, 40% theoretical BSA loaded PHBHV-Diol nanospheres showed the highest percentage increase in mean particle diameter of ~89% for PHBHV-Diol, ~39% for 3HB 3HC and ~29% for Diblock nanospheres, respectively.

4.2.3 SCANNING ELECTRON MICROSCOPY OF THEORETICAL 10%, 20%, 30% AND 40% w/w BSA LOADED PHBHV-DIOL, 3HB 3HC AND DIBLOCK NANOSPHERES, PRIOR TO USE IN RELEASE STUDIES

Scanning electron microscopy of BSA loaded nanospheres was carried out using the method described in Section 2.2.6, page 57. The photograph obtained is shown in Figure 24, below.

FIGURE 24 – SCANNING ELECTRON MICROGRAPH OF THEORETICAL 10% w/w BSA LOADED DIBLOCK NANOSPHERES

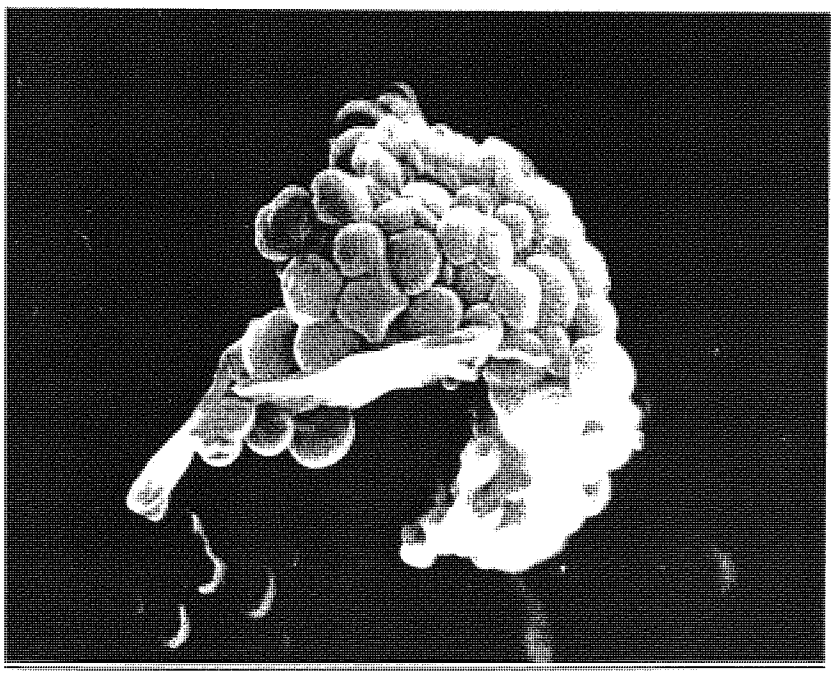

The scanning electron micrograph shows a tight clump of BSA loaded Diblock nanospheres. Print Magnification = 23K (2.4cm = 1μm)

4.2.4 ZETA POTENTIAL MEASUREMENTS OF UNLOADED AND THEORETICAL 10%, 20%, 30% AND 40% w/w BSA LOADED PHBHV-DIOL, 3HB 3HC AND DIBLOCK POLYMER NANOSPHERES, PRIOR TO USE IN RELEASE STUDIES

These studies were carried out to investigate the effects of type of fabrication polymer and theoretical percentage BSA loading on the zeta potential of nanospheres. Zeta potential measurements on all BSA loaded nanosphere preparations was routinely carried out using a Malvern Zeta Master® according to Section 2.2.8, page 59. The results are summarised in Table 12, below.

TABLE 12 - MEAN ZETA POTENTIALS OF UNLOADED AND THEORETICAL 10%, 20%, 30% AND 40% w/w BSA LOADED PHBHV-DIOL, 3HB 3HC AND DIBLOCK POLYMER NANOSPHERES, PRIOR TO USE IN RELEASE STUDIES (mean values ± SEM, n=12)

THEORETICAL % LOADING	POLYMER	MEAN ZETA POTENTIAL (mV)
0	PHBHV-DIOL	-20.97 ± 0.38
10	PHBHV-DIOL	-4.4 ± 0.22[a]
20	PHBHV-DIOL	-5.48 ± 0.57
30	PHBHV-DIOL	-6.15 ± 0.45
40	PHBHV-DIOL	-6.5 ± 0.61
0	3HB 3HC	-10.97 ± 0.74
10	3HB 3HC	-4.23 ± 0.06[a]
20	3HB 3HC	-4.95 ± 0.17
30	3HB 3HC	-6.23 ± 0.045
40	3HB 3HC	-6.8 ± 0.54
0	DIBLOCK	-35.99 ± 0.67[b]
10	DIBLOCK	-15 ± 0.48[a]
20	DIBLOCK	-14.3 ± 0.4
30	DIBLOCK	-14.8 ± 0.42
40	DIBLOCK	-14.39 ± 0.42

a, significantly reduced ($P<0.05$) compared with unloaded nanospheres fabricated from the same polymer.

b, significantly elevated ($P<0.05$) compared with unloaded nanospheres fabricated from PHBHV-Diol and 3HB 3HC.

Unloaded nanospheres fabricated from Diblock polymer had the most negative mean zeta potentials, followed by unloaded PHBHV-Diol nanospheres, with unloaded 3HB 3HC nanospheres showing the least mean zeta potential, Table 12. In all cases loading nanospheres with BSA significantly reduced ($P<0.05$) the mean zeta potential. Loading PHBHV-Diol nanospheres with BSA produced the greatest percentage (~73%) reduction in the mean zeta potential, Table 12. Theoretical loading of both PHBHV-Diol and 3HB 3HC nanospheres with 10% BSA produced the greatest reduction in mean zeta potential. However, in both cases the mean zeta potential began to recover as the theoretical percentage BSA loading was increased from 10% w/w to 40% w/w, Table 12.

4.2.5 DETERMINATION OF THE WEIGHT AVERAGE MOLECULAR MASS (Mw) OF UNLOADED AND THEORETICAL 10%, 20%, 30% AND 40% w/w BSA LOADED PHBHV-DIOL, 3HB 3HC AND DIBLOCK NANOSPHERES, PRIOR TO USE IN RELEASE STUDIES

The weight average molecular mass was measured by Gel Permeation Chromatography using the method described in Section 2.2.9, page 62. The GPC system was calibrated with polystyrene and the results expressed as 'polystyrene equivalent' molecular masses. Since there could be considerable difference between the polystyrene equivalents and the actual molecular weights of the samples it was thought best to regard the results in a comparative manner, with emphasis being placed on any observed differences and trends between the sample values, and not simply on the numerical values of the results themselves. The results of GPC analysis of unloaded and BSA loaded nanospheres have been summarised in Table 13, overleaf.

The apparent molecular weight of unloaded nanospheres fabricated from PHBHV-Diol and Diblock polymers is significantly elevated compared to the molecular weight of virgin PHBHV-Diol and Diblock polymers. This may be due to interference from PVA or cross-linking leading to aggregation. The molecular weight of unloaded 3HB 3HC nanospheres is significantly reduced compared to the molecular weight of virgin 3HB 3HC polymer, Table 13. Gradually increasing the theoretical percentage BSA loading significantly increases the molecular weight of PHBHV-Diol and Diblock nanospheres, but significantly reduces the molecular weight of 3HB 3HC nanospheres, Table 13.

TABLE 13 - MEAN MOLECULAR WEIGHT OF VIRGIN POLYMER, UNLOADED PHBHV-DIOL, 3HB 3HC AND DIBLOCK AND THEORETICAL 10%, 20%, 30% AND 40% w/w BSA LOADED PHBHV-DIOL, 3HB 3HC AND DIBLOCK NANOSPHERES BY RAPRA PRIOR TO USE IN RELEASE STUDIES (mean values ± SEM, n=6)

THEORECTICAL % LOADING	POLYMER	MEAN MOLECULAR WEIGHT (Daltons)
VIRGIN	PHBHV-DIOL	2630 ± 28
0	PHBHV-DIOL	8138 ± 625[a]
10	PHBHV-DIOL	10, 798 ± 493[b]
20	PHBHV-DIOL	13, 475 ± 641[b]
30	PHBHV-DIOL	15, 275 ± 269[b]
40	PHBHV-DIOL	17, 300 ± 515[b]
VIRGIN	3HB 3HC	167, 500 ± 2121
0	3HB 3HC	119, 167 ± 307[c]
10	3HB 3HC	117, 667 ± 882[d]
20	3HB 3HC	114, 000 ± 732[d]
30	3HB 3HC	109, 333 ± 1202[d]
40	3HB 3HC	106, 233 ± 1876[d]
VIRGIN	DIBLOCK	37, 100 ± 707
0	DIBLOCK	58, 914 ± 1067[e]
10	DIBLOCK	61, 750 ± 2666[f]
20	DIBLOCK	65, 317 ± 1413[f]
30	DIBLOCK	77, 425 ± 3068[f]
40	DIBLOCK	83, 625 ± 309[f]

a, significantly elevated ($P<0.05$) compared with virgin PHBHV-Diol polymer.

b, significantly elevated ($P<0.05$) compared with unloaded PHBHV-Diol nanospheres.

c, significantly reduced ($P<0.05$) compared with virgin 3HB 3HC polymer.

d, significantly reduced ($P<0.05$) compared with unloaded 3HB 3HC nanospheres.

e, significantly elevated ($P<0.05$) compared with virgin Diblock polymer.

f, significantly elevated ($P<0.05$) compared with unloaded Diblock polymer.

4.2.6 DETERMINATION OF THE THERMAL CHARACTERISTICS OF VIRGIN POLYMERS, UNLOADED PHBHV-DIOL, 3HB 3HC AND DIBLOCK AND THEORETICAL 10%, 20%, 30% AND 40% w/w BSA LOADED PHBHV-DIOL, 3HB 3HC AND DIBLOCK NANOSPHERES, PRIOR TO USE IN RELEASE STUDIES

Thermal analysis of freshly fabricated unloaded and BSA loaded nanospheres fabricated from PHBHV-Diol, 3HB 3HC and Diblock polymers was performed by Differential Scanning Calorimetry using the method described in Section 2.2.10, page 64. The results of the DSC analysis have been summarised in Table 14.

The thermal characteristics of the virgin polymers have firstly been compared with the data obtained from unloaded nanospheres. This is performed to determine whether the nanosphere fabrication process has affected the thermal characteristics. Secondly, the thermal characteristics of the virgin polymers have been compared with BSA loaded nanospheres to see if loading with BSA at different theoretical percentage loadings affects the thermal characteristics of the nanospheres.

TABLE 14 - THE GLASS TRANSITION TEMPERATURE (Tg), RECRYSTALLISATION TEMPERATURE AND MELTING POINTS OF UNLOADED AND THEORETICAL 10%, 20%, 30% AND 40% w/w BSA LOADED PHBHV-DIOL, 3HB 3HC AND DIBLOCK NANOSPHERES PRIOR TO USE IN RELEASE STUDIES (mean values, n=2)

THEORETICAL % LOADING	POLYMER	Tg (°C)	RECRYSTALLISATION (°C)	MELTING POINT 1 (°C)	MELTING POINT 2 (°C)
VIRGIN	PHBHV-DIOL	-15	59	78	94
0	PHBHV-DIOL	-12	55	80	99
10	PHBHV-DIOL	-10	50	80	100
20	PHBHV-DIOL	-10	35	80	110
30	PHBHV-DIOL	-20	60	85	110
40	PHBHV-DIOL	-10	40	90	120
VIRGIN	3HB 3HC	4	72	112	128
0	3HB 3HC	27	68	118	124
10	3HB 3HC	35	70	120	125
20	3HB 3HC	10	80	122	130
30	3HB 3HC	25	85	125	140
40	3HB 3HC	5	88	131	144
VIRGIN	DIBLOCK	39	65	139	154
0	DIBLOCK	35	61	138	152
10	DIBLOCK	37	66	144	158
20	DIBLOCK	37	67	145	161
30	DIBLOCK	38	69	147	162
40	DIBLOCK	38	71	148	164

From Table 14 and analysis of the thermograms, it can be seen that there is no pattern between the glass transition temperature (Tg) and the theoretical percentage BSA loading or the recrystallisation temperature and the theoretical percentage BSA loading for PHBHV-diol nanospheres. This is also true for the glass transition temperature and the theoretical percentage of BSA loading in 3HB 3HC nanospheres. However, the recrystallisation temperature and two melting points for the BSA loaded 3HB 3HC nanospheres, and all the measured temperature points for BSA loaded Diblock nanospheres, do show positive correlation. All the temperatures increase as the theoretical percentage BSA loading increases. From Table 14 it can also be seen that PHBHV-Diol is the only fabrication polymer that has a Tg below 0°C. The reasons behind these findings are not known and further research would be needed in order to confirm trends and elaborate why these occur.

4.2.7 DETERMINATION OF THE MOISTURE CONTENT OF FREEZE-DRIED VIRGIN PHBHV-DIOL, 3HB 3HC AND DIBLOCK POLYMERS AND UNLOADED AND THEORETICAL 10%, 20%, 30% AND 40% w/w BSA LOADED PHBHV-DIOL, 3HB 3HC AND DIBLOCK NANOSPHERES

The moisture content of freeze-dried nanosphere preparations was determined using Thermogravimetric Analysis as described in Section 2.2.11, page 66. The results of the TGA can be seen in Table 15, below.

TABLE 15 - MOISTURE CONTENT OF FREEZE-DRIED VIRGIN PHBHV-DIOL, 3HB 3HC AND DIBLOCK POLYMERS AND UNLOADED AND THEORETICAL 10%, 20%, 30% AND 40% w/w BSA LOADED PHBHV-DIOL, 3HB 3HC AND DIBLOCK NANOSPHERES (mean values ± SEM, n=3)

THEORETICAL % LOADING	POLYMER	MEAN MOISTURE CONTENT (%)
VIRGIN	PHBHV-DIOL	0.28 ± 0.1
0	PHBHV-DIOL	0.26 ± 0.04
10	PHBHV-DIOL	0.35 ± 0.1
20	PHBHV-DIOL	0.51 ± 0.1
30	PHBHV-DIOL	0.55 ± 0.1
40	PHBHV-DIOL	0.38 ± 0.05
VIRGIN	3HB 3HC	0.4 ± 0.2
0	3HB 3HC	0.16 ± 0.05
10	3HB 3HC	0.42 ± 0.1
20	3HB 3HC	0.33 ± 0.8
30	3HB 3HC	0.57 ± 0.04
40	3HB 3HC	0.45 ± 0.04
VIRGIN	DIBLOCK	0.45 ± 0.1
0	DIBLOCK	0.42 ± 0.1
10	DIBLOCK	0.47 ± 0.1
20	DIBLOCK	0.43 ± 0.17
30	DIBLOCK	0.61 ± 0.13
40	DIBLOCK	0.37 ± 0.12

Moisture content analysis showed that there were no statistically significant differences between the moisture content of virgin polymers and unloaded nanospheres, or between unloaded nanospheres and BSA loaded nanospheres. The freeze-drying process employed effectively removed the majority of the moisture.

4.2.8 DETERMINATION OF THE RESIDUAL PVA CONTENT OF UNLOADED AND THEORETICAL 10%, 20%, 30% AND 40% w/w BSA LOADED PHBHV-DIOL, 3HB 3HC AND DIBLOCK NANOSPHERES, PRIOR TO USE IN RELEASE STUDIES

Determination of the residual PVA content of unloaded and BSA loaded nanospheres was carried out according to the method described in Section 2.2.12, page 67. The results are summarised in Table 16, overleaf.

TABLE 16 - MEAN PERCENTAGE RESIDUAL PVA OF UNLOADED AND THEORETICAL 10%, 20%, 30% AND 40% w/w BSA LOADED PHBHV-DIOL, 3HB 3HC AND DIBLOCK NANOSPHERES, PRIOR TO USE IN RELEASE STUDIES (mean values ± SEM, n=3)

THEORETICAL % BSA LOADING	POLYMER	RESIDUAL % PVA
0	PHBHV-DIOL	12.05 ± 0.68
10	PHBHV-DIOL	11.29 ± 0.44
20	PHBHV-DIOL	10.87 ± 0.47
30	PHBHV-DIOL	12.36 ± 0.27
40	PHBHV-DIOL	11.44 ± 0.23
0	3HB 3HC	14.85 ± 0.25
10	3HB 3HC	15.61 ± 0.49
20	3HB 3HC	12.87 ± 0.14
30	3HB 3HC	14.66 ± 0.74
40	3HB 3HC	12.81 ± 0.33
0	DIBLOCK	11.57 ± 0.09
10	DIBLOCK	16.89 ± 0.14
20	DIBLOCK	13.66 ± 0.53
30	DIBLOCK	12.55 ± 0.61
40	DIBLOCK	14.87 ± 0.81

The theoretical percentage BSA loading had no significant effect on the percentage of residual PVA in nanospheres, irrespective of the polymer used. This suggests that the presence of residual PVA was a function of the fabrication technique used and not of loading with BSA.

4.2.9 DETERMINATION OF RESIDUAL DICHLOROMETHANE IN UNLOADED AND THEORETICAL 10%, 20%, 30% AND 40% w/w BSA LOADED PHBHV-DIOL AND DIBLOCK NANOSPHERES

The concentration of residual DCM within freshly fabricated, freeze-dried unloaded and BSA loaded nanospheres was determined using gas liquid chromatography (GLC), Section 2.2.13, page 69. GLC analysis of the residual DCM in unloaded and BSA loaded 3HB 3HC nanospheres was not possible due to the limited availability of fabrication polymer. The residual solvent levels in unloaded and BSA loaded PHBHV-Diol and Diblock nanospheres have been summarised in Table 17, below.

TABLE 17 - RESIDUAL DCM IN UNLOADED AND THEORETICAL 10%, 20%, 30% AND 40% w/w BSA LOADED PHBHV-DIOL AND DIBLOCK NANOSPHERES (mean values ± SEM, n=3)

POLYMER	THEORETICAL % LOADING	RESIDUAL DCM (ppm)
PHBHV-DIOL	0	0
PHBHV-DIOL	10	10.36 ± 0.41^{a}
PHBHV-DIOL	20	10.42 ± 0.3^{a}
PHBHV-DIOL	30	10.66 ± 0.8^{a}
PHBHV-DIOL	40	10.74 ± 0.47^{a}
DIBLOCK	0	0
DIBLOCK	10	8.38 ± 1.48^{a}
DIBLOCK	20	9.15 ± 0.53^{a}
DIBLOCK	30	10.11 ± 1.14^{a}
DIBLOCK	40	10.48 ± 0.36^{a}

a, significantly increased ($P<0.05$) compared with unloaded nanospheres, irrespective of fabrication polymer.

Residual DCM was not detectable in either of the unloaded nanosphere samples fabricated using either PHBHV-Diol or Diblock polymers. However, irrespective of the fabrication polymer used, compared with unloaded nanospheres, BSA loading significantly increased the level of residual DCM. The concentration of DCM marginally increased, but not significantly, with increasing theoretical percentage BSA loading, Table 17.

4.2.10 DETERMINATION OF TOTAL AMOUNT OF BSA (mg) LOST INTO NANOSPHERE WASHES DURING FABRICATION

Determination of the concentration of BSA lost from the nanosphere preparations into the centrifugation supernatants during washing was carried out using the Bicinchoninic Acid method described in Section 2.2.15, page 71. The results have been summarised in Table 18, below.

TABLE 18 - TOTAL AMOUNT OF BSA (mg) LOST INTO NANOSPHERE WASHES DURING FABRICATION (mean values ± SEM, n=12)

THEORETICAL % LOADING (mg)	POLYMER	TOTAL MEAN BSA LOST (mg)
10 (25)	PHBHV-DIOL	17.68 ± 0.86
20 (50)	PHBHV-DIOL	36.66 ± 5.30
30 (75)	PHBHV-DIOL	63.17 ± 3.73
40 (100)	PHBHV-DIOL	81.72 ± 4.43[a]
10 (25)	3HB 3HC	15.86 ± 1.14
20 (50)	3HB 3HC	39.72 ± 4.28
30 (75)	3HB 3HC	60.88 ± 4.44
40 (100)	3HB 3HC	80.67 ± 5.81[a]
10 (25)	DIBLOCK	14.06 ± 0.63[b]
20 (50)	DIBLOCK	23.1 ± 1.26[c]
30 (75)	DIBLOCK	43.18 ± 10.26[c]
40 (100)	DIBLOCK	50.52 ± 13.60[a,c]

a, significantly elevated ($P<0.05$) compared with 10% BSA loaded nanospheres fabricated from the same polymer.

b, significantly reduced ($P<0.05$) compared with 10% BSA loaded PHBHV-Diol nanospheres.

c, significantly reduced ($P<0.05$) compared with corresponding BSA loaded nanospheres fabricated with either PHBHV-Diol or 3HB 3HC.

For all fabrication polymers, the greater the theoretical percentage BSA loading, the greater the mean total weight of BSA lost into the nanosphere wash solution. For all theoretical percentage BSA loadings, the lowest mean total weight of BSA lost was from nanospheres fabricated from Diblock polymer, Table 18.

4.2.11 DETERMINATION OF THE NANOENCAPSULATION EFFICIENCY AND THE TOTAL AMOUNT OF BSA ENCAPSULATED IN 100mg OF THEORETICAL 10%, 20%, 30% AND 40% w/w BSA LOADED PHBHV-DIOL, 3HB 3HC AND DIBLOCK NANOSPHERES

The effect of the type of polymer and percentage BSA loading on the nanoencapsulation efficiency was investigated by analysing the amount of BSA contained within a known weight of nanospheres. Determination of nanoencapsulation efficiency of BSA into polymer nanospheres was determined using the method described in Section 2.2.17, page 72. These data together with the actual total amount of BSA in 100mg of nanospheres, as used for the release studies, are shown in Table 19, below.

TABLE 19 - NANOENCAPSULATION EFFICIENCY AND TOTAL AMOUNT OF BSA INCORPORATED INTO 100mg OF THEORETICAL 10%, 20%, 30% AND 40% w/w BSA LOADED PHBHV-DIOL, 3HB 3HC AND DIBLOCK NANOSPHERES (mean values ± SEM, n=12)

THEORETICAL % LOADING	POLYMER	TOTAL BSA INCORPORATED INTO 100mg NANOSPHERES (mg)	NANOENCAPSULATION EFFICIENCY (%)
10	PHBHV-DIOL	6.14 ± 0.53	61.40 ± 5.30
20	PHBHV-DIOL	6.83 ± 0.82	34.13 ± 4.08
30	PHBHV-DIOL	9.98 ± 0.15	33.24 ± 0.47
40	PHBHV-DIOL	10.73 ± 1.50[a]	26.82 ± 3.74[b]
10	3HB 3HC	5.20 ± 0.25	52.10 ± 2.50
20	3HB 3HC	6.48 ± .077	32.40 ± 3.90
30	3HB 3HC	7.76 ± 2.15	25.87 ± 7.17
40	3HB 3HC	11.13 ± 2.48[a]	27.83 ± 6.20[b]
10	DIBLOCK	5.45 ± 0.15	54.50 ± 1.50
20	DIBLOCK	8.99 ± 2.30	44.95 ± 11.50
30	DIBLOCK	11.36 ± 2.80	37.85 ± 9.30
40	DIBLOCK	24.16 ± 5.50[a]	24.16 ± 5.50[b]

a, significantly elevated ($P<0.05$) compared with 10% w/w theoretical BSA loaded nanospheres, irrespective of the fabrication polymer used.

b, significantly reduced ($P<0.05$) compared with 10% w/w theoretical BSA loaded nanospheres, irrespective of the fabrication polymer used.

So, the actual total BSA incorporated into nanospheres increases with theoretical percentage BSA loading, irrespective of the fabrication polymer used. The greatest actual total BSA loading was observed for Diblock fabrication nanospheres, Table 19. On the other hand, increasing the theoretical percentage BSA loading significantly reduced the nanoencapsulation efficiency, irrespective of the fabrication polymer used.

4.2.12 *IN VITRO* RELEASE OF BSA FROM THEORETICAL 10%, 20%, 30% AND 40% w/w BSA LOADED PHBHV-DIOL, 3HB 3HC AND DIBLOCK NANOSPHERES INTO HANKS BALANCED SALTS SOLUTION (pH 7.4) AT 37°C FOR 28 DAYS

In vitro release was carried out using the method described in Section 2.2.18, page 73. Unloaded nanospheres fabricated from PHBHV-Diol, 3HB 3HC and Diblock polymers were incubated alongside the BSA loaded nanospheres as a negative control for the release of BCA sensitive components.
Daily release BSA profiles for theoretical 10% and 40% w/w BSA loaded PHBHV-Diol, 3HB 3HC and Diblock nanospheres monitored over 28 days in HBSS (pH 7.4) at 37°C are shown in Figures 25 to 27, below.

FIGURE 25 – DAILY BSA RELEASE PROFILE FOR 10% AND 40% w/w BSA LOADED PHBHV-DIOL NANOSPHERES (mean values ± SEM, n=12)

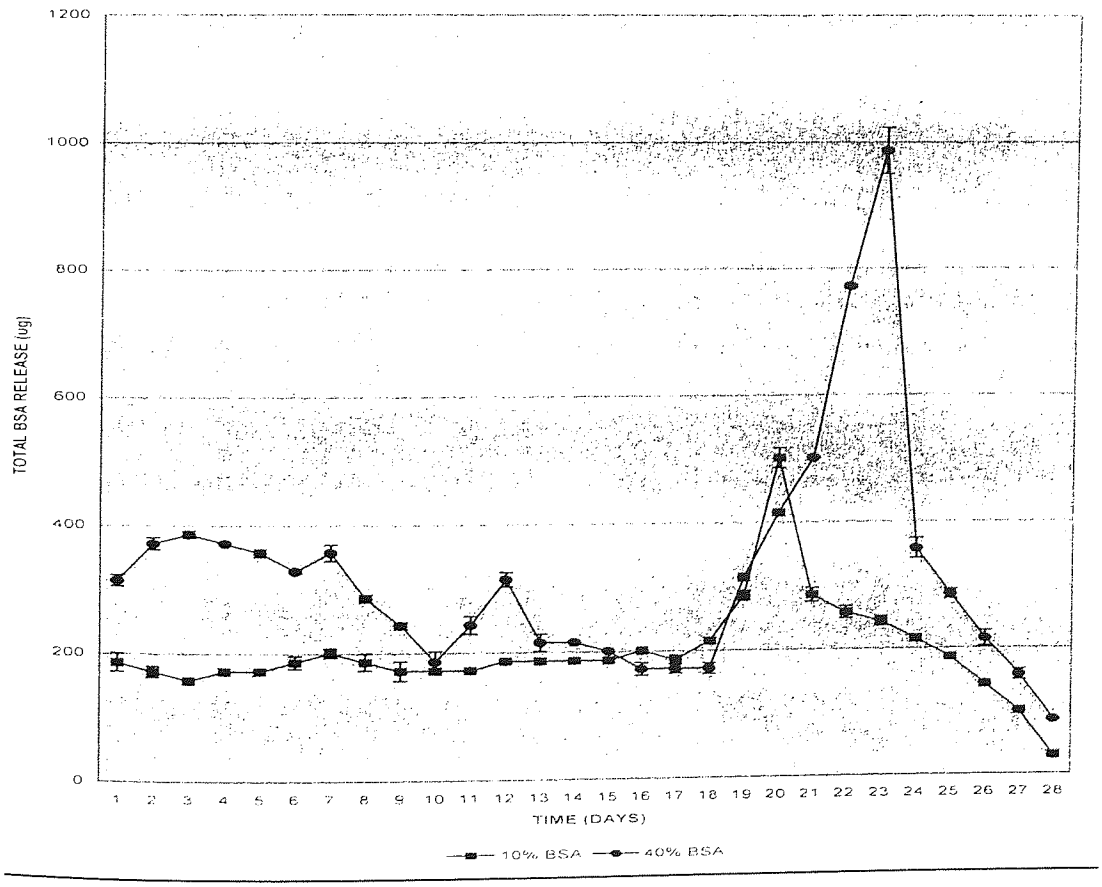

FIGURE 26 – DAILY BSA RELEASE PROFILE FOR 10% AND 40% w/w BSA LOADED 3HB 3HC NANOSPHERES (mean values ± SEM, n=12)

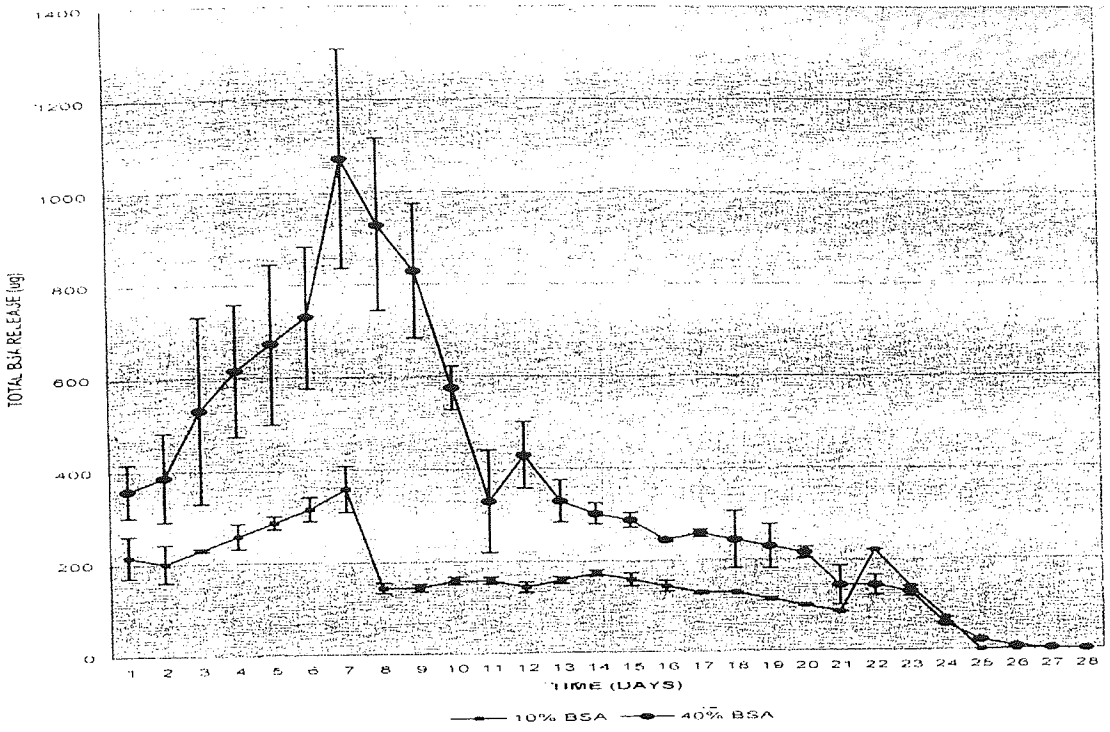

FIGURE 27 – DAILY BSA RELEASE PROFILE FOR 10% AND 40% w/w BSA LOADED DIBLOCK NANOSPHERES (mean values ± SEM, n=12)

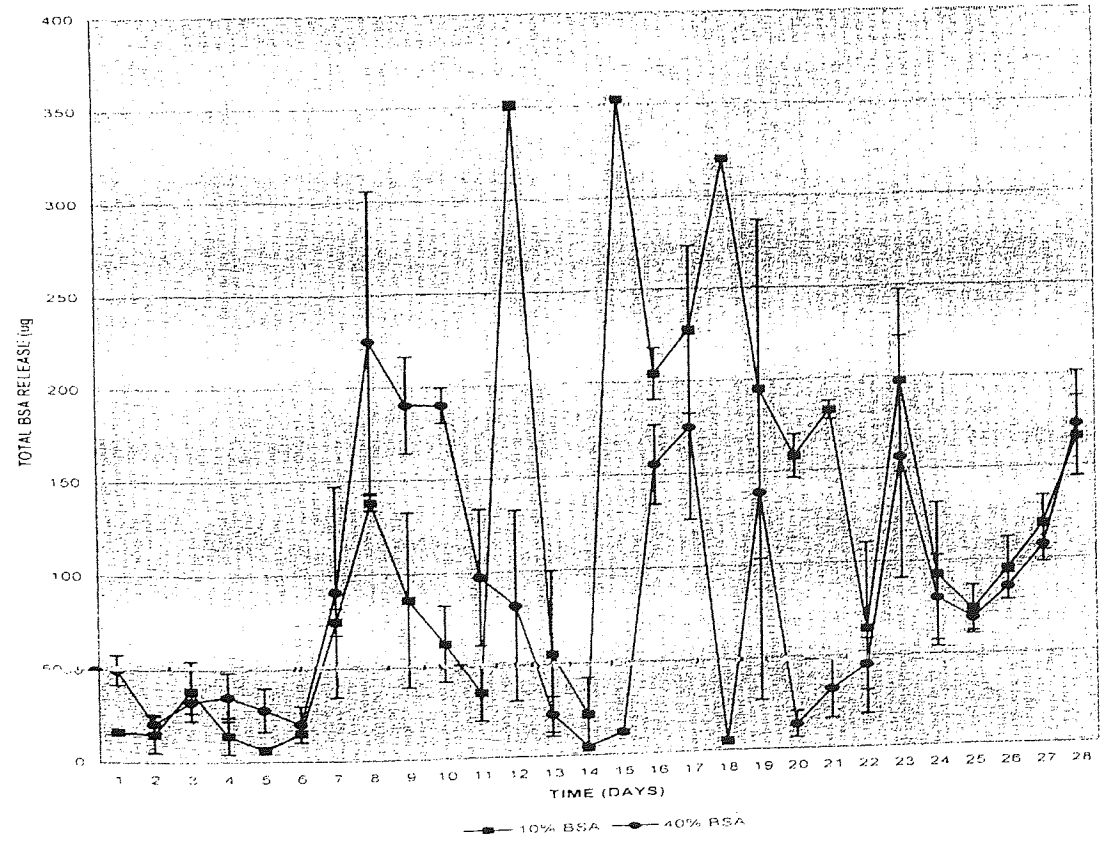

Theoretical 10% and 40% w/w BSA loaded PHBHV-Diol daily release profiles, Figure 25, characteristically show a stable continuous release of BSA for up to 17 days. After 17 days incubation, all samples show a burst release of BSA whose extent was positively correlated to the theoretical percentage of BSA loading. PHBHV-Diol nanospheres theoretically loaded with 10% w/w BSA showed a maximum BSA release of ~500μg/day at day 20 whilst theoretically 40% w/w BSA loaded PHBHV-Diol nanospheres showed a maximum release of ~1000μg/day after this time. Following the burst release phase the amount of BSA released from the PHBHV-Diol nanospheres decreased over time, Figure 25. No further BSA could be detected after 28 days incubation, irrespective of the theoretical percentage BSA loading.

Theoretical 10% BSA loaded 3HB 3HC nanospheres showed a short initial lag phase release period lasting approximately 24 hours, while theoretical 30% w/w BSA loaded 3HB 3HC (See Appendix Section 2.2, page 268) had a lag phase of some three days prior to significant BSA release. Maximum release occurred after 6 - 7 days and reached ~350μg/day from theoretical 10% w/w BSA loaded 3HB 3HC nanospheres to >1000μg/day from theoretical 40% w/w BSA loaded 3HB 3HC nanospheres, Figure 34. Maximum release occurred between six and seven days for theoretical 10%, 20% and 30% w/w BSA loaded 3HB 3HC nanospheres (See Appendix Section 2.2, page 268) and maximum release at seven days for the theoretical 40% w/w BSA loaded 3HB 3HC nanospheres, Figure 26. Following the initial burst release, the amount of BSA released from all BSA loaded 3HB 3HC nanospheres, irrespective of the theoretical percentage BSA loading, gradually decreased over the remainder of the release period, until at 28 days no further BSA could be detected, Figure 34. A further small burst release of BSA did occur after 22 days from theoretical 10% w/w BSA loaded 3HB 3HC nanospheres.
The pattern of release from BSA loaded Diblock nanospheres was rather irregular but appeared to have a much longer initial lag phase than any of the other polymers amounting to some six days. This initial lag phase was followed by 18 days of peaks and troughs in BSA release characterised by large standard errors. Irrespective of theoretical percentage BSA loading, from day 24 until the end of the release study at day 28, the release of BSA appeared to gradually increase on a daily basis, Figure 27. This might suggest that a substantial reservoir of BSA still remained in the nanospheres, and this was in fact proven by post release BSA encapsulation experiments, discussed later.

Representative total cumulative BSA release profiles for theoretical 10% and 40% w/w BSA loaded PHBHV-Diol, 3HB 3HC and Diblock nanospheres over 28 days are illustrated in Figures 28 to 31, overleaf. Total cumulative BSA release profiles for theoretical 20% and 30% w/w BSA loaded nanospheres fabricated using the three polymers are shown in Appendix Section 2.3, page 270.
Profiles for the release of BSA from theoretical 10% and 40% w/w BSA loaded PHBHV-Diol nanospheres look almost sigmoidal in profile with a lag phase of ~5 days and confirmed that the total cumulative release of BSA was positively correlated with the theoretical percentage BSA loading. The total cumulative amount of BSA released increased from a maximum of ~5.5mg after 28 days from theoretical 10% w/w BSA loaded PHBHV-Diol nanospheres to a maximum of ~9mg from theoretical 40% w/w BSA loaded PHBHV-Diol nanospheres over the same time period, Figure 28.

FIGURE 28 – TOTAL CUMULATIVE RELEASE PROFILE FOR 10% AND 40% w/w BSA LOADED PHBHV-DIOL NANOSPHERES (mean values ± SEM, n=12)

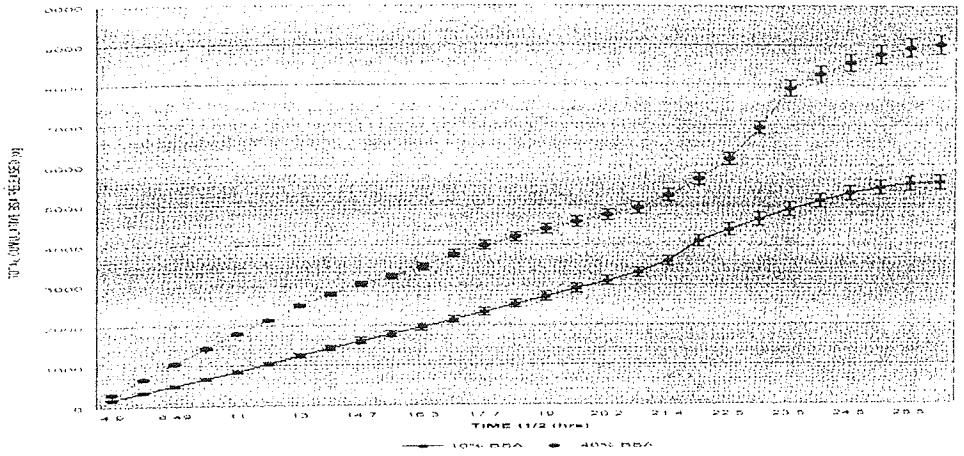

FIGURE 29 – TOTAL CUMULATIVE RELEASE PROFILE FOR 10% AND 40% w/w BSA LOADED 3HB 3HC NANOSPHERES (mean values ± SEM, n=12)

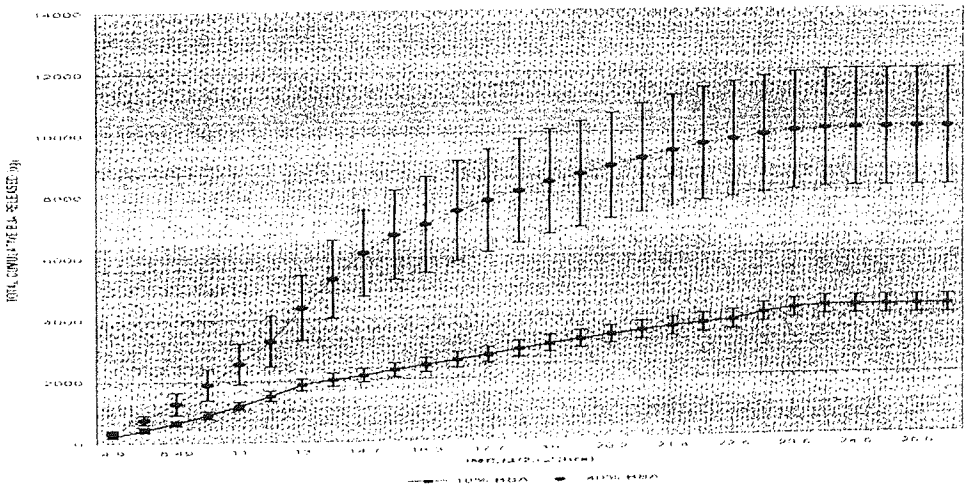

FIGURE 30 – TOTAL CUMULATIVE RELEASE PROFILE FOR 10% AND 40% w/w BSA LOADED DIBLOCK NANOSPHERES (mean values ± SEM, n=12)

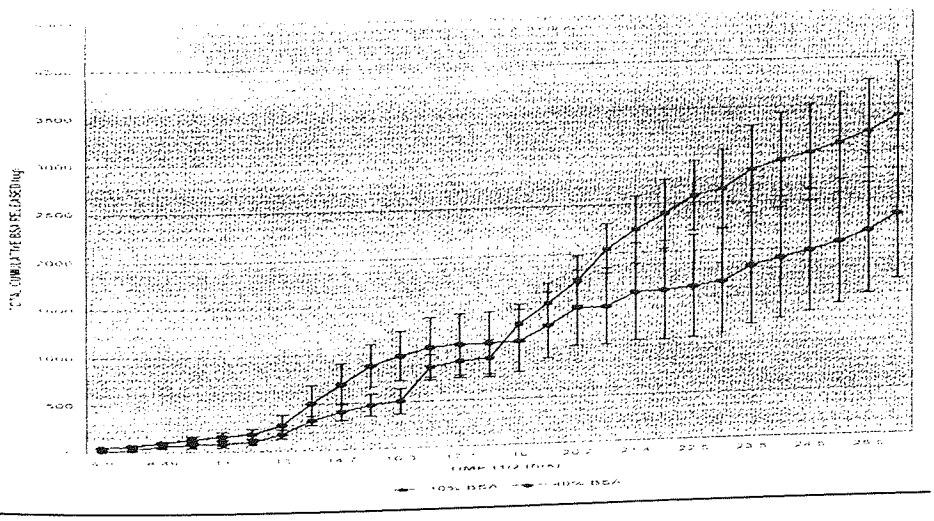

After 28 days, the release of BSA from PHBHV-Diol nanospheres, irrespective of the theoretical percentage BSA loading, had started to plateau, suggesting that the majority of incorporated BSA had been released.

The total cumulative release of BSA from BSA loaded 3HB 3HC nanospheres was positively correlated to the extent of theoretical percentage BSA loading, Figure 29. Total cumulative BSA release significantly increased ($P<0.05$) from a maximum of ~4.3mg from theoretical 10% w/w BSA loaded 3HB 3HC nanospheres after 28 days to a maximum of ~10mg from theoretical 40% w/w BSA loaded nanospheres over the same incubation period. The total cumulative release of BSA reached a maximum at around 22 days for both theoretical 10% and 40% w/w BSA loaded 3HB 3HC nanospheres. After this time no further release of BSA could be detected, Figure 29.

Unlike BSA release from PHBHV-Diol and 3HB 3HC nanospheres, there was no positive correlation between the theoretical percentage BSA loading of Diblock nanospheres and total cumulative BSA release. Irrespective of percentage BSA loading, BSA release was still active after 28 days, Figure 30. Theoretical 10% w/w BSA loaded Diblock nanospheres released the greatest total cumulative amount of BSA over a 28 day release period with a value of ~3.3 mg. The lowest total cumulative release of BSA was observed for theoretical 20% w/w BSA loaded Diblock nanospheres with a value of ~2.4mg BSA, (See Appendix Section 2.3, page 270).

No BSA like activity was detected from unloaded nanospheres fabricated from the three polymers used to fabricate BSA loaded nanospheres, when incubated alongside the BSA loaded nanospheres. Consequently values for unloaded nanospheres do not feature on any profiles or in any tables.

TABLE 20 - TOTAL CUMULATIVE BSA RELEASE AFTER INCUBATION IN HANKS BALANCED SALTS SOLUTION (pH 7.4) AT 37°C FROM THEORETICAL 10%, 20%, 30% AND 40% w/w BSA LOADED PHBHV-DIOL, 3HB 3HC AND DIBLOCK NANOSPHERES (mean values ± SEM, n=12)

THEORETICAL % LOADING	POLYMER	TOTAL CUMUALTIVE RELEASE (mg)
10	PHBHV-DIOL	5.56 ± 0.18
20	PHBHV-DIOL	6.38 ± 0.17
30	PHBHV-DIOL	8.59 ± 0.23
40	PHBHV-DIOL	9.02 ± 0.24[a]
10	3HB 3HC	4.25 ± 0.3
20	3HB 3HC	5.77 ± 0.71
30	3HB 3HC	6.57 ± 1.15
40	3HB 3HC	10.08 ± 1.9[a]
10	DIBLOCK	3.38 ± 0.57[b]
20	DIBLOCK	2.00 ± 0.69[b]
30	DIBLOCK	2.84 ± 0.73[b]
40	DIBLOCK	2.34 ± 0.69[b]

a, significantly elevated ($P<0.05$) compared with theoretical 10% w/w BSA loaded nanospheres fabricated using the same polymer.

b, significantly reduced ($P<0.05$) compared with the same percentage BSA loaded PHBHV-Diol and 3HB 3HC nanospheres.

In the case of PHBHV-Diol and 3HB 3HC nanospheres, the total cumulative BSA release increases with theoretical percentage BSA loading. However, this is not the case with Diblock nanospheres which showed a significantly reduced total cumulative BSA release compared with nanospheres fabricated from PHBHV-Diol and 3HB 3HC at all theoretical percentage BSA loadings, Table 20.

4.2.13 MEAN PERCENTAGE HARVEST AND CONSEQUENT PERCENTAGE WEIGHT LOSS FROM UNLOADED AND THEORETICAL 10%, 20%, 30% AND 40% w/w BSA LOADED PHBHV-DIOL, 3HB 3HC AND DIBLOCK NANOSPHERES AFTER USE IN RELEASE STUDIES

Following the incubation period, the nanospheres were quantitatively harvested and then freeze-dried as described in Section 2.2.5, page 57. The nanospheres were weighed accurately to determine the percentage weight loss during the release period. The results can be seen in Table 21, below.

TABLE 21 - PERCENTAGE WEIGHT LOSS FROM UNLOADED AND THEORETICAL 10%, 20%, 30% AND 40% w/w BSA LOADED PHBHV-DIOL, 3HB 3HC AND DIBLOCK NANOSPHERES AFTER INCUBATION IN HANKS BALANCED SALTS SOLUTION (pH 7.4) AT 37°C, FOR 28 DAYS (mean value ± SEM, n=12)

THEORETICAL % LOADING	POLYMER	WEIGHT AFTER INCUBATION (mg) (% YIELD)	% WEIGHT LOSS
0	PHBHV-DIOL	83.6 ± 0.23	16.4 ± 0.23
10	PHBHV-DIOL	93.0 ± 1.1	7 ± 1.1^{b}
20	PHBHV-DIOL	91.0 ± 0.7	9 ± 0.7^{b}
30	PHBHV-DIOL	90.0 ± 0.6	10 ± 0.6^{b}
40	PHBHV-DIOL	89.0 ± 0.3	11 ± 0.3^{bc}
0	3HB 3HC	75.0 ± 4.4	25 ± 4.4^{a}
10	3HB 3HC	95.0 ± 0.6	5 ± 0.6^{b}
20	3HB 3HC	93.0 ± 1.1	7 ± 1.1^{b}
30	3HB 3HC	89.0 ± 1.7	11 ± 1.7^{b}
40	3HB 3HC	97.0 ± 2.3	3 ± 2.3^{b}
0	DIBLOCK	62.33 ± 2.9	37.7 ± 3^{a}
10	DIBLOCK	68.2 ± 5	31.8 ± 5
20	DIBLOCK	75.5 ± 2	24.5 ± 2^{b}
30	DIBLOCK	74.8 ± 3	25.5 ± 3^{b}
40	DIBLOCK	84.2 ± 5	15.8 ± 5^{b}

a. significant increase in percentage weight loss ($P<0.05$) compared with unloaded PHBHV-Diol nanospheres.

b. significantly reduced percentage weight loss ($P<0.05$) compared with unloaded nanospheres fabricated using the same polymer.

c. significantly elevated ($P<0.05$) compared with theoretical 10% BSA loaded nanospheres fabricated using the same polymer.

Unloaded Diblock nanospheres showed the greatest percentage weight loss in Hank's Balanced Salts Solution (pH 7.4) at 37°C of all the fabrication polymers used. Loading PHBHV-Diol and 3HB 3HC nanospheres with BSA significantly reduced the percentage weight loss, although in both cases the percentage weight loss tended to increase with percentage BSA loading, Table 21. BSA loaded Diblock nanospheres showed the greatest percentage weight loss of all the theoretical percentage BSA loaded nanospheres.

4.2.14 DETERMINATION OF THE RESIDUAL BSA REMAINING IN THEORETICAL 10%, 20%, 30% AND 40% w/w BSA LOADED PHBHV-DIOL, 3HB 3HC AND DIBLOCK NANOSPHERES AFTER INCUBATION IN HANKS BALANCED SALTS SOLUTION (pH 7.4) AT 37 °C FOR 28 DAYS

Determination of the amount of BSA remaining in loaded nanospheres after use in release studies was carried out using the Bicinchoninic Acid assay (Smith *et al*, 1985) described in Section 2.2.15, page 71. No detectable BSA could be extracted from theoretical 10%, 20%, 30% or 40% w/w BSA loaded nanospheres fabricated from either PHBHV-Diol or 3HB 3HC after 28 days incubation. The levels of BSA remaining in BSA loaded Diblock nanospheres after 28 days incubation have been summarised in Table 22.

TABLE 22 - RESIDUAL BSA IN THEORETICAL 10%, 20%, 30% AND 40% w/w BSA LOADED DIBLOCK NANOSPHERES AFTER INCUBATION IN HANKS BALANCED SALTS SOLUTION (pH 7.4) AT 37°C FOR 28 DAYS. (mean value ± SEM, n=12)

POLYMER	THEORETICAL % LOADING	RESIDUAL BSA (mg)	RESIDUAL BSA AS % OF ACTUAL ORIGINAL BSA LOADING
DIBLOCK	10	0.918 ± 0.07	16.83 ± 0.74
DIBLOCK	20	5.43 ± 0.11[a]	60.40 ± 0.71[a]
DIBLOCK	30	7.97 ± 0.32[a]	70.16 ± 1.6[a]
DIBLOCK	40	18.2 ± 1.1[a]	75.33 ± 2.6[a]

a. significantly increased ($P<0.05$) compared with theoretical 10% w/w BSA loaded Diblock nanospheres.

Diblock nanospheres still contained detectable amounts of BSA after 28 days of incubation. The amount of BSA remaining within Diblock nanospheres gradually increased with theoretical percentage BSA loading, Table 22. Extending the release period would be expected to further reduce the amount of residual BSA in all BSA loaded Diblock nanospheres.

4.2.15 DETERMINATION OF THE MEAN PARTICLE DIAMETER OF UNLOADED AND THEORETICAL 10%, 20%, 30% AND 40% w/w BSA LOADED PHBHV-DIOL, 3HB 3HC AND DIBLOCK NANOSPHERES AFTER INCUBATION IN HANKS BALANCED SALTS SOLUTION (pH 7.4) AT 37 °C FOR 28 DAYS

Particle diameter analysis using Photon Correlation Spectroscopy was performed on all harvested nanospheres after use in release studies using the method described in Section 2.2.7, page 58. The results of the particle diameter analysis have been summarised in Table 23, below.

TABLE 23 - MEAN PARTICLE DIAMETER OF UNLOADED AND THEORETICAL 10%, 20% 30% AND 40% w/w BSA LOADED PHBHV-DIOL, 3HB 3HC AND DIBLOCK NANOSPHERES BEFORE AND AFTER INCUBATION IN HANKS BALANCED SALTS SOLUTION (pH 7.4) AT 37°C FOR 28 DAYS

(mean values ± SEM, n=12)

THEORETICAL % BSA LOADING	POLYMER	MEAN DIAMETER BEFORE (nm)	MEAN DIAMETER AFTER (nm)	% DECREASE IN DIAMETER
0	PHBHV-DIOL	275.6 ± 1.79	263.4 ± 0	4.39 ± 0
10	PHBHV-DIOL	295 ± 13.73	266.6 ± 2.9	9.63 ± 0.99
20	PHBHV-DIOL	328.8 ± 5.4	311.7 ± 3.4	5.2 ± 1.03
30	PHBHV-DIOL	384.7 ± 19	368.4 ± 20.4	4.24 ± 5.3
40	PHBHV-DIOL	557.4 ± 19.49	512 ± 7.4[a]	8.15 ± 1.3
0	3HB 3HC	396.51 ± 4.4	388 ± 9.9	8.51 ± 0.16[b]
10	3HB 3HC	504.2 ± 21.46	494.3 ± 4.21	1.97 ± 0.84
20	3HB 3HC	561.6 ± 22.19	543.5 ± 7.18	3.22 ± 1.3
30	3HB 3HC	615.2 ± 13.7	594.3 ± 6.8	3.4 ± 1.1
40	3HB 3HC	703 ± 16.8	665.67 ± 23.73[a]	5.31 ± 3.4
0	DIBLOCK	328 ± 7.57	299.67 ± 5.5	8.64 ± 1.7[b]
10	DIBLOCK	361 ± 8.33	337.67 ± 3.48	6.47 ± 0.97
20	DIBLOCK	401.67 ± 8.1	392.67 ± 4.06	2.19 ± 1.1
30	DIBLOCK	432.3 ± 15.41	420.33 ± 3.53	2.36 ± 0.41
40	DIBLOCK	464.3 ± 17.46	443.3 ± 6.7[a]	4.53 ± 1.4

a, significantly increased ($P<0.05$) compared with unloaded nanospheres, irrespective of the fabrication polymer used.

b, significantly greater ($P<0.05$) compared with unloaded nanospheres fabricated using PHBHV-Diol.

The percentage decrease in diameter was marginally lower in theoretical 20%, 30% and 40% w/w BSA loaded Diblock nanospheres compared with similarly BSA loaded 3HB 3HC and PHBHV-Diol nanospheres, Table 23. Irrespective of the fabrication polymer and theoretical percentage BSA loading used, all nanospheres show a reduction in mean particle diameter following incubation in HBSS for 28 days. The mean particle diameter of all nanosphere preparations irrespective of fabrication polymer and theoretical percentage BSA loading used continued to show a positive correlation with regards to the theoretical BSA loading. This pattern is not mirrored with regard to the percentage decrease in mean particle diameter for nanospheres generated from the same fabrication polymer, Table 23.

Incubation in HBSS for 28 days resulted in a marginal decrease in mean particle diameter for all nanospheres, irrespective of the fabrication polymer or extent of theoretical percentage BSA loading, Table 23.

4.2.16 DETERMINATION OF THE MEAN ZETA POTENTIAL OF UNLOADED AND THEORETICAL 10%, 20%, 30% AND 40% w/w BSA LOADED PHBHV-DIOL, 3HB 3HC AND DIBLOCK NANOSPHERES AFTER INCUBATION IN HANKS BALANCED SALTS SOLUTION (pH 7.4) AT 37°C FOR 28 DAYS

Zeta potential measurements were carried out on harvested nanospheres as described in Section 2.2.8, page 59. The results have been summarised in Table 24.

Unloaded nanospheres showed the greatest negative charge and the incorporation of BSA, irrespective of extent of theoretical percentage BSA loading, significantly lowered the negative charge on nanospheres fabricated from each of the polymers.

Incubation in HBSS for 28 days resulted in a significantly greater negative charge, irrespective of the fabrication polymer or the extent of theoretical percentage BSA loading, Table 24. These results could have been due to the removal of PVA into the incubation media over the 28 day incubation period.

TABLE 24 - MEAN ZETA POTENTIALS OF UNLOADED AND THEORETICAL 10%, 20%, 30% AND 40% w/w BSA LOADED PHBHV-DIOL, 3HB 3HC AND DIBLOCK POLYMER NANOSPHERES BEFORE AND AFTER INCUBATION IN HANKS BALANCED SALTS SOLUTION (pH 7.4) AT 37°C FOR 28 DAYS (mean value ± SEM, n=12)

THEORETICAL % BSA LOADING	POLYMER	MEAN ZETA POTENTIAL (mV) BEFORE	MEAN ZETA POTENTIAL (mV) AFTER
0	PHBHV-DIOL	-20.97 ± 0.38	-26.11 ± 1.27[c]
10	PHBHV-DIOL	-4.4 ± 0.22	-9.7 ± 0.27[c]
20	PHBHV-DIOL	-5.48 ± 0.57	-9.28 ± 0.2[c]
30	PHBHV-DIOL	-6.15 ± 0.45	-8.58 ± 0.23[c]
40	PHBHV-DIOL	-6.5 ± 0.61	-10.03 ± 0.22[bc]
0	3HB 3HC	-10.97 ± 0.74	-14.37 ± 0.12[c]
10	3HB 3HC	-4.23 ± 0.06	-7.95 ± 0.15[c]
20	3HB 3HC	-4.95 ± 0.17	-8.18 ± 0.21[c]
30	3HB 3HC	-6.23 ± 0.045	-7.08 ± 0.06[c]
40	3HB 3HC	-6.8 ± 0.54	-9.88 ± 0.59[bc]
0	DIBLOCK	-35.99 ± 0.67	-45.67 ± 0.83[ac]
10	DIBLOCK	-15 ± 0.48	-29.3 ± 0.81[c]
20	DIBLOCK	-14.3 ± 0.4	-27.73 ± 0.42[c]
30	DIBLOCK	-14.8 ± 0.42	-25.66 ± 0.74[c]
40	DIBLOCK	-14.39 ± 0.42	-25.13 ± 0.6[bc]

a, significantly greater negative charge ($P<0.05$) compared with unloaded PHBHV-Diol and 3HB 3HC.

b, significantly lower negative charge ($P<0.05$) compared with unloaded nanospheres fabricated using the same polymer.

c, significantly greater negative charge ($P<0.05$) compared with mean zeta potential of corresponding nanospheres prior to incubation in HBSS for 28 days.

4.2.17 DETERMINATION OF THE WEIGHT AVERAGE MOLECULAR MASS (Mw) OF UNLOADED AND THEORETICAL 10%, 20%, 30% AND 40% w/w BSA LOADED PHBHV-DIOL, 3HB 3HC AND DIBLOCK NANOSPHERES, AFTER INCUBATION IN HANKS BALANCED SALTS SOLUTION AT 37°C FOR 28 DAYS

The weight average molecular mass of unloaded and BSA loaded nanospheres following incubation in HBSS at 37°C for 28-days was measured using the gel permeation chromatography method described in Section 2.2.9, page 62. The results have been summarised in Table 25.

TABLE 25 – WEIGHT AVERAGE MOLECULAR MASS (Mw) OF UNLOADED AND THEORETICAL 10%, 20%, 30% AND 40% w/w BSA LOADED PHBHV-DIOL, 3HB 3HC AND DIBLOCK NANOSPHERES, BEFORE AND AFTER INCUBATION IN HANKS BALANCED SALTS SOLUTION AT 37°C FOR 28 DAYS (mean value ± SEM, n=6)

THEORETICAL % LOADING	POLYMER	Mw BEFORE (Dalton)	Mw AFTER (Dalton)	MEAN DECREASE IN Mw (Dalton)
0	PHBHV-DIOL	8138 ± 625	7710 ± 363	428 ± 262
10	PHBHV-DIOL	10, 798 ± 493	9770 ± 58	1028 ± 435[c]
20	PHBHV-DIOL	13, 475 ± 641	11, 833 ± 240	1642 ± 401[c]
30	PHBHV-DIOL	15, 275 ± 269	14, 767 ± 176	508 ± 93[c]
40	PHBHV-DIOL	17, 300 ± 515	15, 900 ± 208	1400 ± 307[c]
0	3HB 3HC	119, 167 ± 307	118, 967 ± 103	200 ± 204
10	3HB 3HC	117, 667 ± 882	117, 000 ± 506	667 ± 376[c]
20	3HB 3HC	114, 000 ± 732	113, 500 ± 487	500 ± 245[c]
30	3HB 3HC	109, 333 ± 1202	108, 500 ± 673	833 ± 529[c]
40	3HB 3HC	106, 233 ± 1876	105, 500 ± 1437	1437 ± 439[c]
0	DIBLOCK	58, 914 ± 1067	54, 800 ± 925[a]	4, 114 ± 142[b]
10	DIBLOCK	61, 750 ± 2666	51, 400 ± 1359[a]	10, 350 ± 1307[bc]
20	DIBLOCK	65, 317 ± 1413	58, 950 ± 1097[a]	6367 ± 316[bc]
30	DIBLOCK	77, 425 ± 3068	65, 150 ± 2108[a]	12, 275 ± 1740[bc]
40	DIBLOCK	83, 625 ± 309	74, 233 ± 242[a]	9392 ± 67[bc]

a, significantly reduced ($P<0.05$) compared with corresponding nanospheres prior to incubation in HBSS for 28-days.

b, significantly greater ($P<0.05$) compared with corresponding nanospheres fabricated from PHBHV-Diol and 3HB 3HC.

c, significantly greater ($P<0.05$) compared with unloaded nanospheres fabricated from the same polymer.

All nanospheres, irrespective of fabrication polymer or extent of percentage BSA loading, showed a significant decrease in mean molecular weight after 28 days incubation in HBSS compared with pre-incubation values, Table 13, page 103 and Table 25. Diblock nanospheres, irrespective of the extent of percentage BSA loading, showed a significantly greater decrease in mean molecular weight after incubation than corresponding nanospheres fabricated from PHBHV-Diol or 3HB 3HC, Table 25. BSA loading significantly elevated the reduction in mean molecular weight after incubation, irrespective of the fabrication polymer used, Table 25.

4.2.18 DETERMINATION OF THE RESIDUAL PVA CONTENT OF UNLOADED AND THEORETICAL 10%, 20%, 30% AND 40% w/w BSA LOADED PHBHV-DIOL, 3HB 3HC AND DIBLOCK NANOSPHERES, AFTER INCUBATION IN HANKS BALANCED SALTS SOLUTION AT 37°C FOR 28 DAYS

Analysis of the residual PVA content of unloaded and theoretical 10%, 20%, 30% and 40% w/w BSA loaded PHBHV-Diol, 3HB 3HC and Diblock nanospheres, after incubation in Hanks Balanced Salts Solution at 37°C for 28 days was carried out using the method detailed in Section 2.2.12, page 67. No residual PVA could be detected in nanospheres after 28 days incubation, irrespective of the extent of BSA loading or the fabrication polymer used. This could possibly explain the observed changes in zeta potential before and after incubation in HBSS.

CHAPTER 5

THE INCORPORATION INTO AND RELEASE OF ADMIRE® FROM NANOSPHERES FABRICATED FROM NOVEL MONSANTO POLYALKANOATES

5.1.1 INTRODUCTION

From the preliminary work carried out on the surrogate protein BSA, it was established that loaded nanospheres in the size range of 275.6nm ± 1.79 to 703nm ± 16.8 (mean values ± SEM, n=12) could be fabricated using the double sonication solvent evaporation method (2.3.1), for the nanoencapsulation and release of the Monsanto active Imidacloprid {1-[(6-chloro-3-pyridinyl)methyl]-N-nitro-2-imidazolidinimine}, fabricated using PHBHV-Diol and Diblock.

Imidacloprid *per se* is a broad-spectrum systemic insecticide produced by Monsanto under licence from Bayer, U.S.A. It has a number of common trade names such as Admire®, Confidor®, Advantage®, Gaucho® and Merit®. Throughout the remainder of this work, Imidacloprid {1-[(6-chloro-3-pyridinyl)methyl]-N-nitro-2-imidazolidinimine} will be referred to by its trade name Admire®.

5.1.2 DISCOVERY, SYNTHESIS AND PHYSICO-CHEMICAL PROPERTIES OF ADMIRE®

Most insecticides used in agriculture are based on a very limited number of chemically different classes of substance, the most important of which commercially are phosphates, carbamates and pyrethroids. Unfortunately the widespread use of structurally similar preparations, which have the same mechanism of action, has resulted in the development of insecticide resistance. For example, strains of the important virus-carrying peach-potato aphid (*Myzus persicae*) have developed 'esterase E4' resistance to organophosphate, carbamate and pyrethroid insecticides (Gaucho Booklet, Bayer, 1998). The R_1 and more resistant R_2 strains of the peach-potato aphid are widespread; a third, highly resistant R_3 strain, is found less frequently. Recently *Myzus persicae,* with a new type of resistance, have appeared in the United Kingdom, know as 'MACE aphids'. These possess Modified AcetylCholine Esterase which renders them resistant to dimethyl carbamates such as pirimicarb and triazamate (Diehr *et al,* 1991). Uniquely, as a result of its different mode of action, Admire® offers effective control against the 'MACE aphids', as well as many other resistant insects.

The insecticidal properties of nitromethylene compounds were first discovered by Soloway *et al* (1978), and the chloropyridyl-substituted heterocycles synthesised from this substance class were subsequently found to be powerful insecticides. Other potent insecticides, in addition to the nitromethylene compounds, are the guanidine derivatives and it was studies into these latter compounds that lead to the development of Admire® in February, 1985 by Nihan Bayer Agrochem K.K (Bayer "Pflanzenschutz Nachrichten Bayer" Booklet, 1991). The initial name of the compound chosen for biological development, due to promising preliminary results, was NTN 33983, this later became known as Admire®. All these newly discovered compounds had a mode of action that had not previously been associated with any commercially important insecticide.

The chemical synthesis of Admire® can be carried out via two routes. Both routes use the key intermediate compound 2-chloro-5-chloromethylpyridine (CCMP). Suitable inexpensive starting materials for the preparation of the precursor (CCMP) are the pyridine derivative β-picoline and nicotinic acid. The precursor (CCMP) can itself be synthesised by two routes, as shown below.

FIGURE 31 - SYNTHESIS OF 2-CHLORO-5-CHLOROMETHYLPYRIDINE (CCMP) BY β-PICOLINE – METHOD 1

A very good yield of β-picoline-N-oxide is obtained by oxidising β-picoline with hydrogen peroxide.

β-picoline β-picoline-N-oxide

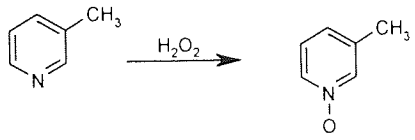

The resulting β-picoline-N-oxide is then subjected to a rearrangement reaction, for example with phosphorus oxychloride, to give 2-chloro-5-methylpyridine (CMP). Chlorination of the methyl group gives the key product 2-chloro-5-chloromethylpyridine (CCMP).

CMP

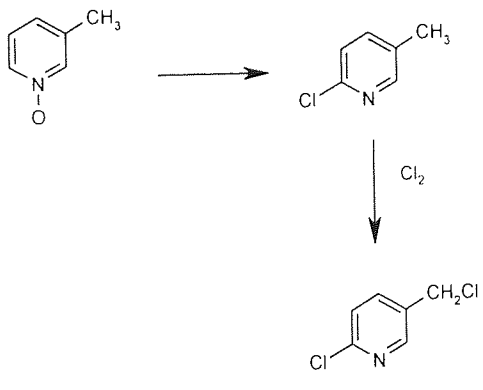

CCMP

FIGURE 32 - SYNTHESIS OF 2-CHLORO-5-CHLOROMETHYLPYRIDINE (CCMP) BY β-PICOLINE – METHOD 2

CCMP can also be synthesised by converting β-picoline into aminopicoline using sodamine. CMP is formed by diazotising the product in the presence of hydrogen chloride. The chlorination stage used in method 1 above is then carried out to produce CCMP.

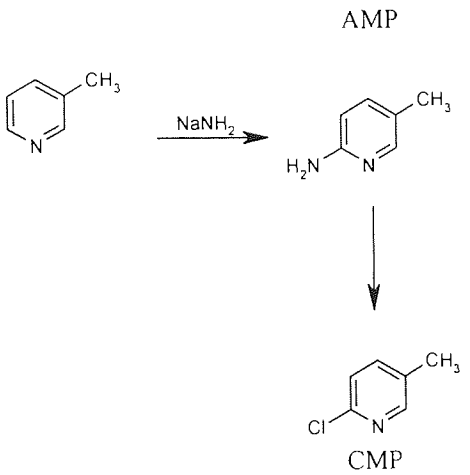

FIGURE 33 - SYNTHESIS OF 2-CHLORO-5-CHLOROMETHYLPYRIDINE (CCMP) BY NICOTINIC ACID.

The two nicotinic acid pathways that can be used differ in that the intermediate via one route is chloronicotinic acid and by the alternative route it is trichloromethylpyridine.

CHLORONICOTINIC ACID PATHWAY

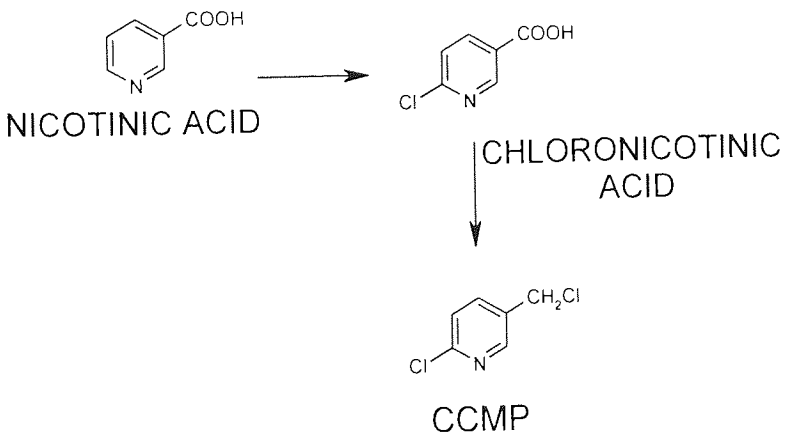

TRICHLOROMETHYLPYRIDINE PATHWAY

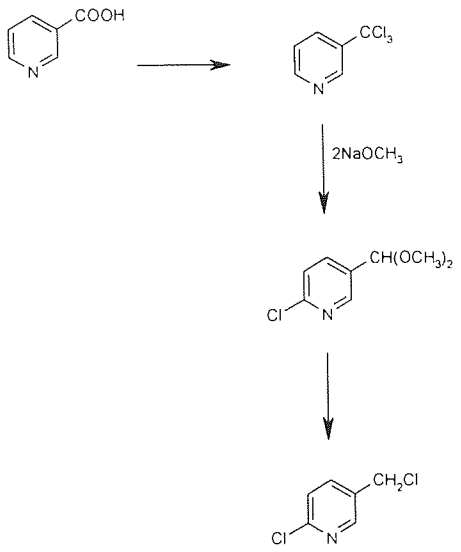

CCMP

PREPARATION OF THE ACTIVE INSECTICIDE - ADMIRE®

Admire® is obtained by alkylating the 2-chloro-5-chloromethylpyridine (CCMP) with ethylenediamine, followed by either ring formation with nitroguanidine or direct reaction with ethylene nitroguanidine (McKay & Wright, 1948).

FIGURE 34 - RING FORMATION PATHWAY FOR THE SYNTHESIS OF ADMIRE®

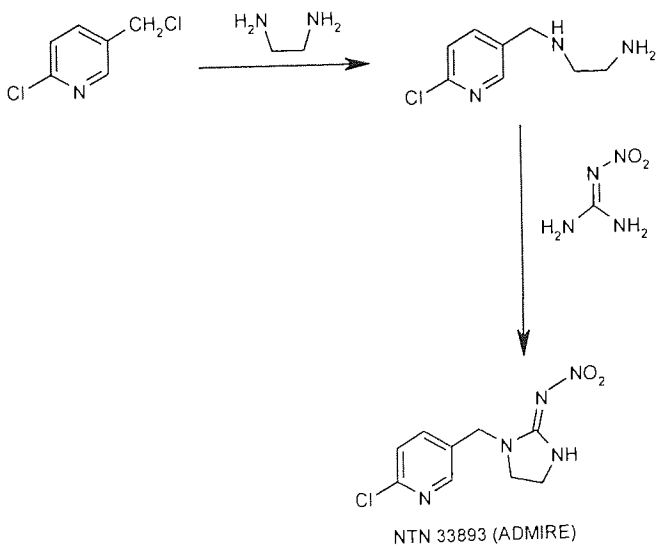

NTN 33893 (ADMIRE)

FIGURE 35 - DIRECT REACTION PATHWAY FOR THE SYNTHESIS OF ADMIRE®

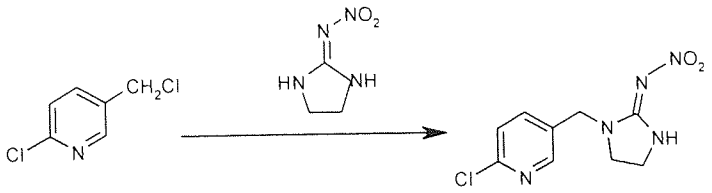

NTN 33893 (ADMIRE)

THE STRUCTURE AND PHYSICO-CHEMICAL PROPERTIES OF ADMIRE®

FIGURE 36 - STRUCTURAL FORMULA OF ADMIRE®:-

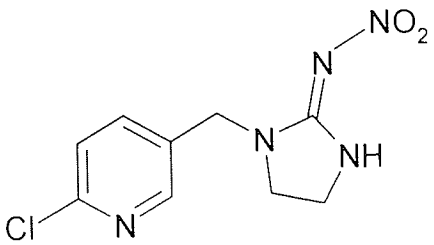

ADMIRE®

The basic properties of Admire® are summarised in Table 26, below.

TABLE 26 – BASIC CHEMICAL CHARACTERISTICS OF ADMIRE®

DESCRIPTION	CHARACTERISTIC
Chemical Name	1-(6-chloro-3-pyridinyl)methyl-4,5-dihydro-N-nitro-1H-imidazole-2-amine
Commercial Name	Admire®
Appearance	Colourless crystals
Empirical Formulae	$C_9H_{10}ClN_5O_2$
Melting Point	143.8°C
Vapour Pressure	2×10^{-9} mbar at 20°C
Solubility at 20°C: (g/1000 ml solvent)	Water: 0.51g/1000ml Dichloromethane: 50-100 g/1000ml 2-propanol: 1-2 g/1000ml
Stability	Stable to hydrolysis at pH 5-11

5.1.3 MODE OF ACTION OF ADMIRE®

Users of insecticides usually expect a very rapid onset of action, after application, to minimise the loss of crops. Apart from a few substances that act by inhibiting insect development, the vast majority of insecticides act by rapidly attacking the insect's nervous system.

The neurones of the insects nervous system consist of a cell body with an axon and dendrites. The axons and dendrites branch out and form numerous contacts with other neurones for the intensive transmission of information (Abbink, 1991). Peripheral axons make contact with muscle fibres and the points of contact are known as synapses. Most synapses are 'chemical' due to the fact that information is transmitted with the aid of chemical substances known as transmitters. Transmitters are stored in vesicles inside the pre-synaptic ends of the neurones. When an action potential reaches a pre-synaptic ending, the transmitter is released and travels across the synaptic cleft and binds to receptors on the post-synaptic membrane, as shown in Figure 37, below.

FIGURE 37 – A NORMAL SYNAPTIC JUNCTION

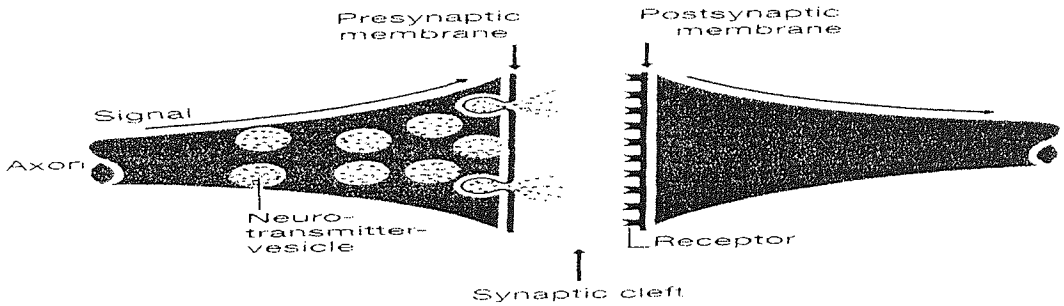

Reproduced with permission from BAYER plc, Bury St Edmunds, Suffolk, IP32 7AH, U.K.

This binding creates a specific change in the conductivity of the post-synaptic membrane for certain ions. In other words it produces a post-synaptic change in potential, and the membrane becomes depolarised. This depolarisation is known as the excitatory post-synaptic potential (EPSP). If the stimulus was weak then the cell membrane would be rapidly re-polarised. However, if the stimulus was strong then the threshold of an 'all or none' response is reached, resulting in an avalanche-like influx of certain ions into the cell. This rapid depolarisation actually reverses the potential. The cell membrane is then re-polarised and the resting potential is restored. The cycle of excitatory postsynaptic potential and rapid de- and re-polarisation (spike potential) is known as the action potential.

The nervous system of an insect employs numerous transmitters including acetylcholine, gamma-aminobutyric acid, glutamate, serotonin and octopamine. The dendrites have excitatory and inhibitory postsynaptic receptors through which they control or modulate the subsequent nerve cell. These principles of synaptic signal transmission suggest the following ways in which the insect nervous system might be targeted by insecticides. These may include the induction or inhibition of pre-synaptic transmitter release, interference with post-synaptic receptors (Gepner *et al,* 1978) and finally by disruption of the concentrations of neurotransmitters, for example by inhibiting either their degradation, which is largely hydrolytic, or their pre-synaptic re-synthesis (Abbink, 1991).

In the case of the transmitter acetylcholine all these can be achieved by phosphates (such as paraoxon) and carbamates. These substances inhibit the enzyme acetylcholinesterase (E.C. 3.1.1.7) localised in the synaptic cleft and thus prevent the degradation of acetylcholine. This results in an extended residence time of the transmitter in the synaptic cleft, ultimately leading to post-synaptic hyperstimulation.
Chlorinated hydrocarbons and pyrethroids (such as cyfluthrin) act on target principle 1 by inducing pre-synaptic transmitter release. The insecticides delay the closure of axonal Na^+ channels so that the membrane potential remains above the threshold for a longer period, resulting in a number of spike potentials being triggered. This huge release of transmitter results in postsynaptic hyperstimulation. Unfortunately for years the only insecticides available were those with an action principle based on interference of synaptic signal transmission, and hence resistance to these insecticides has now developed (Abbink, 1991).

Studies on the motor neurone of the cockroach *Periplaneta americana* have shown that Admire® and its analogues have an excellent insecticidal action, achieved by interfering with target principle 2, post-synaptic receptors. Once released into the synapse, the neurotransmitter cannot exert any effect unless it binds to the receptors in the post-synaptic membrane. Admire® and its analogues prevent the binding of acetylcholine to certain acetylcholine receptors by binding almost completely and virtually irreversibly to them.

Figure 38 below, shows the various sites of action of the main types of insecticides, including that of Admire®.

FIGURE 38 – SITES OF ACTION OF THE MAIN TYPES OF INSECTICIDE INCLUDING ADMIRE®

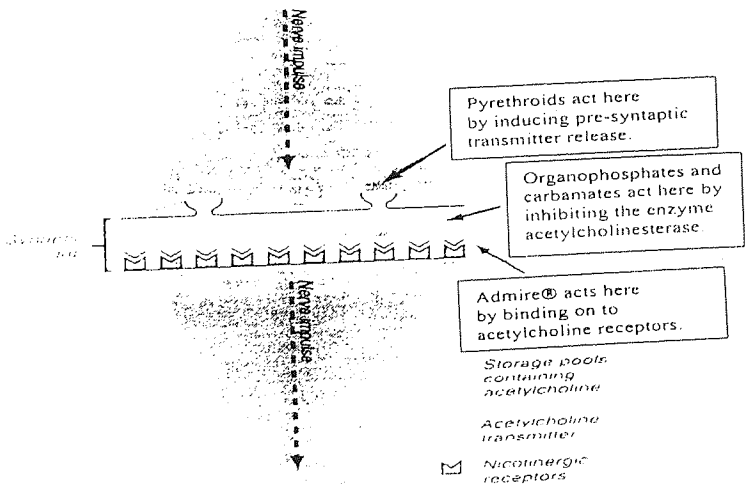

Reproduced with permission from BAYER plc, Bury St. Edmunds, Suffolk, IP32 7AH, U.K.

Acetylcholine receptors play an important role in the process of signal transmission in insect central nervous system and the prevention by Admire® of neurone impulse transmission leads to modified feeding behaviour and subsequent death of the insect (Bayer "Pflanzenschutz Nachrichten Bayer" Booklet, 1991). Insects contain two types of acetylcholine receptors – nicotinic and muscarinic just like warm-blooded animals (Sattelle, 1980). In insects, the nicotinic receptors are much more common than the muscarinergic receptors (Breer and Sattelle, 1987). The pharmacological differences between the two types of receptors in insects and warm-blooded animals mean that the action of Admire® is very specific and only has great affinity for insect nicotinic acetylcholine receptors.

5.1.4 ECOTOXICOLOGY OF ADMIRE®

Admire® is a fairly water soluble (500 mg/litre), non-polar insecticide (Kagabu, 1997) that is extremely effective against sucking insects such as aphids, leaf hoppers, white flies (Chao *et al*, 1997), thrips, scale insects and mealy bugs. Admire® is also effective against some biting pests such as rice water weevils, Colorado beetles, leaf miners, soil insects and termites. For this reason, Admire® is also used to control fleas in dogs and cats (Dryden *et al*, 1999), and is highly effective in controlling sucking and biting lice in dogs (Hanssen *et al*, 1999). However, Admire® has no effect on nematodes or spider mites (Elbert *et al*, 1991). It has also been shown that at comparatively high dose rates Admire® kills adult insects and has an ovicidal effect (Elbert *et al*, 1991). Admire® is active after oral ingestion and by direct contact, but it is not active in the vapour phase. The LD_{95} after oral ingestion by the aphid *M.persicae* is about 2 pg *per* aphid. After topical application it is about 160 pg *per* aphid. After foliar application, Admire® shows good translaminar and acropetal translocation. This is very important because as well as protecting plants at the time of treatment, insecticides must also protect the parts of the plant that grow after treatment, as pests have a predilection for new growth. Treatment with 500 ppm of an Admire® preparation completely protected cotton plants against attack by the aphid *M.persicae* for 5 weeks in tests carried out by Elbert *et al* (1991). By virtue of its good contact action and powerful systemic action after uptake through the root system, Admire® can be applied to the soil and used as a seed dressing where it gives excellent control of pests such as onion maggots, *Diabrotica* species, wire worms, termites and fire ants which live in the soil (Elbert *et al* 1991). After incorporation into the soil, even at concentrations as low as 0.31 ppm, Admire® controlled *M.persicae* for at least 8 weeks. Even when applied at excessively high dose rates, Admire® does not impair the activity of soil microbes (Pfluger & Schmuck, 1991).

In extensive experiments carried out by Elbert *et al* (1991) the biological activity of Admire® was seen to increase with temperature. With a dose rate of 1000 ppm at 10°C, 45% of the test organism, *Plutella xylostella*, were killed under the test conditions, but a temperature increase to 16.5°C saw 90% of the insects killed. A similar pattern was observed for all the other test species examined. It was also found that Admire® was highly photostable. The possible effects of Admire® containing preparations on potentially exposed organisms has been tested and ecologically evaluated in many experiments (Pfluger and Schmuck, 1991). In normal application systems, namely seed dressings, pills and granules, the possibility of contact with Admire®, and hence the risk of side effects, is greatly restricted for many organisms in the environment, such as beneficial species or aquatic animals. However, in such application

systems particular attention has to be paid to the safety of birds. The risk assessments are based on procedures customary to the Food and Agricultural Organisation of the United Nations (1990) and the Environmental Protection Agency, U.S.A (1986). Table 27 below, shows the LC_{50} for a range of animals that may come into contact with Admire®.

TABLE 27 - ECOLOGICAL IMPACT OF ADMIRE® ON A RANGE OF ORGANISMS.

ANIMAL	DEATH RATE COUNT	CONCENTRATION OF ADMIRE® REQUIRED	REFERENCE
RAT	LD_{50}	424-475 mg/kg	BOMANN, 1989a
CANARY	LD_{50}	25-50 mg/kg	GRAU, 1986
PIGEON	LD_{50}	25-50 mg/kg	GRAU, 1987a
TROUT	LC_{50}, 96 HOURS	211 mg/l	GRAU, 1988
CARP	LC_{50}, 96 HOURS	280 mg/l	TAKADA, 1986
EARTHWORM	LC_{50}, 14 DAYS	10.7 mg/kg	HEIMBACH, 1986
WATERFLEA	EC_{50}	85 mg/l	YOUNG *et al*, 1990
GROWTH OF ALGAE	EC_{50}	ABOVE 10 mg/l	HEIMBACH, 1986

From a range of experiments carried out by Schmitt (1989) and Zeller (1990), it was concluded that when applied as a spray in flowering crops during foraging time, Admire® should be classified as dangerous to bees due to its repellent effect, which lasted in excess of a week. Also, with birds, an LC_{50} of 25-50 mg/kg means that Admire® is classified as an acute toxin to birds. In contrast, with an LC_{50} of more than 1000 ppm (Toll 1990 a&b) the subacute toxicity, which is more important for assessing the potential effects of residues in the diet of wild animals, is low. Tests with duck and quail showed no adverse effects on the reproduction rate, the highest concentration had no observed effect at 125-243 mg/kg feed (Toll, 1991 a&b). In practice, under test conditions, neither songbirds (Grau, 1987b) nor upland game birds (Grau, 1987d, Schmuck, 1990 a&b) showed effects which suggests that these birds are not at risk in normal agricultural practice (Pfluger & Schmuck, 1991). The repellent effect of Admire® is also well documented for cereal and corn seed pigeons (Grau, 1987c), and corvids (Grolleau, 1991).

The mammalian toxicity of Admire® is low. The lowest LD_{50} value of 131-168 mg/kg was determined in mice (Bomann, 1989b) and with an LC_{50} value of more than 2400 ppm, the subacute toxicity of Admire® for mammals is also well outside the hazardous range. Mammals exhibit symptoms shortly after ingestion of very high quantities of Admire®, and so it has been concluded that no particular hazard to vertebrates is to be expected under normal practice conditions. It has also been concluded that recommended dosage rates exclude any hazard to fish, waterfleas or algae.

The results of exhaustive tests for possible ecological effects of Admire® demonstrate that, although this compound is highly effective against a broad spectrum of pests, it is also unusually safe in environmental terms. This was echoed by the fact that the synthesis to sales time of Admire® was only 6 years,

compared with the normal time for synthesis to sales of 10 years. By virtue of its biological properties, Admire® has a wide range of uses in controlling economically important pests of rice, cotton, cereals, maize, sugar beet, potatoes, citrus fruits and many other crops (Tomlin, 1994). The latest published results of trials performed by Bayer on fields of sugar beet throughout the 1996 and 1997 growing seasons show significant potential for this insecticide, with sugar yields increased by 18%, and financial returns up by more than £164 *per* hectare over the next best treatment (Bayer Gaucho® Booklet, 1998).

5.1.5 THE DANGERS OF AGROCHEMICALS IN THE ENVIRONMENT

In recent years there has been growing concerns about the use of agricultural chemicals, such as pesticides and fertilisers, and their impact on the environment and ecosystem around farmlands, with growers becoming increasingly scrutinised for contributing to contamination of ground water supplies (Felsot *et al*, 1998).

Agrichemicals, including Admire®, are frequently sprayed onto crops to aid plant growth by killing insects that damage crop growth. However, during rainfall these chemicals are washed off the plants, and leach through the soil irrigation system, eventually ebbing into nearby rivers and lakes. These chemicals can build up to such a level that they begin to destroy *fauna* and *flora* remote from the farmlands where their action was desired, affecting whole ecosystems. Although best management practices have been comprehensively studied for allaying surface transport, field practices for managing leaching have been less developed (Felsot *et al*, 1998). Water management used in irrigated farming reduces leaching, especially of the more water soluble pesticides like aldicarb (Wyman *et al*, 1985), but other farming practices, such as rill irrigation, have been held responsible for significant sediment and pesticide contamination of rivers (Rinella *et al*, 1993). Extensive investigations into the leaching of Admire® by Felsot *et al* (1998), after subsurface drip chemigation, suggest that leaching would be limited. With a water solubility of around 500 mg/l, Admire® would be predicted to leach readily. However, the Admire® sorption coefficient (K_{oc}) in a sandy loam increased from 71 to 893 as initial solution concentrations were reduced from 250 ppm to 0.5 ppm (Cox *et al*, 1997), and a field study of residues by Rouchaud *et al* (1994) showed no leaching. Both these examples support the hypothesis that Admire® is not as leachable as its water solubility might predict (Felsot et al, 1998). Nevertheless, under irrigation conditions unmatched to the water evaporation rate, Admire® can leach to depths of at least 105 cm, therefore entering the water table and causing potential environmental damage.

5.1.6 ROLES AND BENEFITS OF THE NANOENCAPSULATION OF ADMIRE®

In the present work, the nanoencapsulation of Admire® has been studied because of the increasingly severe requirements demanded of the pesticide industry, and the fact that pesticide formulations are now required to satisfy a spectrum of conditions. Amongst these are higher safety (during handling and application, for non-target organisms, and in the environment in general), higher efficacy (initial and residual efficacy at lower dosage), and lower price (low manufacturing costs and low cost/performance ratio). The development of new functional pesticide formulations and new application fields for existing

pesticides, these days, out-weighs the development of new safer pesticides both in terms of cost and time (Tsuji, 1999).

The importance of pesticide delivery systems (PDS) cannot be over emphasised. A PDS can be defined as a technology in which an active ingredient is made available to a specific target at a concentration and for a duration which has been designed to accomplish an intended effect, to enhance the fullest biological efficacy and to reduce its harmful effects. One of the most important PDS is controlled release formulation (Tsuji, 1987 & 1993).

Table 28 below, shows various microencapsulated pesticide products that are already on the market.

TABLE 28 - MICROENCAPSULATED PESTICIDE DELIVERY SYSTEMS CURRENTLY USED IN AGRICULTURE. (Extracted from Tsuji, 1999)

TRADE NAME	ACTIVE INGREDIENT	POLYMERIC WALL MATERIAL	COMPANY
Actellic M20	Pyrimiphosmethyl	Polyurea	Zeneca
Altosid SR-10	Methoprene	Polyamide	Zoecon
Capfos Seed Treatment	Fonofos	Polyurea	Zeneca
Diazinon SL Sol	Diazinon	Polyurea	Nippon Kayaku
Ember MC	Permethrin	Polyurethane	Sumitomo Chemical
MicroSect	Synergized pyrethrins	Polyurea	3M
Tossits	DDT	Gelatin	Wyco International

Nanoencapsulating pesticides has many advantages over the use of conventional dosage forms such as neat spraying. These advantages include the fact that controlled release and longer application intervals lead to improved residual activity and labour saving; degradation of active ingredients by the environment is reduced; toxicity and harmful effects to humans, fish and plants are reduced because the active is protected by the matrix and low level sustained release ensures that the local concentration of the active ingredient outside the capsule is low; lower true dosage and reduced evaporation lead to less environmental pollution; protection of active by polymer matrix leads to masking of any unpleasant odour; reduction of drift in the field, when compared with emulsifiable concentrate formulations; more organisms may be targeted over a longer period of time due to the changed release of the active ingredient resulting from nanoencapsulation and finally, sealing of active ingredient, hence preventing undesirable interaction and loss during storage and handling (Tsuji, 1999).

Not all nanoencapsulation processes will display all these properties, and so it is important to obtain the maximum number of desired characteristics for a given application.

Once applied to the crops, in order to be biologically effective, the pesticide must be released. This can occur via diffusion through the sphere wall and/or destruction of the sphere matrix by mechanical action, hydrolysis, biodegradation by bacteria and fungi, or thermal degradation. Biodegradable polymers, such as PHB-HV, are desirable for agricultural use from the viewpoints of safety and residue.

One example of a polymer that is widely used in controlled release systems is starch. Aqueous gelatinisation of starch at high temperatures, followed by the addition of active agents, drying and grinding, yields encapsulation products that release active ingredients slowly (Wing *et al*, 1990), and the rate of release of the active can be controlled by varying the starch type and particle size. For example, higher amylose content has been shown to give a slower release of alachlor (Tsuji, 1999). As a consequence such immobilised products offer great potential in the reduction of ground water contamination.

There is certainly a demand in the agricultural community for Pesticide Delivery Systems (PDS) that have a longer sustained duration of action, which can be applied simply and easily to agrochemical applicators (Muchembled, 1991), and the potential nanoencapsulation of Admire® may provide such a system.

AIMS

The work presented in this chapter describes the fabrication, characterisation and release of Admire® from loaded nanospheres fabricated using the double sonication solvent evaporation method. A range of loaded nanospheres were fabricated containing theoretical 10 to 40 % w/w Admire® and incubated in rural rainwater at both room temperature (23°C) and fridge temperature (4°C), for a period of up to 37 days. The Admire® concentration was measured spectrophotometrically and release profiles of day to day release and total cumulative release constructed. A significant release of Admire® was easily maintained over the 37 day release period.

5.2 RESULTS

5.2.1 MEAN PERCENTAGE YIELD OF UNLOADED AND THEORETICAL 10%, 20%, 30% AND 40% w/w ADMIRE® LOADED PHBHV-DIOL AND DIBLOCK NANOSPHERES

Unloaded nanospheres and nanospheres theoretically loaded with either 10%, 20%, 30%, or 40% w/w Admire® were routinely fabricated from both PHBHV-Diol and Diblock polymers using the method described in Section 2.2.4, page 56. The mean total weight of nanospheres (mg) produced during fabrication was computed using Equation 2, page 57 and can be seen in Appendix Section 3.1, page 271. The mean percentage yield of nanospheres was computed from the mean total weight of nanospheres and the results are summarised in Table 29, below.

TABLE 29 - MEAN PERCENTAGE YIELD OF UNLOADED AND THEORETICAL 10%, 20%, 30% AND 40% w/w ADMIRE® LOADED NANOSPHERES FABRICATED FROM PHBHV-DIOL AND DIBLOCK POLYMERS (mean values ± SEM, n=12)

THEORETICAL % LOADING	POLYMER	MEAN % YIELD
0	PHBHV-DIOL	71.76 ± 0.83
10	PHBHV-DIOL	68.37 ± 0.94
20	PHBHV-DIOL	66.3 ± 2.4
30	PHBHV-DIOL	64.5 ± 1.7
40	PHBHV-DIOL	61.1 ± 2.2[b]
0	DIBLOCK	66.17 ± 1.4[a]
10	DIBLOCK	57.1 ± 1.5[a]
20	DIBLOCK	59.9 ± 5.4[a]
30	DIBLOCK	49.3 ± 1[a]
40	DIBLOCK	56.1 ± 3.3[ab]

a, significantly reduced ($P<0.05$) compared with similarly loaded PHBHV-Diol nanospheres.

b, significantly reduced ($P<0.05$) compared with unloaded nanospheres fabricated using the same polymer.

The mean percentage yield of unloaded and Admire® loaded nanospheres fabricated from PHBHV-Diol were significantly greater ($P<0.05$), than the mean percentage yield of Diblock fabricated nanospheres,

irrespective of the percentage Admire® loading. The mean theoretical percentage yield of Admire® loaded PHBHV-Diol nanospheres tended to decrease ($P<0.05$) with percentage Admire® loading. However, no such trend was observed for Admire® loaded Diblock nanospheres, Table 29, although the mean percentage yield of theoretical 40% w/w Admire® loaded Diblock nanospheres was significantly lower ($P<0.05$) than the mean percentage yield of unloaded nanospheres fabricated using the same polymer.

5.2.2 DETERMINATION OF THE MEAN PARTICLE DIAMETER OF UNLOADED AND THEORETICAL 10%, 20%, 30% AND 40% w/w ADMIRE® LOADED NANOSPHERES, PRIOR TO USE IN RELEASE STUDIES

Particle diameter analysis performed using photon correlation spectroscopy was carried out on all Admire® loaded nanosphere preparations as described in Method 2.2.7, page 58 and the results have been summarised in Table 30, below.

TABLE 30 – THE EFFECT OF THEORETICAL PERCENTAGE LOADING AND FABRICATION POLYMER ON THE MEAN PARTICLE DIAMETER OF UNLOADED AND THEORETICAL 10%, 20%, 30% AND 40% w/w ADMIRE® LOADED PHBHV-DIOL AND DIBLOCK NANOSPHERES (mean values ± SEM, n=12)

THEORETICAL % LOADING	POLYMER	MEAN DIAMETER (nm)
0	PHBHV-DIOL	275.6 ± 2.1
10	PHBHV-DIOL	455.8 ± 31.7
20	PHBHV-DIOL	521.4 ± 4.6
30	PHBHV-DIOL	578.9 ± 1.9
40	PHBHV-DIOL	624.5 ± 11.4[b]
0	DIBLOCK	328 ± 7.57[a]
10	DIBLOCK	496 ± 7.7
20	DIBLOCK	524.9 ± 4.9
30	DIBLOCK	594.7 ± 3.9
40	DIBLOCK	635.9 ± 5.6[b]

a, significantly increased in diameter ($P<0.05$) compared with unloaded PHBHV-Diol nanospheres.

b, significantly increased in diameter ($P<0.05$) compared with theoretical 10%, 20% and 30% w/w Admire® loaded nanospheres fabricated using the same polymer.

The mean diameter of unloaded Diblock nanospheres is significantly ($P<0.05$) larger than the mean diameter of unloaded PHBHV-Diol nanospheres. Loading nanospheres with Admire® significantly ($P<0.05$) increases the mean diameter of nanospheres irrespective of the fabrication polymer used, Table 30.

5.2.3 ZETA POTENTIAL MEASUREMENTS OF UNLOADED AND THEORETICAL 10%, 20%, 30% AND 40% w/w ADMIRE® LOADED PHBHV-DIOL AND DIBLOCK POLYMER NANOSPHERES, PRIOR TO USE IN RELEASE STUDIES

Zeta potential measurements of all Admire® loaded nanosphere preparations were carried out using a Malvern Zetamaster®, as described in Section 2.2.8, page 59 and the results summarised in Table 31, below.

TABLE 31 - MEAN ZETA POTENTIALS OF UNLOADED AND THEORETICAL 10%, 20%, 30% AND 40% w/w ADMIRE® LOADED PHBHV-DIOL AND DIBLOCK POLYMER NANOSPHERES, PRIOR TO USE RELEASE STUDIES (mean values ± SEM, n=12)

THEORETICAL % LOADING	POLYMER	MEAN ZETA POTENTIAL (mV)
0	PHBHV-DIOL	-20.76 ± 0.38
10	PHBHV-DIOL	-9.1 ± 1
20	PHBHV-DIOL	-8.1 ± 1
30	PHBHV-DIOL	-8.1 ± 1
40	PHBHV-DIOL	-9.2 ± 1.8[b]
0	DIBLOCK	-35.99 ± 0.38[a]
10	DIBLOCK	-13.6 ± 1[a]
20	DIBLOCK	-13.4 ± 0.9[a]
30	DIBLOCK	-13 ± 1.2[a]
40	DIBLOCK	-13.6 ± 2[ab]

a, significantly more negative ($P<0.05$) compared with unloaded and similarly percentage Admire® loaded PHBHV-Diol nanospheres.

b, significantly less negative ($P<0.05$) compared with unloaded nanospheres fabricated using the same polymer.

The mean zeta potential of unloaded Diblock nanospheres was significantly ($P<0.05$) more negative than unloaded PHBHV-Diol nanospheres. Admire® loading significantly reduced the negative charge of nanospheres, irrespective of the fabrication polymer used. Increasing the percentage Admire® loading from theoretical 10% w/w to 40% w/w did not significantly influence the negative charge on nanospheres fabricated from either polymer, Table 31. According to the stability table of Riddick (1968) this puts the Admire® loaded PHBHV-Diol nanospheres into the stability band between 'the range of strong aggregation and precipitation' and 'threshold of agglomeration', and the Admire® loaded Diblock nanospheres into the 'threshold of agglomeration' band. Unloaded PHBHV-Diol nanospheres can be placed in the stability band 'threshold of delicate dispersion', and the unloaded Diblock polymer nanospheres into the stability band 'moderate stability' (Riddick, 1968).

5.2.4 DETERMINATION OF THE WEIGHT AVERAGE MOLECULAR MASS (Mw) OF UNLOADED AND THEORETICAL 10%, 20%, 30% AND 40% w/w ADMIRE® LOADED PHBHV-DIOL AND DIBLOCK NANOSPHERES, PRIOR TO USE IN RELEASE STUDIES

The results obtained from GPC analysis have been summarised in Table 32, below.

TABLE 32 - MEAN WEIGHT AVERAGE MOLECULAR MASS OF UNLOADED AND THEORETICAL 10%, 20%, 30% AND 40% w/w ADMIRE® LOADED PHBHV-DIOL AND DIBLOCK NANOSPHERES, PRIOR TO USE IN RELEASE STUDIES (mean values ± SEM, n=12)

THEORETICAL % LOADING	POLYMER	MEAN MOLECULAR WEIGHT (DALTONS)
0	PHBHV-DIOL	8138 ± 625
10	PHBHV-DIOL	2773 ± 15
20	PHBHV-DIOL	2379 ± 55
30	PHBHV-DIOL	1572 ± 21
40	PHBHV-DIOL	1003 ± 6[b]
0	DIBLOCK	58 914 ± 1067[a]
10	DIBLOCK	58 526 ± 2452
20	DIBLOCK	53 900 ± 2939
30	DIBLOCK	48 575 ± 712
40	DIBLOCK	37 450 ± 56[b]

a, significantly higher ($P<0.05$) compared with unloaded PHBHV-Diol nanospheres

b, significantly lower ($P<0.05$) compared with unloaded nanospheres and theoretical 10%, 20% and 30% w/w Admire® loaded nanospheres fabricated from the same polymer.

The mean weight average molecular mass of unloaded Diblock nanospheres was significantly greater ($P<0.05$) than unloaded PHBHV-Diol nanospheres. Loading with Admire® significantly reduced ($P<0.05$) the mean weight average molecular mass of nanospheres fabricated from both PHBHV-Diol and Diblock polymers. Irrespective of fabrication polymer, increasing the theoretical percentage Admire® loading from 10% w/w to 40% w/w significantly ($P<0.05$) reduced the mean weight average molecular mass of nanospheres, Table 32.

5.2.5 DETERMINATION OF THE THERMAL CHARACTERISTICS OF UNLOADED AND THEORETICAL 10%, 20%, 30% AND 40% w/w ADMIRE® LOADED PHBHV-DIOL AND DIBLOCK NANOSPHERES, PRIOR TO USE IN RELEASE STUDIES

The thermal characteristics of freshly fabricated unloaded PHBHV-Diol and Diblock nanospheres were compared with those of theoretical 10%, 20%, 30% and 40% w/w Admire® loaded nanospheres, using the methods described in Section 2.2.10, page 64. The thermal characteristics of unloaded and Admire® loaded nanospheres are summarised in Table 33, below.

TABLE 33 - THE GLASS TRANSITION TEMPERATURE (Tg), RECRYSTALLISATION TEMPERATURE AND MELTING POINTS OF UNLOADED AND 10%, 20%, 30% AND 40% w/w ADMIRE® LOADED PHBHV-DIOL AND DIBLOCK NANOSPHERES PRIOR TO USE IN RELEASE STUDIES (mean values, n=2)

THEORETICAL % LOADING	POLYMER	Tg (°C)	RECRYSTALLISATION (°C)	MELTING POINT 1 (°C)	MELTING POINT 2 (°C)
0	PHBHV-DIOL	-12	55	80	99
10	PHBHV-DIOL	-15	58	79	94
20	PHBHV-DIOL	-14	60	77	93
30	PHBHV-DIOL	-15	62	75	90
40	PHBHV-DIOL	-13	65	71	84
0	DIBLOCK	36	61	138	152
10	DIBLOCK	37	64	137	152
20	DIBLOCK	39	66	132	151
30	DIBLOCK	35	67	130	151
40	DIBLOCK	37	69	128	150

Irrespective of the theoretical percentage Admire® loading, the Tg of PHBHV-Diol nanospheres is considerably lower than that of Diblock nanospheres, Table 33.

Irrespective of the fabrication polymer, increasing the theoretical percentage Admire® loading appears to have no real effect on the respective values of Tg.

The recrystallisation temperature of unloaded Diblock nanospheres is marginally higher than that of unloaded PHBHV-Diol nanospheres. Irrespective of the fabrication polymer, Admire® loading appears to increase the recrystallisation temperature with highest recrystallisation temperatures appearing with theoretical 40% w/w Admire® loading, Table 33. The melting point temperatures were much higher for unloaded Diblock nanospheres than for unloaded PHBHV-Diol nanospheres and irrespective of fabrication polymer the melting point temperatures generally appear to decrease with theoretical percentage Admire® loading, Table 33.

5.2.6 DETERMINATION OF THE MOISTURE CONTENT OF FREEZE-DRIED UNLOADED AND THEORETICAL 10%, 20%, 30% AND 40% w/w ADMIRE® LOADED PHBHV-DIOL AND DIBLOCK NANOSPHERES PRIOR TO USE IN RELEASE STUDIES

The moisture content of freeze-dried nanosphere preparations was determined using thermogravimetric analysis as described in Section 2.2.11, page 66 and the results are shown in Table 34, below.

TABLE 34 - MOISTURE CONTENT OF FREEZE-DRIED UNLOADED AND THEORETICAL 10%, 20% 30% AND 40% w/w ADMIRE® LOADED PHBHV-DIOL AND DIBLOCK NANOSPHERES PRIOR TO USE IN RELEASE STUDIES (mean values ± SEM, n=3)

THEORETICAL % ADMIRE LOADING	POLYMER	% MOISTURE CONTENT
0	PHBHV-DIOL	0.26 ± 0.04
10	PHBHV-DIOL	0.28 ± 0.1
20	PHBHV-DIOL	0.37 ± 0.05
30	PHBHV-DIOL	0.25 ± 0.1
40	PHBHV-DIOL	0.34 ± 0.2
0	DIBLOCK	0.32 ± 0.1
10	DIBLOCK	0.47 ± 0.1
20	DIBLOCK	0.36 ± 0.14
30	DIBLOCK	0.40 ± 0.2
40	DIBLOCK	0.31 ± 0.04

Moisture content analysis showed that there was no statistically significant difference between the moisture content of unloaded nanospheres and Admire® loaded nanospheres. The freeze-drying process employed effectively removed the majority of the moisture.

5.2.7 DETERMINATION OF THE RESIDUAL PVA CONTENT OF UNLOADED AND THEORETICAL 10%, 20%, 30% AND 40% w/w ADMIRE® LOADED PHBHV-DIOL AND DIBLOCK NANOSPHERES PRIOR TO USE IN RELEASE STUDIES

Determination of the residual PVA content of unloaded and Admire® loaded nanospheres was carried out using the method described in Section 2.2.12, page 67. The theoretical percentage Admire® loading did not affect the percentage of residual PVA in nanospheres irrespective of the fabrication polymer used and hence only the mean overall percentage of residual PVA has been given in Table 35, below.

TABLE 35 - OVERALL MEAN PERCENTAGE RESIDUAL PVA IN PHBHV-DIOL AND DIBLOCK NANOSPHERES PRIOR TO USE IN RELEASE STUDIES (mean values ± SEM, n=15)

POLYMER	% RESIDUAL PVA (n=6 ± SEM)
PHBHV-DIOL	12.5 ± 1
DIBLOCK	12.9 ± 0.6

The overall mean percentage of residual PVA in all nanospheres fabricated from either PHBHV-Diol or Diblock was approximately 12-13 % of the total mass of freeze dried product. Levels of residual PVA in microsphere and nanosphere preparations are not frequently published in the literature, but microsphere preparations containing up to 10% of the total mass of freeze dried product have been reported (Leroux *et al*, 1995). Since residual PVA is approximately linearly related to the specific surface area of the particles (Alléman *et al*, 1993), the levels of residual PVA determined in nanosphere preparations in the present work are consistent with these observations.

5.2.8 DETERMINATION OF RESIDUAL DICHLOROMETHANE IN UNLOADED AND THEORETICAL 10%, 20%, 30% AND 40% w/w ADMIRE® LOADED PHBHV-DIOL AND DIBLOCK NANOSPHERES

Gas-liquid chromatography was used to measure the concentration of residual DCM within freshly fabricated, freeze-dried nanospheres using the method described in Section 2.2.13, page 69. The results of GLC analysis have been summarised in Table 36, overleaf.

TABLE 36 - RESIDUAL DCM IN UNLOADED AND THEORETICAL 10%, 20%, 30% AND 40% w/w ADMIRE® LOADED PHBHV-DIOL AND DIBLOCK NANOSPHERES (mean values ± SEM, n=3)

THEORETICAL % ADMIRE® LOADING	POLYMER	RESIDUAL DCM (ppm)
0	PHBHV-DIOL	0
10	PHBHV-DIOL	10.47 ± 0.45[a]
20	PHBHV-DIOL	10.48 ± 0.32[a]
30	PHBHV-DIOL	10.74 ± 1.8[a]
40	PHBHV-DIOL	10.74 ± 0.47[a]
0	DIBLOCK	0
10	DIBLOCK	10.43 ± 0.36[a]
20	DIBLOCK	11 ± 0.67[a]
30	DIBLOCK	11.48 ± 1.4[a]
40	DIBLOCK	10.62 ± 0.5[a]

a, significantly increased ($P<0.05$) compared with unloaded nanospheres fabricated using the same polymer.

Unloaded nanospheres, irrespective of fabrication polymer, contained no detectable residual solvent. It had presumably been removed by freeze-drying. However, Admire® loaded nanospheres, irrespective of the fabrication polymer used, contained detectable levels of residual DCM amounting to some 10 and 11ppm, Table 36. The residual DCM concentrations measured were all considerably below the recommended UK limits for residual solvent in pharmaceutical preparations, which are set at 250ppm for short-term exposure, and 100ppm for long-term exposure. The levels determined in the present work are also considerably below the acceptable US limits which are set at 500ppm and 2000ppm for long and short-term exposure, respectively.

5.2.9 DETERMINATION OF TOTAL AMOUNT OF ADMIRE® (mg) LOST INTO NANOSPHERE WASHES DURING FABRICATION

Determination of the concentration of Admire® lost from nanosphere preparations into the centrifugation supernatants during washing was carried out as described in Section 2.2.20, page 74. The results of the determinations have been summarised in Table 37, below.

TABLE 37 – TOTAL AMOUNT OF ADMIRE® LOST INTO NANOSPHERE WASHES DURING FABRICATION (mean values ± SEM, n=12)

THEORETICAL % LOADING	POLYMER	MEAN WEIGHT OF ADMIRE® LOST (mg)
10	PHBHV-DIOL	14.74 ± 0.32
20	PHBHV-DIOL	24.77 ± 0.44
30	PHBHV-DIOL	27.01 ± 0.1
40	PHBHV-DIOL	28.33 ± 0.1[b]
10	DIBLOCK	17.23 ± 0.75[a]
20	DIBLOCK	27.03 ± 2.25
30	DIBLOCK	38.39 ± 1.92[a]
40	DIBLOCK	47.74 ± 2.6[ab]

a, significantly increased ($P<0.05$) compared with similarly Admire® loaded PHBHV-Diol nanospheres.
b, significantly increased ($P<0.05$) compared with theoretical 10% w/w Admire® loaded nanospheres fabricated with the same polymer.

From the overall mean total amount of Admire® lost from the nanospheres after 3 cycles of washes it can be seen that there is a positive correlation between the theoretical percentage loading of Admire®, and the overall mean total loss of Admire® after these cycles of washes. Admire® loaded Diblock nanospheres lost significantly greater amounts of Admire® during the 3 cycles of washes than PHBHV-Diol nanospheres, Table 37. Irrespective of the fabrication polymer used, increasing the theoretical percentage Admire® loading significantly increased the amount of Admire® lost into the washing medium of 3 cycles of harvesting and washing, Table 37. The 30 % w/w Diblock nanospheres lost on average approximately 15 % more Admire® than the 30 % w/w PHBHV-Diol nanospheres and 40% w/w Diblock nanospheres approximately 19 % more than the equivalent PHBHV-Diol nanospheres after 3 cycles of harvesting and washing, Table 37.

5.2.10 DETERMINATION OF THE NANOENCAPSULATION EFFICIENCY AND THE TOTAL AMOUNT OF ADMIRE® ENCAPSULATED IN 100 mg OF THEORETICAL 10%, 20%, 30% AND 40% w/w ADMIRE® LOADED PHBHV-DIOL AND DIBLOCK NANOSPHERES

The nanoencapsulation efficiency for Admire® loaded nanospheres was determined using isopropanol as described in Section 2.2.21, page 74. This method, however, did not prove to be very accurate for determination of the nanoencapsulation efficiency of Admire®. The main problem was the low solubility of Admire® in isopropanol (1-2 g/l). Crushing and grinding the Admire® loaded nanospheres in an

attempt to release as much of the entrapped Admire® as possible, prior to suspension in isopropanol, also proved to be ineffective. In order to give some indication of the maximum amount of Admire® that might be encapsulated, the known amount of Admire® lost in the washing cycles was subtracted from the original encapsulation quantity. From this calculated maximum amount of Admire® remaining and the known percentage yield the nanoencapsulation efficiency for 100 mg of nanospheres was calculated. The results have been summarised in Table 38, below.

TABLE 38 – THE APPROXIMATE NANOENCAPSULATION EFFICIENCY AND TOTAL AMOUNT OF ADMIRE® INCORPORATED INTO 100 mg OF THEORETICAL 10%, 20%, 30% AND 40% w/w ADMIRE® LOADED PHBHV-DIOL AND DIBLOCK NANOSPHERES

(mean values ± SEM, n=12)

THEORETICAL % LOADING	POLYMER	COMPUTED MAXIMUM ADMIRE® LOADING IN 100 mg (mg)	NANOENCAPSULATION EFFICIENCY (%)
10	PHBHV-DIOL	4.10 ± 0.375	41.00
20	PHBHV-DIOL	10.09 ± 0.83	50.46
30	PHBHV-DIOL	19.20 ± 0.87	63.40
40	PHBHV-DIOL	28.67 ± 1.8	71.67[a]
10	DIBLOCK	3.10 ± 0.669	31.00
20	DIBLOCK	9.10 ± 2.9	45.50
30	DIBLOCK	14.64 ± 2.17	48.80
40	DIBLOCK	20.90 ± 5.7	52.25[a]

a, significantly elevated ($P<0.05$) compared with theoretical 10% w/w Admire® loaded nanospheres, irrespective of the fabrication polymer used.

The Admire® nanoencapsulation efficiency and the computed maximum Admire® loading increased significantly ($P<0.05$) with theoretical percentage Admire® loading, irrespective of the fabrication polymer used. The capacity of the two polymers to nanoencapsulate Admire® was not significantly different at all theoretical percentage Admire® loadings used.

5.2.11 *IN VITRO* RELEASE OF ADMIRE® FROM THEORETICAL 10%, 20%, 30% AND 40% w/w ADMIRE® LOADED PHBHV-DIOL AND DIBLOCK NANOSPHERES INTO RAINWATER AT 4°C AND 23°C

In vitro release was carried out as described in Section 2.2.22, page 75.
Unloaded PHBHV-Diol and Diblock nanospheres were incubated alongside the Admire® loaded nanospheres to act as controls.
Examples of daily release profiles for 10% and 40% w/w Admire® loaded PHBHV-Diol nanospheres and 10% and 40% w/w Admire® loaded Diblock nanospheres over 37 days incubation into rural rainwater at 4°C and 23°C are illustrated in Figures 39 to 42 below. The remainder of the daily release profiles are shown in Appendix Section 3.2, page 274.

Generally the higher the theoretical percentage Admire® loading, the higher the initial concentration of Admire® released from both PHBHV-Diol and Diblock polymer nanospheres.
It can also be seen that, with the exception of theoretical 10% w/w Admire® loaded nanospheres fabricated from both PHBHV-Diol and Diblock polymers (Figures 39 and 41), initial release is slightly higher for both PHBHV-Diol and Diblock nanospheres incubated at 23°C, compared to those incubated at 4°C. This is presumably due to the increased solubility of Admire® at the higher temperature.
PHBHV-Diol nanospheres loaded with theoretical 20% w/w Admire® (Appendix Section 3.2, Page 274) and theoretical 30% w/w Admire® (Appendix Section 3.2, page 274), incubated at both 4°C and 23°C, showed initial stable release followed by spike releases after 5 and 12 days, followed again by sustained release over the remainder of the 37 day release period. These short bursts only lasted for one day in each case.

Diblock nanospheres loaded with theoretical 40% w/w Admire® and incubated at 4°C, Figure 42, showed initial sustained release followed by a single one day spike release at day 5, followed again by sustained release over the remainder of the 37 day incubation period. In contrast, Diblock nanospheres loaded with theoretical 40% w/w Admire® and incubated at 23°C, Figure 42, showed a drop in release rate from day 2 to day 8, followed by a sustained increase in Admire® release lasting from day 9 to day 27 of the incubation period. Diblock nanospheres loaded with theoretical 30% w/w Admire® (Appendix Section 3.2, Page 274) also showed one day spike releases at both 5 and 12 days when incubated at 4°C, but only at day 5 when incubated at 23°C.

Profiles for theoretical 10% w/w Admire® (Figures 39 and 41) and theoretical 20% w/w Admire® (Appendix Section 3.2, Page 274) all showed an initial drop in Admire® release in the initial part of the release profile, followed by small periods of release at 4-5 days, followed by further sustained release.

All Admire® loaded nanospheres fabricated from either PHBHV-Diol or Diblock polymers were able to release detectable amounts of Admire® for up to 37-days.

FIGURE 39 – DAILY ADMIRE RELEASE PROFILES FOR 10% w/w ADMIRE LOADED PHBHV-DIOL NANOSPHERES INTO RURAL RAINWATER AT 4 DEGREES CELCIUS AND 23 DEGREES CELCIUS (mean values ± SEM, n=12)

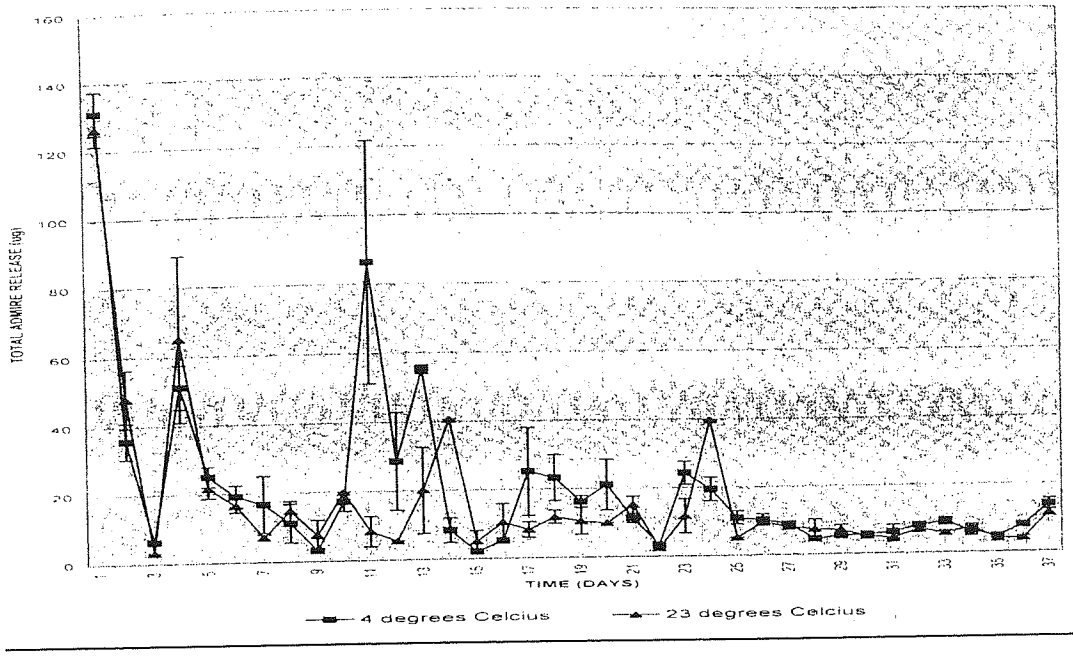

FIGURE 40 – DAILY ADMIRE RELEASE PROFILES FOR 40% w/w ADMIRE LOADED PHBHV-DIOL NANOSPHERES INTO RURAL RAINWATER AT 4 DEGREES CELCIUS AND 23 DEGREES CELCIUS (mean values ± SEM, n=12)

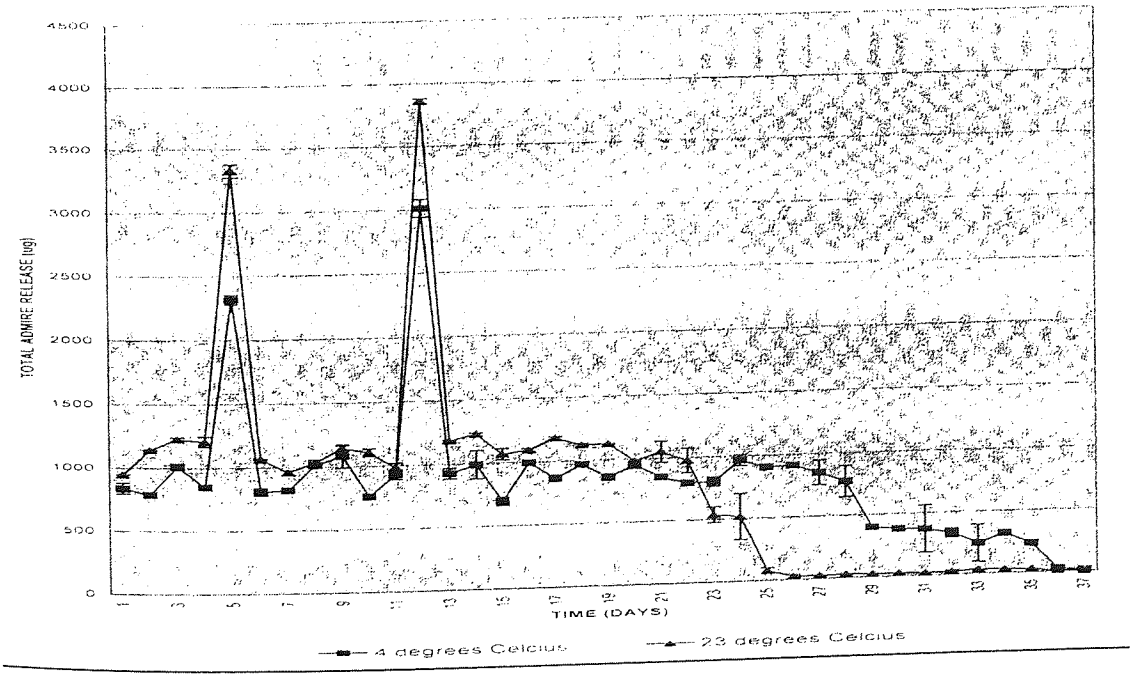

FIGURE 41 – DAILY ADMIRE RELEASE PROFILES FOR 10% w/w ADMIRE LOADED DIBLOCK NANOSPHERES INTO RURAL RAINWATER AT 4 DEGREES CELCIUS AND 23 DEGREES CELCIUS (mean values ± SEM, n=12)

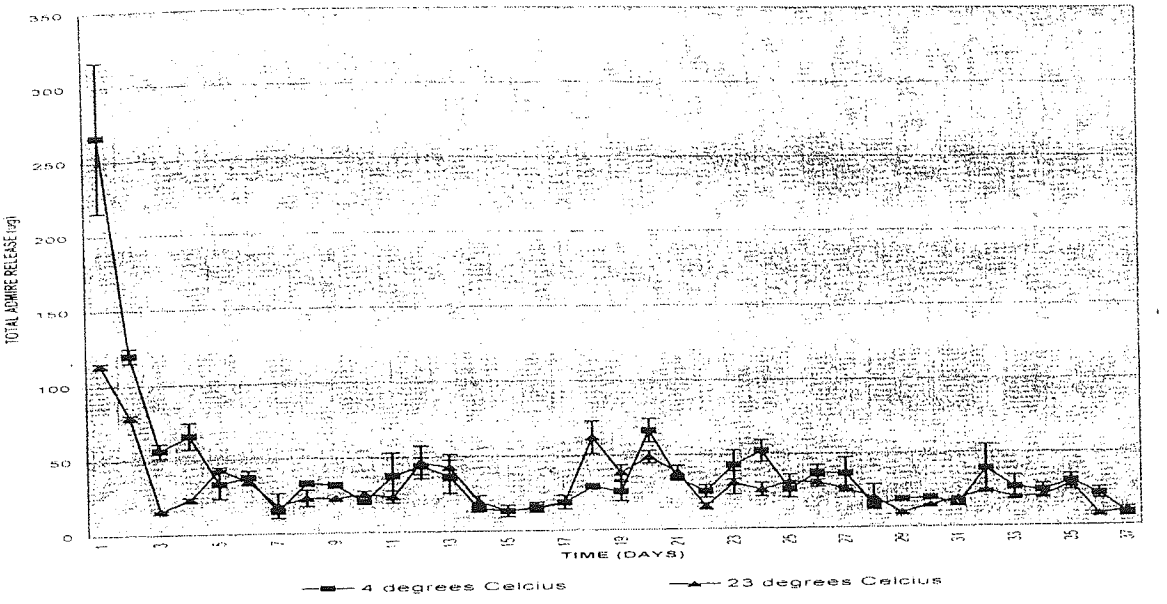

FIGURE 42 – DAILY ADMIRE RELEASE PROFILES FOR 40% w/w ADMIRE LOADED DIBLOCK NANOSPHERES INTO RURAL RAINWATER AT 4 DEGREES CELCIUS AND 23 DEGREES CELCIUS (mean values ± SEM, n=12)

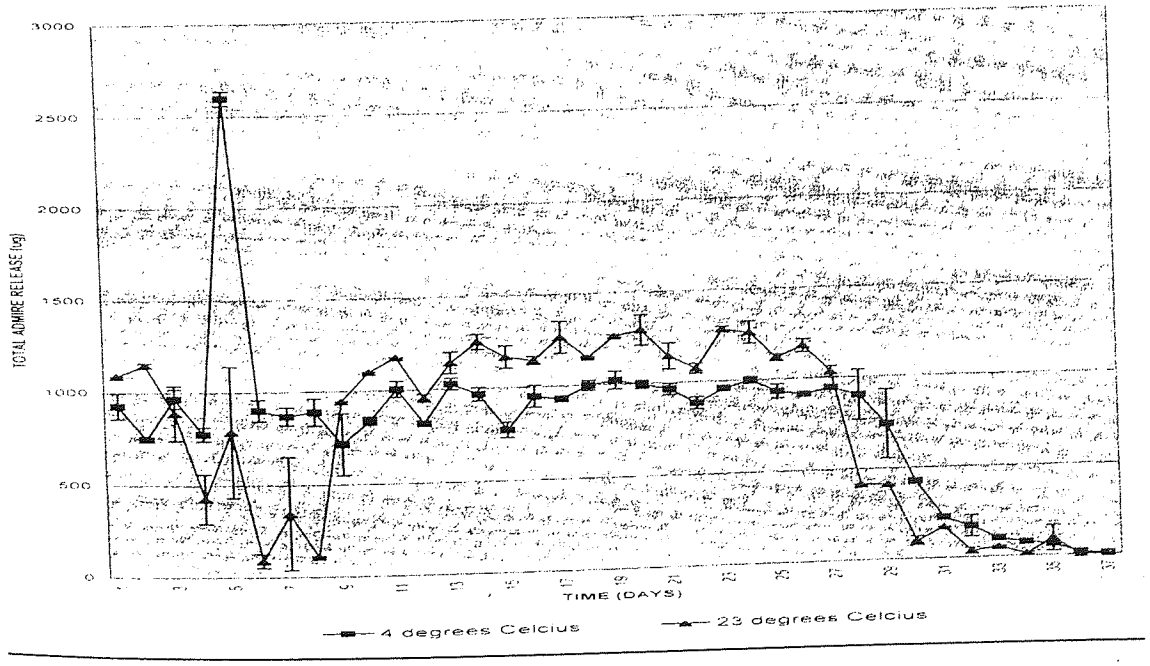

Representative examples of total cumulative Admire® release profiles from 10% and 40% w/w Admire® loaded PHBHV-Diol nanospheres and 10% and 40% w/w Admire® loaded Diblock nanospheres over 37 days incubation in rural rainwater at 4°C and 23°C are shown in Figures 43 to 46. The total cumulative Admire® release profiles for 20% w/w and 30% w/w Admire® loaded nanospheres at 4°C and 23°C are shown in the Appendix Section 3.3, page 276.

Theoretical 40% w/w Admire® loaded nanospheres fabricated from both PHBHV-Diol and Diblock polymer and incubated at 4°C and 23°C released the highest concentration of Admire® over the 37 day release period, Figures 44 and 46. The 10% w/w Admire® loaded nanospheres fabricated from both PHBHV-Diol and Diblock polymer and incubated at either 4°C or 23°C released the lowest concentration of Admire® over the 37 day release period, Figures 43 and 45.

Irrespective of the fabrication polymer, the total cumulative release of Admire® tended to increase significantly with increasing theoretical percentage Admire® loading at both 4°C and 23°C. Increasing the temperature from 4°C to 23°C did not significantly influence the total cumulative release of Admire® from nanospheres fabricated from the same polymer, Table 39. However, the total cumulative release of Admire® from Diblock nanospheres was marginally lower than that from PHBHV-Diol nanospheres at both 4°C and 23°C and theoretical 20%, 30% and 40% w/w Admire® loaded nanospheres, Table 39. Nanospheres fabricated from either PHBHV-Diol or Diblock polymer released approximately the same total cumulative quantity of Admire® for each theoretical percentage loading. The results of total cumulative release after the 37-day incubation period for all Admire® loaded nanosphere samples can be seen in Table 39, overleaf.

No Admire® like activity was detected from unloaded nanospheres fabricated from the two polymers used to fabricated Admire® loaded nanospheres. Consequently values for unloaded nanospheres do not feature on any profiles or in any tables.

FIGURE 43 – TOTAL CUMULATIVE RELEASE PROFILES FOR 10% w/w ADMIRE LOADED PHBHV-DIOL NANOSPHERES INTO RURAL RAINWATER AT 4 DEGREES CELCIUS AND 23 DEGREES CELCIUS (mean values ± SEM, n=12)

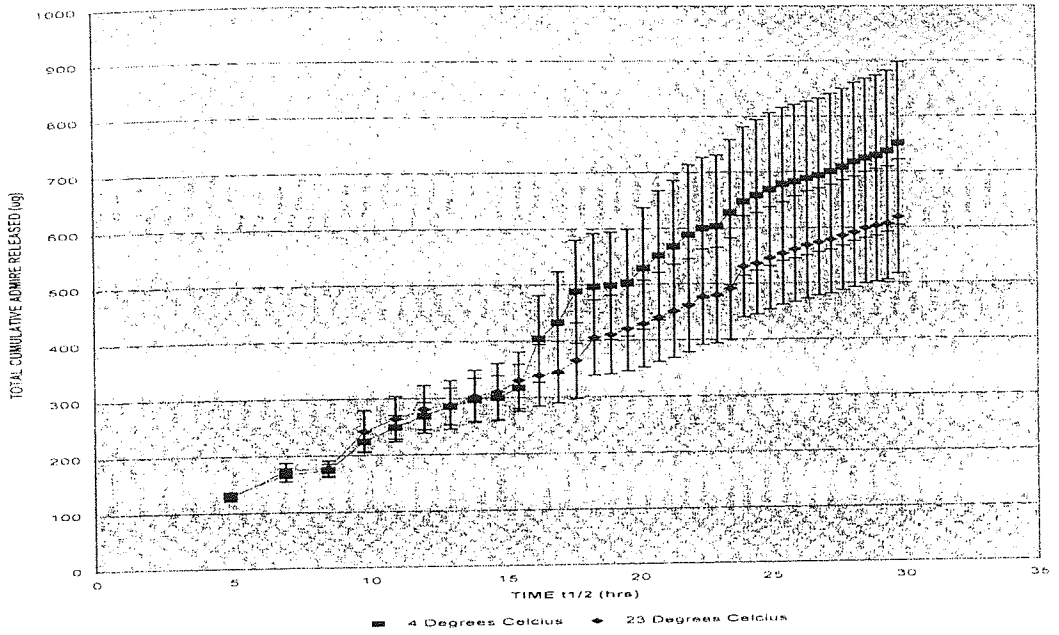

FIGURE 44 – TOTAL CUMULATIVE RELEASE PROFILES FOR 40% w/w ADMIRE LOADED PHBHV-DIOL NANOSPHERES INTO RURAL RAINWATER AT 4 DEGREES CELCIUS AND 23 DEGREES CELCIUS (mean values ± SEM, n=12)

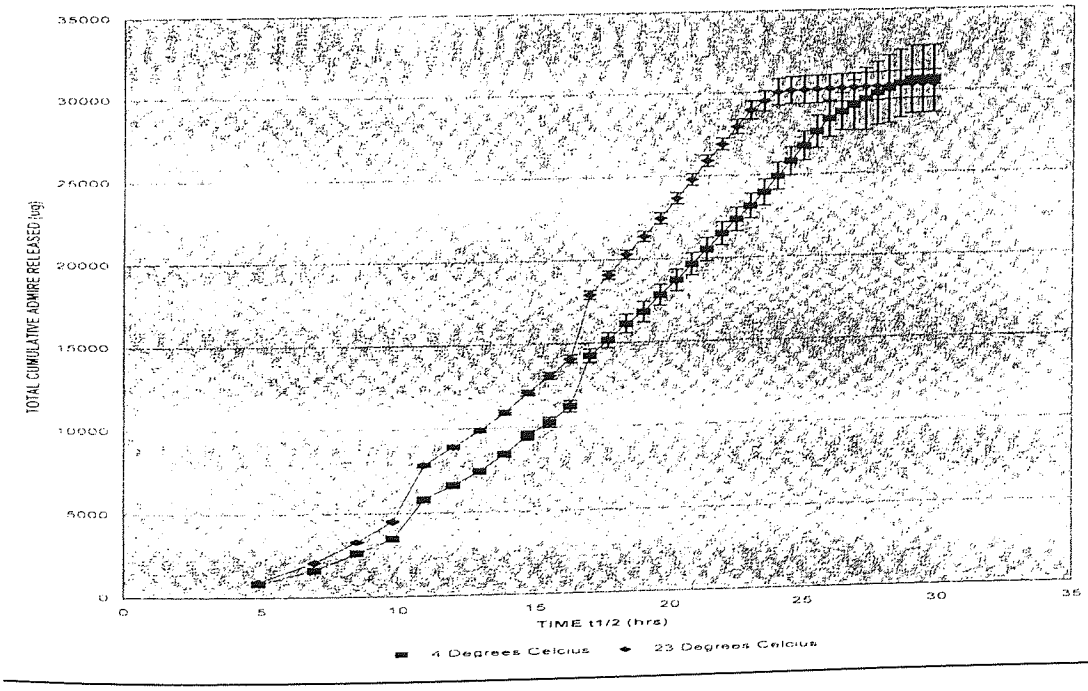

FIGURE 45 – TOTAL CUMULATIVE RELEASE PROFILES FOR 10% w/w ADMIRE LOADED DIBLOCK NANOSPHERES INTO RURAL RAINWATER AT 4 DEGREES CELCIUS AND 23 DEGREES CELCIUS (mean values ± SEM, n=12)

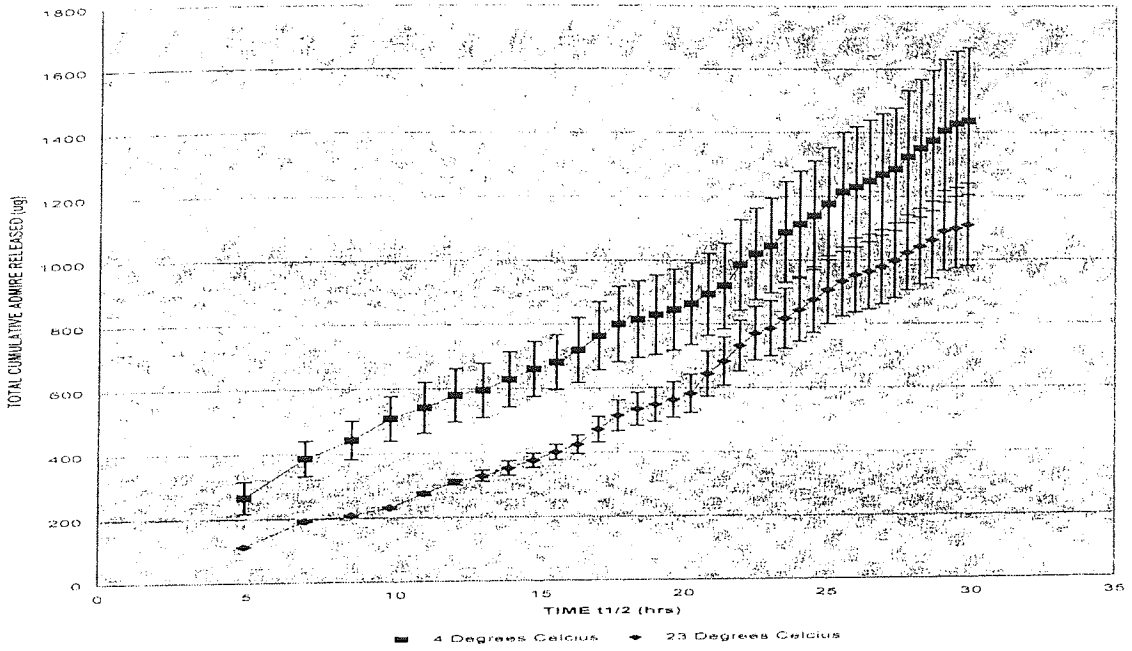

FIGURE 46 – TOTAL CUMULATIVE RELEASE PROFILES FOR 10% w/w ADMIRE LOADED DIBLOCK NANOSPHERES INTO RURAL RAINWATER AT 4 DEGREES CELCIUS AND 23 DEGREES CELCIUS (mean values ± SEM, n=12)

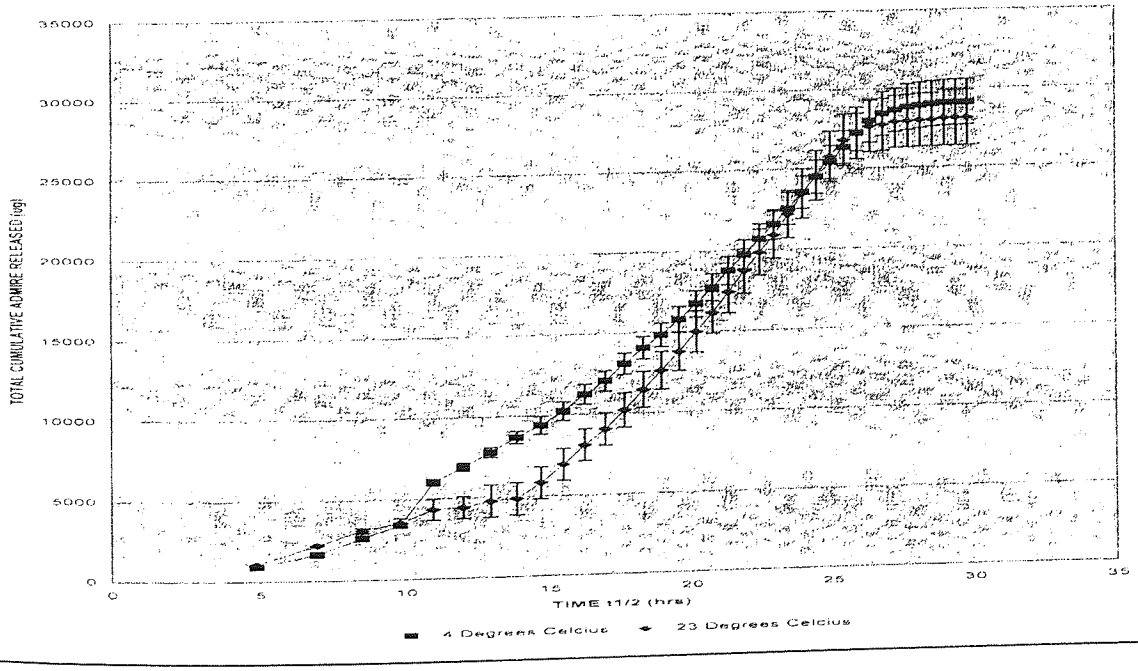

TABLE 39 - TOTAL CUMULATIVE ADMIRE® RELEASE AFTER 37 DAYS INCUBATION IN RURAL RAINWATER AT 4°C AND 23°C FROM THEORETICAL 10%, 20%, 30% AND 40% w/w ADMIRE® LOADED PHBHV-DIOL AND DIBLOCK NANOSPHERES (mean values ± SEM, n=3)

THEORETICAL % ADMIRE® LOADING	POLYMER	INCUBATION TEMPERATURE (°C)	TOTAL CUMULATIVE ADMIRE® (mg)
10	PHBHV-DIOL	4	0.75 ± 0.15
20	PHBHV-DIOL	4	3.65 ± 0.54
30	PHBHV-DIOL	4	15.10 ± 0.95
40	PHBHV-DIOL	4	30.7 ± 1.5[a]
10	PHBHV-DIOL	23	0.62 ± 0.1
20	PHBHV-DIOL	23	4.23 ± 0.23
30	PHBHV-DIOL	23	18.33 ± 1.03
40	PHBHV-DIOL	23	30.38 ± 0.84[a]
10	DIBLOCK	4	1.44 ± 0.23
20	DIBLOCK	4	3.02 ± 0.55
30	DIBLOCK	4	10.74 ± 1.03
40	DIBLOCK	4	29.11 ± 1.4[a]
10	DIBLOCK	23	1.11 ± 0.1
20	DIBLOCK	23	3.87 ± 0.56
30	DIBLOCK	23	11.7 ± 1.17
40	DIBLOCK	23	28.13 ± 1.8[a]

a, significantly increased ($P<0.05$) compared with theoretical 10% w/w Admire® loaded nanospheres fabricated using the same polymer and incubated at the same temperature.

5.2.13 MEAN PERCENTAGE HARVEST AND PERCENTAGE WEIGHT LOSS FROM UNLOADED AND THEORETICAL 10%, 20%, 30% AND 40% w/w ADMIRE® LOADED PHBHV-DIOL AND DIBLOCK NANOSPHERES AFTER USE IN RELEASE STUDIES

After use in Admire® release studies, all nanospheres samples were freeze-dried as described in Section 2.2.5, page 57. The samples were then weighed accurately to determine the percentage weight loss that had occurred over the 37 day release period. The results have been summarised in Table 40, overleaf.

TABLE 40 - PERCENTAGE WEIGHT LOSS FROM UNLOADED AND THEORETICAL 10%, 20%, 30% AND 40% w/w ADMIRE® LOADED PHBHV-DIOL AND DIBLOCK NANOSPHERES AFTER INCUBATION IN RURAL RAINWATER AT 4°C AND 23°C FOR 37 DAYS (mean values ± SEM, n=6)

THEORETICAL % LOADING	POLYMER	INCUBATION TEMPERATURE (°C)	INITIAL MEAN WEIGHT (mg)	HARVESTED MEAN WEIGHT (mg)	% WEIGHT LOSS
0	PHBHV-DIOL	4	100 ± 0	82.3 ± 1	18.7 ± 1
10	PHBHV-DIOL	4	100 ± 0	92 ± 1[b]	8 ± 1
20	PHBHV-DIOL	4	100 ± 0	84 ± 2	16 ± 2
30	PHBHV-DIOL	4	100 ± 0	82 ± 3	18 ± 3
40	PHBHV-DIOL	4	100 ± 0	75 ± 2[a]	25 ± 2
0	PHBHV-DIOL	23	100 ± 0	80.4 ± 1	19.6 ± 1
10	PHBHV-DIOL	23	100 ± 0	89 ± 3[b]	11 ± 3
20	PHBHV-DIOL	23	100 ± 0	88 ± 5	12 ± 5
30	PHBHV-DIOL	23	100 ± 0	86 ± 9	14 ± 9
40	PHBHV-DIOL	23	100 ± 0	71 ± 5[a]	29 ± 5
0	DIBLOCK	4	100 ± 0	87.8 ± 1	12.2 ± 1
10	DIBLOCK	4	100 ± 0	88 ± 3	12 ± 3
20	DIBLOCK	4	100 ± 0	87 ± 4	13 ± 4
30	DIBLOCK	4	100 ± 0	85 ± 5	15 ± 5
40	DIBLOCK	4	100 ± 0	74 ± 3[a]	26 ± 3
0	DIBLOCK	23	100 ± 0	84.2 ± 1	15.8 ± 1
10	DIBLOCK	23	100 ± 0	89 ± 1[b]	11 ± 1
20	DIBLOCK	23	100 ± 0	88 ± 1	12 ± 1
30	DIBLOCK	23	100 ± 0	81 ± 4	19 ± 4
40	DIBLOCK	23	100 ± 0	70 ± 8[a]	30 ± 8

a, significantly reduced ($P<0.05$) compared with theoretical 10% w/w Admire® loaded nanospheres fabricated from the same polymers and incubated at the same temperature.

b, significantly increased ($P<0.05$) compared with unloaded nanospheres fabricated from the same polymer and incubated at the same temperature.

Over the incubation period, the mean percentage weight loss was marginally greater from unloaded PHBHV-Diol nanospheres than from unloaded Diblock nanospheres at both 4°C and 23°C.

Theoretical 10% w/w Admire® loading significantly reduced the percentage weight loss from PHBHV-Diol nanospheres at both 4°C and 23°C and from Diblock nanospheres incubated at 23°C, Table 40. Increasing the theoretical percentage Admire® loading from 10% to 40% w/w significantly increased the mean percentage weight loss, irrespective of the fabrication polymer and the incubation temperature used. This might suggest that the majority of the percentage weight loss was attributed to Admire® release from the polymer nanospheres. Increasing the incubation temperature from 4°C to 23°C had no significant effect on the percentage weight loss from unloaded and Admire® loaded nanospheres, irrespective of the fabrication polymer used.

5.2.14 DETERMINATION OF THE MEAN PARTICLE DIAMETER OF UNLOADED AND THEORETICAL 10%, 20%, 30% AND 40% w/w ADMIRE® LOADED PHBHV-DIOL AND DIBLOCK NANOSPHERES AFTER INCUBATION IN RAINWATER AT 4°C AND 23°C FOR 37 DAYS (mean values ± SEM, n=6)

Particle diameter analysis using photon correlation spectroscopy was performed on all nanospheres harvested from Admire® release studies as described in Section 2.2.7, page 58 and the results have been summarised in Table 41, overleaf.

Irrespective of the fabrication polymer, theoretical Admire® loading and incubation temperature, all nanospheres showed a reduction in mean particle diameter following incubation in rural rainwater for 37 days, Table 41. The theoretical percentage loading of Admire®, irrespective of the fabrication polymer, had no significant effect on the percentage decrease in mean particle diameter over the 37 day incubation period.

TABLE 41 - MEAN PARTICLE DIAMETER OF UNLOADED AND THEORETICAL 10%, 20%, 30% AND 40% w/w ADMIRE® LOADED PHBHV-DIOL AND DIBLOCK NANOSPHERES AFTER INCUBATION IN RURAL RAINWATER AT 4°C AND 23°C FOR 37 DAYS (mean values ± SEM, n=6)

POLYMER	THEO. % ADMIRE® LOADING	INCUBATION TEMP. (°C)	MEAN DIAMETER BEFORE (nm)	MEAN DIAMETER AFTER (nm)	% DECREASE IN DIAMETER
PHBHV-DIOL	0	4	275.6 ± 2.1	272.7 ± 6	1.02 ± 6
PHBHV-DIOL	10	4	455.8 ± 31.7	430.7 ± 21.4	5.5 ± 4
PHBHV-DIOL	20	4	521.4 ± 4.6	504.3 ± 7.9	3.3 ± 1.5
PHBHV-DIOL	30	4	578.9 ± 1.9	553.6 ± 4.7	4.37 ± 0.8
PHBHV-DIOL	40	4	624.5 ± 11.4	608.3 ± 16.2[a]	3.1 ± 2
PHBHV-DIOL	0	23	275.6 ± 2.1	269.4 ± 4.2	2.2 ± 4.2
PHBHV-DIOL	10	23	455.8 ± 31.7	427.2 ± 15.8	6.3 ± 3
PHBHV-DIOL	20	23	521.4 ± 4.6	503.2 ± 6.9	3.5 ± 1.3
PHBHV-DIOL	30	23	578.9 ± 1.9	546.1 ± 14.3	5.67 ± 2.5
PHBHV-DIOL	40	23	624.5 ± 11.4	597.4 ± 18[a]	4.34 ± 2.9
DIBLOCK	0	4	328 ± 7.57	322.6 ± 1.4[b]	1.65 ± 1.4
DIBLOCK	10	4	496 ± 7.7	475.5 ± 8.6	4.14 ± 1.7
DIBLOCK	20	4	524.9 ± 4.9	508.7 ± 7	3.09 ± 1.3
DIBLOCK	30	4	594.7 ± 3.9	575.7 ± 3[a]	3.4 ± 0.07
DIBLOCK	40	4	635.9 ± 5.6	609.5 ± 6.5[a]	4.15 ± 1
DIBLOCK	0	23	328 ± 7.57	318.4 ± 6.7[b]	2.9 ± 6.7
DIBLOCK	10	23	496 ± 7.7	471.3 ± 2.4	4.98 ± 0.5
DIBLOCK	20	23	524.9 ± 4.9	505.3 ± 4.2	3.73 ± 0.8
DIBLOCK	30	23	594.7 ± 3.9	563.3 ± 12.7	5.28 ± 2
DIBLOCK	40	23	635.9 ± 5.6	600.3 ± 4.4[a]	5.6 ± 0.07

a, significantly greater in diameter ($P<0.05$) compared with unloaded nanospheres incubated at the same temperature and fabricated from the same polymer.

b, significantly greater in diameter ($P<0.05$) compared with unloaded PHBHV-Diol nanospheres incubated at the same temperature.

5.2.15 DETERMINATION OF THE MEAN ZETA POTENTIAL OF UNLOADED AND THEORETICAL 10%, 20% 30% AND 40% w/w ADMIRE® LOADED PHBHV-DIOL AND DIBLOCK NANOSPHERES AFTER INCUBATION IN RAINWATER AT 4°C AND 23 °C FOR 37 DAYS

Zeta potential measurements were carried out on harvested nanospheres as described in Section 2.2.8, page 59. Temperature had no significant effect on the mean zeta potential of nanospheres, whether Admire® loaded or unloaded or whether fabricated with PHBHV-Diol or Diblock polymer. Only data based on changes in zeta potential caused by increasing the theoretical percentage Admire® loading or using different fabrication polymers have been summarised in Table 42.

TABLE 42 - MEAN ZETA POTENTIALS OF UNLOADED AND THEORETICAL 10%, 20% 30% AND 40% w/w ADMIRE® LOADED PHBHV-DIOL AND DIBLOCK NANOSPHERES BEFORE AND AFTER INCUBATION IN RURAL RAINWATER FOR 37 DAYS (mean values ± SEM, n=12)

POLYMER	THEORETICAL % ADMIRE® LOADING	MEAN ZETA POTENTIAL BEFORE (mV)	MEAN ZETA POTENTIAL AFTER (mV)
PHBHV-DIOL	0	-20.76 ± 0.38	-29.5 ± 0.88[c]
PHBHV-DIOL	10	-9.1 ± 1	-20.6 ± 0.4[c]
PHBHV-DIOL	20	-8.1 ± 1	-15.0 ± 0.3[c]
PHBHV-DIOL	30	-8.1 ± 1	-16.7 ± 0.5[c]
PHBHV-DIOL	40	-9.2 ± 1.8	-13.1 ± 1.4[bc]
DIBLOCK	0	-35.99 ± 0.38	-45 ± 2.19[ac]
DIBLOCK	10	-13.6 ± 1	-20.2 ± 0.1[c]
DIBLOCK	20	-13.4 ± 0.9	-15.0 ± 1[c]
DIBLOCK	30	-13 ± 1.2	-13.3 ± 0.6
DIBLOCK	40	-13.6 ± 2	-14.5 ± 0.6[b]

a, significantly greater negative charge ($P<0.05$) compared with unloaded PHBHV-Diol nanospheres.

b, significantly lower negative charge ($P<0.05$) compared with unloaded nanospheres fabricated using the same polymer.

c, significantly greater negative charge ($P<0.05$) compared with mean zeta potential of corresponding nanospheres prior to incubation in rural rainwater for 37-days.

So, unloaded nanospheres showed the greatest negative charge and the incorporation of Admire®, irrespective of the extent of theoretical percentage Admire® loading, significantly lowered the negative charge on nanospheres fabricated from each of the polymers. The zeta potentials became more negative after 37 days incubation in rural rainwater, irrespective of the theoretical percentage Admire® loading and fabrication polymer, Table 42. With the exception of theoretical 30% w/w and 40% w/w Admire® loaded Diblock nanospheres, incubation in rural rainwater for 37 days resulted in a significantly greater negative charge, irrespective of the fabrication polymer or extent of theoretical percentage Admire® loading, Table 42. This could be due to steric reasons. The loss of the relatively high residue PVA content of the nanospheres during incubation could have played an important role in increasing the negative charge displayed by the nanospheres.

5.2.16 DETERMINATION OF THE WEIGHT AVERAGE MOLECULAR MASS (Mw) OF UNLOADED AND THEORETICAL 10%, 20%, 30% AND 40% w/w ADMIRE® LOADED PHBHV-DIOL AND DIBLOCK NANOSPHERES AFTER INCUBATION IN RURAL RAINWATER AT 4°C AND 23 °C FOR 37 DAYS

The weight average molecular mass was determined using gel permeation chromatography as described in Section 2.2.9, page 62. Preliminary analysis of the results confirmed that temperature had no significant effect upon the weight average molecular mass of unloaded and Admire® loaded nanospheres fabricated from either PHBHV-Diol or Diblock polymer, prior to use in and after being harvested from release studies after 37-days incubation. The results summarised in Table 43 have been presented in a simplified fashion to take account of this.

TABLE 43 – THE MEAN WEIGHT AVERAGE MOLECULAR MASS OF UNLOADED AND THEORETICAL 10%, 20%, 30% AND 40% w/w ADMIRE® LOADED PHBHV-DIOL AND DIBLOCK NANOSPHERES BEFORE AND AFTER INCUBATION IN RURAL RAINWATER FOR 37 DAYS (mean values ± SEM, n=3)

POLYMER	THEORETICAL % ADMIRE® LOADING	MEAN Mw BEFORE (DALTONS)	MEAN Mw AFTER (DALTONS)	MEAN DECREASE IN Mw (DALTONS)
PHBHV-DIOL	0	8138 ± 625	3741 ± 15	4397 ± 15
PHBHV-DIOL	10	2773 ± 15	1835 ± 15	938 ± 15
PHBHV-DIOL	20	2379 ± 55	1685 ± 15	694 ± 15
PHBHV-DIOL	30	1572 ± 21	1258.5 ± 56	313.5 ± 56
PHBHV-DIOL	40	1003 ± 6	863.5 ± 122[b]	139.5 ± 122[b]
DIBLOCK	0	58 914 ± 1067	57 773 ± 240[a]	1141 ± 240
DIBLOCK	10	58 526 ± 2452	55 250 ± 750	3376 ± 750
DIBLOCK	20	53 900 ± 2939	48 250 ± 1050	5650 ± 1050
DIBLOCK	30	48 575 ± 712	43250 ± 150	5325 ± 150
DIBLOCK	40	37 450 ± 56	35 688 ± 1463[b]	1763 ± 1463[b]

a. significantly greater ($P<0.05$) compared with unloaded PHBHV-Diol nanospheres.

b. significantly reduced ($P<0.05$) compared with theoretical 10% w/w Admire® loaded nanospheres fabricated from the same polymer.

The mean weight average molecular weight of unloaded and Admire® loaded nanospheres, irrespective of the fabrication polymer, decrease as the theoretical percentage Admire® loading increases for both fabrication polymers. The reduction in mean weight average molecular weight of nanospheres before use in release studies and after being harvested after 37 days incubation for all Admire® loaded PHBHV-Diol and Diblock nanospheres was extremely significant, Table 43.

5.2.17 DETERMINATION OF THE GLASS TRANSITION TEMPERATURE (Tg), RECRYSTALLISATION TEMPERATURE AND MELTING POINTS OF UNLOADED AND THEORETICAL 10%, 20%, 30% AND 40% w/w ADMIRE® LOADED PHBHV-DIOL AND DIBLOCK NANOSPHERES, AFTER INCUBATION IN RURAL RAINWATER FOR 37 DAYS

DSC analysis was performed on nanospheres harvested from release studies using the method described in Section 2.2.10, page 64. These data have been summarised in Table 44. Since the incubation temperature in release studies had no significant effect upon the thermal characteristics of the nanospheres, this parameter has been omitted from Table 44.

TABLE 44 - THE GLASS TRANSITION TEMPERATURE (Tg), RECRYSTALLISATION TEMPERATURE AND MELTING POINTS OF UNLOADED AND THEORETICAL 10%, 20%, 30% AND 40% w/w ADMIRE® LOADED PHBHV-DIOL AND DIBLOCK NANOSPHERES AFTER INCUBATION IN RURAL RAINWATER FOR 37 DAYS (mean values, n=2)

POLYMER	THEO. % ADMIRE® LOADING	Tg (°C)	RECRYSTALLISATION TEMPERATURE (°C)	MELTING POINT 1 (°C)	MELTING POINT 2 (°C)
PHBHV-DIOL	0	-6	56	90	105
PHBHV-DIOL	10	-9	62	87	105
PHBHV-DIOL	20	-9	64	85	101
PHBHV-DIOL	30	-8	67	82	97
PHBHV-DIOL	40	-10	71	80	94
DIBLOCK	0	40	63	140	156
DIBLOCK	10	41	66	140	156
DIBLOCK	20	40	67	135	154
DIBLOCK	30	39	69	134	153
DIBLOCK	40	40	71	132	155

The thermal profiles for harvested unloaded and Admire® loaded nanospheres incubated for 37 days show similar patterns to the pre-release nanospheres (Table 33, page 138), irrespective of the fabrication polymer used, Table 44. Recrystallisation temperature increased with increased theoretical percentage Admire® loading, while in contrast the two melting points tended to decrease. The recrystallisation temperature and the two melting point temperatures for unloaded and theoretical percentage Admire® loaded nanospheres, irrespective of the fabrication polymers used, increased marginally after 37 days incubation, Table 44. Irrespective of the theoretical percentage Admire® loading, the Tg of PHBHV-Diol nanospheres remains considerably lower than that of Diblock nanospheres following incubation in rural rainwater for 37 days.

Irrespective of the fabrication polymer, increasing the theoretical percentage Admire® loading appears to have no real effect on the respective values of Tg. The melting point of Admire® is 144°C but is not seen on the thermal profiles because the drug is not crystalline.

5.2.18 DETERMINATION OF THE RESIDUAL PVA CONTENT OF UNLOADED AND THEORETICAL 10%, 20%, 30% AND 40% w/w ADMIRE® LOADED PHBHV-DIOL AND DIBLOCK NANOSPHERES, AFTER INCUBATION IN RAINWATER AT 4°C AND 23°C FOR 37 DAYS

Residual PVA was measured by colorimetric assay as described in Section 2.2.12, Page 67. Following incubation in rural rainwater at either 4°C or 23°C for 37-days, no residual PVA was detectable in any of the harvested nanosphere samples, irrespective of either the fabrication polymer or theoretical percentage Admire® loading used. It may be that any residual PVA was dissolved in the rural rainwater by periodic aggitation, during the Admire® release period.

CHAPTER 6

THE INCORPORATION INTO AND RELEASE OF GIBBERELLIC ACID POTASSIUM SALT (GA_3K) FROM NANOSPHERES FABRICATED FROM NOVEL MONSANTO POLYALKANOATES

6.1 INTRODUCTION

6.1.1 DISCOVERY OF GIBBERELLINS

The gibberellins are tetracyclic diterpene plant growth regulators which influence a range of developmental processes in higher plants including stem elongation, germination, dormancy, flowering, sex expression and enzyme induction (Salisbury and Ross, 1992). Plants that either cannot synthesise sufficient gibberellins, or that are unable to respond to them, are developmental dwarfs. Dwarf plants such as dwarf peas and dwarf French beans are popular in agriculture and horticulture because they are more manageable than their taller zenotypes, making them less likely to be damaged by wind and rain.

The first observations of the effects of gibberellins can be traced back to Japanese farmers who noticed a phenomenon of abnormal elongation in certain rice plants, which soon became unhealthy and sterile (Riley, 1987). The Japanese gave this disease the name 'bakanae' meaning foolish seedling. In 1898, the agent responsible for the disease 'bakanae' was shown by the Japanese plant pathologist, Shotaro Hori, to be a fungal pathogen belonging to the genus *Fusarium* (Hori, 1898). In 1926, Eiichi Kurusawa discovered that culture filtrates from dried rice seedlings caused considerable elongation in rice plants. From this he concluded that 'bakanae' was caused by a secreted chemical substance that stimulated shoot elongation, inhibited chlorophyll formation and suppressed root growth (Kurosawa, 1926). He also concluded that the substance was secreted by the fungal species *Gibberella fujikuroi.* It was not until 1935 that Teiyiro Yabuta was able to isolate the active compound from *Gibberella fujikuroi,* which he named 'gibberellin'. This compound was found to stimulate growth when applied to rice roots (Yabuta, 1935). The work on gibberellins was put on hold during World War II, and at that point in time the Western civilisation did not have access to any of these early observations (Arteca, 1996). In the early 1950s workers in both the US and UK discovered the early Japanese papers and commenced work on gibberellins. In the US, John Mitchell reported optimum fermentation procedures for the fungus, as well as the effects of fungal extracts on the growth of broad bean (*Vicia faba*) seedlings (Mitchell and Angel, 1951). At the Akers Research Laboratories (ICI) in the UK, British workers isolated an entirely new compound from *G. fujikuroi* and named it gibberellic acid (Brian *et al*, 1954). In 1955, American scientists also isolated a new compound, in addition to what they thought was gibberellin A from *G. fujikuroi*, which they called gibberellin X (Stodola *et al*, 1955). An exchange of samples between scientists led to the discovery that gibberellin A was actually made up of three compounds, which Japanese scientists named GA_1, GA_2 and GA_3. It was also confirmed that gibberellin X, GA_3 and gibberellic acid were all the same compound and today the latter two are synonymous terms used to describe the compound (Takahashi *et al*, 1955). In the mid- 1950s evidence that gibberellins were in fact naturally occurring substances in higher plants began to appear in the literature (Salisbury and Ross, 1992). Using techniques that had been used to isolate gibberellins from the fungus, M. Radley at ICI, UK demonstrated the presence of gibberellin-like substances in higher plants (Radley, 1956). In the USA, the first report of a gibberellin-like substance in maize came from Phinney *et al* (1957) using dwarf maize mutants to assay for activity in plant extracts. In 1958, MacMillan and Suter were the first to isolate and identify GA_1 from plants (MacMillan and

Suter, 1958). The same year Went and Murashige also identified GA_1 in higher plants (Salisbury and Ross, 1992). This was rapidly followed by the isolation of gibberellins A_5, A_6 and A_8 from runner beans (*Phaseolus multiflorus*) (Macmillan *et al*, 1959, 1960 and 1962).

The number of gibberellins discovered and isolated from fungal and plant origins rapidly increased in the 1960s. In 1968 Macmillan and Takahashi proposed that gibberellins be assigned the numbers gibberellin A_{1-x} irrespective of their origin, in order to reduce any confusion between compounds (Macmillan and Takahashi, 1968). Over the past few years, with the improvement of analytical equipment, the number of identified gibberellins has risen to ~125 and the assignment of identifying codes has proved to be very useful.

6.1.2 BIOSYNTHESIS AND METABOLISM OF GIBBERELLINS

Gibberellins, are synthesised from acetyl CoA via a long and complex mevalonic acid pathway. They all have either 19 or 20 carbon units which are grouped into either four or five ring systems. The exact location of gibberellin production is unknown. They are believed to be synthesised in young tissues of the shoots and also the developing seeds, but it is still uncertain whether young root tissues also produce the hormones. Some evidence also points to the leaves as a possible site of gibberellin biosynthesis (Sponsel, 1995; Salisbury and Ross, 1992). Gibberellins are formed using the following pathway.

Firstly three acetyl CoA molecules are oxidised by two NADPH molecules to produce three CoA molecules as a side product and mevalonic acid. The mevalonic acid is then phosphylated by ATP and decarboxylated to form isopentyl pyrophosphate. Four isopentyl pyrophosphate molecules form geranylgeranyl pyrophosphate. These serve as the donor for all gibberellic acid carbon atoms. The geranylgeranyl pyrophosphate is subsequently converted to copalylpyrophosphate which has two ring systems. Copalylpyrophosphate is then converted to kaurene which has four ring systems and subsequent oxidations produce kaurenol (alcohol form), kaurenal (aldehyde form), and kaurenoic acid, respectively. Kaurenoic acid is then converted to the aldehyde form of GA_{12} by decarboxylation. GA_{12} is the first true gibberellane ring system, and has 20 carbons. From the aldehyde form of GA_{12} arise both 20 and 19 carbon gibberellins, but by many more complex mechanisms. To biosynthesis GA_3, the aldehyde form of GA_{12} is first converted to GA_{12} and then to GA_{53}. This in turn is converted to GA_{20}, which is subsequently converted to GA_5. Finally the GA_5 is converted to GA_3.

Figure 47, shows the pathway for the biosynthesis of GA_3 from mevalonic acid.

FIGURE 47 - BIOSYNTHESIS PATHWAY FOR GA_3 FROM MEVALONIC ACID (Reproduced with the permission of Peter Hedden, IACR-Long Ashton Research Station, University of Bristol, Bristol, BS41 9AF, UK)

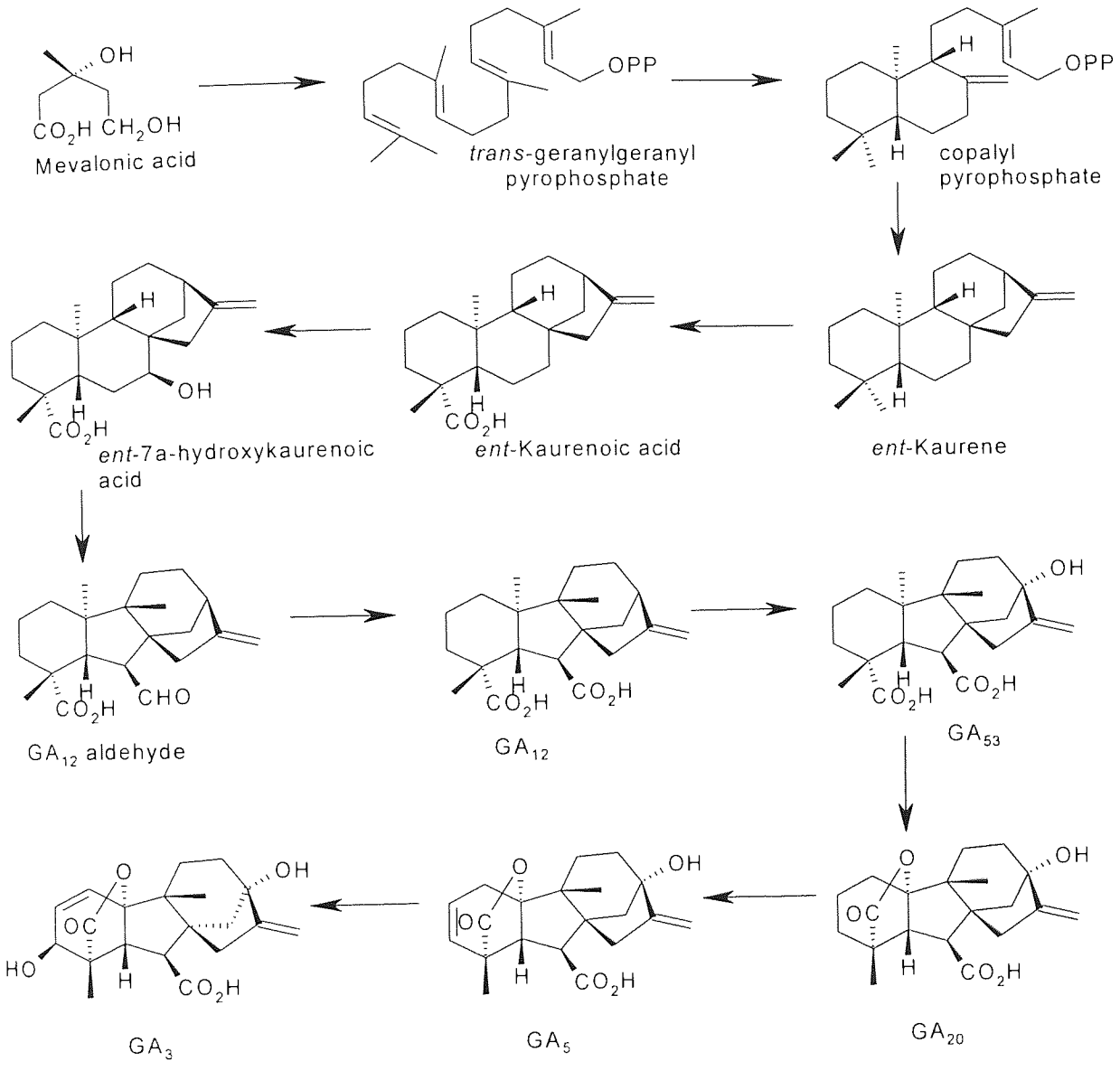

The potassium salt of Gibberellic A_3 (GA_3K) was supplied by Monsanto, for use in nanoencapsulation studies. The structure of GA_3K is shown in Figure 48, overleaf.

FIGURE 48 - THE STRUCTURE OF GA_3K

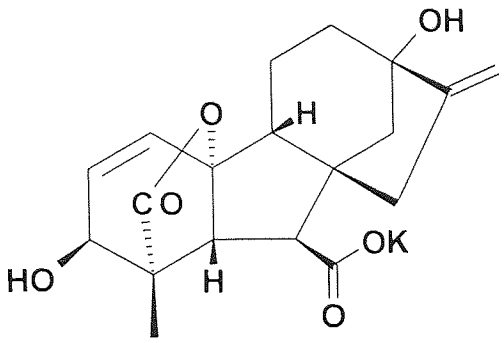

During active growth plants will quickly metabolise most gibberellins by hydroxylation to inactive conjugates. However, GA_3 is degraded much more slowly than the other gibberellins, which explains why the symptoms initially associated with the hormone in the disease 'bakanae', are present. It has been suggested that inactive conjugates are stored and translocated via the phloem and xylem before they become activated in the target tissue at a predetermined time (Arteca, 1996; Sponsel, 1995).

6.1.3 NATURAL FUNCTIONS OF GIBBERELLINS

Active gibberellins show many physiological effects, each depending on the type of gibberellin present, as well as the species of plant. Amongst the gibberellins, GA_3 has received the greatest attention (Davies, 1995; Mauseth, 1991; Raven, 1992; Salisbury and Ross, 1992). It stimulates stem elongation by stimulating cell division and elongation; flowering in response to long days; the breaking of seed dormancy in some plants that require stratification or light to induce germination; enzyme production (α-amylase) in germinating cereal grains for mobilisation of seed reserves; the induction of maleness in dioecious flowers (sex expression); parthenocarpic (seedless) fruit production, and finally GA_3 can delay senescence in leaves and citrus fruits.

6.1.4 COMMERCIAL USE OF GIBBERELLIN A_3

Gibberellins are involved in a wide range of developmental processes in plants and these processes can be manipulated by either the exogenous application of gibberellin inhibitors, which block the biosynthesis of endogenous gibberellins or by the application of bio-active gibberellins. The inhibition of gibberellin biosynthesis has been used to reduce the stem height of cereal crops and flowering pot plants such as lilies and orchids, as well as control the height of bedding plants.

The commercial application of gibberellic acid is usually in the form of GA_3 or GA_{4+7}. The application of very low concentrations of gibberellic acid can have a profound effect on crops, but timing the application is critical. The dose needs careful consideration because too much can have an opposite effect

to the one desired, where as too little may require the plant to be repeatedly treated to sustain the desired levels of gibberellic acid (Riley, 1987). If applied at the correct time and in the correct concentration, then gibberellic acid can assist in a whole spectrum of horticultural applications ranging from overcoming dormancy to root formation (Riley, 1987).

6.1.5 AIMS

The work presented in this chapter describes the fabrication, characterisation, and release of Gibberellic A_3 Potassium Salt (GA_3K) from loaded nanospheres fabricated using the double sonication solvent evaporation method. A range of loaded nanospheres were fabricated containing theoretical 10% w/w to 40% w/w GA_3K and incubated in rural rainwater at both room temperature (23°C) and fridge temperature (4°C), for a period of 28 days. The GA_3K concentration was measured spectrophotometrically and release profiles of day to day release and total cumulative release constructed.

6.2 MATERIALS AND METHODS

6.2.1 MATERIALS

Table 45 below, describes some of the basic physico-chemical characteristics of GA_3K, relevant to the incorporation of GA_3K into polymer nanospheres.

TABLE 45 – PHYSICO-CHEMICAL CHARACTERISTICS OF GA_3K

DESCRIPTION	CHARACTERISTICS
CHEMICAL NAME	Gibberellic A_3K (GA_3K)
APPEARANCE	Crystalline powder, with a yellow cast
EMPIRICAL FORMULAE	$C_{19}H_{21}O_6K$
MOLECULAR WEIGHT	384.5
MELTING POINT	223-225°C
PURITY GRADE	≅ 95%
SOLUBILITY	Clear to slightly hazy yellow at 50mg + 1ml methanol : water (1:1). Slightly soluble in water. Soluble in methanol, ethanol, isopropanol and acetone.
STABILITY	Stable, stored at room temperature
ORAL TOXICITY	LD_{50} = 1000 – 25000mg/kg in mice, dog and rat.
DERMAL TOXICITY	LD_{50} = > 2000mg/kg in rabbit.

6.2.2 GENERAL METHODS

The polymer nanospheres were fabricated using the double sonication solvent evaporation method as described in Section 2.2.4, page 56. Before and after use in release studies the polymer nanospheres were subjected to the same series of physico-chemical methods as the nanospheres used in the previous chapters' release studies. These included determination of mean particle diameter (Section 2.2.7, page 58), zeta potential (Section 2.2.8, page 59), weight average molecular mass (Section 2.2.9, page 62), thermal characteristics (Section 2.2.10, page 64), moisture content (Section 2.2.11, page 66) and finally determination of the residual PVA (Section 2.2.12, page 67) and DCM (Section 2.2.13, page 67) concentrations.

6.2.3 METHODS FOR THE DETECTION OF GA_3K

6.2.3.1 INVESTIGATION OF THE MEASUREMENT OF GA_3K CONCENTRATION USING NEGATIVE ELECTROSPRAY GAS CHROMATOGRAPHY-MASS SPECTROSCOPY (GC-MS)

Detection and measurement of the GA_3K concentration in fabrication washes and release samples was attempted by gas chromatography – mass spectroscopy (GC-MS), using a negative electrospray method, described below.

Exactly 1ml of filtered release sample was placed into a glass mass spectroscopy vial. To this was added exactly 10µl of deuteriated GA_3 (50ng dGA_3) dissolved in HPLC methanol. The sample was mixed thoroughly, capped with a rubber seal and stored at 4°C until required. A 30µl sample was injected with a microsyringe into the mass spectrometer (Hewlett Packard Electrospray Accessory 59987A; Hewlett Packard Mass Spectroscopy Engine 5989B; Hewlett Packard 1100 series Liquid Chromatography column) and eluted with a 90% methanol, 10% water mixture at a flow rate of 250µl *per* minute. A graphical printout of the area of each peak was produced. A calibration curve was generated by injecting a range of GA_3K concentrations dissolved in filtered rainwater, each containing 50ng internal standard (dGA_3), into the mass spectrometer. From these data, an area ratio standard curve was produced as shown in Figure 49, overleaf.

Calculation of the area ratio was achieved by dividing the area of the peak produced by GA_3K (Area 345), by the area of the peak produced by dGA_3 (Area 347), as shown in Equation 10, below.

EQUATION 10 - CALCULATION OF THE AREA RATIO IN THE NEGATIVE ELECTROSPRAY METHOD OF GA_3K MEASUREMENT

$$\text{Area ratio} = \frac{\text{Area 345}}{\text{Area 347}}$$

A typical area ratio standard curve is shown in Figure 49 below and generated by the injection of a range of GA_3K concentrations dissolved in filtered rainwater, each containing 50ng of internal standard (dGA_3).

FIGURE 49 – GC-MS NEGATIVE ELECTROSPRAY STANDARD CALIBRATION CURVE FOR THE AREA RATIO OF GA_3K TO dGA_3 (mean values ± SEM, n=3)

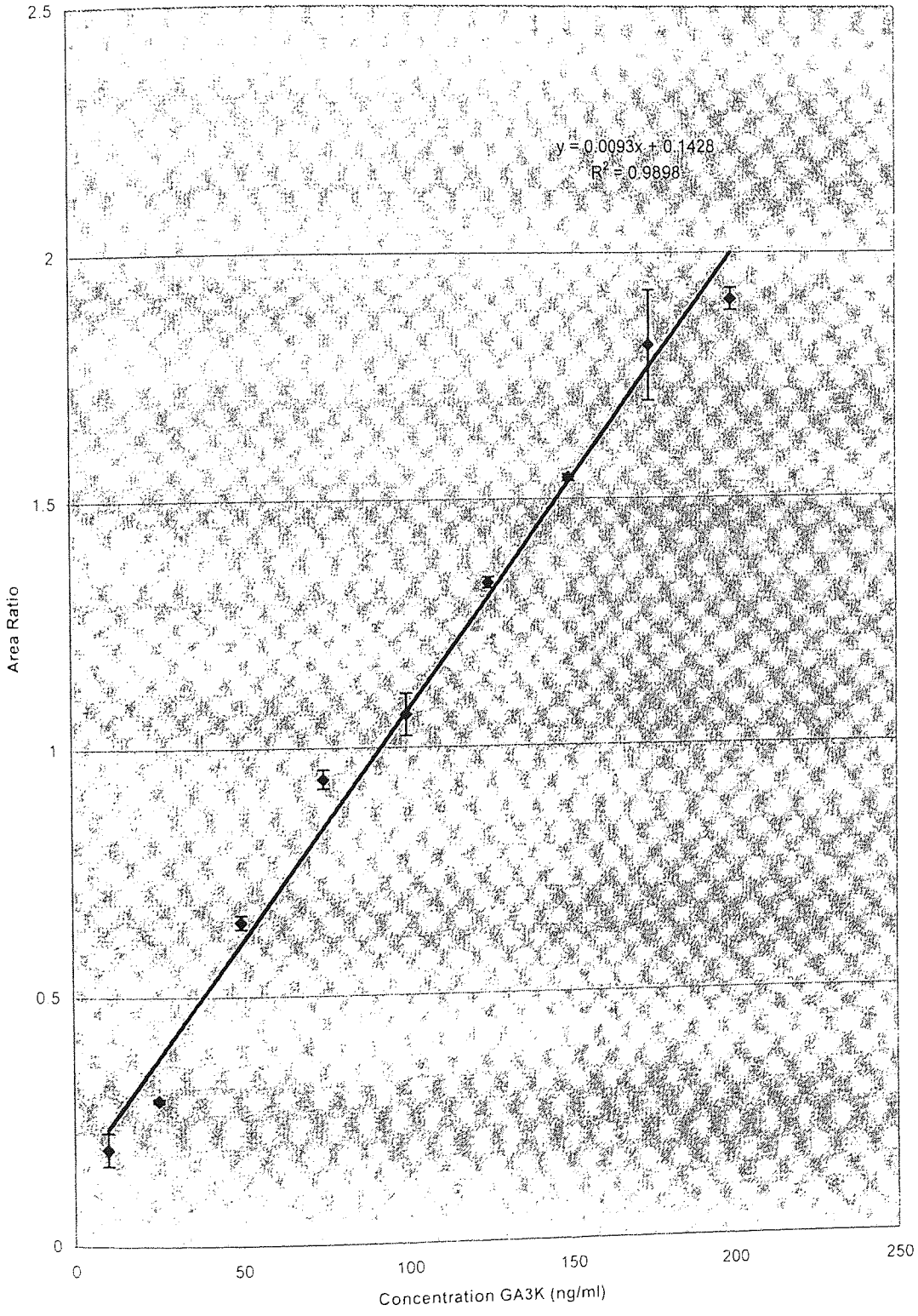

However, when release samples were injected into the mass spectrometer, ionisation of both the added internal standard (dGA_3) and the GA_3K, was almost completely suppressed. Repeated analysis of samples gave erratic results, and the readings for dGA_3 were consistently lower than in the standard samples. This suggested that there was a contaminant in the fabrication wash and release samples, causing a suppression of the ionisation. It became apparent that because of the great sensitivity of the mass spectrometer, even the smallest quantities of PVA, F68 or soluble polymer debris in the fabrication wash and release study samples caused a dramatic suppression in the ionisation of the dGA_3 and GA_3K. This was confirmed by discussion with Peter Hedden at IACR-Long Ashton Research Station, University of Bristol, Bristol, BS41 9AF, UK. Attempts to remove these contaminants, prior to injection into the mass spectrometer, proved unsuccessful. Hence another method of monitoring GA_3K was investigated, involving reverse phase-HPLC.

6.2.3.2 INVESTIGATION OF THE POSSIBILITIES OF USING REVERSE PHASE - HIGH PERFORMANCE LIQUID CHROMATOGRAPHY (RP-HPLC) FOR THE DETERMINATION OF GA_3K CONCENTRATIONS

High performance liquid chromatography (HPLC) is a popular analytical separation technique because of its high sensitivity and versatility and its possible use for the measurement of GA_3K in release samples was investigated in the present work. HPLC is a quantitative technique, capable of separating either non-volatile or thermally fragile compounds on the basis of charge. In normal phase HPLC the solid stationary phase is highly polar, and the mobile phase is very non-polar. Non-polar compounds travel rapidly with the solvent, whereas polar compounds are absorbed tightly onto the stationary phase. In reverse phase-high performance liquid chromatography (RP-HPLC) the solid stationary phase is non-polar, for example, a hydrocarbon, whereas the mobile phase is a highly polar species, such as methanol.
In the present work, 20µl of sample containing sorbic acid as an internal standard was injected (Shimadzu SIL-6B Auto Injector) into an RP-HPLC system (LC-6A Liquid Chromatograph). A system controller (Shimadzu SCL-6B) maintained the flow rate of the mobile phase (35% methanol : 65% 0.1% phosphoric acid) at 1ml *per* minute through the column (Phenomenex Luna C18 (2) 150mm × 4.6mm, RP fitted with a guard column). The GA_3K and sorbic acid peaks were monitored using a UV detector (Shimadzu SPD-6A), at 208nm (the λ max of GA_3K in mobile phase). The elution profile recorded sample peaks together with retention times, heights, areas and concentrations, and these were evaluated using a Shimadzu C-R6A Chromatopac.
A typical printout from the RP-HPLC analysis of a standard sample of GA_3K is shown in Figure 50, overleaf.

FIGURE 50 – TYPICAL PRINTOUT FROM THE RP-HPLC ANALYSIS OF A STANDARD SAMPLE CONTAINING 1000µg/ml GA_3K IN HPLC METHANOL

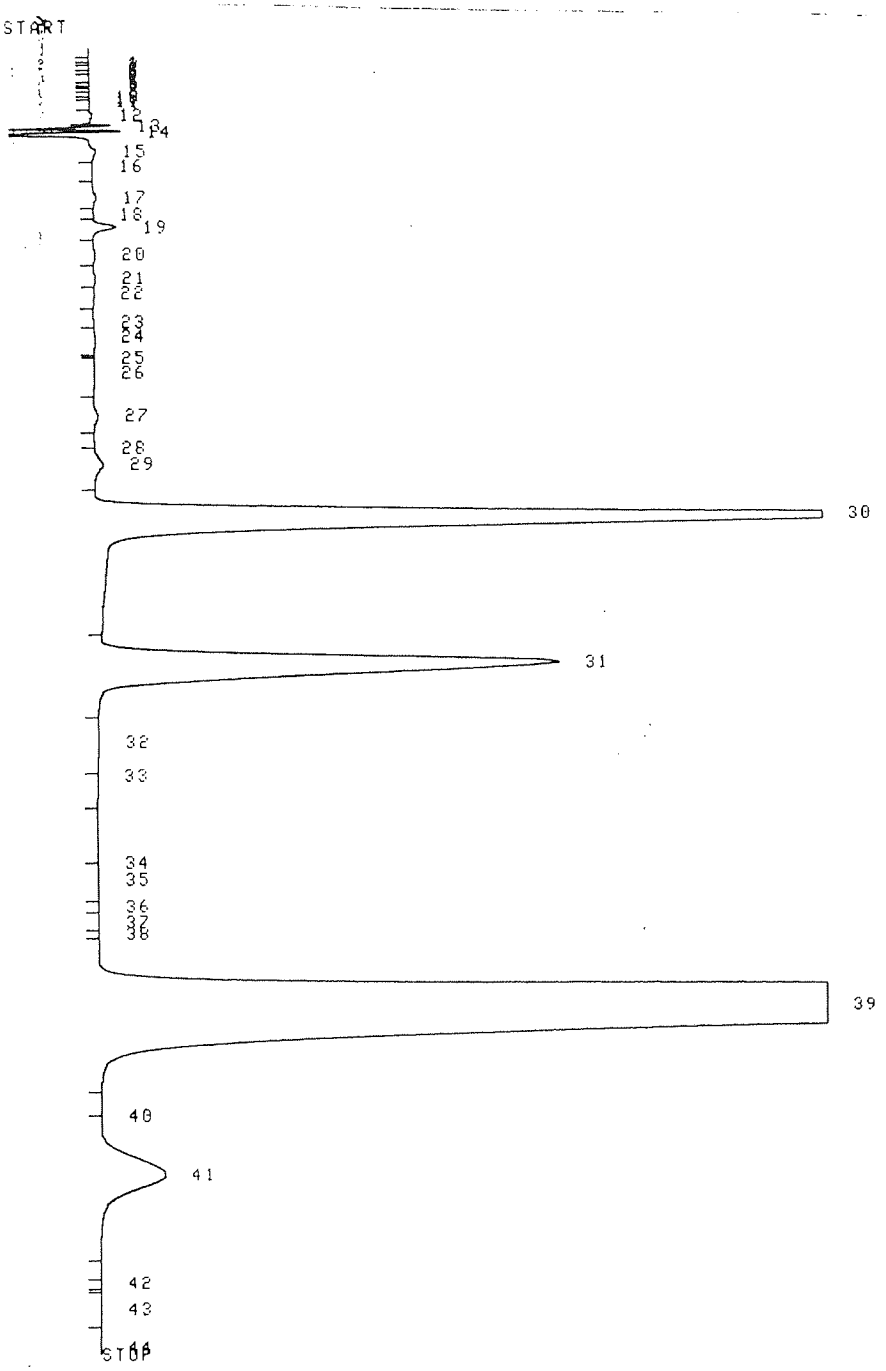

Trace shows four distinct peaks, all of which form part of the GA_3K compound.

As shown in Figure 50 above, the 'pure' (95-99.5%) GA_3K (G1025) supplied by Sigma Chemical Company appears to contain a range of compounds. The purity of the GA_3K (G1025) compound had only been assessed using thin-layer chromatography, which is not a quantitative method and useful only for

separating constituent compounds or GA_3- like compounds. It was also established that to produce GA_3K, Sigma mixes gibberellic acid (G7645), itself a mix of gibberellins, with potassium hydroxide. It seems possible that the multitude of peaks seen on the RP-HPLC trace are in fact either contaminating gibberellins or even other unrelated compounds. Repeated analysis with fresh release samples produced different patterns of peaks and peak heights on each run. Analysis by RP-HPLC was therefore assumed to be unreliable and was discontinued. Hence another method of measuring GA_3K was investigated involving the use of simple absorption maxima, as described in Section 2.2.27, page 77.

6.3 RESULTS

6.3.1 MEAN PERCENTAGE YIELD OF UNLOADED AND THEORETICAL 10%, 20%, 30% AND 40% w/w GA_3K LOADED PHBHV-DIOL AND DIBLOCK NANOSPHERES

Nanospheres theoretically loaded with either 10%, 20%, 30% or 40% w/w GA_3K were routinely fabricated from both PHBHV-Diol and Diblock polymers using the method described in Section 2.2.23, page 75. Unloaded PHBHV-Diol and Diblock nanospheres were fabricated using the same technique to act as controls. Mean percentage yields for unloaded and GA_3K loaded nanospheres were computed using Equation 2, page 57 and the results have been summarised in Table 46, below.

TABLE 46 – THE EFFECT OF THEORETICAL PERCENTAGE GA_3K LOADING AND FABRICATION POLYMER ON THE MEAN PERCENTAGE YIELD OF NANOSPHERES

(mean values ± SEM, n=6)

THEORETICAL % LOADING	POLYMER	MEAN % YIELD
0	PHBHV-DIOL	71.76 ± 0.83
10	PHBHV-DIOL	75.3 ± 0.72
20	PHBHV-DIOL	67.9 ± 1.8
30	PHBHV-DIOL	60.9 ± 0.61
40	PHBHV-DIOL	47.9 ± 1.5[b]
0	DIBLOCK	66.17 ± 1.4[a]
10	DIBLOCK	61.27 ± 3.4
20	DIBLOCK	57.1 ± 0.92
30	DIBLOCK	51.5 ± 0.54
40	DIBLOCK	42.5 ± 0.66[b]

a, significantly reduced ($P<0.05$) compared with unloaded PHBHV-diol nanospheres.

b, significantly reduced ($P<0.05$) compared with unloaded nanospheres fabricated from the same polymer.

Mean percentage yield of Diblock nanospheres was significantly lower ($P<0.05$) than that of PHBHV-Diol fabricated nanospheres, whether unloaded or loaded with increasing amounts of GA_3K. Irrespective of the fabrication polymer, increasing the theoretical percentage GA_3K loading significantly reduced ($P<0.05$) the mean percentage yield of nanospheres, Table 46.

6.3.2 DETERMINATION OF THE MEAN PARTICLE DIAMETER OF UNLOADED AND THEORETICAL 10%, 20%, 30% AND 40% w/w GA_3K LOADED NANOSPHERES, PRIOR TO USE IN RELEASE STUDIES

Particle diameter analysis was performed by photon correlation spectroscopy (PCS) on all unloaded and GA_3K loaded nanosphere samples, using the technique described in Section 2.2.7, page 58 and the results have been summarised in Table 47, below.

TABLE 47 – THE EFFECT OF THEORETICAL PERCENTAGE GA_3K LOADING AND FABRICATION POLYMER ON THE MEAN PARTICLE DIAMETER OF NANOSPHERES

(mean values ± SEM, n=6)

THEORETICAL % LOADING	POLYMER	MEAN DIAMETER (nm)
0	PHBHV-DIOL	275.6 ± 1.79
10	PHBHV-DIOL	509 ± 11.29
20	PHBHV-DIOL	565 ± 20.5
30	PHBHV-DIOL	600.8 ± 7.9
40	PHBHV-DIOL	616 ± 3.6[b]
0	DIBLOCK	328 ± 7.57[a]
10	DIBLOCK	534 ± 4
20	DIBLOCK	549.7 ± 8.4
30	DIBLOCK	601.8 ± 7.7
40	DIBLOCK	646.1 ± 12[b]

a, significantly greater ($P<0.05$) compared with mean diameter of unloaded PHBHV-Diol.

b, significantly elevated ($P<0.05$) compared with mean diameter of unloaded nanospheres fabricated from the same polymer.

GA_3K loading significantly increases the mean diameter of both PHBHV-Diol and Diblock nanospheres, Table 47. The mean particle diameter of unloaded PHBHV-Diol nanospheres is significantly smaller ($P<0.05$) than the mean particle diameter of unloaded Diblock nanospheres, Table 47.

6.3.3 SCANNING ELECTRON MICROSCOPY OF SAMPLES OF UNLOADED AND THEORETICAL 10%, 20%, 30% AND 40% w/w GA_3K LOADED PHBHV-DIOL AND DIBLOCK NANOSPHERES, PRIOR TO USE IN RELEASE STUDIES

Scanning electron microscopy of unloaded and GA_3K loaded nanospheres to elaborate surface morphology was carried out using the method detailed in Section 2.2.6, page 57. Due to the small size of the nanospheres and the limited resolution of the equipment available, it was only possible to obtain an image of theoretical 30% w/w GA_3K loaded Diblock nanospheres. A typical scanning electron micrograph of the theoretical 30% w/w GA_3K loaded Diblock nanospheres is shown in Figure 51, below.

FIGURE 51 – TYPICAL SCANNING ELECTRON MICROGRAPH OF THEORETICAL 30% w/w GA_3K LOADED DIBLOCK NANOSPHERES

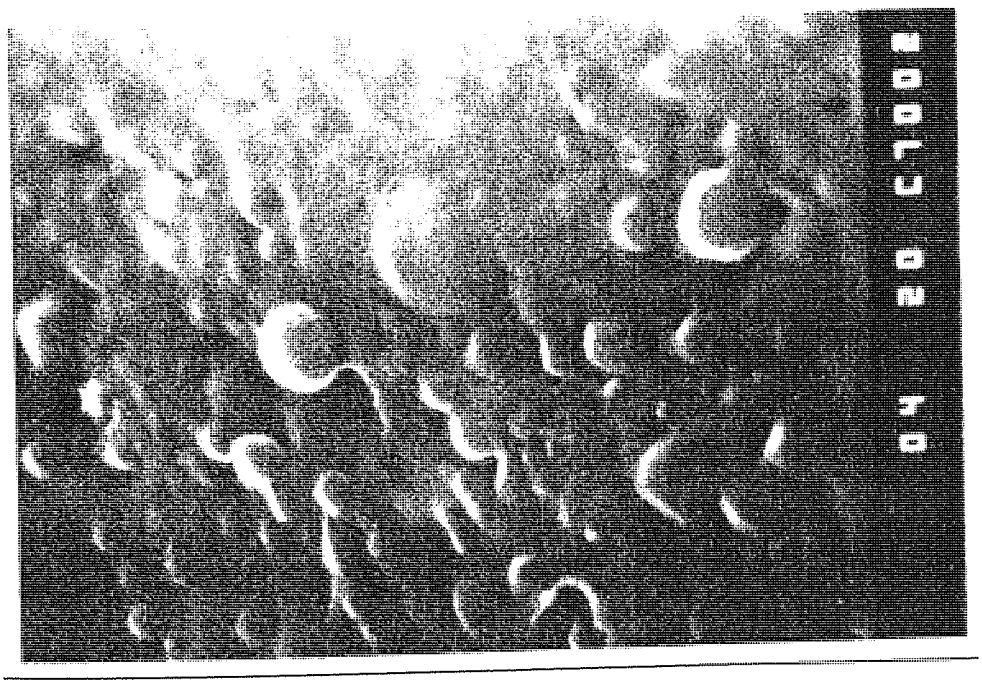

Figure 51 above, shows GA_3K loaded Diblock nanospheres associated with what appears to be a film of PVA. Print magnification = 30,600 (3cm = 1μM).

6.3.4 ZETA POTENTIAL MEASUREMENTS OF UNLOADED AND THEORETICAL 10%, 20%, 30% AND 40% w/w GA_3K LOADED PHBHV-DIOL AND DIBLOCK POLYMER NANOSPHERES, PRIOR TO USE IN RELEASE STUDIES

Zeta potential measurements of all unloaded and GA_3K loaded nanosphere preparations were carried out using a Malvern ZetaMaster®, as described in Section 2.2.8, page 59 and the results are shown in Table 48, overleaf.

TABLE 48 - MEAN ZETA POTENTIAL OF UNLOADED AND THEORETICAL 10%, 20%, 30% AND 40% w/w GA_3K LOADED PHBHV-DIOL AND DIBLOCK POLYMER NANOSPHERES, PRIOR TO USE IN RELEASE STUDIES (mean values ± SEM, n=6)

THEORETICAL % LOADING	POLYMER	MEAN ZETA POTENTIAL (mV)
0	PHBHV-DIOL	-20.76 ± 0.38
10	PHBHV-DIOL	-12.85 ± 0.58
20	PHBHV-DIOL	-11.92 ± 0.46
30	PHBHV-DIOL	-10.3 ± 0.27
40	PHBHV-DIOL	-8.78 ± 0.58[b]
0	DIBLOCK	-35.99 ± 0.67[a]
10	DIBLOCK	-11.8 ± 0.45
20	DIBLOCK	-11.23 ± 0.52
30	DIBLOCK	-9.93 ± 0.85
40	DIBLOCK	-8.03 ± 0.71[b]

a, significantly more negative ($P<0.05$) compared with unloaded PHBHV-Diol nanospheres.
b, significantly less negative ($P<0.05$) compared with either unloaded or theoretical 10% GA_3K loaded nanospheres fabricated using the same polymer.

The mean zeta potential of unloaded Diblock nanospheres is significantly more negative ($P<0.05$) than that of unloaded PHBHV-Diol nanospheres, Table 48. Increasing the theoretical percentage GA_3K loading significantly reduced ($P<0.05$) the negative charge of nanospheres, irrespective of the fabrication polymer used, Table 48. The mean zeta potentials of GA_3K loaded PHBHV-Diol and GA_3K loaded Diblock nanospheres are in the stability band known as the 'threshold of agglomeration' (Riddick, 1968). The unloaded PHBHV-Diol nanospheres are in the stability band known as the 'threshold of delicate dispersion', whereas the unloaded Diblock nanospheres are in the stability band known as 'moderate stability' (Riddick, 1968).

6.3.5 DETERMINATION OF THE WEIGHT AVERAGE MOLECULAR MASS (Mw) OF SAMPLES OF UNLOADED AND THEORETICAL 10%, 20%, 30% AND 40% w/w GA_3K LOADED PHBHV-DIOL AND DIBLOCK NANOSPHERES, PRIOR TO USE IN RELEASE STUDIES

The weight average molecular mass was measured using gel permeation chromatography, according to the method described in Section 2.2.9, page 62. The results obtained from GPC analysis have been summarised in Table 49, overleaf.

TABLE 49 – MEAN WEIGHT AVERAGE MOLECULAR MASS FOR SAMPLES OF UNLOADED AND THEORETICAL 10%, 20%, 30% AND 40% w/w GA_3K LOADED PHBHV-DIOL AND DIBLOCK NANOSPHERES PRIOR TO USE IN RELEASE STUDIES (mean values ± SEM, n=3)

THEORETICAL % LOADING	POLYMER	MEAN MOLECULAR MASS (Daltons)
0	PHBHV-DIOL	8138 ± 625
10	PHBHV-DIOL	2977 ± 81
20	PHBHV-DIOL	2543 ± 98
30	PHBHV-DIOL	2477 ± 74
40	PHBHV-DIOL	2227 ± 46[a]
0	DIBLOCK	58914 ± 1067
10	DIBLOCK	38133 ± 1717
20	DIBLOCK	36800 ± 850
30	DIBLOCK	35933 ± 145
40	DIBLOCK	35533 ± 706[b]

a, significantly reduced ($P<0.05$) compared with theoretical 10% w/w GA_3K loaded and unloaded nanospheres fabricated from the same polymer.

b, significantly reduced ($P<0.05$) compared with unloaded nanospheres fabricated from the same polymer.

Increasing the theoretical percentage GA_3K loading reduces the mean molecular mass of nanospheres, irrespective of the fabrication polymer used, Table 49.

6.3.6 DETERMINATION OF THE THERMAL CHARACTERISTICS OF SAMPLES OF UNLOADED AND THEORETICAL 10%, 20%, 30% AND 40% w/w GA_3K LOADED PHBHV-DIOL AND DIBLOCK NANOSPHERES, PRIOR TO USE IN RELEASE STUDIES

DSC analysis of freshly fabricated unloaded and GA_3K loaded PHBHV-Diol and Diblock nanospheres was carried out using the method described in Section 2.2.10, page 64 and the results have been summarised in Table 50, overleaf.

TABLE 50 - DSC ANALYSIS OF NANOSPHERE SAMPLES SHOWING THE GLASS TRANSITION TEMPERATURE (Tg), RECRYSTALLISATION TEMPERATURE AND MELTING POINTS OF UNLOADED AND THEORETICAL 10%, 20%, 30% AND 40% w/w GA_3K LOADED PHBHV-DIOL AND DIBLOCK NANOSPHERES, PRIOR TO USE IN RELEASE STUDIES (mean values, n=2)

THEO. % LOADING	POLYMER	Tg (°C)	RECYRSTALLISATION (°C)	MELTING POINT 1 (°C)	MELTING POINT 2 (°C)
0	PHBHV-DIOL	-12	55	80	99
10	PHBHV-DIOL	-14	57	81	99
20	PHBHV-DIOL	-12	58	83	100
30	PHBHV-DIOL	-13	61	84	104
40	PHBHV-DIOL	-15	63	86	105
0	DIBLOCK	36	61	138	152
10	DIBLOCK	36	64	141	152
20	DIBLOCK	35	66	143	153
30	DIBLOCK	37	67	145	157
40	DIBLOCK	33	70	146	158

GA_3K loading appears to have little appreciable effect on the Tg of either PHBHV-Diol or Diblock fabricated nanospheres. However, irrespective of the fabrication polymer used, increasing the theoretical percentage GA_3K loading tended to marginally increase the recrystallisation temperature and melting point temperatures of the nanospheres, Table 50.

6.3.7 DETERMINATION OF MOISTURE CONTENT OF FREEZE-DRIED UNLOADED AND THEORETICAL 10%, 20%, 30% AND 40% w/w GA_3K LOADED PHBHV-DIOL AND DIBLOCK NANOSPHERES, PRIOR TO USE IN RELEASE STUDIES

The moisture content of freeze-dried nanosphere preparations was determined using thermogravimetric analysis as described in Section 2.2.11, page 66 and the results of analyses have been summarised in Table 51, overleaf.

TABLE 51 - MOISTURE CONTENT OF FREEZE-DRIED UNLOADED AND THEORETICAL 10%, 20%, 30% AND 40% w/w GA_3K LOADED PHBHV-DIOL AND DIBLOCK NANOSPHERES, PRIOR TO USE IN RELEASE STUDIES (mean values ± SEM, n=6)

POLYMER	THEORETICAL % LOADING	MEAN MOISTURE CONTENT (%)
PHBHV-DIOL	0	0.36 ± 0.04
PHBHV-DIOL	10	0.34 ± 0.1
PHBHV-DIOL	20	0.43 ± 0.07
PHBHV-DIOL	30	0.37 ± 0.05
PHBHV-DIOL	40	0.39 ± 0.1
DIBLOCK	0	0.42 ± 0.1
DIBLOCK	10	0.38 ± 0.05
DIBLOCK	20	0.41 ± 0.1
DIBLOCK	30	0.38 ± 0.07
DIBLOCK	40	0.44 ± 0.04

Moisture content analysis showed that there was no statistically significant difference between the moisture content of unloaded and GA_3K loaded nanospheres, irrespective of the fabrication polymer, Table 51. There is no statistically significant difference between the moisture content of nanospheres fabricated from PHBHV-Diol compared to those fabricated from Diblock polymer, Table 51.

6.3.8 DETERMINATION OF THE RESIDUAL PVA CONTENT OF UNLOADED AND THEORETICAL 10%, 20%, 30% AND 40% w/w GA_3K LOADED PHBHV-DIOL AND DIBLOCK NANOSPHERES, PRIOR TO USE IN RELEASE STUDIES

Determination of the residual PVA content of unloaded and GA_3K loaded nanospheres was carried out using the methods described in Section 2.2.12, page 67 and the results have been summarised in Table 52, overleaf.

TABLE 52 – MEAN PERCENTAGE RESIDUAL PVA CONTENT OF UNLOADED AND THEORETICAL 10%, 20%, 30% AND 40% w/w GA_3K LOADED PHBHV-DIOL AND DIBLOCK NANOSPHERES PRIOR TO USE IN RELEASE STUDIES (mean values ± SEM, n=3)

THEORETICAL % LOADING	POLYMER	MEAN RESIDUAL PVA (%)
0	PHBHV-DIOL	12.1 ± 0.7
10	PHBHV-DIOL	26.93 ± 0.22
20	PHBHV-DIOL	27.12 ± 0.26
30	PHBHV-DIOL	44.2 ± 0.98
40	PHBHV-DIOL	54.56 ± 3.24[a]
0	DIBLOCK	11.6 ± 0.09
10	DIBLOCK	13.09 ± 0.26
20	DIBLOCK	16.27 ± 1.88
30	DIBLOCK	17.62 ± 0.49
40	DIBLOCK	21.75 ± 0.19[a]

a, significantly increased ($P<0.05$) compared with unloaded and theoretical 10% to 30% w/w GA_3K loaded nanospheres fabricated using the same polymer.

Fabrication polymer has no significant effect on the mean residual PVA content of unloaded nanospheres, Table 52. Irrespective of the fabrication polymer, increasing the theoretical percentage GA_3K loading significantly increased ($P<0.05$) the mean percentage residual PVA of nanospheres, Table 52. The mean residual percentage PVA associated with GA_3K loaded PHBHV-Diol nanospheres was always significantly greater than the mean percentage PVA associated with GA_3K loaded Diblock nanospheres, Table 52.

6.3.9 DETERMINATION OF RESIDUAL DICHLOROMETHANE IN SAMPLES OF UNLOADED AND THEORETICAL 10%, 20%, 30% AND 40% w/w GA_3K LOADED PHBHV-DIOL AND DIBLOCK NANOSPHERES, PRIOR TO USE IN RELEASE STUDIES

Gas liquid chromatography was used to measure the concentration of DCM in freshly fabricated freeze-dried nanospheres using the method described in Section 2.2.13, page 69. Irrespective of the fabrication polymer used, increasing the theoretical percentage GA_3K loading had no significant effect on residual DCM concentration. On this basis, results have been abbreviated to tabulate only the mean concentration of DCM in GA_3K loaded and unloaded nanospheres, Table 53.

TABLE 53 - RESIDUAL DCM IN UNLOADED AND THEORETICAL 10%, 20%, 30% AND 40% w/w GA_3K LOADED PHBHV-DIOL AND DIBLOCK NANOSPHERES, PRIOR TO USE IN RELEASE STUDIES (mean values ± SEM, n=6)

POLYMER	GA_3K LOADED / UNLOADED	OVERALL MEAN CONCENTRATION OF DCM (ppm)
PHBHV-DIOL	GA_3K LOADED	14.65 ± 3.74
PHBHV-DIOL	UNLOADED	0
DIBLOCK	GA_3K LOADED	14.04 ± 1.45
DIBLOCK	UNLOADED	0

Significant and largely similar concentrations of residual DCM could be detected in the GA_3K loaded samples fabricated from both PHBHV-Diol and Diblock polymers, whereas DCM was not detected in either of the unloaded nanosphere samples. These concentrations of residual DCM in both GA_3K loaded PHBHV-Diol nanospheres and GA_3K loaded Diblock nanospheres were considered to be below the recommended UK (100ppm - <250ppm) and US (500ppm - <2000ppm) limits for both long and short-term exposure (Martindale 31st Edition, 1996).

6.3.10 DETERMINATION OF TOTAL AMOUNT OF GA_3K (mg) LOST INTO NANOSPHERE WASHES DURING THE FABRICATION PROCESS

Assessment of the amount of GA_3K lost from nanosphere preparations into centrifugation supernatants during washing with double distilled water, was carried out as described in Section 2.2.24, page 76 and the results are shown in Table 54, below.

TABLE 54 – TOTAL AMOUNT OF GA_3K (mg) LOST INTO NANOSPHERE WASHES DURING THE FABRICATION PROCESS (mean values ± SEM, n=6)

THEORETICAL % LOADING	POLYMER	OVERALL MEAN GA_3K LOST(mg)
10	PHBHV-DIOL	2.91 ± 0.4
20	PHBHV-DIOL	19.9 ± 0.7
30	PHBHV-DIOL	40.06 ± 0.39
40	PHBHV-DIOL	70.73 ± 2[a]
10	DIBLOCK	3.48 ± 0.62
20	DIBLOCK	25.3 ± 1.6
30	DIBLOCK	49.6 ± 1.3
40	DIBLOCK	70.01 ± 1.3[a]

a, significantly increased ($P<0.05$) compared with theoretical 10%, 20% and 30% w/w GA_3K loaded nanospheres fabricated using the same polymer.

The type of fabrication polymer used had no significant effect on the amount of GA_3K lost during harvesting or washing. However, the overall amount of GA_3K lost from nanospheres increased significantly with increase in theoretical percentage GA_3K loading, Table 54.

6.3.11 DETERMINATION OF THE NANOENCAPSULATION EFFICIENCY AND THE TOTAL AMOUNT OF GA_3K ENCAPSULATED IN 100mg OF THEORETICAL 10%, 20%, 30% AND 40% w/w GA_3K LOADED PHBHV-DIOL AND DIBLOCK NANOSPHERES PRIOR TO USE IN RELEASE STUDIES

The effect of the type of polymer and percentage GA_3K loading on the nanoencapsulation efficiency was investigated by analysing the amount of GA_3K contained within a known weight of nanospheres. Determination of the nanoencapsulation efficiency of GA_3K was carried out using the method described in Section 2.2.25, page 76 and the results of these determinations, together with the computed total amount of GA_3K in 100mg of freeze-dried nanospheres is shown in Table 55, below.

TABLE 55 - NANOENCAPSULATION EFFICIENCY AND TOTAL AMOUNT OF GA_3K INCORPORATED IN 100mg OF THEORETICAL 10%, 20%, 30% AND 40% w/w GA_3K LOADED PHBHV-DIOL AND DIBLOCK NANOSPHERES PRIOR TO USE IN RELEASE STUDIES (mean values ± SEM, n=6)

THEORETICAL % LOADING	POLYMER	TOTAL GA_3K INCORPRATED INTO 100mg NANOSPHERES (mg)	NANOENCAPSULATION EFFICIENCY (%)
10	PHBHV-DIOL	8.84 ± 2.10	88.40 ± 5.6
20	PHBHV-DIOL	16.26 ± 0.67	81.3 ± 2.28
30	PHBHV-DIOL	19.68 ± 0.79	65.60 ± 1.6
40	PHBHV-DIOL	23.35 ± 0.90[a]	58.38 ± 1.1[b]
10	DIBLOCK	8.60 ± 0.44	86.00 ± 2.7
20	DIBLOCK	15.74 ± 0.8	78.70 ± 2.29
30	DIBLOCK	17.36 ± 0.84	57.87 ± 1.4
40	DIBLOCK	25.84 ± 2.01[a]	64.60 ± 2.2[b]

a, significantly increased ($P<0.05$) compared with theoretical 10% w/w GA_3K loaded nanospheres fabricated with the same polymer.
b, significantly reduced ($P<0.05$) compared with theoretical 10% w/w GA_3K loaded nanospheres fabricated with the same polymer.

The type of fabrication polymer used has no significant effect on either the amount of GA_3K incorporated *per* 100mg of nanospheres or the resulting nanoencapsulation efficiency calculated for each theoretical percentage GA_3K loading. The percentage nanoencapsulation efficiency significantly ($P<0.05$) decreases with increasing theoretical percentage GA_3K loading.

6.3.12 RELEASE OF GA_3K FROM THEORETICAL 10%, 20%, 30% AND 40% w/w GA_3K LOADED PHBHV-DIOL AND DIBLOCK NANOSPHERES INTO RURAL RAINWATER AT 4°C AND 23°C FOR 28 DAYS

The release of GA_3K into rural rainwater at 4°C and 23°C over 28 days was monitored as described in Section 2.2.26, page 77. Unloaded PHBHV-Diol and Diblock nanospheres were incubated alongside the GA_3K loaded nanospheres to act as controls for GA_3K like activity in release samples.

The measurement of GA_3K concentration was attempted by both negative electrospray and RP-HPLC, but for reasons outlined previously, Section 6.2, these techniques did not prove successful, and consequently all GA_3K release profiles were constructed using data obtained by the spectrophotometric analysis of GA_3K in daily collected release samples. Typical daily GA_3K release profiles for theoretical 10% and 40% w/w GA_3K loaded PHBHV-Diol nanospheres and theoretical 10% and 40% w/w GA_3K loaded Diblock nanospheres over 28 days incubation into rural rainwater at 4°C and 23°C have been illustrated in the text in Figures 52 to 55, overleaf. The remainder of the daily release profiles are shown in Appendix Section 4.2, page 280.

FIGURE 52 – DAILY GA_3K RELEASE PROFILES FOR 10% w/w GA_3K LOADED PHBHV-DIOL NANOSPHERES INTO RURAL RAINWATER AT 4 DEGREES CELCIUS AND 23 DEGREES CELCIUS (mean values ± SEM, n=3)

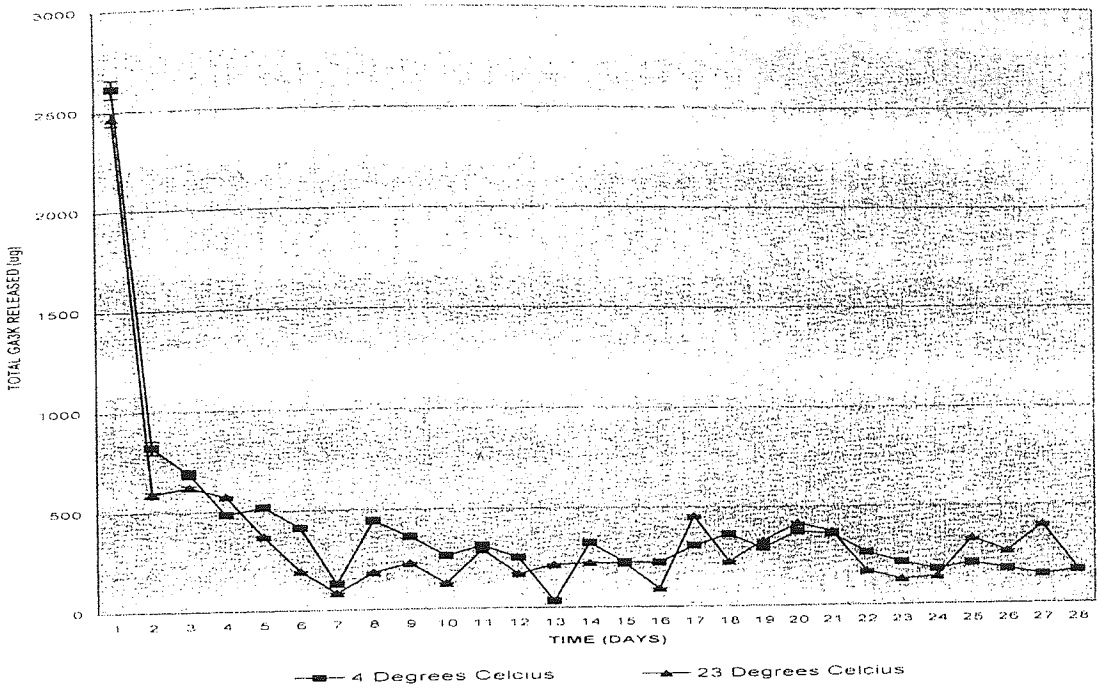

FIGURE 53 – DAILY GA_3K RELEASE PROFILES FOR 40% w/w GA_3K LOADED PHBHV-DIOL NANOSPHERES INTO RURAL RAINWATER AT 4 DEGREES CELCIUS AND 23 DEGREES CELCIUS (mean values ± SEM, n=3)

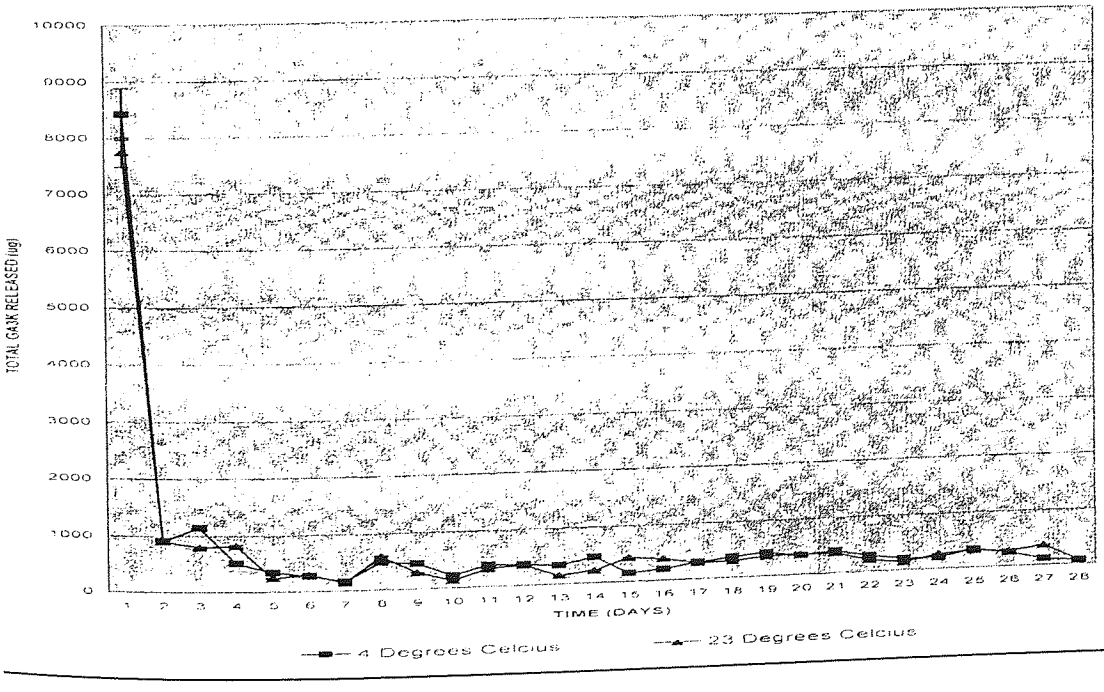

FIGURE 54 – DAILY GA_3K RELEASE PROFILES FOR 10% w/w GA_3K LOADED DIBLOCK NANOSPHERES INTO RURAL RAINWATER AT 4 DEGREES CELCIUS AND 23 DEGREES CELCIUS (mean values ± SEM, n=3)

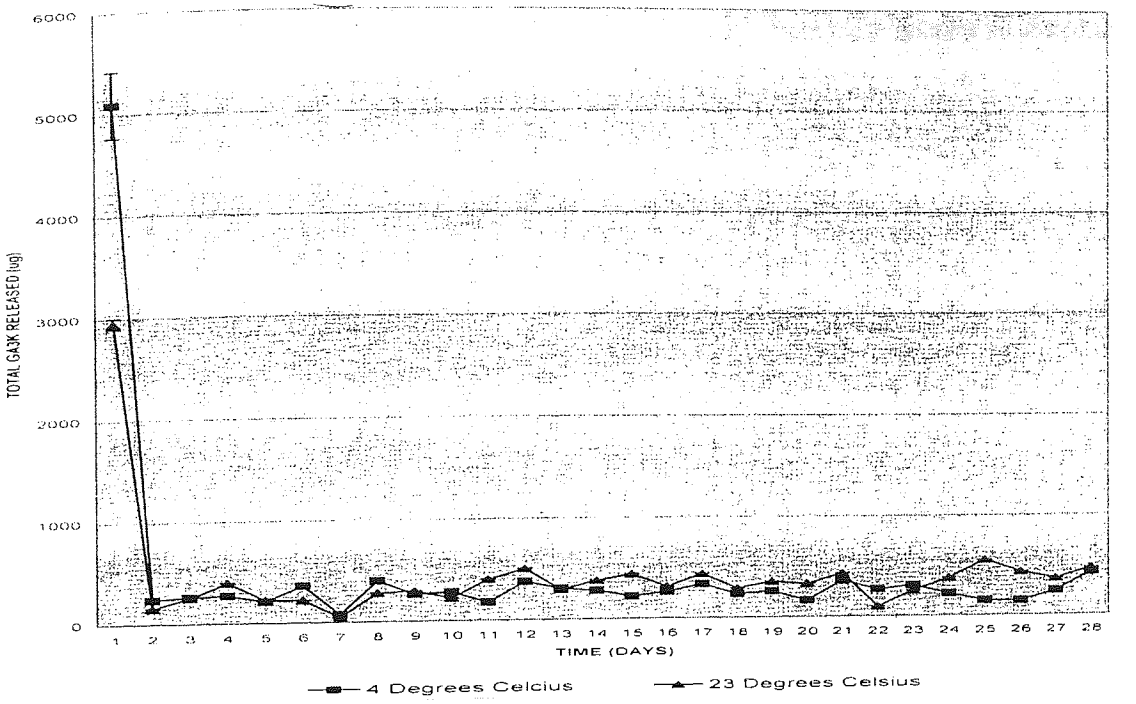

FIGURE 55 – DAILY GA_3K RELEASE PROFILES FOR 40% w/w GA_3K LOADED DIBLOCK NANOSPHERES INTO RURAL RAINWATER AT 4 DEGREES CELCIUS AND 23 DEGREES CELCIUS (mean values ± SEM, n=3)

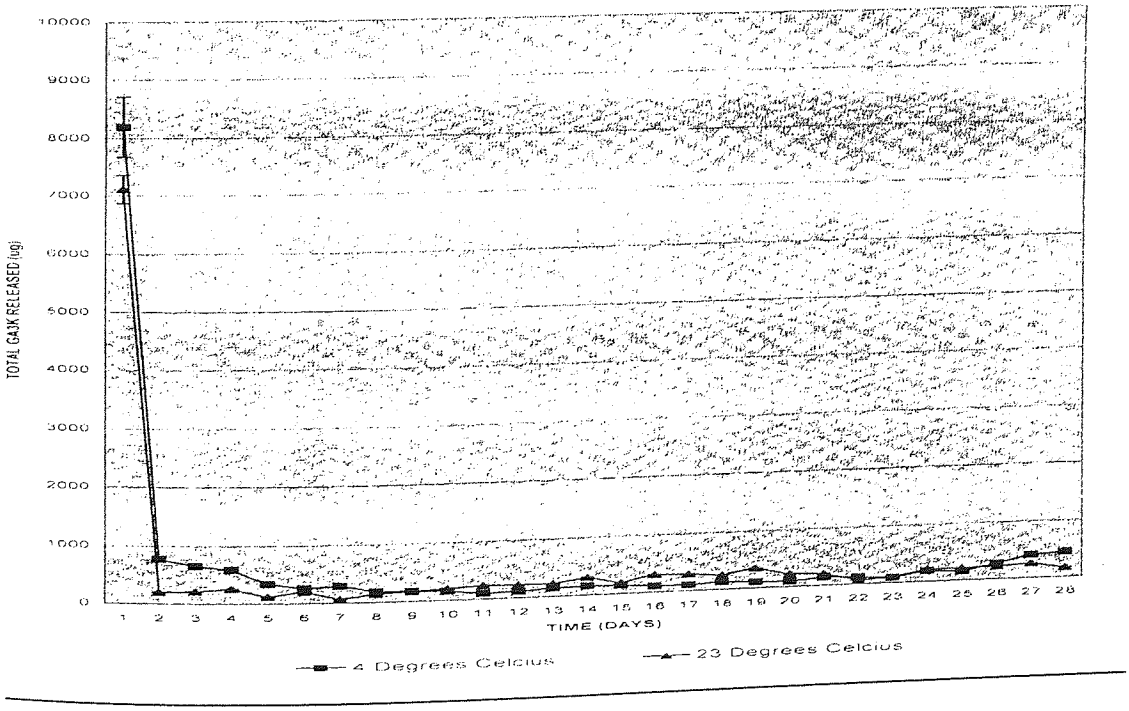

GA_3K release from nanosphere samples, irrespective of either the fabrication polymer or theoretical percentage loading used, was characterised by an initial burst release of the active followed, after 24 hours, by low-level sustained release continuing for up to 28 days. The extent of the initial burst release phase was positively correlated with the theoretical percentage GA_3K loading for all nanosphere samples used. The release of GA_3K from all nanosphere samples, was greatest from those samples incubated in rural rainwater at 4°C compared with those incubated at 23°C.

Typical total cumulative GA_3K release profiles for theoretical 10% w/w and 40% w/w GA_3K loaded PHBHV-Diol nanospheres, and theoretical 10% w/w and 40% w/w GA_3K loaded Diblock nanospheres over 28 days incubation into rural rainwater at 4°C and 23°C have been illustrated in Figures 56 to 59, below. The remainder of the total cumulative release profiles are illustrated in the Appendix Section 4.3, page 282.

The total cumulative release of GA_3K from GA_3K loaded PHBHV-Diol and Diblock nanospheres was positively correlated to the extent of theoretical percentage GA_3K loading, Figures 56 to 59. There were no statistically significant differences between the total cumulative release of GA_3K from GA_3K loaded PHBHV-Diol and Diblock nanospheres incubated in rural rainwater at either 4°C or 23°C. Total cumulative GA_3K release from GA_3K loaded PHBHV-Diol nanospheres significantly increased ($P<0.05$) from a maximum of ~10mg from theoretical 10% w/w GA_3K loaded nanospheres after 28 days incubation, to a maximum of ~18mg from theoretical 40% w/w GA_3K loaded nanospheres, over the same incubation period, Table 56. Unlike GA_3K release from GA_3K loaded PHBHV-Diol nanospheres, there only appeared to be a marginal increase in total cumulative release from GA_3K loaded Diblock nanospheres as the theoretical percentage GA_3K loading increased. Total cumulative GA_3K release increased from a maximum of ~12mg from theoretical 10% w/w GA_3K loaded Diblock nanospheres to a maximum of ~14mg from theoretical 40% W/W GA_3K loaded nanospheres, over the same incubation period, Table 56.

No GA_3K-like activity was detected from unloaded nanospheres fabricated from the two polymers used to fabricate GA_3K loaded nanospheres, when incubated alongside the GA_3K loaded nanospheres. Consequently, values from unloaded nanospheres do not feature on any profiles or in any tables.

FIGURE 56 – TOTAL CUMULATIVE RELEASE PROFILES FOR 10% w/w GA_3K LOADED PHBHV-DIOL NANOSPHERES INTO RURAL RAINWATER AT 4 DEGREES CELCIUS AND 23 DEGREES CELCIUS (mean values ± SEM, n=3)

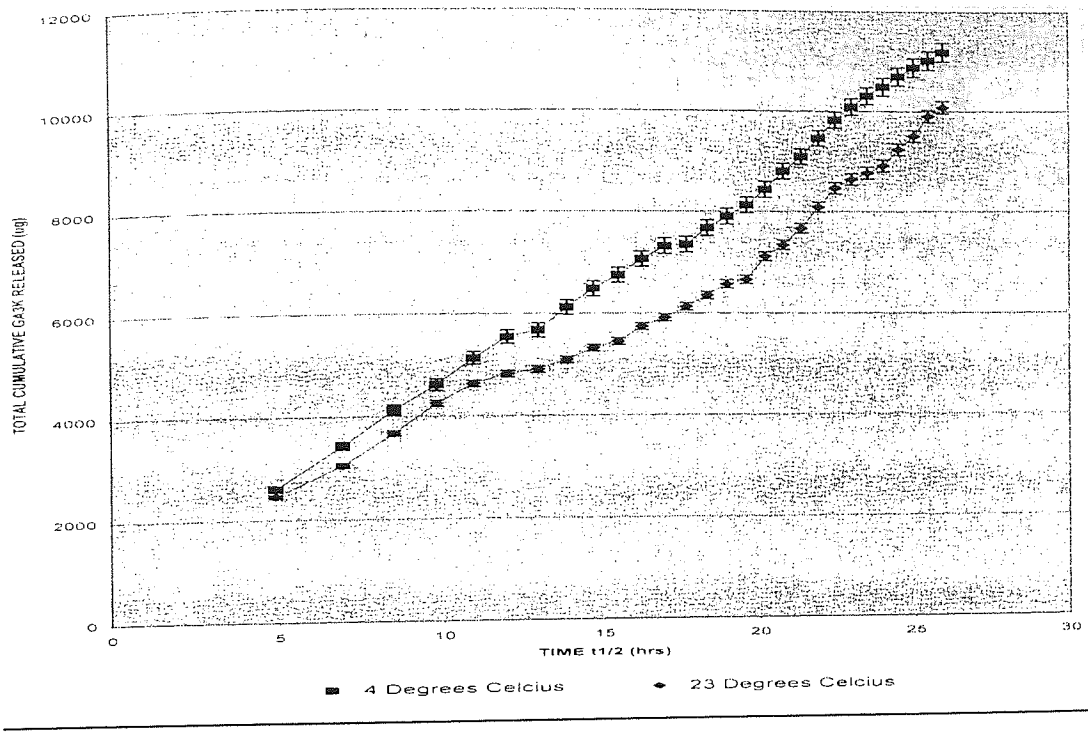

FIGURE 57 – TOTAL CUMULATIVE RELEASE PROFILES FOR 40% w/w GA_3K LOADED PHBHV-DIOL NANOSPHERES INTO RURAL RAINWATER AT 4 DEGREES CELCIUS AND 23 DEGREES CELCIUS (mean values ± SEM, n=3)

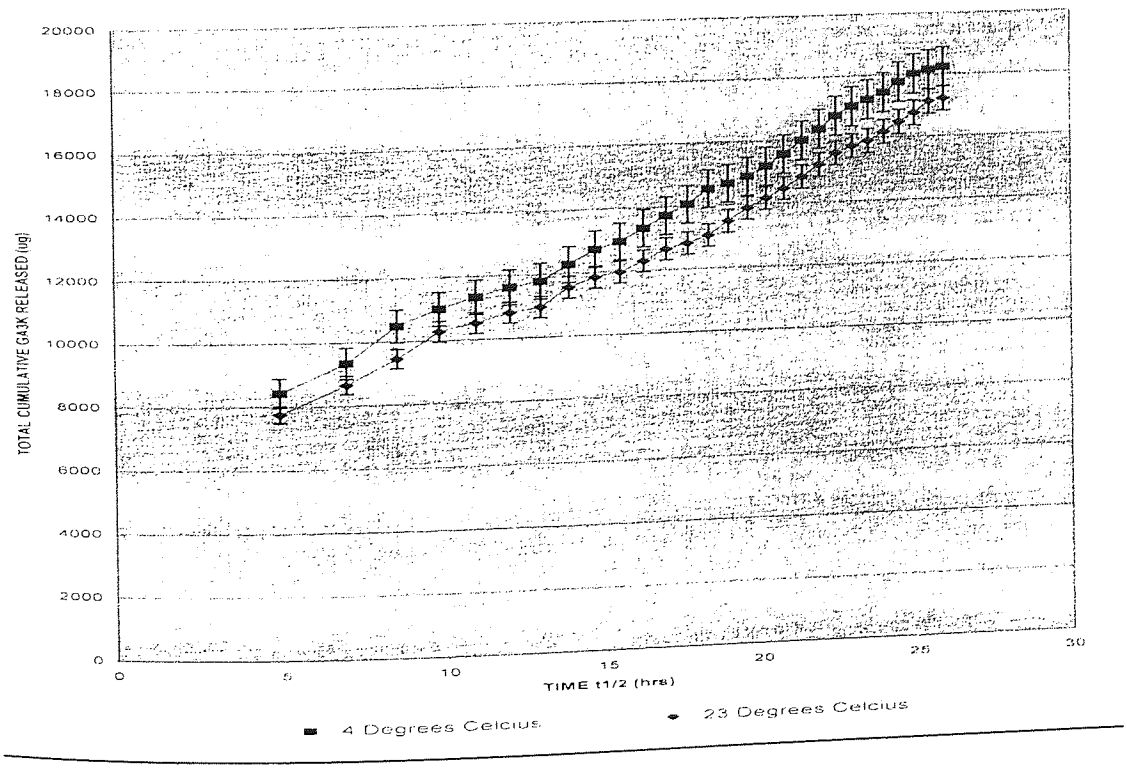

FIGURE 58 – TOTAL CUMULATIVE RELEASE PROFILES FOR 10% w/w GA_3K LOADED DIBLOCK NANOSPHERES INTO RURAL RAINWATER AT 4 DEGREES CELCIUS AND 23 DEGREES CELCIUS (mean values ± SEM, n=3)

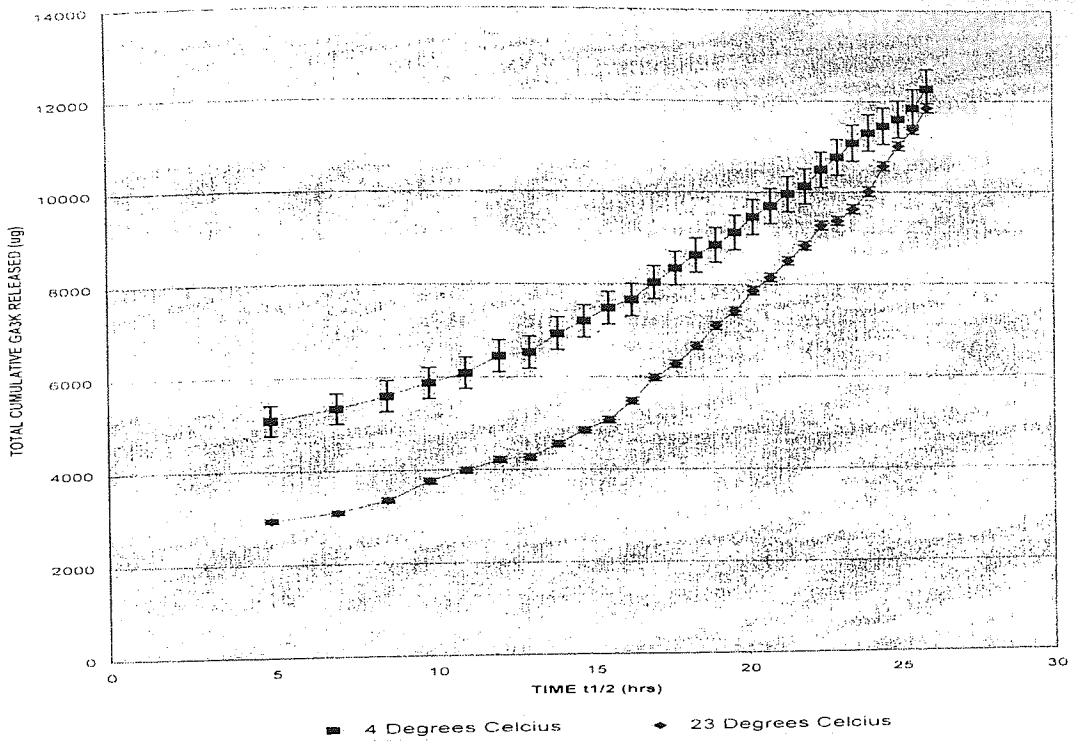

FIGURE 59 – TOTAL CUMULATIVE RELEASE PROFILES FOR 40% w/w GA_3K LOADED DIBLOCK NANOSPHERES INTO RURAL RAINWATER AT 4 DEGREES CELCIUS AND 23 DEGREES CELCIUS (mean values ± SEM, n=3)

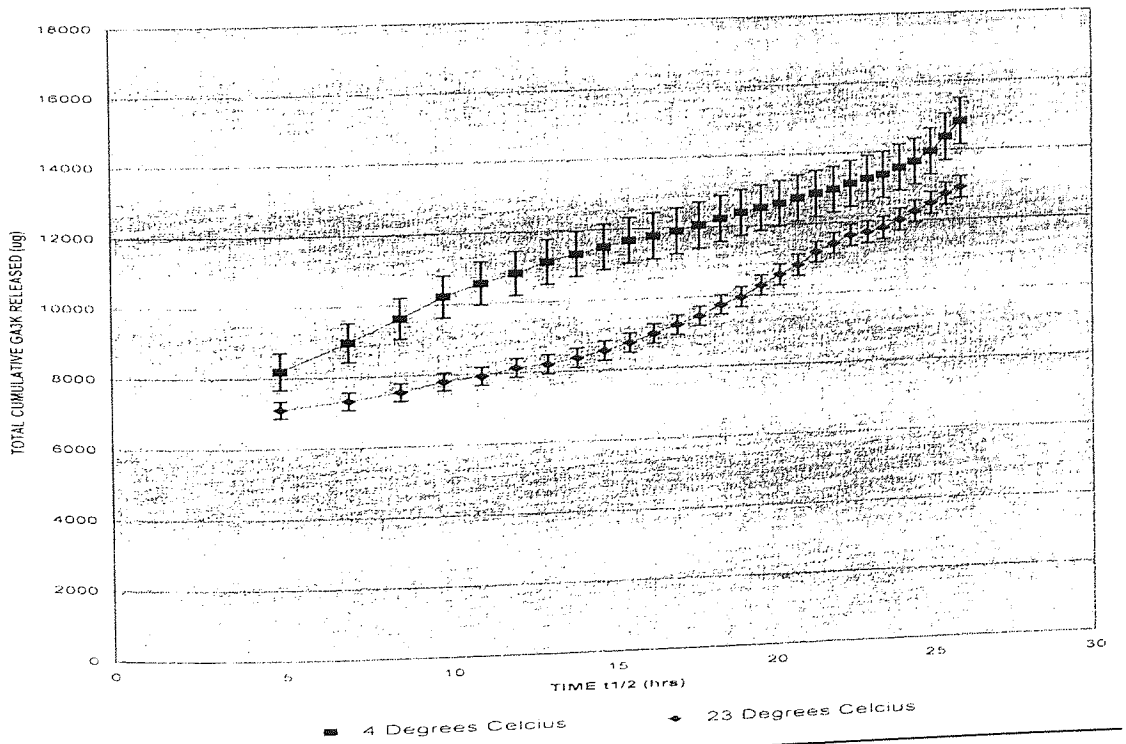

TABLE 56 - TOTAL CUMULATIVE RELEASE OF GA_3K AFTER 28 DAYS INCUBATION IN RURAL RAINWATER AT 4°C AND 23°C FROM THEORETICAL 10%, 20%, 30% AND 40% w/w GA_3K LOADED PHBHV-DIOL AND DIBLOCK NANOSPHERES (mean values ± SEM, n=3)

THEORETICAL % LOADING	POLYMER	INCUBATION TEMPERATURE (°C)	TOTAL CUMUALTIVE RELEASE (mg)
10	PHBHV-DIOL	4	11.19 ± 0.19
20	PHBHV-DIOL	4	14.93 ± 0.69
30	PHBHV-DIOL	4	15.37 ± 0.58
40	PHBHV-DIOL	4	18.24 ± 0.6[ab]
10	PHBHV-DIOL	23	10.08 ± 0.12
20	PHBHV-DIOL	23	12.45 ± 0.16
30	PHBHV-DIOL	23	15.81 ± 0.37
40	PHBHV-DIOL	23	17.23 ± 0.4[ab]
10	DIBLOCK	4	12.78 ± 0.43
20	DIBLOCK	4	12.99 ± 0.44
30	DIBLOCK	4	13.70 ± 0.61
40	DIBLOCK	4	14.84 ± 0.67
10	DIBLOCK	23	11.85 ± 0.1
20	DIBLOCK	23	12.03 ± 0.13
30	DIBLOCK	23	12.67 ± 0.22
40	DIBLOCK	23	12.92 ± 0.3

a, significantly increased ($P<0.05$) compared with theoretical 10% w/w GA_3K loaded nanospheres fabricated from the same polymer and incubated at the same temperature.
b, significantly increased ($P<0.05$) compared with theoretical 40% w/w GA_3K loaded nanospheres fabricated from Diblock polymer and incubated at the same temperature.

Although not always statistically significant, the total cumulative release of GA_3K tends to increase with increasing theoretical percentage GA_3K loading for nanospheres fabricated from PHBHV-Diol. In addition, the total cumulative release of GA_3K from PHBHV-Diol nanospheres tends to be marginally greater than that from Diblock nanospheres at both 4°C and 23°C, Table 56. Increasing the incubation temperature from 4°C to 23°C appears to marginally reduce the total cumulative release of GA_3K from GA_3K loaded Diblock nanospheres, Table 56.

6.3.14 MEAN PERCENTAGE HARVEST AND CONSEQUENT PERCENTAGE WEIGHT LOSS FROM UNLOADED AND THEORETICAL 10%, 20%, 30% AND 40% w/w GA_3K LOADED PHBHV-DIOL AND DIBLOCK NANOSPHERES AFTER 28 DAYS INCUBATION IN RELEASE STUDIES

After use in release studies, all nanosphere samples were quantitatively harvested and then freeze-dried according to the method detailed in Section 2.2.5, page 57 and weighed accurately to determine the percentage weight loss that had occurred over the 28 day incubation period. The results of these studies have been summarised in Table 57, below.

TABLE 57 - PERCENTAGE WEIGHT LOSS FROM UNLOADED AND THEORETICAL 10%, 20%, 30% AND 40% w/w GA_3K LOADED PHBHV-DIOL AND DIBLOCK NANOSPHERES AFTER INCUBATION IN RURAL RAINWATER AT 4°C AND 23°C FOR 28 DAYS (mean values ± SEM, n=3)

THEO. % LOADING	POLYMER	INCUBATION TEMPERATURE (°C)	INITIAL MEAN WT (mg)	HARVESTED MEAN WT (mg)	% WEIGHT LOSS
0	PHBHV-DIOL	4	100 ± 0	80.29± 0.63	19.71 ± 0.63[c]
10	PHBHV-DIOL	4	100 ± 0	75.36 ± 1	23.64 ± 1
20	PHBHV-DIOL	4	100 ± 0	65.06 ± 1.1	34.94 ± 1.1
30	PHBHV-DIOL	4	100 ± 0	58.8 ± 0.9	41.2 ± 0.89
40	PHBHV-DIOL	4	100 ± 0	51.7 ± 0.87[a]	48.30 ± 0.87[bd]
0	PHBHV-DIOL	23	100 ± 0	80.4 ± 0.56	19.58 ± 0.57[c]
10	PHBHV-DIOL	23	100 ± 0	77.9 ± 1.3	22.1 ± 1.3
20	PHBHV-DIOL	23	100 ± 0	64.94 ± 2	35.06 ± 2
30	PHBHV-DIOL	23	100 ± 0	57.8 ± 1.9	42.19 ± 1.9
40	PHBHV-DIOL	23	100 ± 0	52.58 ± 1.1[a]	47.42 ± 1.1[bd]
0	DIBLOCK	4	100 ± 0	87.86 ± 0.8	12.14 ± 0.8
10	DIBLOCK	4	100 ± 0	81.84 ± 0.8	18.16 ± 0.81
20	DIBLOCK	4	100 ± 0	74.6 ± 1.6	25.4 ± 1.59
30	DIBLOCK	4	100 ± 0	64.41 ± 2.7	35.59 ± 2.7
40	DIBLOCK	4	100 ± 0	62.85 ± 0.6[a]	37.15 ± 0.61[b]
0	DIBLOCK	23	100 ± 0	84.25 ± 1.4	15.79 ± 1.4
10	DIBLOCK	23	100 ± 0	82.68 ± 0.7	17.32 ± 0.66
20	DIBLOCK	23	100 ± 0	76.3 ± 1.3	23.7 ± 1.3
30	DIBLOCK	23	100 ± 0	66.39 ± 2.5	33.61 ± 2.5
40	DIBLOCK	23	100 ± 0	64.06 ± 2.1[a]	35.94 ± 2.1[b]

a, significantly reduced ($P<0.05$) compared with unloaded nanospheres fabricated using the same polymer and incubated at the same temperature.
b, significantly increased ($P<0.05$) compared with unloaded nanospheres fabricated using the same polymer and incubated at the same temperature.
c, significantly increased ($P<0.05$) compared with unloaded Diblock nanospheres incubated at the same temperature.
d, significantly increased ($P<0.05$) compared with theoretical 40% w/w GA_3K loaded Diblock nanospheres incubated at the same temperature.

The percentage weight loss from unloaded PHBHV-Diol nanospheres was significantly greater than that from unloaded Diblock nanospheres at both 4°C and 23°C, Table 57. This may be the result of a more rapid biodegradation of low molecular weight PHBHV-Diol compared with Diblock polymer in rural rainwater.

The percentage weight loss from theoretical 40% w/w GA_3K loaded nanospheres was significantly greater than that from unloaded nanospheres fabricated from the same polymer and incubated at the same temperature, Table 57.

Increasing the incubation temperature from 4°C to 23°C had no significant effect on the percentage weight loss from either unloaded or theoretical 10% to 40% w/w GA_3K loaded nanospheres fabricated from the same polymer, Table 57.

A large proportion of the additional weight loss not accounted for by release of GA_3K could be attributed to loss of residual PVA.

6.3.15 DETERMINATION OF RESIDUAL GA_3K REMAINING IN THEORETICAL 10%, 20%, 30% AND 40% w/w GA_3K LOADED PHBHV-DIOL AND DIBLOCK NANOSPHERES AFTER INCUBATION IN RURAL RAINWATER FOR 28 DAYS AT 4°C AND 23 °C

Determination of the residual GA_3K in nanospheres harvested from release studies after 28 days incubation at both 4°C and 23°C was carried out using the method described in Section 2.2.25, page 76 and the results have been summarised in Table 58, below.

TABLE 58 - RESIDUAL GA_3K IN THEORETICAL 10%, 20%, 30% AND 40% w/w GA_3K LOADED PHBHV-DIOL AND DIBLOCK NANOSPHERES AFTER INCUBATION IN RURAL RAINWATER FOR 28 DAYS AT 4°C AND 23°C (mean values ± SEM, n=3)

THEORETICAL % LOADING	POLYMER	INCUBATION TMPERATURE (°C)	RESIDUAL GA_3K AS % OF ACTUAL ORIGINAL GA_3K LOADING
10	PHBHV-DIOL	4	0
20	PHBHV-DIOL	4	0.79± 0.09
30	PHBHV-DIOL	4	1.13 ± 0.58
40	PHBHV-DIOL	4	3.1 ± 0.3[a]
10	PHBHV-DIOL	23	0.64 ± 0.05
20	PHBHV-DIOL	23	1.46 ± 0.34
30	PHBHV-DIOL	23	1.9 ± 0.4
40	PHBHV-DIOL	23	3.7 ± 0.6[a]
10	DIBLOCK	4	0
20	DIBLOCK	4	0.13 ± 0.04
30	DIBLOCK	4	1.7 ± 0.2
40	DIBLOCK	4	7.78 ± 0.6[ab]
10	DIBLOCK	23	0.46 ± 0.1
20	DIBLOCK	23	0.8 ± 0.17
30	DIBLOCK	23	1.7 ± 0.6
40	DIBLOCK	23	8.05 ± 1.2[ab]

a, significantly increased ($P<0.05$) compared with theoretical 10%, 20% and 30% w/w GA_3K loaded nanospheres fabricated from the same polymer and incubated at the same temperature over 28 days.
b, significantly increased ($P<0.05$) compared with theoretical 40% w/w GA_3K loaded PHBHV-Diol nanospheres incubated at the same temperature.

Apart from 10% w/w GA_3K loaded PHBHV-Diol nanospheres and 10% w/w GA_3K loaded Diblock nanospheres incubated in rural rainwater at 4°C, there remained significant amounts of residual GA_3K in the nanospheres after 28 days incubation, Table 58.

Irrespective of fabrication polymer and incubation temperature, the amount of GA_3K remaining in nanospheres after 28 days incubation tended to increase with increasing theoretical percentage GA_3K loading. The amount of GA_3K remaining in theoretical 40% w/w GA_3K loaded Diblock nanospheres was significantly greater than the amount remaining in similarly loaded PHBHV-Diol nanospheres after 28 days incubation at both 4°C and 23°C, Table 58.

6.3.16 DETERMINATION OF THE MEAN PARTICLE DIAMETER OF UNLOADED AND THEORETICAL 10%, 20%, 30% AND 40% w/w GA_3K LOADED PHBHV-DIOL AND DIBLOCK NANOSPHERES, AFTER INCUBATION IN RURAL RAINWATER AT 4°C AND 23°C, FOR 28 DAYS

Particle diameter analysis (Section 2.2.7, page 58) was performed on all nanosphere preparations after incubation for 28 days at either 4°C or 23°C in rural rainwater. The results of the particle diameter analysis can be seen in Table 59, below.

TABLE 59 - MEAN PARTICLE DIAMETER OF UNLOADED AND THEORETICAL 10%, 20%, 30% AND 40% w/w GA_3K LOADED PHBHV-DIOL AND DIBLOCK NANOSPHERES AFTER INCUBATION IN RURAL RAINWATER AT 4°C AND 23°C FOR 28 DAYS (mean values ± SEM, n=3)

THEO. % LOADING	POLYMER	INCUBATION TEMP. (°C)	MEAN DIAMETER BEFORE (nm)	MEAN DIAMETER AFTER (nm)	% DECREASE
0	PHBHV-DIOL	4	275.6 ± 1.79	272.7 ± 6	1.02 ± 2.2
10	PHBHV-DIOL	4	509 ± 11.29	407.3 ± 4.6	19.98 ± 1.1[a]
20	PHBHV-DIOL	4	565 ± 20.5	433.56 ± 7.3	23.26 ± 1.68[a]
30	PHBHV-DIOL	4	600.8 ± 7.9	538.5 ± 25.98	10.37 ± 4.8[a]
40	PHBHV-DIOL	4	616 ± 3.6	565.2 ± 22.96	8.25 ± 4.06[a]
0	PHBHV-DIOL	23	275.6 ± 1.79	269.4 ± 4.2	2.2 ± 1.6
10	PHBHV-DIOL	23	509 ± 11.29	398.88 ± 12.2	21.63 ± 3.1[a]
20	PHBHV-DIOL	23	565 ± 20.5	484.2 ± 3.7	14.3 ± 0.76[a]
30	PHBHV-DIOL	23	600.8 ± 7.9	548.8 ± 30.5	8.66 ± 5.56[a]
40	PHBHV-DIOL	23	616 ± 3.6	565.5 ± 25.5	8.2 ± 4.51[a]
0	DIBLOCK	4	328 ± 7.57	322.6 ± 1.4[b]	1.65 ± 0.4
10	DIBLOCK	4	534 ± 4	500.03 ± 9.5[c]	6.36 ± 1.9[a]
20	DIBLOCK	4	549.7 ± 8.4	497.6 ± 7.8[c]	9.48 ± 1.57[a]
30	DIBLOCK	4	601.8 ± 7.7	563.77 ± 20.4[c]	6.32 ± 3.62[a]
40	DIBLOCK	4	646.1 ± 12	613.6 ± 9.1[c]	5.03 ± 1.48[a]
0	DIBLOCK	23	328 ± 7.57	318.4 ± 6.7[b]	2.9 ± 2.1
10	DIBLOCK	23	534 ± 4	502.5 ± 12.9[c]	5.9 ± 2.57[a]
20	DIBLOCK	23	549.7 ± 8.4	514.9 ± 8.96[c]	6.33 ± 0.17[a]
30	DIBLOCK	23	601.8 ± 7.7	583.47 ± 3.1[c]	3.05 ± 0.5
40	DIBLOCK	23	646.1 ± 12	612.5 ± 20.2[c]	5.2 ± 3.2[a]

a, significantly elevated percentage decrease in diameter ($P<0.05$) compared with unloaded nanospheres fabricated using the same polymer and incubated at the same temperature.
b, significantly increased ($P<0.05$) compared with diameter of unloaded PHBHV-Diol nanospheres incubated at both 4°C and 23°C.
c, significantly increased ($P<0.05$) compared with the diameter of similarly GA_3K loaded PHBHV-Diol nanospheres incubated at both 4°C and 23°C.

Loading both PHBHV-Diol and Diblock nanospheres with GA_3K, significantly elevated the mean percentage decrease in nanosphere diameter after 28 days incubation, irrespective of incubation temperature compared with unloaded nanospheres.

Irrespective of both fabrication polymer and incubation temperature, the greatest mean percentage decrease in nanosphere diameter was observed for theoretical 20% w/w GA_3K loaded nanospheres, Table 59.

Irrespective of incubation temperature and percentage GA_3K loading, the mean diameter of GA_3K loaded PHBHV-Diol nanospheres was significantly smaller than the mean diameter of GA_3K loaded Diblock nanospheres, Table 59.

6.3.17 DETERMINATION OF THE MEAN ZETA POTENTIAL OF UNLOADED AND THEORETICAL 10%, 20%, 30% AND 40% w/w GA_3K LOADED PHBHV-DIOL AND DIBLOCK NANOSPHERES AFTER INCUBATION IN RURAL RAINWATER AT 4°C AND 23°C FOR 28 DAYS

Zeta potential measurements on all harvested and freeze-dried nanospheres were determined using the method described in Section 2.2.8, page 59. The values obtained after 28 days incubation were compared with zeta potential measurements obtained prior to use in release studies and the results have been summarised in Table 60, overleaf.

TABLE 60 - MEAN ZETA POTENTIAL OF UNLOADED AND THEORETICAL 10%, 20%, 30% AND 40% w/w GA_3K LOADED PHBHV-DIOL AND DIBLOCK NANOSPHERES AFTER INCUBATION IN RURAL RAINWATER AT 4°C AND 23°C FOR 28 DAYS (mean values ± SEM, n=3)

THEO. % LOADING	POLYMER	INCUBATION TEMPERATURE (°C)	MEAN ZETA POTENTIAL BEFORE (mV)	MEAN ZETA POTENTIAL AFTER (mV)
0	PHBHV-DIOL	4	-20.76 ± 0.38	-27.97 ± 0.39[c]
10	PHBHV-DIOL	4	-12.85 ± 0.58	-20.06 ± 1.4[c]
20	PHBHV-DIOL	4	-11.92 ± 0.46	-18.17 ± 0.87[c]
30	PHBHV-DIOL	4	-10.3 ± 0.27	-14.99 ± 0.95[c]
40	PHBHV-DIOL	4	-8.78 ± 0.58	-14.64 ± 0.9[bc]
0	PHBHV-DIOL	23	-20.76 ± 0.38	-31.03 ± 1.36[c]
10	PHBHV-DIOL	23	-12.85 ± 0.58	-21.61 ± 0.95[c]
20	PHBHV-DIOL	23	-11.92 ± 0.46	-19.89 ± 1.1[c]
30	PHBHV-DIOL	23	-10.3 ± 0.27	-19.58 ± 0.41[c]
40	PHBHV-DIOL	23	-8.78 ± 0.58	-15.34 ± 1.4[bc]
0	DIBLOCK	4	-35.99 ± 0.67	-44.35 ± 2.7[ac]
10	DIBLOCK	4	-11.8 ± 0.45	-30.86 ± 0.64[c]
20	DIBLOCK	4	-11.23 ± 0.52	-25.57 ± 1.2[c]
30	DIBLOCK	4	-9.93 ± 0.85	-19.6 ± 0.6[c]
40	DIBLOCK	4	-8.03 ± 0.71	-15.67 ± 0.79[bc]
0	DIBLOCK	23	-35.99 ± 0.67	-45.65 ± 1.68[ac]
10	DIBLOCK	23	-11.8 ± 0.45	-28.85 ± 0.7[c]
20	DIBLOCK	23	-11.23 ± 0.52	-25.05 ± 0.7[c]
30	DIBLOCK	23	-9.93 ± 0.85	-20.48 ± 1.7[c]
40	DIBLOCK	23	-8.03 ± 0.71	-19.06 ± 2.1[bc]

a, significantly elevated negative charge ($P<0.05$) compared with unloaded PHBHV-Diol nanospheres at both 4°C and 23°C.

b, significantly reduced negative charge ($P<0.05$) compared with theoretical 10% w/w GA_3K loaded nanospheres, irrespective of incubation temperature and fabrication polymer used.

c, significantly greater negative charge ($P<0.05$) compared with mean zeta potential of corresponding nanospheres prior to incubation in rural rainwater at both 4°C and 23°C.

Unloaded nanospheres showed the greatest negative charge and the incorporation of GA_3K, irrespective of the extent of theoretical percentage GA_3K loading, significantly lowered the negative charge on nanospheres fabricated from PHBHV-Diol and Diblock polymers, Table 60.

The zeta potential of all nanospheres became significantly more negative after 28 days incubation in rural rainwater at both 4°C and 23°C, irrespective of the fabrication polymer or theoretical percentage GA_3K loading, Table 60, compared to the mean zeta potential of corresponding nanospheres prior to use in release studies.

The zeta potential of unloaded nanospheres after incubation in rural rainwater remains significantly more negative than the zeta potential of GA_3K loaded nanospheres fabricated from each polymer. The zeta potential of unloaded Diblock nanospheres after incubation in rural rainwater also remains significantly more negative than the zeta potential of unloaded PHBHV-Diol nanospheres incubated at the same temperature, Table 60.

6.3.18 DETERMINATION OF THE WEIGHT AVERAGE MOLECULAR MASS (Mw) OF UNLOADED AND THEORETICAL 10%, 20%, 30% AND 40% w/w GA_3K LOADED PHBHV-DIOL AND DIBLOCK NANOSPHERES AFTER INCUBATION IN RURAL RAINWATER AT 4°C AND 23°C FOR 28 DAYS

The weight average molecular mass of harvested, freeze-dried nanospheres was determined using the method described in Section 2.2.9, page 62, to show what effect 28 days incubation has on the weight average molecular mass of the polymers. The decrease in weight average molecular mass resulting from 28 days incubation was calculated by subtracting the weight average molecular mass obtained prior to incubation from the weight average molecular mass obtained after incubation. No statistically significant difference was observed in mean weight average molecular mass between nanospheres incubated at 4°C and 23°C. The results have been summarised in Table 61, overleaf.

TABLE 61 – WEIGHT AVERAGE MOLECULAR MASS OF UNLOADED AND THEORETICAL 10%, 20%, 30% AND 40% w/w GA_3K LOADED PHBHV-DIOL AND DIBLOCK NANOSPHERES AFTER INCUBATION IN RURAL RAINWATER FOR 28 DAYS

(mean values ± SEM, n=3)

THEORETICAL % LOADING	POLYMER	MEAN MOLECULAR MASS BEFORE (Daltons)	MEAN MOLECULAR MASS AFTER (Daltons)	DECREASE IN MOLECULAR MASS (Daltons)
0	PHBHV-DIOL	8138 ± 625	3741 ± 15	4397 ± 610[b]
10	PHBHV-DIOL	2977 ± 81	2558 ± 133	419 ± 52
20	PHBHV-DIOL	2543 ± 98	2485 ± 40	58 ± 58
30	PHBHV-DIOL	2477 ± 74	2198 ± 118	279 ± 44
40	PHBHV-DIOL	2227 ± 46	2215 ± 5	12 ± 41
0	DIBLOCK	58 914 ± 1067	57 773 ± 240	1141 ± 827
10	DIBLOCK	38 133 ± 1717	34 175 ± 1775	3958 ± 58[a]
20	DIBLOCK	36 800 ± 850	34 475 ± 525	2325 ± 325[a]
30	DIBLOCK	35 933 ± 145	33 850 ± 50	2083 ± 95[a]
40	DIBLOCK	35 533 ± 706	34 350 ± 300	1183 ± 406[a]

a, significantly greater ($P<0.05$) decrease in weight average molecular mass after incubation compared to corresponding theoretical GA_3K loaded PHBHV-Diol nanospheres.

b, significantly greater ($P<0.05$) decrease in weight average molecular mass after incubation compared to unloaded Diblock nanospheres.

Following incubation in rural rainwater for 28 days, the weight average molecular mass of all nanospheres, irrespective of theoretical percentage GA_3K loading or fabrication polymer, showed a marginal decrease compared to the weight average molecular mass of corresponding nanospheres prior to use in release studies, Table 61.

Incubation of GA_3K loaded Diblock nanospheres in rural rainwater for 28 days, irrespective of theoretical percentage GA_3K loading, resulted in a significantly greater decrease in weight average molecular mass than corresponding GA_3K loaded PHBHV-Diol nanospheres, Table 61.

6.3.19 DETERMINATION OF THE RESIDUAL PVA CONTENT OF UNLOADED AND THEORETICAL 10%, 20%, 30% AND 40% w/w GA_3K LOADED PHBHV-DIOL AND DIBLOCK NANOSPHERES AFTER INCUBATION IN RURAL RAINWATER AT 4°C AND 23°C FOR 28 DAYS

Following 28 days incubation in rural rainwater at both 4°C and 23°C, no residual PVA could be detected in any of the nanosphere samples, irrespective of either the fabrication polymer used or the theoretical percentage GA_3K loading used. It was assumed that residual PVA was released concomitantly with GA_3K during the incubation period, which could explain the suppression in ionisation experienced when the GC-MS negative electrospray method was investigated for the detection of GA_3K in release study samples. The loss of PVA can also explain the additional weight loss showed by nanospheres following incubation, which cannot be attributed to drug release alone.

CHAPTER 7

BIODEGRADATION OF UNLOADED PHBHV-DIOL, 3HB 3HC AND DIBLOCK NANOSPHERES IN PHYSIOLOGICAL MEDIA AND RURAL RAINWATER

7.1 INTRODUCTION

The *in vitro* hydrolytic degradation of commercially available polyester copolymers, such as poly-(β-hydroxybutyrate-hydroxyvalerate), (PHB-HV) (Holland *et al*, 1987; Atkins and Peacock, 1996) and poly-(lactide-co-glycolide) (Hutchinson and Furr, 1990; Swarbrick and Boylan, 1990; Jalil and Nixon, 1990c) in simple aqueous buffers has been well characterised.

For drug delivery applications it is important to understand the mechanism of biodegradation of unloaded PHBHV-Diol, 3HB 3HC and Diblock polymer nanospheres. The reasons for this are to show the differences between chemical hydrolysis of Monsanto polymers and possible additional enzymatic hydrolysis; to establish whether biodegradation plays a part in the release mechanism of actives from the polymers over the 28 day incubation period and finally to show how the polymers biodegrade in the different body compartments and the rate at which they biodegrade.

Each incubation media containing the unloaded nanospheres was aspirated daily and analysed to ensure that soluble polymer degradation products and residual fabrication components such as PVA and F68 were not interfering with the assay technique for the active. All physico-chemical properties that were determined for active loaded nanospheres were also determined for unloaded nanospheres and the results compared statistically to see if the fabrication polymer, incubation media or incubation temperature had any influence on the rate of biodegradation.

The incubation of unloaded nanospheres was carried out to characterise the mechanisms of polymer biodegradation and predict the rate of biodegradation *in vivo,* with new-born calf serum used to mimic serum; pancreatin to mimic the small intestine, and in the external environment, where rural rainwater at 4°C and 23°C was used.

A decrease in polymer weight average molecular mass, as measured by GPC analysis during incubation, would suggest some form of biodegradation. If the molecular weight decreases to a point where soluble oligomers and monomers are formed, then significant mass loss from the nanospheres would occur and rapid active release would be expected.

Incubation in Hank's balanced salts solution (pH 7.4) at 37°C exposes the nanospheres to physical concentrations of buffer salts at body temperature and will provide information on the occurrence of simple chemical hydrolysis under physiological conditions.

Incubation in non-heat treated new born calf serum (pH 7.1) at 37°C was also carried out to provide information on the potential effects of serum enzymes, such as carboxylic ester hydrolase (E.C.3.1.1.1.), acetylcholine acylhydrolase (E.C.3.1.1.8), and acetylcholine acetylhydrolase (E.C.3.1.1.7), and serum protein (α-β globulin factors) adsorption on nanosphere biodegradation in parenteral application.

Incubation in porcine pancreatin (1.5% porcine pancreatin in HBSS, containing 2% w/v penicillin/streptomycin and 0.25mgml^{-1} amphotericin B) at 37°C, which comprises a non-sterile mixture of enzymes including lipase, amylase, phospholipase A2, cholesterol ester hydrolase, trypsin, chymotrypsin, serine proteases and carboxypeptidase A (Atkins, 1997), was carried out to mimic the biodegradation of nanospheres in the small intestine. There is evidence to suggest that enzymatic degradation might aggravate the underlying simple hydrolytic process of biodegradation of polymer nanospheres when incubated in porcine pancreatin, leading to the breakdown of the ester bonds in the polymer. The addition of both penicillin/streptomycin and amphotericin B to the non-sterile pancreatin solution was required to suppress *in vitro* broad spectrum microbial activity, since polyesters are known to be susceptible to biodegradation by both bacteria and fungi (Koosha *et al*, 1989; Yamada *et al*, 1993).

In order to investigate the possible environmental biodegradation of the novel Monsanto polyesters and their potential for use as an agricultural active delivery system in soil and to prevent run off from food crops, unloaded nanospheres were incubated in rural rainwater at 4°C and 23°C and the results compared with the release of GA_3K and Admire®, under the same incubation conditions to show how biodegradation had effected release.

7.2 RESULTS

7.2.1 MEAN PERCENTAGE HARVEST AND CONSEQUENT PERCENTAGE WEIGHT LOSS FROM UNLOADED PHBHV-DIOL, 3HB 3HC AND DIBLOCK NANOSPHERES AFTER 28 DAYS INCUBATION IN PHYSIOLOGICAL MEDIA AT 37°C AND RURAL RAINWATER AT 4°C AND 23°C

Unloaded nanospheres were incubated in physiological media at 37°C and rural rainwater at 4°C and 23°C for 28 days to see the effect of incubation on physico-chemical properties of the nanospheres.

Following the incubation period of 28 days, the nanospheres were quantitatively harvested and then freeze-dried as described in Section 2.2.5, page 57. The nanospheres were weighed accurately to determine the percentage weight loss during the release period. The results can be seen in Table 62, below.

TABLE 62 - MEAN PERCENTAGE HARVEST AND MEAN PERCENTAGE WEIGHT LOSS FROM UNLOADED NANOSPHERES FABRICATED FROM PHBHV-DIOL, 3HB 3HC AND DIBLOCK POLYMERS AFTER 28 DAYS INCUBATION IN PHYSIOLOGICAL MEDIA AT 37°C AND RURAL RAINWATER AT 4°C AND 23°C (mean values ± SEM, n=6)

POLYMER	MEDIUM	TEMP (°C)	% WEIGHT LOSS
PHBHV-DIOL	HBSS	37	16.37 ± 0.23
PHBHV-DIOL	NCS	37	20.5 ± 0.46
PHBHV-DIOL	PANC	37	18.2 ± 3.7
PHBHV-DIOL	RAIN WATER	4	8.7 ± 0.14
PHBHV-DIOL	RAIN WATER	23	9.3 ± 0.2
DIBLOCK	HBSS	37	37.67 ± 2.9[a]
DIBLOCK	NCS	37	26.6 ± 3.3[b]
DIBLOCK	PANC	37	33.7 ± 1.45
DIBLOCK	RAIN WATER	4	12.4 ± 1.6[c]
DIBLOCK	RAIN WATER	23	14.8 ± 1.3[d]
3HB 3HC	HBSS	37	25 ± 4.4
3HB 3HC	NCS	37	19.73 ± 2.7
3HB 3HC	PANC	37	34.5 ± 9.2

a, significantly greater ($P<0.05$) percentage weight loss than PHBHV-Diol and 3HB 3HC nanospheres incubated in the same physiological media.

b, significantly greater ($P<0.05$) percentage weight loss than PHBHV-Diol and 3HB 3HC nanospheres incubated in the same physiological media.

c, significantly greater ($P<0.05$) percentage weight loss than PHBHV-Diol nanospheres incubated in rural rainwater at 4°C.

d, significantly greater ($P<0.05$) percentage weight loss than PHBHV-Diol nanospheres incubated in rural rainwater at 23°C.

Incubation in non heat treated new born calf serum caused the greatest percentage weight loss of PHBHV-Diol nanospheres, suggesting that the PHBHV-Diol was susceptible to enzymatic biodegradation as well as simple chemical hydrolysis, Table 62. The lowest percentage weight loss from unloaded PHBHV-Diol nanospheres was observed after incubation in rural rainwater at 4°C. Increasing the incubation temperature of rural rainwater from 4°C to 23°C caused a marginal increase in the observed percentage weight loss from unloaded PHBHV-Diol nanospheres, indicating that temperature may have an effect on polymer biodegradation.

Hank's balance salts solution caused the greatest weight loss with Diblock nanospheres, suggesting that simple chemical hydrolysis played an important role in the biodegradation of Diblock polymer, Table 62. The lowest percentage weight loss from unloaded Diblock nanospheres was observed after incubation in rural rainwater at 4°C. Increasing the incubation temperature of rural rainwater from 4°C to 23°C caused a marginal increase in the observed percentage weight loss from unloaded Diblock nanospheres, Table 62, indicating that temperature of incubation medium may have an effect on the rate of biodegradation.

Incubation in porcine pancreatin caused the greatest percentage weight loss of 3HB 3HC nanospheres, suggesting that 3HB 3HC was susceptible to the cocktail of enzymes present in the small intestine, Table 62. Lowest percentage weight loss for unloaded 3HB 3HC nanospheres was observed after incubation in non heat treated new born calf serum at 37°C, Table 62. This would suggest that the enzymes present in new born calf serum were not as effective at hydrolysing 3HB 3HC as those enzymes found in porcine pancreatin.

Weight loss could also be attributed to a loss of residual PVA which is discussed later in this section.

7.2.2 MEAN PARTICLE DIAMETER OF UNLOADED NANOSPHERES FABRICATED FROM PHBHV-DIOL, 3HB 3HC AND DIBLOCK POLYMERS AFTER 28 DAYS INCUBATION IN PHYSIOLOGICAL MEDIA AT 37°C AND RURAL RAINWATER AT 4°C AND 23°C

Particle diameter analysis using photon correlation spectroscopy was performed on all unloaded nanosphere samples after 28 days incubation, as described in Section 2.2.7, page 58. The results of the mean particle diameter analysis have been summarised in Table 63, below.

TABLE 63 - MEAN PARTICLE DIAMETER OF UNLOADED NANOSPHERES FABRICATED FROM PHBHV-DIOL, 3HB 3HC AND DIBLOCK POLYMERS BEFORE AND AFTER INCUBATION FOR 28 DAYS IN PHYSIOLOGICAL MEDIA AT 37°C AND RURAL RAINWATER AT 4°C AND 23°C (mean values ± SEM, n=6)

POLYMER	MEDIUM	TEMP (°C)	MEAN DIAMETER BEFORE INCUBATION (nm)	MEAN DIAMETER AFTER INCUBATION (nm)	% DECREASE
PHBHV-DIOL	HBSS	37	275.6 ± 1.79	263.4 ± 0	4.39 ± 1.79
PHBHV-DIOL	NCS	37	275.6 ± 1.79	257.8 ± 0.8	6.42 ± 0.99[b]
PHBHV-DIOL	PANC	37	275.6 ± 1.79	261.8 ± 1.3	4.97 ± 0.49
PHBHV-DIOL	RAINWATER	4	275.6 ± 1.79	272.7 ± 6	1.02 ± 4.21
PHBHV-DIOL	RAINWATER	23	275.6 ± 1.79	269.4 ± 4.2	2.2 ± 2.41
DIBLOCK	HBSS	37	328 ± 7.57	299.67 ± 5.5	8.64 ± 2.07[a]
DIBLOCK	NCS	37	328 ± 7.57	315.7 ± 3.6	3.75 ± 3.97
DIBLOCK	PANC	37	328 ± 7.57	303.7 ± 2.6	7.41 ± 4.97[c]
DIBLOCK	RAINWATER	4	328 ± 7.57	322.6 ± 1.4	1.65 ± 6.17
DIBLOCK	RAINWATER	23	328 ± 7.57	318.4 ± 6.7	2.9 ± 0.87
3HB 3HC	HBSS	37	396.51 ± 4.4	388 ± 9.9[d]	2.14 ± 5.5
3HB 3HC	NCS	37	396.51 ± 4.4	391.7 ± 6.8[d]	1.21 ± 2.4
3HB 3HC	PANC	37	396.51 ± 4.4	389.2 ± 6.5[d]	1.84 ± 2.1

a, significantly increased ($P<0.05$) compared with percentage decrease in mean particle diameter of PHBHV-Diol and 3HB 3HC nanospheres in HBSS.

b, significantly increased ($P<0.05$) compared with percentage decrease in mean particle diameter of Diblock and 3HB 3HC nanospheres in NCS.

c, significantly increased ($P<0.05$) compared with percentage decrease in mean particle diameter of PHBHV-Diol and 3HB 3HC nanospheres in porcine pancreatin.

d, significantly increased ($P<0.05$) compared to the mean particle diameter of PHBHV-Diol and Diblock nanospheres.

Prior to incubation, the low molecular weight polymer PHBHV-Diol (1500 Daltons), produced nanospheres with the smallest mean particle diameter, Table 63. In contrast, the high molecular weight polymer, 3HB 3HC (172 000 Daltons), produced nanospheres with the largest mean particle diameter. Statistical analysis using one-way analysis of variance confirmed the differences in mean particle diameter between the three fabrication polymers to be extremely significant. Following incubation, the pattern of mean particle diameter remained unchanged, Table 63.

Of the physiological media, new born calf serum brought about the greatest percentage decrease in mean particle diameter of PHBHV-Diol nanospheres suggesting that enzymatic hydrolysis was also occurring in this situation, in addition to simple chemical hydrolysis, such as that seen when incubated in HBSS, Table 63. In contrast, the percentage decrease in mean particle diameter in rural rainwater was relatively low compared to that seen in physiological media and appeared to increase with increasing incubation temperature, suggesting that temperature did play a part in the biodegradation process.

Diblock nanospheres showed their greatest percentage decrease in mean particle diameter in HBSS compared with other physiological media, suggesting that biodegradation of this polymer was largely by simple chemical hydrolysis with little enzymatic contribution. In rural rainwater the percentage decrease in mean particle diameter was relatively low compared to that seen in physiological media and again appeared to be increased by increasing incubation temperature.

In comparison with the other polymers, 3HB 3HC nanospheres appeared to be relatively resistant to the physiological media showing relatively low percentage decreases in mean particle diameter after incubation, with HBSS producing the greatest percentage decrease, Table 63.

7.2.3 ZETA POTENTIAL MEASUREMENTS OF UNLOADED NANOSPHERES FABRICATED FROM PHBHV-DIOL, 3HB 3HC AND DIBLOCK POLYMERS BEFORE AND AFTER 28 DAYS INCUBATION IN PHYSIOLOGICAL MEDIA AT 37°C AND RURAL RAINWATER AT 4°C AND 23°C

The measurement of zeta potential of unloaded nanospheres before and after incubation was carried out using a Malvern ZetaMaster® as described in Section 2.2.8, page 59. The results have been summarised in Table 64, overleaf.

TABLE 64 - MEAN ZETA POTENTIALS OF UNLOADED NANOSPHERES FABRICATED FROM PHBHV-DIOL, 3HB 3HC AND DIBLOCK POLYMERS BEFORE AND AFTER INCUBATION FOR 28 DAYS IN PHYSIOLOGICAL MEDIA AT 37°C AND RURAL RAINWATER AT 4°C AND 23°C (mean values ± SEM, n=6)

POLYMER	MEDIUM	TEMP (°C)	MEAN ZETA POTENTIAL (mV)
PHBHV-DIOL	BEFORE INCUBATION	21	*-20.97 ± 0.38[a]
PHBHV-DIOL	HBSS	37	-26.11 ± 1.27
PHBHV-DIOL	NCS	37	-28.5 ± 1.74
PHBHV-DIOL	PANC	37	-21.63 ± 1.74
PHBHV-DIOL	RAINWATER	4	-27.97 ± 0.39
PHBHV-DIOL	RAINWATER	23	-31.03 ± 1.36
DIBLOCK	BEFORE INCUBATION	21	*-35.99 ± 0.67[a]
DIBLOCK	HBSS	37	-45.67 ± 0.83
DIBLOCK	NCS	37	-40.17 ± 1.28
DIBLOCK	PANC	37	-41.18 ± 1.77
DIBLOCK	RAINWATER	4	-44.35 ± 2.7
DIBLOCK	RAINWATER	23	-45.65 ± 1.68
3HB 3HC	BEFORE INCUBATION	21	*-10.97 ± 0.74[a]
3HB 3HC	HBSS	37	-14.37 ± 0.12
3HB 3HC	NCS	37	-16.8 ± 1.7
3HB 3HC	PANC	37	-11.7 ± 0

* n=36

a, significantly less negative ($P<0.05$) compared with unloaded nanospheres fabricated from the same polymer and incubated for 28 days in physiological media.

.

The mean zeta potential of all unloaded nanosphere samples, irrespective of either fabrication polymer or incubation media, became more negative following incubation, Table 64. This could be due to the removal of residual PVA. After incubation, all the unloaded Diblock nanospheres, irrespective of the incubation medium, were elevated to the stability band known as 'fairly good stability' (Riddick, 1968). After incubation, the unloaded Diblock nanospheres were the most negative of the three types of polymer nanospheres, suggesting that the Diblock nanospheres would be the most stable in aqueous suspension. Unloaded Diblock nanospheres incubated in HBSS at 37°C for 28 days gave the most negative zeta potential, Table 64. This was closely followed by unloaded Diblock nanospheres incubated in rural rainwater, pH 6.24 at 4°C and 23°C, suggesting that the nanospheres are more stable in aqueous media.

The most negative zeta potential for unloaded PHBHV-Diol nanospheres was observed following incubation for 28 days in rural rainwater, pH 6.24, at 4°C and 23°C, just putting these nanospheres into the stability band known as 'moderate stability' (Riddick, 1968), Table 64.

The most positive zeta potentials observed after incubation were those of unloaded 3HB 3HC nanospheres, irrespective of the incubation media. On the other hand the most negative zeta potential for unloaded 3HB 3HC nanospheres was observed after incubation in NCS, pH 7.1, at 37°C for 28 days, Table 64, just putting them into the stability band known as 'threshold of delicate dispersion' (Riddick, 1968). Following 28 days incubation in HBSS and pancreatin at 37°C the unloaded 3HB 3HC nanospheres remained in the stability band known as 'threshold of agglomeration' (Riddick, 1968).

7.2.4 DETERMINATION OF THE WEIGHT AVERAGE MOLECULAR MASS OF UNLOADED NANOSPHERES FABRICATED FROM PHBHV-DIOL, 3HB 3HC AND DIBLOCK POLYMERS BEFORE AND AFTER 28 DAYS INCUBATION IN PHYSIOLOGICAL MEDIA AT 37°C AND RURAL RAINWATER AT 4°C AND 23°C

The weight average molecular mass was measured by gel permeation chromatography, using the method detailed in Section 2.2.9, page 62. The results obtained from GPC analysis have been summarised in Table 65.

TABLE 65 - MEAN WEIGHT AVERAGE MOLECULAR MASS OF UNLOADED NANOSPHERES FABRICATED FROM PHBHV-DIOL, 3HB 3HC AND DIBLOCK POLYMERS BEFORE AND AFTER 28 DAYS INCUBATION IN PHYSIOLOGICAL MEDIA AT 37°C AND RURAL RAINWATER AT 4°C AND 23°C (mean values ± SEM, n=3)

POLYMER	MEDIUM	TEMP (°C)	MEAN Mw BEFORE INCUBATION (Daltons)	MEAN Mw AFTER INCUBATION (Daltons)	MEAN DECREASE IN Mw (Daltons)
PHBHV-DIOL	HBSS	37	8138 ± 625	7710 ± 363	428 ± 262
PHBHV-DIOL	NCS	37	8138 ± 625	6873 ± 186	1265 ± 439
PHBHV-DIOL	PANC	37	8138 ± 625	7762 ± 63	376 ± 562
PHBHV-DIOL	RAINWATER	4	8138 ± 625	3741 ± 15	4397 ± 610[d]
PHBHV-DIOL	RAINWATER	23	8138 ± 625	3741 ± 15	4397 ± 610[d]
DIBLOCK	HBSS	37	58 914 ± 1067	54 800 ± 925	4114 ± 142[a]
DIBLOCK	NCS	37	58 914 ± 1067	43 250 ± 161	15 664 ± 906[b]
DIBLOCK	PANC	37	58 914 ± 1067	56 425 ± 392	2489 ± 675[c]
DIBLOCK	RAINWATER	4	58 914 ± 1067	57 773 ± 240	1141 ± 827
DIBLOCK	RAINWATER	23	58 914 ± 1067	57 773 ± 240	1141 ± 827
3HB 3HC	HBSS	37	119 167 ± 307	118 967 ± 103	200 ± 204
3HB 3HC	NCS	37	119 167 ± 307	118 317 ± 233	850 ± 74
3HB 3HC	PANC	37	119 167 ± 307	118 183 ± 384	984 ± 77

a, significantly greater mean decrease in molecular weight ($P<0.05$) compared with mean decrease in molecular weight of PHBHV-Diol and 3HB 3HC nanospheres incubated in HBSS.
b, significantly greater mean decrease in molecular weight ($P<0.05$) compared with mean decrease in molecular weight of PHBHV-Diol and 3HB 3HC nanospheres incubated in NCS.
c, significantly greater mean decrease in molecular weight ($P<0.05$) compared with mean decrease in molecular weight of PHBHV-Diol and 3HB 3HC nanospheres incubated in porcine pancreatin.
d, significantly greater mean decrease in molecular weight ($P<0.05$) compared with mean decrease in molecular weight of Diblock nanospheres incubated in rural rainwater.

The molecular weight of PHBHV-Diol, Diblock and 3HB 3HC unloaded polymer nanospheres, before incubation, were 8138 ± 625 Daltons (n=6), 58 914 ± 106 Daltons (n=6) and 119 167 ± 307 Daltons (n=6) respectively, Table 65. This compares with the mean molecular weights of PHBHV-Diol, Diblock and 3HB 3HC, according to Monsanto, of 1500 Daltons, 37 000 Daltons and 172 000 Daltons, respectively. The results obtained by GPC in the present study, and expressed as 'polystyrene equivalents' probably show the variation in GPC analysis which can occur due to changes in instrumentation.

All unloaded nanospheres, irrespective of fabrication polymer or incubation media, showed a marginal decrease in mean molecular weight after 28 days incubation in either physiological media at 37°C, or rural rainwater at 4°C or 23°C, Table 65, suggesting that biodegradation had taken place.

Diblock nanospheres showed a significantly greater decrease in mean molecular weight after incubation in physiological media for 28 days than corresponding nanospheres fabricated from PHBHV-Diol or 3HB 3HC polymers, Table 65. The greatest mean decrease in molecular weight for Diblock nanospheres was observed after incubation in new born calf serum, which suggested that biodegradation of this polymer was a result of both simple chemical hydrolysis and enzymatic hydrolysis.

PHBHV-Diol nanospheres showed a significantly greater decrease in mean molecular weight after incubation in rural rainwater at both 4°C and 23°C, compared to Diblock nanospheres, Table 65. The increase in temperature had no statistical effect on the mean decrease in molecular weight for either fabrication polymer.

7.2.5 DETERMINATION OF THE THERMAL CHARACTERISTICS OF UNLOADED NANOSPHERES FABRICATED FROM PHBHV-DIOL AND DIBLOCK POLYMERS BEFORE AND AFTER INCUBATION IN PHYSIOLOGICAL MEDIA AT 37°C AND RURAL RAINWATER AT 4°C AND 23°C

Thermal analysis by differential scanning calorimetry (DSC) (Section 2.2.10, page 64) was only performed on PHBHV-Diol and Diblock nanospheres that had been harvested from rural rainwater after 28 days incubation at 4°C and 23°C. No significant difference was observed between the thermal characteristics of unloaded PHBHV-Diol and Diblock nanosphere samples that had been incubated at 4°C and 23°C.

TABLE 66 - SUMMARISED RESULTS OF DSC ANALYSIS SHOWING GLASS TRANSITION TEMPERATURE (Tg), RECRYSTALLISATION TEMPERATURE AND MELTING POINT TEMPERATURES FOR UNLOADED NANOSPHERES FABRICATED FROM PHBHV-DIOL AND DIBLOCK POLYMERS BEFORE AND AFTER INCUBATION IN RURAL RAINWATER (mean values, n=2)

POLYMER	Tg (°C)	RECRYSTALLISATION TEMPERATURE (°C)	MELTING POINT 1 (°C)	MELTING POINT 2 (°C)
PHBHV-DIOL – BEFORE INCUBATION	-12	55	80	99
DIBLOCK – BEFORE INCUBATION	35	61	138	152
PHBHV-DIOL – AFTER INCUBATION	-6	56	90	105
DIBLOCK – AFTER INCUBATION	40	63	140	156

It can be seen from Table 66 above, that the Tg of PHBHV-Diol and Diblock nanospheres had marginally increased following incubation in rural rainwater for 28 days. The Tg, recrystallisation and melting point temperatures of unloaded Diblock nanospheres remained considerably higher than those of the unloaded PHBHV-Diol nanospheres, following incubation for 28 days in rural rainwater, Table 66.

7.2.6 DETERMINATION OF THE RESIDUAL PVA CONTENT OF UNLOADED PHBHV-DIOL, 3HB 3HC AND DIBLOCK NANOSPHERES BEFORE AND AFTER INCUBATION IN PHYSIOLOGICAL MEDIA AT 37°C AND RURAL RAINWATER AT 4°C AND 23°C

The residual PVA content of the unloaded nanospheres before and after incubation was determined following the method detailed in Section 2.2.12, page 67. The results of the PVA determination can be seen in Table 67.

TABLE 67 - MEAN PERCENTAGE RESIDUAL PVA IN UNLOADED NANOSPHERES FABRICATED FROM PHBHV-DIOL, 3HB 3HC AND DIBLOCK POLYMERS BEFORE AND AFTER INCUBATION IN PHYSIOLOGICAL MEDIA AT 37°C AND RURAL RAINWATER AT 4°C AND 23°C (mean values ± SEM, n=12)

POLYMER	BEFORE / AFTER INCUBATION	MEAN RESIDUAL PVA (%)
PHBHV-DIOL	BEFORE	12.1 ± 0.7
3HB 3HC	BEFORE	13.84 ± 0.58[a]
DIBLOCK	BEFORE	11.6 ± 0.09
PHBHV-DIOL	AFTER	0[b]
3HB 3HC	AFTER	0[b]
DIBLOCK	AFTER	0[b]

a, significantly greater mean percentage residual PVA ($P<0.05$) compared to PHBHV-Diol and Diblock polymer nanospheres.

b, significantly reduced mean percentage residual PVA ($P<0.05$) compared to corresponding polymer nanospheres before incubation.

Prior to incubation, unloaded 3HB 3HC nanospheres contained significantly more residual PVA than unloaded PHBHV-Diol or Diblock nanospheres. No residual PVA was detected in any of the polymer nanosphere samples after incubation for 28 days in physiological media at 37°C or rural rainwater at 4°C and 23°C. This would suggest that the majority of the PVA was released along with the active, into the incubation media.

CHAPTER 8

DETERMINATION OF THE RATE OF BIODEGRADATION OF PHBHV-DIOL, PHB, AND CELLULOSE BY THE MICROBIAL CONTENT OF GREEN GARDEN WASTE COMPOST

8.1 INTRODUCTION

A composting study using the International Standard ISO/FDIS 14855 method of determining the ultimate aerobic biodegradation and disintegration of plastic materials under controlled composting conditions by the analysis of evolved carbon dioxide was used to measure the ultimate aerobic biodegradation of PHBHV-Diol and PHB, using cellulose polymer as a control. The biodegradation of polymers under composting conditions was carried out to identify how the polymers would act and biodegrade when used in the environment, for example as Pesticide Delivery Systems (PDS).

Analysis of the innate ability of polymers to biodegrade and the rate of biodegradation of the polymers used to fabricate agrochemical loaded drug delivery nanospheres was deemed to be very important in light of the recent introduction of environmental regulations (Evens and Sikdar, 1990; Cimmino *et al*, 1991; Musmeci *et al*, 1994) regarding environmental pollution with non-degradable plastics. Currently there is an on-going world-wide research effort to develop biodegradable polymers from renewable sources (Kaplan *et al*, 1993; Thayer, 1990). These polymers can be placed into three categories: firstly, natural polymers such as cellulose starch and proteins; secondly, modified natural polymers prepared by biological and/or chemical modifications, such as cellulose acetate, lignocellulose esters (Thiebaud and Borredon, 1995) and polyalkanoates, such as PHBHV (Brandl *et al*, 1988; Doi *et al*, 1992), and PHBHV-Diol; and finally composite materials which combine natural biodegradable materials and a synthetic biodegradable polymer, such as starch-vinylalcohol-copolymer (Bastioli *et al*, 1994).

These biodegradable materials may be a viable solution for some plastic items, especially those that are either litter prone, not easily collected or not easily recycled, such as the plastics used in agriculture (Mayer *et al*, 1994). Some of these materials would also make ideal materials for the fabrication of biodegradable agrochemical loaded nanospheres which could be applied to the land without the fear of accumulation, pollution and run off.

The development of biodegradable materials has created the need to evaluate and monitor the biodegradation of these polymers in different environments, when dumping in marine, freshwater, compost or landfill sites. Therefore, many organisations such as the American Society of Testing and Materials, the Organisation for Economic Co-operation and Development, the European Committee of Normalisation and the Japanese Biodegradable Plastics Society have developed standard laboratory test procedures for evaluating potentially biodegradable materials (Calmon-Decriaud *et al*, 1998). The work presented in this thesis covers the biodegradation of three polymer powders using a green waste composting method initially outlined in a draft by the European Committee of Normalisation and described as International Standard ISO/FDIS 14855 '*Determination of the ultimate aerobic biodegradation and disintegration of plastic materials under controlled composting conditions – method by analysis of evolved carbon dioxide*' (Appendix Section 1.1, page 246).

8.1.2 THE PROCESS OF BIODEGRADATION

Biodegradation is the natural and complex process (Calmon-Decriaud *et al*, 1998; Groenhof, 1998) of decomposition facilitated by biochemical mechanisms, and each standard organisation gives its own definition of a biodegradable polymer. The definition used in this thesis is that given by the European Committee of Normalisation (May, 1993) and is defined as being 'a degradable material in which the degradation results from the action of micro-organisms and ultimately the material is converted to water, carbon dioxide and/or methane and a new cell biomass'. Although biodegradability can be defined as the intrinsic capacity of a material to be degraded by the action of micro-organisms, there are two more precise definitions available depending on the final fate of the polymers (Battersby *et al*, 1994; Buchanan *et al*, 1993). These being, 'Primary Biodegradability', whereby the polymer loses specific properties resulting from an alteration in its chemical structure, and 'Ultimate Biodegradability', as determined by the method utilised in this thesis, whereby the polymer is total degraded by micro-organisms with the production of carbon dioxide. In some cases this mineralisation is not complete because some end products of polymer breakdown are resistant to degradation and remain as oligomers (Calmon-decriaud *et al*, 1998).

These considerations introduce the concept of 'environmentally acceptable biodegradable polymers' (Swift, 1994). To be classed as a biodegradable polymer, the polymer only has to be capable of being partially degraded, but to become an 'environmentally acceptable biodegradable polymer', the polymer must be either totally mineralised, or if only partially mineralised, then it must not produce any environmentally harmful residues.

Ecotoxicity should be investigated, when substantial degradation of test material has occurred, to try and highlight any possible negative ecotoxic effects. The ecotoxicity tests must be performed in a bid to maximise the sensitivity and to give the highest assurance of the absence of toxic compounds (Degli-Innocenti and Bastioli, 1997).

8.1.3 COMPOSTING

The International Standard (ISO/FDIS 14855) method used in the present work really analyses the compostability of the polymers. Compostability is the ability of a material to be degraded by micro-organisms in a compost made of green garden waste and relies on organic carbon being converted to carbon dioxide. The polymer samples are intensively composted in static reactors containing an iso-standard compost (which has undergone a 10 day analysis period, prior to the addition of the samples, to ensure its suitability). A continuous airflow, that is 100% free of carbon dioxide, is provided so that carbon dioxide produced from the reactor vessels can be monitored by infrared.

The compost used in the analysis is carefully selected mature phase mesophilic compost. The entire composting process is divided into three phases and involves a succession of bacteria, actinomycetes and other fungi, whose numbers are dictated by the availability of specific nutrients and also temperature. The

early phase of composting is known as the mesophilic phase and involves mainly bacteria and fungi. The subsequent phase, known as the thermophilic phase is characterised by the abundance of actinomycetes and bacteria, and the final curing stage, which is again known as the mesophilic stage often involves higher fungi (Groenhof, 1998). The phases and associated temperatures of the composting process are shown in Figure 60, below.

FIGURE 60 - CONSTITUENT PHASES AND TEMPERATURE PROFILE OF THE COMPOSTING PROCESS WITH ITS ASSOCIATED PHASES OF MICROBIAL ACTIVITY (Groenhof, 1998).

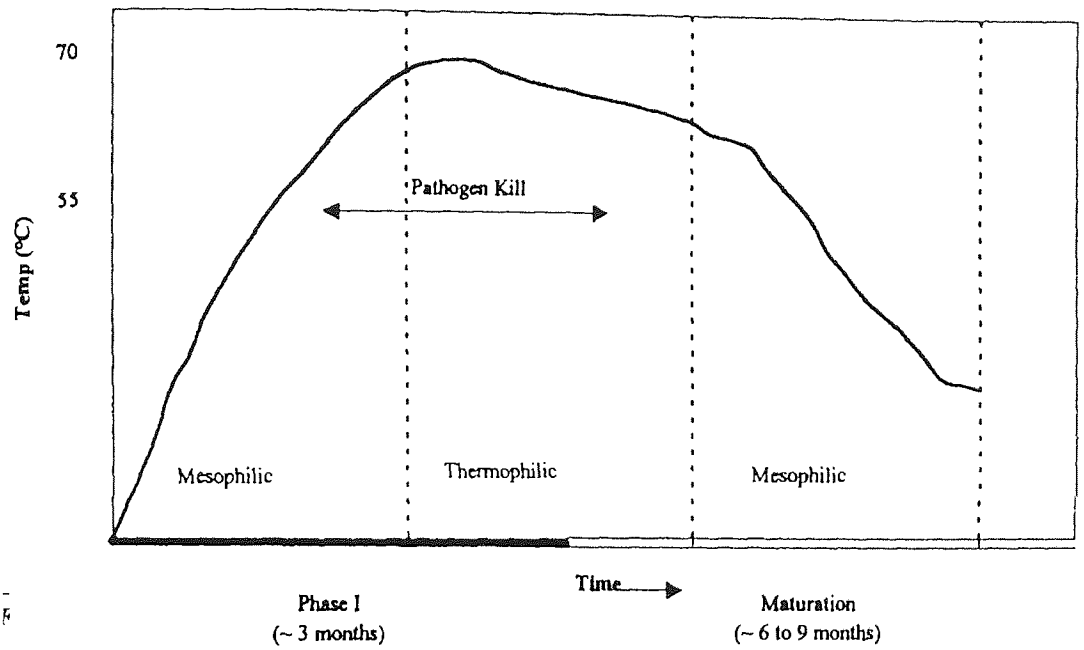

The entire composting process takes around 9 – 12 months and will have resulted in a ≅50% reduction in the volume of material, as well as its sanitation. The high temperatures, often 60°C - 70°C, kill weed seeds and pathogens making it safe for use. Thermophilic phase compost is not used in the reactor vessels because in this phase the compost is biodegrading rapidly, creating its own heat and producing large volumes of carbon dioxide. The carbon dioxide produced from the compost itself would mask the carbon dioxide being produced from the biodegradation of the polymers invalidating the experiment. Mature phase mesophilic compost (6 months old green waste compost) has been used instead of thermophilic phase compost, which is heated to an optimum composting temperature of 58°C ± 2 with a moisture content of ~50%. The mature phase mesophilic compost has the advantage of producing very little carbon dioxide of its own, making the detection of carbon dioxide generated from the biodegradation of the polymers that much easier.

Table 68 below, shows the basic chemical characteristics of the three polymers used in the composting study.

TABLE 68 - BASIC CHEMICAL CHARACTERISTICS OF CELLULOSE, PHBHV-DIOL AND PHB USED IN THE COMPOSTING STUDY

CHARACTERISTIC	CELLULOSE	PHBHV-DIOL	PHB
MOLECULAR WEIGHT (Daltons)	$(324)_n$	1500	$(50)_n$
APPEARANCE	FINE WHITE POWDER	FINE WHITE POWDER	FINE WHITE POWDER

The chemical structures of cellulose, PHBHV-Diol and PHB, respectively, used in the composting studies are shown below, Figure 61.

FIGURE 61 – CHEMICAL STRUCTURE OF POLYMERS USED IN COMPOSTING

CELLULOSE

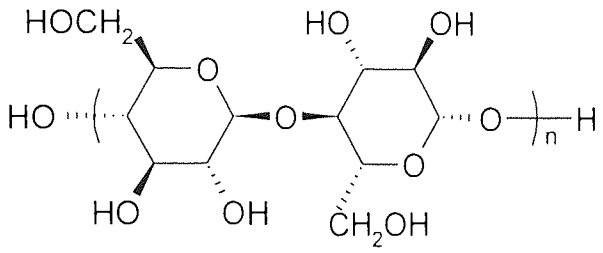

PHBHV-DIOL

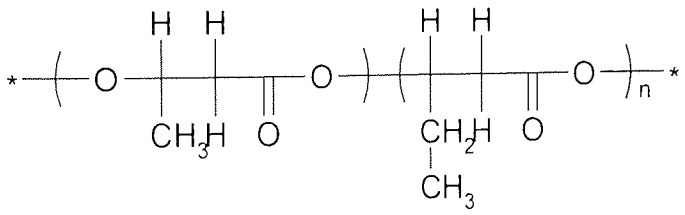

PHB

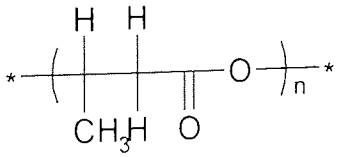

The monitoring of biodegradation in terms of carbon dioxide production was selected over direct weight loss methods, because it was not feasible to harvest and weigh polymer after biodegradation once it had been mixed into the compost. The cumulative theoretical mass of carbon dioxide generated, as a measure of the biodegradation of the polymers, was determined for 75 days of composting, using the method described in Section 2.2.29, page 78.

8.2 RESULTS

8.2.1 ANALYSIS OF COMPOST OVER 10 DAY INCUBATION PERIOD

Six month old mesophilic compost was analysed for moisture content (Section 2.2.30), percentage volatile solids (Section 2.2.31), percentage nitrogen (Section 2.2.33) and pH (Section 2.2.32), according to the International Standard (ISO/FDIS 14855) (Appendix Section 1.1, page 246) method followed in this study. Table 69 below, shows the levels of various parameters in M602 green waste compost initially and after the 10 day incubation period.

TABLE 69 - ANALYSES OF COMPOST BEFORE AND AFTER THE 10 DAY INCUBATION PERIOD.

ANALYSIS	IN INITIAL COMPOST	IN COMPOST AFTER 10 DAY INCUBATION
% WATER	49.99	53.82
% VOLATILE SOLIDS	36.5	37.8
% CARBON	21	21.7
% NITROGEN	0.72	0.68
PH	7.9	7.7

Humidified air was drawn through the compost at a rate of 100ml *per* minute and this was responsible for the increased percentage water content, Table 69.

8.2.2 CARBON DIOXIDE EVOLUTION OVER THE 10 DAY INCUBATION PERIOD

The International Standard ISO/FDIS 14855 required that the compost produce between 50mg and 150mg of carbon dioxide per gram of volatile solids, over the incubation period of 10 days. The rate of carbon dioxide evolution *per* day from the compost over the 10 day incubation period is shown overleaf, Table 70.

TABLE 70 - DAILY CARBON DIOXIDE EVOLUTION FROM THE COMPOST OVER THE INITIAL 10 DAY INCUBATION PERIOD

Day	Reactor 1	Reactor 2	Reactor 3	Reactor 4	Reactor 5	Reactor 6	Mean	$g.CO_2$/day
1	0.88	0.86	0.91	0.92	0.89	0.86	0.887	2.336
2	0.73	0.76	0.89	0.82	0.75	0.79	0.790	2.082
3	0.62	0.63	0.66	0.69	0.66	0.64	0.650	1.713
4	0.53	0.48	0.51	0.43	0.58	0.52	0.508	1.339
5	0.47	0.42	0.41	0.34	0.47	0.47	0.430	1.133
6	0.41	0.35	0.39	0.26	0.36	0.31	0.347	0.913
7	0.36	0.32	0.34	0.22	0.35	0.27	0.310	0.817
8	0.31	0.31	0.28	0.24	0.27	0.26	0.278	0.733
9	0.23	0.26	0.26	0.25	0.31	0.33	0.273	0.720
10	0.21	0.17	0.24	0.22	0.26	0.26	0.227	0.597
				Total mass CO_2 evolved(g)				**12.385**

From the total mass of carbon dioxide evolved from the compost over the 10 day incubation period (12.385g), the mass of carbon dioxide *per* gram of volatile solids was calculated using Equation 5, page 81. For compost M602 the mass of carbon dioxide *per* gram of volatile solids was calculated as **115.67 mg *per* gram.** This value was within the limits set for ISO/FDIS 14855, and so the compost was used in the biodegradation study.

8.2.3 CHEMICAL ANALYSIS OF M602 COMPOST OVER 75 DAY BIODEGRADATION PERIOD.

Full chemical analysis of the compost was carried out on a weekly basis over 75 days of composting and can be seen in Appendix Section 5.1, page 285. Table 71 overleaf, shows a summary of the data obtained after week one and week eleven of the composting period.

TABLE 71 - CHEMICAL ANALYSIS OF M602 GREEN GARDEN WASTE COMPOST IN EACH REACTION VESSEL AFTER WEEK ONE AND WEEK ELEVEN OF THE BIODEGRADATION PERIOD

WEEK	SAMPLE	pH	% NITROGEN	% WATER	% CARBON	% VOLATILE SOLIDS
1	NO POLYMER	7.8	0.62	52.86	21.26	37.00
1	PHBHV-DIOL 1	7.8	0.66	51.57	23.68	41.20
1	PHBHV-DIOL 2	7.7	0.61	54.30	24.83	43.20
1	CELLULOSE 1	7.6	0.57	48.69	25.63	44.60
1	CELLULOSE 2	7.7	0.60	54.49	24.54	42.70
1	PHB	7.8	0.55	53.82	24.90	43.40
11	NO POLYMER	8.6[a]	0.09[b]	51.22	14.00[c]	24.40[d]
11	PHBHV-DIOL 1	8.4[a]	0.18[b]	53.60	14.48[c]	25.20[d]
11	PHBHV-DIOL 2	8.3[a]	0.14[b]	50.90	15.12[c]	26.30[d]
11	CELLULOSE 1	8.2[a]	0.11[b]	52.70	15.12[c]	26.30[d]
11	CELLULOSE 2	8.3[a]	0.06[b]	54.60	16.44[c]	28.60[d]
11	PHB	8.4[a]	0.16[b]	52.30	14.54[c]	25.30[d]

a, significantly increased ($P<0.05$) compared with the pH of corresponding samples after one week of composting.

b, significantly reduced ($P<0.05$) compared with percentage nitrogen of corresponding samples after one week of composting.

c, significantly reduced ($P<0.05$) compared with percentage carbon of corresponding samples after one week of composting.

d, significantly reduced ($P<0.05$) compared with percentage volatile solids of corresponding samples after one week of composting.

The pH of the compost in each of the reaction vessels became significantly more alkaline ($P<0.05$) over the 75 day composting period. The overall mean pH after week one was 7.73 ± 0.03 (n=6), which increased to 8.37 ± 0.056 (n=6), after the 75 day period.

The percentage nitrogen content of the compost in each of the reaction vessels also decreased significantly ($P<0.05$) over the composting period. The overall mean percentage nitrogen content of the compost after week one was 0.60 % ± 0.016 (n=6) and this decreased to a mean of 0.12 % ± 0.018 (n=6).

The water content of the soil remained fairly constant throughout the 75 day composting period, Table 71. However, the water content of one of the two reactor vessels containing PHBHV-Diol polymer did eventually become waterlogged and by week nine it had a percentage moisture content of 66.4%. To counteract this, additional compost was added to this reactor vessel in order to absorb the excess moisture. The water content of the reactor had returned to within the optimum composting range (~50%)

by the following week. The overall mean moisture content of the compost after week one was 52.62 % ± 0.9 (n=6) and after the 75 days of composting, the mean moisture content was 52.55 % ± 0.57 (n=6). The percentage carbon and percentage volatile solids within the compost samples decreased significantly ($P<0.05$) over the 75 day composting period. The percentage carbon content of the compost in the background reactor vessel, which contained no polymer, predictably showed the lowest carbon content each week.

By the end of the 75 day composting period, the visual appearance of the compost had changed. The compost appeared to be less fibrous and the bulk had been reduced. The remaining compost also appeared to be a lot wetter, even though analysis of the moisture content showed this not to be true.

8.2.4 MEASUREMENT OF THE BIODEGRADATION OF CELLULOSE, PHBHV-DIOL AND PHB IN TERMS OF CARBON DIOXIDE EVOLUTION, OVER 45 DAYS

The biodegradation of the test polymers was based on the amount of carbon dioxide release calculated with respect to the theoretical value of carbon dioxide that could be produced from the complete biodegradation of the polymer. Computation of the theoretical weight of carbon dioxide produced by a given weight of cellulose, PHBHV-Diol and PHB has been carried out using Equations 6.1, 6.2 and 6.3, respectively, in Section 2.2.29, page 78.

The mean cumulative daily percentage biodegradation of cellulose, PHBHV-Diol and PHB polymers, shown in terms of the evolution of carbon dioxide over the initial 45 day composting period has been summarised in Table 72, overleaf.

TABLE 72 – MEAN CUMULATIVE DAILY PERCENTAGE BIODEGRADATION OF CELLULOSE, PHBHV-DIOL AND PHB POLYMERS, CALCULATED FROM THE EVOLUTION OF CARBON DIOXIDE OVER 45 DAYS

DAY	MEAN CELLULOSE	MEAN PHBHV-DIOL	PHB
0	0	0	0
1	0.18	2.10	0.41
2	0.83	4.03	0.77
3	1.65	5.63	1.06
4	3.08	6.80	1.49
5	4.23	7.80	1.94
6	4.88	8.89	2.35
7	5.58	10.01	2.66
8	6.25	11.25	3.46
9	6.98	12.34	4.66
10	7.87	13.50	6.09
11	8.94	14.65	7.48
12	9.98	15.68	9.16
13	10.90	16.64	10.73
14	11.74	17.78	12.10
15	12.59	18.63	13.18
16	13.35	19.43	14.06
17	13.99	20.13	14.86
18	14.59	20.78	15.60
19	15.47	21.68	16.67
20	16.46	22.74	18.06
21	17.46	23.90	18.96
22	18.32	25.01	20.51
23	19.32	26.00	21.64
24	20.26	27.09	22.80
25	21.28	28.25	23.89
26	22.31	29.48	25.02
27	23.26	30.412	26.05
28	24.08	31.40	27.09
29	25.11	32.98	28.12
30	26.14	34.15	29.20
31	27.26	35.19	30.21
32	28.25	36.04	31.21
33	29.11	37.05	32.55
34	29.97	38.08	33.59
35	30.75	39.15	34.49
36	32.93	41.94	36.32
37	33.89	42.94	37.64
38	34.86	44.23	39.00
39	35.77	45.62	40.04
40	36.77	46.96	41.18
41	37.86	48.37	42.23
42	39.04	49.60	43.39
43	40.05	50.63	44.66
44	41.31	51.77	46.00
45	42.72	52.99	47.45

In order to pass the ISO/FDIS 14855 validity criteria, the degree of biodegradation of the cellulose reference material, after 45 days, had to be greater than 70%. As can be seen from day 45 in Table 72 above, this was not achieved.

The total cumulative theoretical mean percentage carbon dioxide production from the ultimate aerobic composting of cellulose, PHBHV-Diol and PHB polymers over 45 days has been illustrated in Figure 62.

FIGURE 62 – TOTAL CUMULATIVE THEORETICAL MEAN % CARBON DIOXIDE PRODUCTION FROM THE ULTIMATE AEROBIC COMPOSTING OF CELLULOSE, PHB AND PHBHV-DIOL OVER 45 DAYS IN M602 GREEN GARDEN WASTE COMPOST (mean values ± SEM, n=2)

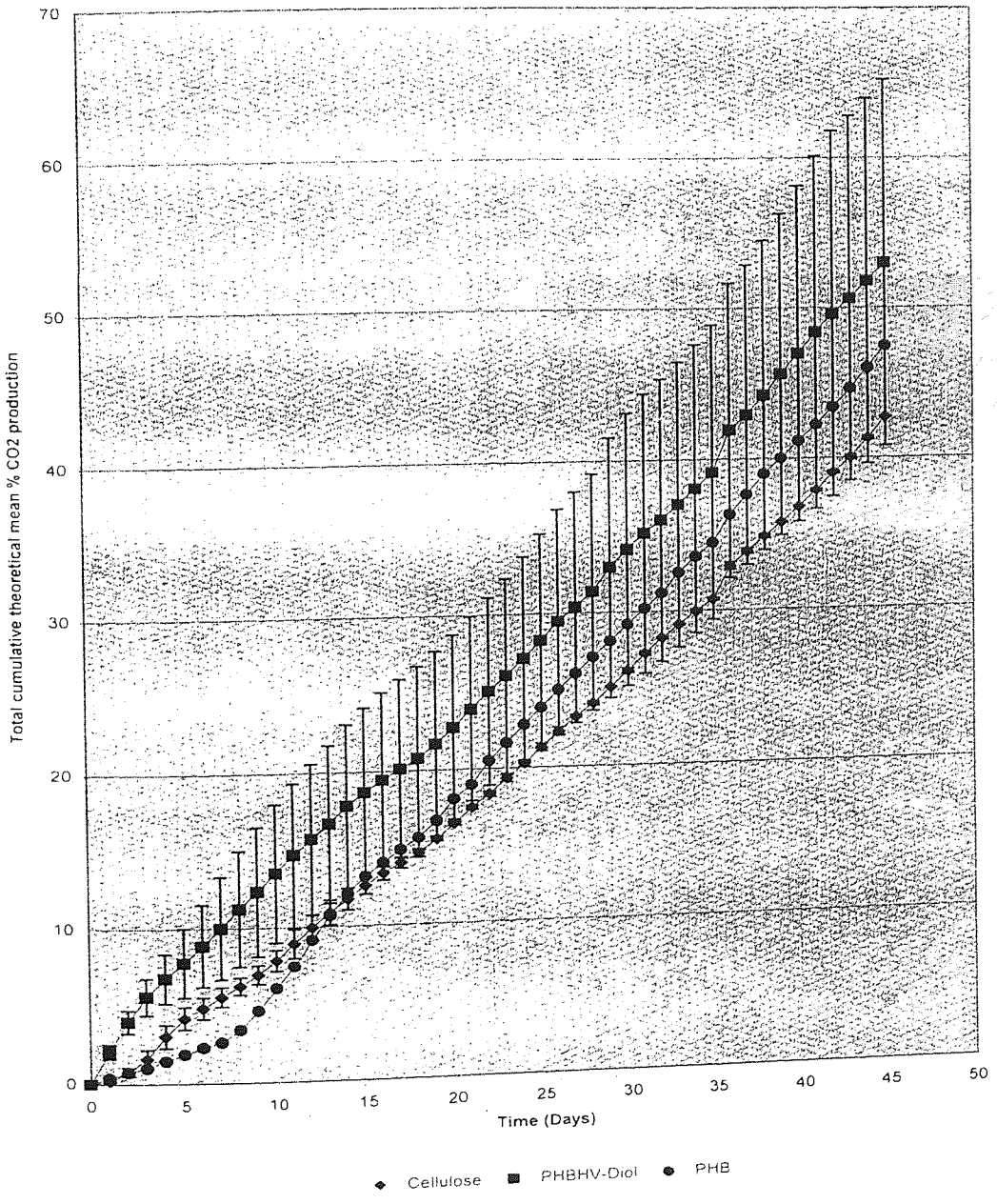

The biodegradation of all three polymers proceeds rapidly from the onset of composting with PHBHV-Diol showing the most rapid biodegradation. This observation is consistent with the fact that PHBHV-Diol had the lowest molecular weight of the three test polymers (1500 Daltons). The rate of biodegradation of PHB exceeded that of cellulose after 14 days, Figure 62. However, the differences between the total cumulative theoretical mean percentage carbon dioxide produced from the ultimate aerobic composting of cellulose, PHB and PHBHV-Diol over 45 days is not statistically significant and could be the result of natural variation.

8.2.5 THE RATE OF BIODEGRADATION OF CELLULOSE, PHBHV-DIOL AND PHB IN TERMS OF CARBON DIOXIDE EVOLUTION, OVER 75 DAYS OF COMPOSTING

Since the criteria for biodegradation validity had not been achieved, it was decided to continue the exposure of the polymers to composting for a further 30 days. Compost studies were terminated after 75 days and the cumulative daily percentage biodegradation of cellulose, PHBHV-Diol and PHB polymers, in terms of carbon dioxide evolution over the entire 75 day composting period have been summarised in Appendix Section 5.2, page 289. Table 73 overleaf, summarises the total cumulative percentage biodegradation of cellulose, PHBHV-Diol and PHB in terms of carbon dioxide evolution after the entire 75 day composting period.

TABLE 73 – TOTAL PERCENTAGE BIODEGRADATION OF CELLULOSE, PHBHV-DIOL AND PHB POLYMERS AFTER 75 DAYS COMPOSTING IN M602 GREEN GARDEN WASTE COMPOST

CELLULOSE 1	CELLULOSE 2	MEAN CELLULOSE	PHBHV-DIOL 1	PHBHV-DIOL 2	MEAN PHBHV-DIOL	PHB
73.58	74.78	74.18	80.13	71.08	75.60	84.03

PHB showed the greatest biodegradation after 75 days composting in green garden waste M602 compost. This was marginally greater than the biodegradation of PHBHV-Diol and cellulose polymers over the same time period, Table 73.

Polymer biodegradation expressed in terms of the total cumulative theoretical mean percentage carbon dioxide production from the ultimate aerobic composting of cellulose, PHBHV-Diol and PHB polymers over 75 days composting is shown in Figure 63.

FIGURE 63 – TOTAL CUMULATIVE THEORETICAL MEAN % CARBON DIOXIDE PRODUCTION FROM THE ULTIMATE AEROBIC COMPOSTING OF CELLULOSE, PHB AND PHBHV-DIOL OVER 75 DAYS IN M602 GREEN GARDEN WASTE COMPOST (mean values ± SEM, n=2)

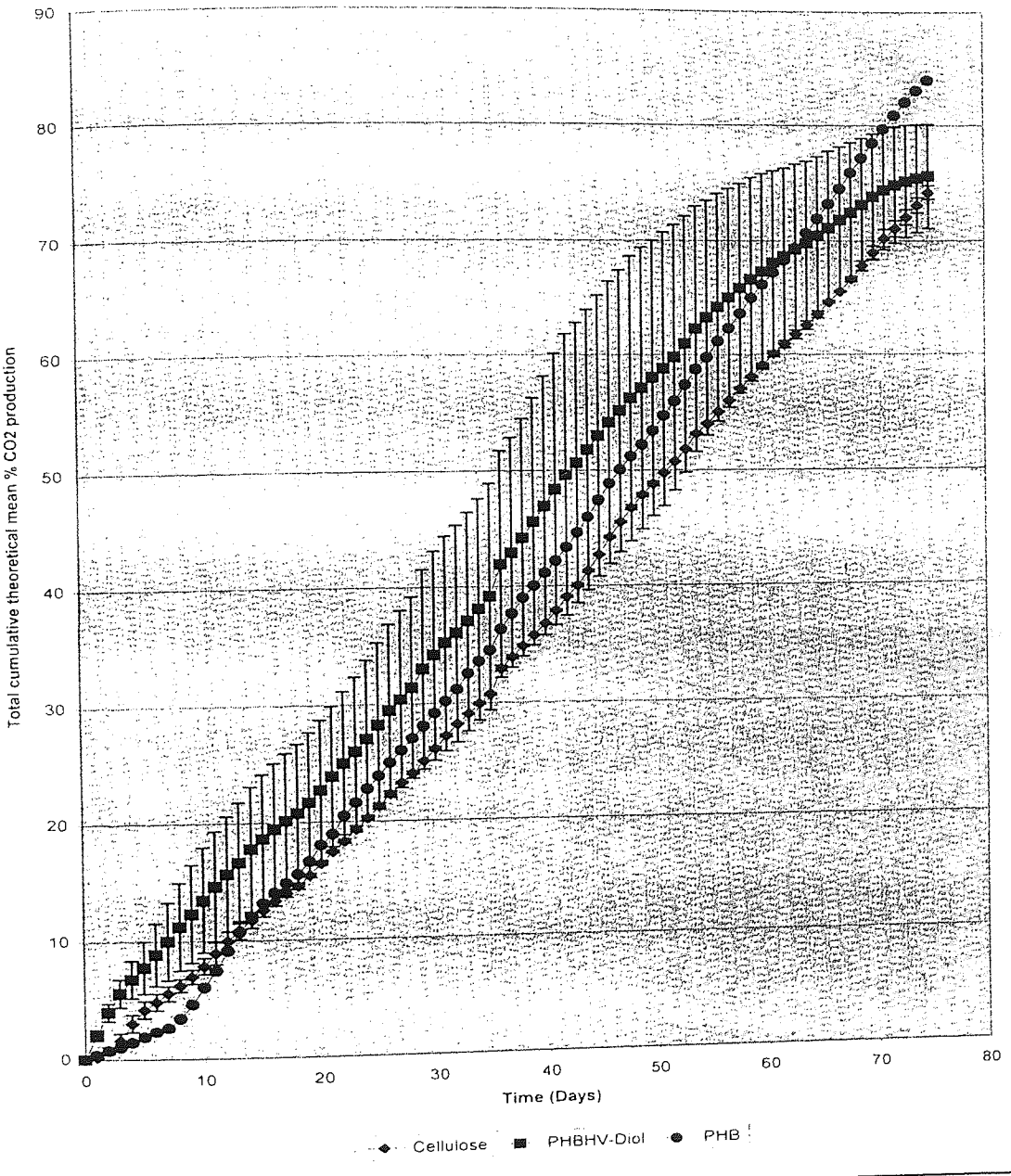

Rapid biodegradation of PHBHV-Diol, compared to cellulose and PHB, continued until day 60, after which the rate began to fall away. After day 14, the rate of biodegradation of PHB was always greater than that of cellulose and after day 63, the percentage biodegradation of PHB exceeded that of PHBHV-Diol. After the 75 day composting period, PHB showed the greatest percentage biodegradation, Figure 63.

CHAPTER 9

DISCUSSION

The pharmaceutical and agricultural effectiveness of a polymer based active delivery vehicle relies heavily on the reproducibility of the methods employed to produce it, which in turn will effect the reproducibility of its performance *in vitro* and *in vivo*.

Preliminary evaluation of microsphere/nanosphere fabrication techniques demonstrated that the F68 double sonication solvent evaporation fabrication method could be used to reproducibly generate very small nanospheres from a range of polyesters supplied by Monsanto, St.Louis, Missouri, USA. The technique could be used to fabricate nanospheres loaded with the surrogate protein BSA and an insecticide Admire® and a plant growth factor Gibberellic Acid A_3 – potassium salt.

Physico-chemical characteristics of the nanospheres has shown that the mean particle diameter of nanospheres loaded with BSA, Admire® and GA_3K increased as the theoretical percentage loading increased. Unloaded nanospheres fabricated from PHBHV-Diol, Diblock and 3HB 3HC were always significantly smaller than those loaded with active, irrespective of the active incorporated. Irrespective of the active incorporated, the largest nanospheres were fabricated using the high molecular weight polymer 3HB 3HC (172 kD), followed in turn by those fabricated from Diblock (37 kD) and PHBHV-Diol (1.5 kD). The same pattern of sizing was also true for the unloaded nanospheres fabricated from the same polymers. The increase in nanosphere mean particle diameter brought about by using different fabrication polymers was a function of the higher molecular weight of the fabrication polymer. The less soluble the polymers were in organic solvent, the more viscous the resulting solution became and the larger the final diameter of the resultant nanospheres. Jalil and Nixon (1990) have reported similar observations.

The interaction of colloidal carriers such as nanospheres with phagocytes and their cellular uptake in the GI tract is influenced by their surface characteristics (Japson *et al*, 1993). Surface charge is known to alter the phagocytosis of a carrier (Tabata and Ikada, 1990) and nanosphere sequestration by the RES can be prevented via the application of hydrophilic coatings based on the poloxamer and poloxamine series. For example, poloxamer 407 has been reported to redirect polystyrene latex to the endothelial cells of the bone marrow (Pouton *et al*, 1992) and poloxamine 908 coated systems are retained by the spleen (Moghimi *et al*, 1991). Non-charged particles are considered less likely to be recognised by the RES (Wilkins and Myers, 1966). It has been documented by Stossel *et al* (1972), that particles with a large negative or large positive charge are more rapidly ingested than those with a weak negative charge. This work was confirmed by Tabata and Ikada (1988) who found that rate of phagocytosis of microspheres with negative and positive zeta potentials of equal numerical value was not significantly different and that phagocytosis occurred more rapidly with increasing negative zeta potential. However, it is the surface hydrophobicity, as opposed to the zeta potential, that has the greatest influence on the rate of microsphere ingestion by macrophages (Tabata and Ikada, 1990). The zeta potential of microspheres and nanospheres, in both a pharmaceutical and agricultural context, is related to certain aspects of colloidal stability such as the ability of microspheres or nanospheres to coagulate

and aggregate. The higher the negativity of the zeta potential, the more repulsion energy is present between the nanospheres, and therefore the less likely they are to aggregate, but the more rapidly they are likely to be phagocytosed, *in vivo*.

The mean zeta potential of BSA loaded nanospheres in the present work was considerably more positive than that of unloaded nanospheres fabricated from the same polymer, irrespective of the theoretical percentage BSA loading used. This might suggest a possible steric effect due to pendant chains or that the incorporated BSA was in some way reducing the extent of the negative charge on the nanospheres making them more positive and increasing the likelihood of flocculation. On the other hand, a combination of the effect of BSA and the presence of excessive residual PVA might have increased the tendency of the nanospheres to aggregate. Yamako and co-workers (1993) found that residual PVA could reduce the absolute negative charge on the surface of microspheres. The incorporation of BSA into nanospheres might alter the distribution of PVA within the nanospheres and hence effect the net surface charge. In the present study the PVA content of BSA loaded nanospheres, irrespective of either the fabrication polymer used or theoretical percentage BSA loading was in the region of 11 to 17% w/w. Hence *in vivo*, BSA loaded Diblock nanospheres, irrespective of the theoretical percentage BSA loading, would be expected to be phagocytosed the slowest, whereas BSA loaded 3HB 3HC nanospheres, irrespective of the theoretical percentage BSA loading would probably be phagocytosed in the shortest period of time. Although the colloidal stability of the BSA loaded Diblock nanospheres was the greatest compared to BSA loaded PHBHV-Diol and 3HB 3HC nanospheres, with a mean zeta potential of ~14mV BSA loaded Diblock nanospheres were still only in the stability band defined as 'threshold of agglomeration' (Riddick, 1968). Following incubation in HBSS at 37°C all nanosphere samples, both unloaded and BSA loaded, irrespective of the fabrication polymer used, became more electronegative. This increased electronegativity could be due to the release of encapsulated BSA from the surface layers and internal matrix of the nanosphere reducing the nanospheres to a more 'unloaded' state. On the other hand the increased electronegativity could be due either to the removal of residual PVA or a combination of the two. Unloaded nanospheres incubated as controls concomitant with BSA loaded nanospheres also showed an increase in electronegativity when incubated in HBSS at 37°C suggesting that the loss of residual PVA *per se* might have a profound effect on the surface charge of the nanospheres and hence improve their stability in aqueous suspension.

The zeta potential of Admire® loaded PHBHV-Diol and Diblock nanospheres followed an identical pattern to that of BSA loaded nanospheres. However, the incorporation of GA_3K into PHBHV-Diol and Diblock nanospheres did not. Unloaded Diblock nanospheres were more negatively charged than unloaded PHBHV-Diol nanospheres, but loading with GA_3K, irrespective of the theoretical percentage GA_3K loading used, resulted in PHBHV-Diol nanospheres becoming more negatively charged than the Diblock nanospheres. The total amount of GA_3K that could be loaded into the PHBHV-Diol and Diblock nanospheres at each theoretical percentage loading was not significantly different, and so on this basis the increase in the negative charge

observed for the GA_3K loaded PHBHV-Diol nanospheres was not a result of GA_3K loading. However, the residual PVA content of GA_3K loaded PHBHV-Diol nanospheres was significantly greater than that of GA_3K loaded Diblock nanospheres, irrespective of the theoretical percentage GA_3K loading. This however contradicts the findings of Yamako and co-workers (1993) and the results obtained for BSA and Admire® loaded nanospheres and would require further research to ascertain an exact reason for the findings.

Determination of the weight average molecular mass of the virgin polymers by GPC confirmed that PHBHV-Diol had the lowest molecular weight, followed by Diblock, with 3HB 3HC having the highest weight average molecular mass. However, these values did not correspond with the molecular weights supplied by Monsanto for these novel polyesters. In the present study the weight average molecular mass of unloaded polymer nanospheres was shown to be lower than that of BSA loaded polymer nanospheres indicating that the incorporation of BSA was increasing the nanosphere weight average molecular mass. The weight average molecular mass of BSA loaded PHBHV-Diol nanospheres also increased in line with increased theoretical percentage BSA loading, confirming that the incorporation of BSA was dramatically increasing the weight average molecular mass of PHBHV-Diol nanospheres. This may indicate molecular aggregation. Further work would be required to confirm this. However, the incorporation of BSA did not increase the high weight average molecular mass of 3HB 3HC nanospheres. Here the mean weight average molecular mass of virgin 3HB 3HC was significantly higher than that of unloaded and BSA loaded 3HB 3HC nanospheres. In contrast, loading with the active Admire® significantly reduced the mean weight average molecular mass of nanospheres fabricated from both PHBHV-Diol and Diblock polymers. Irrespective of the fabrication polymer used, increasing the theoretical percentage Admire® loading from 10% w/w to 40% w/w significantly reduced the mean weight average molecular mass. Determination of the weight average molecular mass of unloaded and GA_3K loaded nanospheres showed that, irrespective of the fabrication polymer used, the weight average molecular mass of unloaded nanospheres was significantly greater than that of GA_3K loaded nanospheres irrespective of the theoretical percentage GA_3K loading. However, increasing the theoretical percentage GA_3K loading had no significant effect on the mean weight average molecular mass of GA_3K loaded PHBHV-Diol and Diblock nanospheres.

Thermal analysis of virgin fabrication polymers and unloaded and active loaded nanospheres was performed using DSC to provide information on the glass transition temperature (Tg), recrystallisation temperature, melting point temperatures and possibly confirmation of nanosphere matrix loading. In addition, a decrease in the Tg caused by the incorporation of active materials within polymer nanospheres can indicate whether the active has been incorporated and formed a molecular dispersion within the nanosphere matrix by chemically interacting with the polymer (Benoit *et al*, 1986). If the drug interacts with the polymer to form either a true or partial solution, it will plasticise the polymer and lower the characteristic Tg (Pepper, 1997). When this occurs, the drug in solution will be thermodynamically stable and homogenously dispersed in the polymer matrix, which is the ultimate result. If the nanoencapsulated drug has little affinity with the polymer

then the glass transition temperature will not be effected and the drug will form crystals due to phase separation. The results obtained for BSA loaded Diblock nanospheres are supported by work done by Pepper (1997), but tend to contradict work published by Jalil and Nixon (1990c). On the thermal profiles there were no endotherms present which corresponded with known melting point of the encapsulated BSA. Melting of the crystalline regions of BSA occurs at ~230°C (Pepper, 1997). This suggests that the BSA was either molecularly dispersed throughout the polymer matrix of the nanospheres, or that BSA does not form crystals under nanosphere formulation conditions. The presence of an endotherm corresponding to the melting of crystalline BSA would suggest that BSA was incorporated in particulate form within the polymer matrix. However, the absence of an endotherm does not always mean that BSA is molecularly dispersed (Watts *et al*, 1990). From the present work there was evidence to suggest that the incorporated BSA existed in solution rather than in the crystalline state within the polymer matrix. Tg values obtained for the both Admire® and GA_3K loaded PHBHV-Diol and Diblock nanospheres were unaffected by an increase in theoretical percentage active loading. However the actives were known to be incorporated or associated in some way with the nanospheres due to the profiles obtained in release studies and analysis of the nanoencapsulation efficiency. However, increasing the theoretical percentage Admire® and GA_3K loading did marginally increase the recrystallisation temperature, irrespective of the fabrication polymer used. The two melting point temperatures associated with the two components of the copolymer generally appeared to decrease with increasing theoretical percentage Admire® loading, irrespective of the fabrication polymer used. In contrast, the two melting point temperatures of GA_3K loaded PHBHV-Diol and Diblock nanospheres tended to marginally increase, with increasing theoretical percentage GA_3K loading.

Analysis of the moisture content of unloaded and active loaded nanospheres using thermogravimetric analysis showed that the freeze-drying process employed was highly effective in removing the majority of the residual moisture. There was no significant difference between the moisture content of nanosphere samples, irrespective of either the fabrication polymer or theoretical percentage active loading used. This means that biodeterioration would be kept to a minimum, increasing the products shelf life.

Solvent evaporation methods of nanosphere preparation have the disadvantage that emulsification stabilisers, in this case PVA, binds onto the surface of nanospheres (Verrecchia *et al*, 1993; Boury *et al*, 1995; Landry *et al*, 1996, Boury *et al*, 1997; Shakesheff *et al*, 1997). This can cause the nanospheres to become very sticky and clump together preventing good stereoscan electron microscopy. However, depending on the intended destination of the nanospheres, some of the initial disadvantages can become advantages. For example, the surface binding of PVA prevents the uptake of nanospheres by macrophages (Tabata and Ikada, 1990), enhances particle uptake into the mucosal lymphoid tissue from mucosal surfaces due to the hydrophobicity of the nanospheres (Frey *et al*, 1996; Jani *et al*, 1989; Lavelle *et al*, 1995) and finally, decreases nanosphere biodegradation and active release by making the polymer matrix inaccessible to hydrolytic enzymes (Landry *et al*, 1996; Landry *et al*, 1997). In the present work the levels of residual PVA found in unloaded and BSA,

Admire® and GA_3K loaded nanospheres were all higher than those reported in the literature. Unloaded, BSA and Admire® loaded nanospheres contained between 11% and 17% PVA w/w irrespective of the fabrication polymer used. Loading nanospheres with GA_3K using the F68 method resulted in higher residual PVA levels of between 11% and 55% w/w, with the mean percentage residual PVA associated with GA_3K loaded PHBHV-Diol nanospheres being significantly greater than the PVA levels associated with GA_3K loaded Diblock nanospheres. Leroux *et al* (1995) have reported that PVA makes up some 10% of the total mass of freeze-dried microspheres while Alleman *et al* (1993) have reported that the level of residual PVA is approximately linearly related to the specific surface area of the microparticles. Lee and colleagues (1999) have shown that the PVA content *per* weight of microparticles tends to increase with specific surface area as the particle diameter decreases. Scholes *et al* (1999) reported that the cleaning techniques of water washing with centrifugation and GPC are equally effective in removing unbound PVA from nanosphere suspensions following manufacture, but that both these techniques left the surface of the nanospheres dominated by the presence of surfactant. Scholes and colleagues (1999) have also reported that the difficulty in removing the PVA after washing might indicate that the PVA chains have been physically incorporated into the nanosphere surface during the emulsification process. A study by Lee and colleagues (1999) concluded that PVA is bound irreversibly onto the surface of nanospheres. In the present work nanospheres were subjected to three washing and centrifugation steps but the PVA levels were still high. Lee and colleagues (1999) were unable to reduce the residual PVA by further washing, possibly because the residual PVA may have become either adsorbed or highly associated with the surface layer of nanospheres via either hydrophobic interactions or hydrogen bonding.

In the present work, when DSC determinations were carried out on either unloaded or active loaded nanospheres, no broad evaporation endotherms were evident at ~60-80°C. Their absence would tend to indicate that either no residual DCM was present in the nanospheres or the levels of residual solvent present were too low to be detected. Analysis of unloaded and active loaded nanospheres by the much more sensitive method of GLC confirmed that the levels of DCM within active loaded preparations, at 11ppm, were well below the maximum short term and long term UK (250ppm/100ppm) and US (2000ppm/500ppm) DCM exposure limits specified by the UK Medicines Control Agency and the US Food and Drug Administration. DCM could not be detected in unloaded nanospheres and it was assumed that the low levels of DCM present in active loaded nanospheres resulted from DCM having a higher affinity for the incorporated active than the polymer alone. The DCM levels obtained in the present work are consistent with the results obtained by O'Hagan and co-workers (1994) who reported residual DCM levels of below 250ppm. Other members of our laboratory have observed residual DCM levels in poly-lactide microspheres of well below 10ppm using GLC (Conway, 1996).

Nanospheres fabricated from PHBHV-Diol, 3HB 3HC and Diblock polymers using the F68 double sonication solvent evaporation method have been used for the incorporation and release of the surrogate protein bovine

serum albumin V over 28 days. In addition PHBHV-Diol and Diblock polymers have been used for the incorporation and release of the insecticide Admire® and the plant growth factor GA_3K over 37 and 28 days respectively. The amount of active agent incorporated significantly increased with increasing theoretical percentage loading, irrespective of either the active or fabrication polymer used. Daily and total cumulative release profiles were produced for each active encapsulated. Daily release profiles for BSA loaded PHBHV-Diol nanospheres were characterised by the absence of a burst-release phase for BSA immediately upon incubation in HBSS. This could be attributed to strong binding between the BSA and the nanosphere surface. After 17 days incubation, all BSA loaded PHBHV-Diol nanospheres showed a short but pronounced burst-release that was proportional to the theoretical percentage BSA loading, followed by a gradual decline in BSA release, thereafter. The absence of an early initial burst release could be due to the sparse distribution of BSA at the compressed periphery of the nanosphere created by solvent evaporation and a greater concentration of BSA at the central core. As the HBSS gradually penetrated the nanospheres, low levels of BSA at the periphery would be dissolved and leach out of the polymer matrix into the surrounding medium, leaving channels and pores for further BSA release. After ~17 days, sudden mass leaching of the central core BSA could have occurred, resulting in a dumping of most of the BSA and a subsequent decline in further active release of BSA.

Daily release profiles for BSA loaded 3HB 3HC nanospheres showed a far earlier but more pronounced burst release than was observed with BSA loaded PHBHV-Diol nanospheres during incubation in HBSS. This may be due either to the formation of larger pores and channels in nanospheres as encapsulated BSA dissolved or the distribution of significant BSA closer to the surface of the nanospheres during fabrication with 3HB 3HC.

The daily release of BSA from BSA loaded Diblock nanospheres was rather irregular but appeared to have a much longer initial lag phase than any of the other polymers of some six days. This was followed by 18 days of sporadic peaks and troughs and a further four days of gradually increasing BSA release, suggesting that the Diblock nanospheres still contained a significant reservoir of BSA. BSA entrapment in Diblock nanospheres may have taken the form of pockets of BSA at the periphery of the nanospheres, rather than the accumulation of BSA in a central core.

The total cumulative amount of BSA released over the 28 day incubation period increased with theoretical percentage BSA loading, irrespective of the fabrication polymer used.

Daily release profiles for Admire® loaded PHBHV-Diol and Diblock nanospheres showed that the higher the theoretical percentage Admire® loading, the higher the initial concentration of Admire® released from nanospheres. With the exception of theoretical 10% w/w Admire® loaded PHBHV-Diol and Diblock nanospheres, the initial release of Admire® was slightly higher from nanospheres incubated at 23°C, compared with those incubated at 4°C. This was presumably due to the increased solubility of Admire®

diffusing from nanospheres at the higher temperature. Daily release profiles for theoretical 10% and 20% w/w Admire® loaded PHBHV-Diol nanospheres were characterised by an initial drop in Admire® release followed by a spike of Admire® release at day 5, subsequently followed by sustained Admire® release over the remainder of the 37 day release period. Daily release profiles for theoretical 30% and 40% w/w Admire® loaded PHBHV-Diol nanospheres were characterised by initial stable release followed by a series of one day spike releases of Admire® on day 5 and day 12, followed by sustained release for the remainder of the 37 day release period. The spikes of Admire® release could be due to either pockets of encapsulated Admire® being released from the nanosphere matrix or sporadic crumbling of the nanosphere matrix releasing stored Admire®. The relatively smooth sustained release around the spikes of release suggests that the majority of the Admire® had been evenly distributed throughout the nanospheres matrix during fabrication.

Daily release profiles for 10% w/w and 20% w/w Admire® loaded Diblock nanospheres showed an initial burst release lasting up to 3 days followed by stable sustained release over the remainder of the 37 day incubation period. This may be due to an increased accumulation of Admire® close to the surface of the nanospheres during fabrication. Diblock nanospheres loaded with 30% w/w Admire® showed a similar pattern of release to 30% w/w Admire® loaded PHBHV-Diol nanospheres with spikes of Admire® release at day 5 and day 12, followed by sustained release for the remainder of the 37 day release period. Diblock nanospheres loaded with 40% w/w Admire® showed a unique pattern of Admire® release. This took the form of irregular initial peaks and troughs of release over the first 9 days followed by 18 days of increased sustained release and a subsequent decline in release over the remainder of the 37 day release period. This would suggest that the majority of the Admire® was situated in a ring around the core of the nanospheres and released by polymer erosion.

Irrespective of the fabrication polymer used, the total cumulative release of Admire® significantly increased with increasing theoretical percentage Admire® loading at both 4°C and 23°C. Increasing the incubation temperature from 4°C to 23°C did not significantly influence the total cumulative release of Admire® from nanospheres fabricated from the same polymer.

Daily release profiles for GA_3K loaded PHBHV-Diol and Diblock nanospheres showed an initial burst release of the active followed, after 24 hours, by low-level sustained release continuing for up to 28 days. The extent of the initial burst release phase was positively correlated with the theoretical percentage GA_3K loading for all nanospheres used. This might suggest that a small quantity of GA_3K was associated with the surface of the nanospheres giving rise to the burst release while the majority of the incorporated GA_3K was evenly distributed throughout the nanosphere matrix during fabrication. The release of GA_3K was greatest from nanospheres incubated in rural rainwater at 4°C compared with those incubated at 23°C.

Irrespective of the fabrication polymer used, the total cumulative release of GA_3K increased with increasing theoretical percentage GA_3K loading when incubated at both 4°C and 23°C. There was some indication that the total cumulative release of GA_3K from PHBHV-Diol nanospheres was marginally greater than that from Diblock nanospheres at both 4°C and 23°C.

Following incubation, all nanospheres samples were freeze-dried and accurately weighed in order to measure any weight loss that had occurred during the incubation period. Measurement of the percentage weight loss from BSA loaded nanospheres following incubation in HBSS at 37°C for 28 days and from Admire® and GA_3K incubated in rural rainwater at 4°C and 23°C for 37 and 28 days respectively showed that there had been weight loss in addition to that accounted for by the release of active. It may be that the additional weight loss was due to the loss of residual PVA incorporated during nanosphere fabrication and the loss of matrix polymer by simple chemical hydrolysis, such as scission of ester bonds. Surface erosion in the form of random chain scission at the polymer/medium interface would account for a small proportion of the percentage weight loss from nanospheres and the reduction in mean particle diameter. The majority of the percentage weight loss would occur as a result of bulk erosion. Here products of chain scission are thought to diffuse out from the amorphous regions of the polymer matrix through surface pores previously occupied by solubilised active, causing significant percentage weight loss. Increasing the theoretical percentage GA_3K and Admire® loading from 10% to 40% w/w greatly increased the mean percentage weight loss after 28 and 37 days incubation respectively, irrespective of the fabrication polymer and incubation temperature used. These observations suggest that the majority of the percentage weight loss from loaded nanospheres was due to the release of Admire® and GA_3K from the polymer nanospheres.
Incubation of unloaded and BSA loaded PHBHV-Diol, 3HB 3HC and Diblock nanospheres in HBSS at 37°C for 28 days and the incubation of unloaded, Admire® loaded and GA_3K loaded PHBHV-Diol and Diblock nanospheres in rural rainwater at 4°C and 23°C all resulted in a reduction in the mean particle diameter of the nanospheres. This could be the result either of simple chemical hydrolysis of the polymer at the surface of the nanospheres or the removal of active or residual PVA from the periphery of the nanospheres.

Following incubation in rural rainwater at both 4°C and 23°C, GA_3K and Admire® loaded nanospheres, irrespective of fabrication polymer, became more electronegative. As with BSA loaded nanospheres this could be due either to the release of active from nanospheres or the removal of the surface bound PVA following surface erosion of the polymer matrix.

The BSA, GA_3K and Admire® loaded nanospheres all showed a reduction in weight average molecular mass following incubation. This would suggest that degradation of the polymer matrix was occurring. The intrinsic differences in molecular weight between the three nanosphere fabrication polymers remained identical to values obtained for pre-incubation samples.

The DSC thermal profiles observed for harvested Admire® loaded nanospheres incubated for 37 days showed similar patterns to loaded pre-incubation nanospheres, irrespective of the fabrication polymer used. The recrystallisation temperature and the two melting point temperatures increased marginally after the incubation period.

In order to throw some light on the mechanisms of polymer biodegradation *in vivo*, unloaded nanospheres were incubated in new-born calf serum to mimic serum, in pancreatin to mimic the enzymatic environment of the small intestine and in HBSS to investigate the effect of physiological concentrations of buffer salts. Work by Williams (1982) suggested that the rate of *in vivo* polyester biodegradation might be faster than the rate of *in vitro* biodegradation due to possible polymer breakdown by proteins, enzymes and lipids. Unloaded nanospheres were also incubated in rural rainwater at 4°C and 23°C to mimic exposure to the external environment and see if temperature had any significant effect on biodegradation.

The extent of the percentage weight loss by nanospheres fabricated from the three different polymers depended on the type of incubation media used. Unloaded PHBHV-Diol nanospheres showed the greatest percentage weight loss after incubation in NCS suggesting that this polymer was susceptible to a mixture of serum enzymes, such as carboxylic ester hydrolase (E.C.3.1.1.1.), acetylcholine acylhydrolase (E.C.3.1.1.8), and acetylcholine acetylhydrolase (E.C.3.1.1.7), and serum protein (α-β globulin factors). Both enzymatic and hydrolytic degradation was assumed to have occurred. The lowest percentage weight loss from PHBHV-Diol nanospheres was observed after incubation in rural rainwater suggesting that simple chemical hydrolysis in this environment was probably very slow. Unloaded Diblock nanospheres showed the greatest percentage weight loss after incubation in HBSS suggesting that this polymer was susceptible to simple chemical hydrolysis and incubation of unloaded Diblock nanospheres in rural rainwater at 4°C resulted in the lowest percentage weight loss. It may be that either the increased incubation temperature when incubated in HBSS at 37°C instead of rural rainwater at 4°C, or the mixture of buffer salts was having an effect on the biodegradation of this polymer. Unloaded 3HB 3HC nanospheres showed the greatest percentage weight loss after incubation in porcine pancreatin and the lowest percentage weight loss after incubation in NCS. This would suggest that the mixture of enzymes found in porcine pancreatin were significantly more active in terms of the enzymatic degradation of 3HB 3HC than the serum enzymes found in NCS.

Unloaded PHBHV-Diol nanospheres showed the greatest reduction in mean particle diameter following incubation in NCS for 28 days at 37°C. Unloaded Diblock nanospheres showed the greatest reduction in mean particle diameter following incubation in HBSS for 28 days at 37°C. This reduction in the mean particle diameter of PHBHV-Diol nanospheres was assumed to be due to enzymatic action and the removal of PVA bound onto the surface of the nanospheres. The reduction in mean particle diameter of unloaded Diblock nanospheres was assumed to be due to surface erosion by simple chemical hydrolysis. The high molecular weight polymer 3HB 3HC showed a significantly lower decrease in mean particle diameter after

incubation in physiological media compared to PHBHV-Diol and Diblock polymer nanospheres. Unloaded 3HB 3HC nanospheres showed the greatest decrease in mean particle diameter after incubation for 28 days in HBSS at 37°C, even though the greatest percentage weight loss from these nanospheres was observed after incubation in porcine pancreatin.

Unloaded Diblock nanospheres had the most negative zeta potential of nanospheres generated from the three fabrication polymers both before and after incubation in physiological media and rural rainwater, suggesting that Diblock nanospheres were the most stable in aqueous suspension.

In nature, polymers are degraded preferentially by hydrolytic reactions. The presence of ester, ether or amide bonds facilitates biological degradation (Brandl *et al*, 1995). The physicochemical and microbiological parameters of the environmental ecosystem, primary material properties and material processing, affect the extent of biodegradation (Brandl *et al*, 1995) in the environment. Microbially formed polyhydroxyalkanoates, such as PHB can be completely mineralised to water and carbon dioxide in aerobic systems (Krupp and Jewell, 1992).

Currently only a very limited range of items made from PHA's are commercially available. Articles made from PHB are advertised as being completely biodegradable in natural ecosystems and are therefore environmentally friendly (Brandl *et al*, 1995). However, only a few studies reporting PHA degradation in natural ecosystems such as soil, compost, freshwater, seawater or land infill sites have been published (Brandl and Puchner, 1992; Gilmore *et al*, 1992; Mergaert 1992; Mergaert *et al*, 1993; Kimura et al, 1994).

In order to investigate the environmental biodegradation of polymer nanospheres with a view to their potential use in the delivery of insecticides and growth factors, a novel composting technique was chosen based on the International Standard ISO/FDIS 14855 (Appendix Section 1.1, page 246) method which provides the means for determining the ultimate aerobic biodegradation and disintegration of polymer materials under controlled composting conditions by the analysis of evolved carbon dioxide.

The results of this study showed that after 45 days of composting PHBHV-Diol had been biodegraded the most out of the three polymers tested. In our hands the technique did not fully meet the requirements of the International Standard ISO/FDIS 14855, as biodegradation of the cellulose reference material, after 45 days, was not greater than 70%. However, this may have been because the microflora present in the compost were better able to biodegrade PHBHV-Diol than either cellulose or PHB. Doi and co-workers (1990b) have shown that the rate of enzymatic degradation was markedly increased and was associated with a decrease in the crystallinity of the polymer. This might explain why the less crystalline copolymer, PHBHV-Diol, was more rapidly biodegraded. After 75 days of composting, the total percentage biodegradation of PHB at 84% had passed that of PHBHV-Diol at 75% and that of cellulose at 74%, suggesting that the microflora in the

M602 green garden waste compost were very capable of biodegrading the PHA polymers. The breakdown products generated from all the polymers during composting were clearly not toxic or they would have stopped microbial biodegradation. A number of bacteria and fungi excrete PHA depolymerases which are capable of hydrolysing solid PHA into water-soluble oligomers and monomers, and they utilise the resulting products as nutrients within their cells (Doi, 1997).

CHAPTER 10

REFERENCES

Abbink, J. (1991). The biochemistry of imidacloprid. In: *Pflanzenschutz-Nachrichten Bayer*, **44**, 183-195.

Akhtar, S., Pouton, C.W. (1989) Biodegradable polymers in drug delivery. *Drug News Prospect* **2** 89-93.

Allemann, E., Gurny, R., & Doelker, E. (1993). Drug-loaded nanoparticles - Preparation methods and drug targeting issues, *Eur. J. Pharm. Biopharm.* **39(5)**: 173-191.

Anderson, A.J., & Dawes, E.A. (1990). Occurrence, Metabolism, Metabolic Role and Industrial Uses of Bacterial Polyhrdroxyalkanoates. *Microbial Reviews*, 450-472..

Andres, R., Merkle, H.P., Schurr, W. and Zeigler, R. (1983). *Journal of Pharmalogical Sciences,* **72**, 1481-1483.

Anile, S.T., Sanders, L.M., Chaplin, M.D., Kushinsky, S. and Nerenburg, C. (1984). LHRH and its analogues, *Contraceptives and therapeutic applications* (editors, Vickery, B.H. and Nester, Jr), (MTP Press), 421-435.

Arshady, R. (1991). Preparation of biodegradable microspheres and microcapsules. 2: Polylactides and related polyesters. *Journal of Controlled Release*, **17**, 1-22.

Arturson, P., Laakso, T., & Edman, P. (1983) Acrylic microspheres in vivo IX: blood elimination kinetics and organ distribution of picroparticles with different surface characteristics, *Journal of Pharmaceutical Sciences*, **72**, 1415-1420.

Arshardy, R. (1991). Preparation of biodegradable microspheres and microcapsules: 2 Polylactides and related polyesters, *Journal of Controlled Release* **8**, 285-291.

Arteca, R. (1996). *Plant Growth Substances: Principles and Applications.* New York: Chapman & Hall.

Atkins, T.W. (1997). Fabrication of microcapsules using poly(ethylene adipate) and a blend of poly(ethylene adipate) with poly(hydroxybutyrate-hydroxyvalerate): incorporation and release of bovine serum albumin, *Biomaterials*, **18**, 173-180.

Atkins, T.W. (1998). Biodegradation of poly(ethylene adipate) microcapsules in physiological media, *Biomaterials*, **19**, 61-67.

Atkins, T.W. and Peacock, S.J. (1996). In vitro biodegradation of polyhydroxybutyrate-hydroxyvalerate microspheres exposed to Hank's buffer, newborn calf serum, pancreatin and synthetic gastric juice. *J. Biomater. Sci Polym* Ed 7, 1075-84.

Atkins, T.W., & Peacock, S.J.(1996) The incorporation and release of bovine serum albumin from poly-hydroxybutyrate-hydroxyvalerate microspheres. *J.Microencapsulation*, **Vol. 13, No 6**, 709-717.

Bastioli, C., Belloti, V. and Rallis, A. (1994). Microstructure and melt flow behaviour of a starch based polymer. *Rheol Acta*, **33**: 307-316.

Battersby, N.S., Pack, S.E. and Watkinson, R.J. (1992). A correlation between the biodegradability of oil products in the CEC $_{L}$-33-T82 and modified sturm tests. *Chemosphere* **24**: 1989-2000.

Bauer, H., & Owen, A.J. (1988). Some structural and mechanical properties of bacterially produced poly-β-hydroxybutyrate-co-β-hydroxyvalerate. *Colloid polym.Sci* **266**: 241-247.

Bazile, D.V., Ropert, C., Huve, P., Verrechia, T., Marland, M., Frydman, A., Veillard, M. and Spenlehauer, G. (1992). Body distribution of fully degradable (^{14}C)-poly(lactic acid) nanoparticles coated with albumin for parenteral administration of progesterone. *Biomaterials*, **13**, 1093-1102.

Beck, L.R., Cawsar, K.R., Lewis, K.H., Cosgrove, R.J., Ridde, C.T., Lowey, S.L., & Epperly, T. (1979). A new long-lasting injectable microcapsule system for the administration of progesterone. *Fertility Sterility*, **31**, 545-551.

Benita, S. (1999). "Microparticulate Drug Delivery Systems: Release Kinetics Models" In, Arshady, R. *Microspheres, Microcapsules and Liposomes*, Citus Press, **Vol 2**, 259-282.

Benita, S., Benoit, J.P., Fuisieux, F and Thies, C. (1984). Characterisation of drug loaded poly (d,l-lactide) microspheres. *Journal of Pharmaceutical Sciences*, **73**, 12, 1721-1724.

Bloembergen, S., Holden, D.A., Bluhm, T.L., Hamer, G.K., & Marchessault, R.H. (1989). Isodimorphism in synthesising poly (β-hydroxybutyrate-β-hydroxyvalerate) stereoregular copolymers from racemic β-lactones. *Macromolecules* **22**, 1663-1669.

Bloembergen, S., Holden, D.A., Bluhm, T.L., Hamer, G.K., & Marchessault, R.H. (1986). Studies of composition and crystallinity of bacterial poly (β-hydroxybutyrate-co-β-hydroxyvalerate). *Macromolecules*, **19**, 2865-2871.

Bomann, W. (1989a). NTN 33893, Untersuchungen zur akuten oralen Toxizität an Ratten, Intern report 18594, Bayer AG. In: Pfluger, W. and Schmuck, R. (1991). Ecotoxicological profile of imidacloprid *Pflanzenschutz-Nachrichten Bayer*, **44**, 145-158.

Bomann, W. (1989b). NTN 33893, Untersuchungen zur akuten oralen Toxizität an Mäusen, Intern report 18593ä, Bayer AG. In: Pfluger, W. and Schmuck, R. (1991). Ecotoxicological profile of imidacloprid *Pflanzenschutz-Nachrichten Bayer*, **44**, 145-158.

Boury, F., Olivier, E., Proust, J.E. & Benoit, J.P. (1994). Interactions of poly(∝-hydroxy acids) with poly(vinyl alcohol) at the air/water and at the dichloromethane/water interfaces. *J.Colloid Interface Sci.* **162**, 37-48.

Brandl, H., Gross, R.A., Lenz, R.W. and Fuller, R.C. (1988). Pseudomonas oleovorans as source of poly(β-hydroxyalkanoates) for potential applications as biodegradable polyesters. *Appl. Env. Microbiol.* **54**: 1977-1982.

Breer, H. and Sattelle, D.B. (1987). Molecular properties and functions of insect acetylcholine receptors. *Journal of Insect Physiology*, **33**, 771-790.

Brian, P.W., Elson, G.W., Hemming, H.G. and Radley, M. (1954). The plant-growth promoting properties of gibberellic acid, a metabolic product of the fungus Gibberella fujikuroi. *J. Sci. Food. Agr.* **5**: 602:612.

Buchanan, C.M., Gardner, R.M. and Komarek, R.J. (1993). Aerobic biodegradation of cellulose acetate. *J. Appl. Polym. Sci.* **47**: 1709-1719.

Calmon-Decriaud, A., Bellon-Maurel, V. and Silvestre, F. (1998). Standard methods for Testing the Aerobic Biodegradation of Polymeric Materials. Review and Perspectives. *Advances in Polymer Science*, **135**, 207-226.

Cavalier, M., Benoit, J.P. & Thies, C. (1986). The formation and characterisation of hydrocortisone loaded poly ((±)-lactide) microspheres. *Journal of Pharmacy and Pharmacology*, **38**, 249-253.

Chao, S.L., Dennehy, T.J. and Casida, J.E. (1997). Whitefly (*Hemiptera aleyrodidae*) binding site for imidacloprid and related insecticides: a putative nicotinic acetylcholine receptor. *J.Economic Entomology*, **90** (4), 879-82.

Cimmino, A., Conte, C. and Incitte, S. (1991). Biodegradability of plastic bags: chemical and regulatory aspects. *Rass Chem* **43**: 109-116.

Conti, B., Genta, I., Modena, T. and Pavanetto, F. (1995). Investgation on process parameters involved in poly (lactide-co-glycolide) microsphere preparation. *Drug Development and Industrial Pharmacy*, **21**, 5, 615-622.

Conway, B.R. (1996). *The delivery of bioactive proteins using biodegradable microspheres*. Aston University Ph.D. Thesis.

Cox, L., Koskinen, W.C. and Yen, P.Y. (1997). Sorption-desorption of imidacloprid and its metabolites in soils. *Journal of Agricultural Food Chemistry*, **45**, 1468-1472.

Davies, P.J. (1995). *Plant Hormones: Physiology, Biochemistry and Molecular biology.* Dordrecht: Kluwer.

Deasy, P.B. (1984) Microencapsulation and related drug processes. (Marcel Dekkar, New York).

Degli-Innocenti, F. and Bastioli, C. (1997). Definition of compostability criteria for packaging: Initiatives in Italy. *Journal of Environmental Polymer Degradation*, **5** (4), 183-189.

DeLuca, P.P., Hickey, A.J., Hazrati, A.M., Wedlund, P., Rypacek, F., & Kanke, M. (1987) Porous biodegradable microspheres for parenteral administration. In: *Topics in Pharmaceutical Sciences*, 1987, Bremeir, D.D., & Speiser, P., Eds., Elsevier Science Publishers, Amsterdam.

Diehr, H.J., Gallenkamp, B., Jelich, K., Lantzsch, R. and Shiokawa, K. (1991). Synthesis and chemical-physical properties of the insecticide imidacloprid (NTN 33893). In: *Pflanzenschutz-Nachrichten Bayer*, **44**, 107-112.

Doi, Y.A., Tamaki, A., Kunioka, M., & Soga, K. (1987). Biosynthesis of an unusual copolyester (10 mol% 3-hydroxybutyrate and 90 mol% 3-hydroxyvalerate units) in *Alcaligenes eutrophus* from pentanoic acid. *J.Chem.Soc.Chem.Commun.*, 1635-1636.

Doi, Y., Kunioka, M., Nakamura, Y., & Soga, K. (1988). Nuclear magnetic resonance studies on unusual bacterial copolyesters of 3-hydroxybutyrate and 4-hydroxybutyrate. *Macromolecules* **21** : 2722-2727.

Doi, Y., Kanesawa, Y., Kawaguchi, Y., and Kunioka, M. (1989). Hydrolytic degradation of microbial poly(hydroxyalkanoates). *Makromol.Chem.Rapid.Commun.* **10:** 227-230.

Doi, Y., Segaura, A., & Kunioka, M. (1990). Biosynthesis and characterisation of poly (3-hydroxybutyrate-co-4-hydroxybutyrate) in *Alcaligenes eutrophus*. *Int.J.Biol.Macromol.* **12**:106-111.

Doi, Y., Kumagai, Y., Tanahashi, N. and Mukai, K. (1992). Structural effects on the biodegradation of microbial and synthetic poly(hydroxyalkanoates). In: Vert, M., Feijen, J., Albertsson, A., Scott, G. and Chiellini, E. (Eds) *Biodegradable polymers and plastics.* The Royal Society of Chemistry, Cambridge, 139-148.

Doi, Y. (1997) Polyhydroxyalkanoates. In: *Handbook of Biodegradable Polymers*. (Editors: Domb, A.J; Kost, J; Wiseman, D.M) Harwood Academic Publishers, 78-86.

Dryden, M.W., Perez, H.R. and Ulitchny, D.M. (1999). Control of fleas on pets and in homes by use of imidacloprid or lufenuron and a pyrethrin spray. *Journal of American Veterinary Medical Association*, **215**, (1), 36-39.

Elbert, A., Becker, B., Hartwig, J. and Erdelen, C. (1991). In: *Pflanzenschutz-Nachrichten Bayer*, **44**, 113-136.

Eldridge, J.H., Hammond, C.J., Medbroek, J.A., Staces, J.K., Gilley, R.M., & Tice, T.R., (1990). Controlled vaccine release in the gut-associated lymphoid tissue. 1. Orally administered biodegradable microspheres target the Peyer's patches. *Journal of Controlled Release*, **11**: 205-214.

Embleton, J.K., & Tighe, B.J. (1992). Polymers for biodegradable medical devices IX: Microencapsulation studies: effect of polymer composition and process parameters on polyhydroxybutyrate-hydroxyvalerate microcapsule morphology. *Journal of microencapsulation*, **9 (1)**, 73-87.

Evans, J.D. and Sikdar, S.K. (1990). Biodegradable plastics: an idea whose time has come. *Chemtech* **20**: 38-42.

Felsot, A.S., Cone, W., Yu, J. and Ruppert, J.R. (1998). Distribution of Imidacloprid in soil following subsurface drip chemigation. *Bull. Environ. Contam. Toxicol.*, **60**, 363-370.

Frey, A., Giannasca, K.T., Weltxin, R. (1996). Role of the glycocalyx in regulating access of microparticles to apical plasma membranes of intestinal epithelial cells: implication for microbial attachment and oral vaccine targeting. *J.Exp.Med.* **184,** 1045-1059.

Gangrade, N., & Price, J.C. (1992). Properties of implantable pellets prepared from a biodegradable polyester. *Drug Development and Industrial Pharmacy*, **18 (15),** 1633-1648.

Gaucho® Booklet, (1998). *Your surest way to higher beet yields - Gaucho®, sugar beet seed treatment.* Bayer, Bury St. Edmunds, U.K.

Gepner, J.I., Hall, L.M. and Sattelle, D.B. (1978): Insect acetylcholine receptors as a site of insecticide action. *Nature*, **276**, 188-190.

Gibbons, A., (1992) Biotech's Second Generation, *Science,* **256**, 766-768.

Grau, R. (1986). NTN 33893, Akute Vogeltoxizität oral, orientierend / Kanarienvogel, Intern report VK300, Bayer AG. In: Pfluger, W. and Schmuck, R. (1991). Ecotoxicological profile of imidacloprid *Pflanzenschutz-Nachrichten Bayer*, **44**, 145-158.

Grau, R. (1987a). NTN 33893, Akute Vogeltoxizität oral / Taube, Intern report VT113, Bayer AG. In: Pfluger, W. and Schmuck, R. (1991). Ecotoxicological profile of imidacloprid *Pflanzenschutz-Nachrichten Bayer*, **44**, 145-158.

Grau, R. (1987b). Modifizierte Annahmeversuche nach BBARichtlinie 251 mit dem insektiziden Wirkstoff NTN 33893 als 70 WS rot und blau auf Weizen an Haussperlingen, Intern report V 5/87, Bayer AG. In: Pfluger, W. and Schmuck, R. (1991). Ecotoxicological profile of imidacloprid *Pflanzenschutz-Nachrichten Bayer*, **44**, 145-158.

Grau, R. (1987c). Modifizierte Annahmeversuche nach BBARichtlinie 251 an Tauben mit NTN 33893 70 WS auf Mais (1000 g Wirkst. / dt), Intern report V 4/87, Bayer AG. In: Pfluger, W. and Schmuck, R. (1991). Ecotoxicological profile of imidacloprid *Pflanzenschutz-Nachrichten Bayer*, **44**, 145-158.

Grau, R. (1987d). Modifizierte Annahmeversuche nach BBARichtlinie 251 an Japanischen Wachteln mit NTN 33893 70 WS auf Weizen (200 g Wirkst. / dt), Intern report V 3/87, Bayer AG. In: Pfluger, W. and Schmuck, R. (1991). Ecotoxicological profile of imidacloprid *Pflanzenschutz-Nachrichten Bayer*, **44**, 145-158.

Grau, R. (1988). NTN 33893, Acute toxicity to Rainbow Trout. Intern report FF210, Bayer AG. In: Pfluger, W. and Schmuck, R. (1991). Ecotoxicological profile of imidacloprid *Pflanzenschutz-Nachrichten Bayer*, **44**, 145-158.

Groenhof, A.C. (1998). Composting: Renaissance of an age-old technology. *Biologist*, **45** (4), 164-167.

Gursel, I., & Hasirci, V. (1995). Properties and drug release behaviour of poly (3-hydroxybutyric acid) and various poly (3-hydroxybutyrate-hydroxyvalerate) copolymer microcapsules. *J. Microencapsulation*, **Vol. 12, No. 2**, 185-193.

Hanssen, I., Mencke, N., Asskildt, H., Ewald-Hamm, D. and Dorn, H. (1999). Field study on insecticidal efficacy of Advantage® against natural infestations of dogs with lice. *Parasitology Research*, **85**, (4), 347-8.

Heimbach, F. (1986). Wachstumshemmung von Grünalgen (*Scenedesmus subspicatus*) durch NTN 33893. Intern report HBF/A1 27, Bayer AG. In: Pfluger, W. and Schmuck, R. (1991). Ecotoxicological profile of imidacloprid *Pflanzenschutz-Nachrichten Bayer*, **44**, 145-158.

Heller, J., Sparer, R.V., & Zentner, C.M., (1990) Poly (ortho esters) In: *Biodegradable Polymers as Drug Delivery Systems*, Chasin, M., & Langer, R., Eds, Marcell Dekker, New York 121.

Higuchi, T. (1963). Mechanisms sustained action medication. Theoretical analysis of rate of release of solid drugs dispersed in solid matrices. *Journal of Pharmaceutical Sciences*, **52**, 12, 1145-1149.

Hoffman, A., Donbrow, M., Gross, S.T., Benita, S. and Bahat, S. (1986). Fundamentals of release mechanism interpretation in multiparticulate systems: determination of substrate release from single microcapsules and relation between individual and ensemble release kinetics, *International Journal of Pharmacology*, **29**, 195.

Holland, S.J., Jolly, A.M., Tighe, B.J., Yasin, M., (1987). Polymers for biodegradable medical devices (II): Hydroxybutyrate-hydroxyvalerate copolymers: hydrolytic degradation studies, *Biomaterials*, **8**, 289-295.

Holland, S.J., Tighe, B.J. and Gould, P.L. (1986). Polymers for biodegradable medical devices 1. The potential of polyesters as controlled molecular release systems. *Journal of Controlled Release*, **4**, 155-180.

Holland, S.J., Yasin, M., & Tighe, B.J., (1990) Polymers for biodegradable medical devices. *Biomaterials* **11** 206-215.

Holmes, P.A. (1985). Applications of PHB - a microbially produced biodegradable thermoplastic. *Phys.Technol.***16** : 32-36.

Holmes, P.A. (1988). Biologically produced (R)-3-hydroxyalkanoate polymers and copolymers, P. 1-65. In: D.C.Bassett (Eds), *Developments in crystalline polymers - 2.* Elsevier Applied Science Publishers, London.

Hora, M.S., Rana, R.K., Nunberg, J.H., Tice, T.R., Gilley, R.M., & Hudson, M.E. (1990). Release of human serum albumin from poly(lactide-co-glycolide) microspheres. *Pharm. Res.* 7: 1190-1194.

Hori, S. (1898). Some observations on 'bakanae' disease of the rice plant. *Mem. Agric. Res. Sta (Tokyo)* **12**: 110-119.

Hutchinson, F.G. and Furr, B.J.A. (1990). Biodegradable polymer systems for the sustained release of polypeptides. *Journal of Controlled Release*, **13**, 279-294.

Hutchinson, F.G., & Furr, B.J.A. (1987). Biodegradable carriers for the sustained release of polypeptides. *Trends in Biotechnology*, **5**, 102-106.

Jalil, R. and Nixon, J.R. (1990c). Biodegradable poly(lactic acid) and poly(lactide-co-glycolide) microcapsules: Problems associated with preparative techniques and release properties. *Journal of Microencapsulation*, **7**, 3, 297-325.

Jalil, R. Nixon, J.R. (1990a). Microencapsulation using poly (l-lactic acid). II: Preparative variables affecting microsphere properties. *Journal of Microencapsulation*, **7**, 1, 25-39.

Jalil, R. Nixon, J.R. (1990b). Microencapsulation using poly (l-lactic acid). III: Effect of polymer molecular weight on the microcapsule properties. *Journal of Microencapsulation,* **7**, 1, 41-52.

Jalil, R., & Nixon, J.R.,(1989) Microencapsulation using poly(l-lactic acid) I: Microcapsule properties affected by the preparative technique. *Journal of Microencapsulation*, **6 (4)**, 473-484.

Jamahidi, K., Hyon, S.H., Nakamura, T., Ikada, Y., Shimizu, Y. and Teramatsu, T. (1986). *In vitro and in vivo* degradation of poly-L-lactide fibres. In: Christel, P., Meunier, A. and Lee, A.J.C. editors. *Biological and biomechanical performance of biomaterials.* Amsterdam: Elsevier Science, 227-32.

Jani, P., Halbert, G.W., Langridge, J. & Florence, A.T. The uptake and translocation of latex nanospheres and microspheres after oral administration to rats. *J.Pharm. Pharmacol.* **41**, 809-812.

Jeffery, H., Davis, S.S. and O'Hagan, D.T. (1993). The preparation and characterisation of poly(lactide-co-glycolide) microparticles. I. Oil-in water emulsion solvent evaporation. *International Journal of Pharmaceutics*, 77, 169-175.

Julienne, M.C., Alonso, M.J., Gomez Amoza, J.L. and Benoit, J.P. (1992). Preparation of poly (d,l-lactide/glycolide) nanoparticles of controlled particle size distribution: Application of experimental designs. *Drug Development and Industrial Pharmacy,* **18**, 10, 1063-1077.

Kagabu, S. (1997). Chloronicotinyl insecticides-discovery, application and future perspective. *Rev. Toxicol.* **1**:75-129.

Kaplan, D.L., Mayer, J.M., Ball, D., McCassie, J., Allan, A.L. and Stenhouse, P. (1993). *Fundamentals of biodegradable polymers. Biodegradable polymers and packaging.* 1-43.

Kojima, T., Nakano, M., Juni, Inoue, S., & Yoshida, Y., (1985). Preparation and evaluation *in vitro* and *in vivo* of polycarobnate microspheres containing dibucaine, *Chemical Pharmaceutical Bulletin*, **33**, 5119-5125.

Koosha, F., Muller, R.H. and Davis, S.S. (1989). Polyhydroxybutyrate as a drug carrier. *Critical Reviews in Therapeutic Drug Carrier Systems*, **6**, 117-29.

Kramer, P.A., (1974) Albumin microspheres are vehicles for achieving specificity in drug delivery. *Journal of Pharmaceutical Sciences*, **63**, 646-647.

Kulkarni, R.K., More, E.G., Hegyeli, A.F., and Leonard, F. (1971) Biodegradable poly(lactic acid) polymers. *Journal of Biomedical Materials Research*, **5**, 169-181.

Kunioka, M., Kawaguchi, Y., & Doi, Y.(1989). Production of biodegradable copolyesters of 3-hydroxybutyrate and 4-hydroxybutyrate by *Alcaligenes eutrophus. Appli.microbiol.Biotechnol.* **30**: 569-573.

Kurosawa, E. (1926). Experimental studies on the nature of the substance secreted by the 'bakanae' fungus. *Nat. Hist. Soc. Formosa.* **16**: 213-227.

Kwong, A.K., Chou, S., Sun, A.M., Sefton, M.V. and Goosen, M.F.A. (1986). In vitro and in vivo release of insulin from poly(lactic acid) microbeads and pellets, *Journal of Controlled Release*, **4**, 47-62.

Landry, F.B., Bazile, D.V., Spenlehauer, G., Veillard, M. & Kreuter, J. (1996). Degradation of poly(D,L-lactic acid) nanoparticles coated with albumin in model digestive fluids (USP XXII). *Biomaterials* **17**, 715-723.

Lavelle, E.C., Sharif, S., Thomas, N.W., Holland, J. & Davis, S.S. (1995). The importance of gastrointestinal uptake of particles in the design of oral delivery systems. *Adv.Drug.Del.Rev.* **18**, 5-22.

Leong, K.W., Kost, J., Marthiowitz, E., and Langer. (1986). Poly anjydrites for controlled release of bioactive agents, *Biomaterials* **7**, 364-371.

Leroux, J.C., Alleman, E., Doelkar, E & Gurny R. (1995). New approach for the preparation of nanoparticles by emulsification-diffusion method. *Eur.J.Pharm.Biopharm.* 41: 14-18.

Li, C., Yang, D.J., Kunan, L.R., and Wallace, S. (1993). Polyamino acid microspheres; preparation, characterisation and distribution after intravenous injection in rats. *International Journal of Pharmaceutics*, **94**, 143-151.

Lohmann, D.G. (1992). Biodegradable polymers and additives in agricultural controlled release systems. In: Kopecek, J. (Ed), *Proc. Inter. Symp. Control. Res. Bioact. Mater.*, Controlled Release Society, **19**, 170-171.

Lowry, O.H., Rosebrough, N.J., Farr, A.L., & Randal, R.J.(1951). *Journal of biological chemistry*, **193**: 265-275.

Macmillan, J. and Suter, P.J. (1958). The occurrence of gibberellin A1 in higher plants: Isolation from the seed of runner bean *(Phaseolus multiflorus). Naturwiss* **45**, 46.

MacMillan, J. and Takahashi, N. (1968). Proposed procedure for the allocation of trivial names to the giberellins. *Nature*, **217**: 170-171.

MacMillan, J., Seaton, J.C. and Suter, P.J. (1959). A new plant-growth promoting acid-gibberellin A5 from the seed of *Phaseolus multiflorus. Proc. Chem.* Soc. 325.

MacMillan, J., Seaton, J.C. and Suter, P.J. (1960). Isolation of gibberellin A1 and gibberellin A5 from *Phaseolus multiflorus.Tetrahedron*, **11**, 60-66.

MacMillan, J., Seaton, J.C. and Suter, P.J. (1962). Isolation and structure of gibberellin A6 and gibberellin A8. *Tetrahedron*, **18**, 349-355.
Malamataris, S. and Augerinos, A. (1990). Controlled release of indomethacin microspheres prepared by using an emulsion solvent-diffusion technique. *International Journal of Pharmaceutics*, **62**, 105-111.

Martindale, The Extra Pharmacopoeia, 31st Edition, 1996. Edited by James E.F. Reynolds. The Pharmaceutical Press.

Martinez, B., Lairion, F. Pena, M.B., Di Rocco, P. and Nasucchio, M.C. (1997). *In vivo* ciprofloxacin release from poly (lactide-co-glycolide) microspheres. *Journal of Microencapsulation*, **14**, 2, 155-161.

Mathot, V.B.F. (1994). *Calorimetry and thermal analysis of polymers*, (Hanser Press) Ch **5**, 105-169

Mauseth, J.D. (1991). *Botany: An introduction to plant biology*. Philadelphia: Saunders 348-415.

Mayer, J., Allen, A.L., Dell, P.A. and Kaplan, D.L. (1994). Development of biodegradable materials: balancing degradability and performance. *Polym. Prep* **34**: 910-911.

McKay, A.F. and Wright, G.F. (1948). *J. Am. Cham. Soc.* **70**, 430.

Mitchell, J.E. and Angel, C.R. (1951). The growth-stimulating properties of a metabolic product of *Fusarium moniliforme. Phytopath.*, **41**, 26-27.

Muchembled, C. (1991). Development of insecticidal treatments in beet. In: *Pflanzenschutz-Nachrichten Bayer*, **44**, 175-182.

Muller, R.H., Davis, S.S., Illum, L., & Mak, E. (1986). Particle charge and surface hydrophobicity of colloidal carriers. In : "*Targetting of drugs with synthetic sytems*", (G.Gregoriadis, J.Senior, & G.Poste, eds), Plenum Press, N.Y, p239.

Musmeci, L., Gucci, P.M. and Voltera, L. (1994). Paper as reference material in "Sturm test" applied to insoluble substances. *Env. Toxicol. Water Quality*. **9**: 83-86.

Nihant, N., Schugens, C., Grandfils, C., Jerome, R., & Teyssie, P. (1994). Polylactide microspheres prepared by double emulsion/evaporation technique. I. Effect of primary emulsion stability, *Pharm. Res.* **11**: 1479 - 1484.

Ogawa, Y., Yamamoto, M., Okada, H., Yashiki, T., & Shimamoto, T. (1988). A new technique to efficiently entrap leuprolide acetate into microcapsules of polylactic acid on copoly(lactic-glycolic) acid. *Chemical and Pharmaceutical Bulletin* **36 (3),** 1095-1103.

Park, T.G. (1994). Degradation of poly(d,l-lactic acid) microspheres: Effect of molecular weight. *Journal of Controlled Release*, **30,** 161-173.

Pavanetto, F., Genta, I., Giunchedi, P. and Conti, B. (1993). Evaluation of spray drying as a method for poly(lactide) and poly(lactide-co-glycolide) microsphere preparation. *Journal of Microencapsulation*, **10**, 4, 487-497.

Peacock, S.J. (1995). *Incorporation and release of macromolecules from biodegradable polymer vehicles*. Aston University Ph.D. Thesis.

Pepper, T. (1997). *Microencapsulation of novel immunogens*. Aston University Ph.D. Thesis.

Peter, T. (1975). Serum albumin, in "*The plasma proteins – structure, function and genetic control*", Vol. 1, (F.W. Putnam, ed.), Academic Press, London, 133-181.

Pfluger, W. and Schmuck, R. (1991). Ecotoxicological profile of imidacloprid. In: *Pflanzenschutz-Nachrichten Bayer*, **44**, 145-158.

Phinney, B.O., West, C.A., Ritzel, M.B. and Neely, P.M. (1957). Evidence for gibberellin-like substances from flowering plants. *Proc. Nat. Acad. Sci. (U.S.A.)*. **43**, 398-404.

Pitt, C.G., Gratzl, M.M., Jeffcoat, R.A., Ziweidinger, R., & Schindler, A. (1979) Sustained drug delivery systems II: Factors affecting release rates from poly (ε-caprolactone) and related biodegradable polyesters. *Journal of Pharmaceutical Sciences,* **68**, 1534-1538.

Pitt, C.G. (1990). The controlled parentreal delivery of peptides and proteins. *International Journal of Pharmaceutics*, **59**, 173-196.

Priede, M.A. (1996). Technology of Plant Regulator Fusicoccin and Gibberellin Production. In: BIOBALT, 1996 Abstract Book.

Poulton, C.W., Kennedy, J., Notarlinni, L.J., & Gould, P. (1988). Biocompatability of poly-β-hydroxybutyrate and related copolymers. *Proceedings of the 15th International Symposium on Controlled Release of Bioactive Materials*, **15**, 179-180, Controlled Release Society, Inc.

Radley, M. (1956). Occurrence of substances similar to gibberellic acid in higher plants. *Nature* **178**: 1070-1071.

Raven, P.H., Evert, R.F. and Eichhorn, S.E. (1992). *Biology of plants*. New York: Worth, 545-572.

Richardson, M.J. (1994). "DSC on polymers: Experimental Conditions" in *Calorimetry and thermal analysis of polymers*, (Hanser Press), Ch. 6, 169-189.

Riddick, T.M. (1968). "Control of colloid stability through Zetapotential", **Vol. 1**, Livingstone, N.Y.

Riley, J.M. (1987). Gibberellic Acid for fruit set and seed germination. In: *California Rare Fruit Growers Journal*. **19**, 10-12.

Rinella, J.F., Hamilton, P.A. and McKensie, S.W. (1993). Persistence of the DDT pesticide in the Yakima River Basin Washington. *U.S Geological Survey Circular* **1090**, Denver, CO.

Rouchard, J., Gustin, F. and Wauters, A. (1994). Soil bio-degradation and leaf transfer of insecticide imidacloprid applied in seed dressing in sugar beet crops. *Bull. Environ. Contam. Toxicol.* **53** : 344-350.

Reusch, R.N., & Sadoff, H.L. (1988). Putative structure and functions of a poly-β-hydroxybutyrate/calcium phosphate channel in bacterial plasma membranes. *Proceedings of the National Academy of Science*, USA, **85**, 4176-4180.

Reusch, R.N.(1989). Poly-β-hydroxybutyrate/calcium polyphosphate complexes in eukaryotic membranes. *Proc.Soc.Exp.Biol.Med*, **191**: 377-381.

Sah, H., Toddywala, R., & Chien Y.W. (1995). Biodegradable microcapsules prepared by a W/O/W technique: effects of shear force to make a primary W/O emulsion on their morphology and protein release. *J.Microencapsulation*, **vol. 12, No. 1**, 59-69.

Salisbury, F.B. and Ross, C.W. (1992). *Plant physiology*. Belmont, CA: Wadsworth, 357-407 and 531-548.

Sampath, S. S., Garvin, K. and Robinson, D.H. (1992). Preparation and characterisation of biodegradable poly (l-lactic acid) gentamicin delivery systems. *International Journal of Pharmaceutics*, **78**, 165-174.

Sanders, L.M., & Hendren, R.W. (1997) Protein Delivery - Physical Systems.

Sattelle, D.B. (1980). Acetylcholine receptors of insects. *Adv. Insect Physiology*, **15**, 215-315.

Schmitt, H.W. (1989). Nützlingsschonung im Obstbau. Intern report VAZ 41/88, Bayer AG. In: Pfluger, W. and Schmuck, R. (1991). Ecotoxicological profile of imidacloprid *Pflanzenschutz-Nachrichten Bayer*, **44**, 145-158.

Schmuck, R. (1990a). Modified acceptance tests with Japanese quail (*Coturnix coturnix japonica*) using the active ingredient NTN 33893 as 70 WS on orange coloured sugar beet seeds. Intern report SXR/WA 01, Bayer AG. In: Pfluger, W. and Schmuck, R. (1991). Ecotoxicological profile of imidacloprid *Pflanzenschutz-Nachrichten Bayer*, **44**, 145-158.

Schmuck, R. (1990b). Modified acceptance tests with Japanese quail (*Coturnix coturnix japonica*) using the active ingredient NTN 33893 as 70 WS on blue coloured sugar beet seeds. Intern report SXR/WA 02, Bayer AG. In: Pfluger, W. and Schmuck, R. (1991). Ecotoxicological profile of imidacloprid *Pflanzenschutz-Nachrichten Bayer*, **44**, 145-158.

Scholes, P.D., Coombes, A,G,A., Illum, L., Davis, S.S., Vert, M. and Davies, M.C. (1993). The preparation of sub-200 nm poly(lactide-co-glycolide) microspheres for site specific drug delivery. *Journal of Controlled Release*, **25**, 145-153.

Schwope, A.D., Wise, D.L., & Howes, J.F. (1975) Lactic/glycolic acid polymers as narcotic antagonist delivery systems. *Life Sciences* **17**, 1877-1886.

Shakesheff, K.M., Evora, C., Soriano, I & Langer, R. (1997). The adsorption of poly(vinyl alcohol) to biodegrade microparticles studied by X-ray photoelectron spectroscopy (XPS). *J.Colloid Interface Sci*, **185**, 538-547.

Smith, P.K., Krohn, R.I., Hemasen, G.T., Mallia, A.K., Gartner, F.H., Provenazo, M.D., Fujimoto, E.T., Goeke, N.M., Olson, B.J., & Klenk, D.C. (1985). Measurement of protein using Bicinchoninic Acid. *Anal. Biochem*, **150** : 76-85.

Soloway, S.B., Henry, A.C., Kollmeyer, W.D., Padgett, W.M., Powell, J.E., Roman, S.A., Tiemann, C.H., Corey, R.A. and Horne, C.A. (1978). *Advances in Pesticide Science*, Fourth International Congress of Pesticide Chemistry Zurich, Switzerland, July 24-28, 1978, **Part 2**, 206-217.

Sponsel, V.M. (1995). Gibberellin biosynthesis and metabolism. In: *Plant Hormones: Physiology, Biochemistry and Molecular Biology.* Dordrecht: Kluwer, 66-97.

Stodola, F.H., Raper, K.B., Fennell, D.I., Conway, H.F., Sohns, V.E., Langford, C.T. and Jackson, R.W. (1955). The microbiological production of gibberellins A and X. *Arch. Biochem. Biophys.* **54**: 240-245.

Suzuki, K., & Price, J.C. (1985) Microencapsulation and dissolution properties of a neuroleptic in biodegradable polymer, poly (d l-lactide). *Journal of Pharmaceutical Sciences,* **74**, 21-24.

Swarbrick, J. and Boylan, J.C. (1990). Biodegradable polyester polymers as drug carriers. In: *Encyclopaedia of pharmaceutical technology*, **Vol 2**. New York: Marcel Dekker, 1-13.

Swift, G. (1994). Expectations for biodegradation testing methods. In: Doi, Y. and Fukuda, K. (Eds) *Biodegradable Plastics and Polymers*. Elsevier, 228-236.

Tabata, Y. and Ikada, Y. (1988). Effect of size and surface charge of polymer microspheres on their phagocytosis by macrophages, *Biomaterials*, 9, 356.

Tabata, Y., & Ikada, Y. (1990). Phagocytosis of polymer microspheres by macrophagess, *Adv. Polym. Sci.* **94** : 107-141.

Takada, T. (1986). NTN 33893 Acute fish toxicity on common carp (preliminary test). Report RW 86102, Nitokuno. In: Pfluger, W. and Schmuck, R. (1991). Ecotoxicological profile of imidacloprid ; *Pflanzenschutz-Nachrichten Bayer*, **44**, 145-158.

Takahashi, N., Kitamura, H., Kawarada, A., Stea, Y., Takai, M., Tamura, S. and Sumiki, Y. (1955). Isolation of gibberellins and their properties. *Bull. Agric. Chem. Soc. Japan.* **19**: 267-277.

Thayer, A. (1990). Degradable plastics generate controversy in solid waste issues. *Chemical and Engineering News*. **68**: 7-24.

Theeuwes, F., Anwar, H. and Higuchi, T. (1974). Quantitative analytical method for determination of drugs dispersed in polymers using Differential Scanning Calorimetry. *Journal of Pharmaceutical Sciences* **63** (3), 427-429.
Thiebaud, S. and Borredon, M.E. (1995). Solvent-free esterification of wood with fatty acid chloride. *Bioresource Technology*, **52**.

Tikhonov, V.N., & Mustafin, I.S. (1965). *Zh.Anal.Khim.* **20**: 390-392.

Toll, P.A. (1990a). Technical NTN 33893, A subacute dietary LD_{50} with mallard ducks. Report No. 100238, Mobay Chemical Corporation. . In: Pfluger, W. and Schmuck, R. (1991). Ecotoxicological profile of imidacloprid *Pflanzenschutz-Nachrichten Bayer*, **44**, 145-158.

Toll, P.A. (1990b). Technical NTN 33893. Subacute dietary LC_{50} with bobwhite quail. Report No. 100241, Mobay Chemical Corporation. In: Pfluger, W. and Schmuck, R. (1991). Ecotoxicological profile of imidacloprid *Pflanzenschutz-Nachrichten Bayer*, **44**, 145-158.

Toll, P.A. (1991a). Technical NTN 33893, A one generation reproduction study with bobwhite quail. Report No. 101203, Mobay Chemical Corporation. In: Pfluger, W. and Schmuck, R. (1991). Ecotoxicological profile of imidacloprid *Pflanzenschutz-Nachrichten Bayer*, **44**, 145-158.

Toll, P.A. (1991b). Technical NTN 33893, A one generation reproduction study with mallard duck. Report No. 101205, Mobay Chemical Corporation. In: Pfluger, W. and Schmuck, R. (1991). Ecotoxicological profile of imidacloprid *Pflanzenschutz-Nachrichten Bayer*, **44**, 145-158.

Tomlin, C. (1994). *The pesticide manual*; British Crop Protection Council, Surrey, U.K. The Royal Society of Chemistry, Cambridge, U.K.

Tsai, D.C., Havard, S.A., Hogan, T.F., Malonga, C.J., Kandzari, S.J., & Ma, J.K.H. (1986). Preparation and *in vitro* evaluation of polylactic acid - mitomycin C microcapsules. *Journal of microencapsulation*, **3 (3),** 181-193.

Tsuji, K. (1987). Controlled release formulation. In: Greenhalgh, R. and Robert, T.R. (Eds), *Pesticide science and biotechnology*, Blackwell Scientific Publications, Oxford, 223-30.

Tsuji, K. (1993). Formulation technology – controlled release technology in pesticide formulation. In: Iwamura, Y., Ueno, T. and Kamoshita, K. (Eds), *Development of medicine*, **Vol, 18**, *Development of pesticide I*, Hirokawa Shoten, Tokyo, 101-24.

Tsuji, K. (1995). Application to pesticide slow release systems. In: Dohi, Y. (Ed in Chief), *Handbook of Biodegradable Plastics*, NTS, Tokyo, 555-566.

Tsuji, K. (1999). Microcapsules in Agriculture. In: Arshady, R. *Microspheres, Microcapsules and Liposomes*, **Vol 1**, Citus Books.

Verrechia, T., Huve, P., Bazile D., Veillard M., Spenlehauer G., Couvreur P. (1993). Adsorption/desortion of human serum albumin at the surface of poly(lactic acid) nanoparticles prepared by a solvent evaporation process. *Journal of Biomed.Mat.Res,* **Vol 27,** 1019-1028.

Watts, P.J., Davies, M.C., & Melia, C.D. (1990). Microencapsulation using emulsification/solvent evaporation; an overview of the techniques and applications. *CRC critical reviews in Therapeutic Drug Carrier Systems*, 7, 235-259.

Widder, K.J. and Senyei, A.E. (1984). Magnetic albumin microspheres in drug delivery, in "*Microspheres and drug therapy: pharmaceutical, immunological and medical aspects*" (S.S. Davis, L.Illum, J.G. McVie and E.Tomlinson, eds), Elsevier, Amsterdam, 393.

Wing, R.E., Doane, W.M. and Schreiber, M.M. (1990). Starch-encapsulated herbicides: approach to reduce groundwater contamination, *Pesticide Formulations and Applications Systems,* **10**, 17-25.

Wood, D.A. (1980) Biodegradable drug delivery systems. *International Journal of Pharmaceutics,* **7**, 1-18.

Wyman, J.A., Jensen, J.O., Curwen, D., Jones, R.L. and Marquardt, T.E. (1985). Effects of application procedures and irrigation on degradation and movement of aldicarb residues in soil. *Environ. Toxicol. Chem.*, **4**, 641-651.

Yabuta, T. (1935). Biochemistry of the 'bakanae' fungus of rice. *Agr. Hort. (Tokyo)* **10:** 17-22.
Yamada, K., Mukai, K. and Doi, Y. (1993). Enzymatic degradation of poly(hydroxyalkanoates) by *Pseudomonas pichettii. International Journal Bio. Macromole.* **15**, (4), 215-220.

Yates, D.J. (1998). The suitability of biodegradable poly (dl-lactide-co-glycolide) 75:25 microspheres for the sustained release of antibiotics. Aston University Ph.D thesis.

Young, B.M. and Hicks, S.L. (1990). Acute Toxcity of NTN 33893 to Daphnia magna. Report No. 100245, Mobay Chemical Corporation. In: Pfluger, W. and Schmuck, R. (1991). Ecotoxicological profile of imidacloprid *Pflanzenschutz-Nachrichten Bayer*, **44**, 145-158.

Zeller, B. (1990). Bienverträglichkeit von NTN 33893. Intern report 39/1990. In: Pfluger, W. and Schmuck, R. (1991). Ecotoxicological profile of imidacloprid *Pflanzenschutz-Nachrichten Bayer*, **44**, 145-158.

APPENDIX

Aston University

Content has been removed for copyright reasons

Aston University

Content has been removed for copyright reasons

SECTION 1.2

CONVERSION FACTOR FOR READING ON IR DETECTOR

The IR detector gives the percentage volume of carbon dioxide in the air, which is pulled through the detector at 100ml/min. The reading is taken as a steady value over one minute.

A reading of X = Vml CO_2 in 100ml air *per* minute

If the GMV is taken as $24dm^3$ at room temperature and pressure, then

Vml CO_2 = V × 44 ÷24000g in 1 minute

= 1.83×10^{-3}Vg *per* minute.

Mass of carbon dioxide per day is therefore,

$1.83 \times 10^{-3}V \times 60 \times 24$g
= 2.64V g per day

This can be converted to percentage of the total theoretical mass carbon dioxide produced by the polymers by using Equations 9.1, 9.2 and 9.3.

SECTION 2.1

MEAN TOTAL WEIGHT OF UNLOADED AND BSA LOADED NANOSPHERES PRODUCED DURING FABRICATION

THEORETICAL % LOADING	POLYMER	MEAN TOTAL WEIGHT (mg)
0	PHBHV-DIOL	179.4 ± 1.2
10	PHBHV-DIOL	153.25 ± 0.5
20	PHBHV-DIOL	151 ± 1.9
30	PHBHV-DIOL	148.75 ± 2.6
40	PHBHV-DIOL	154 ± 2
0	3HB 3HC	172.4 ± 3.2
10	3HB 3HC	172.25 ± 0.8
20	3HB 3HC	172.25 ± 2.7
30	3HB 3HC	170.68 ± 0.5
40	3HB 3HC	169.68 ± 1.3
0	DIBLOCK	165.43 ± 2
10	DIBLOCK	155.28 ± 3.2
20	DIBLOCK	160 ± 5.1
30	DIBLOCK	129.8 ± 1.5
40	DIBLOCK	103.68 ± 2.6

SECTION 2.2

DAILY BSA RELEASE PROFILES

FIGURE 1 – DAILY BSA RELEASE PROFILE FOR THEORETICAL 20% AND 30% w/w BSA LOADED PHBHV-DIOL NANOSPHERES (mean values ± SEM, n=12)

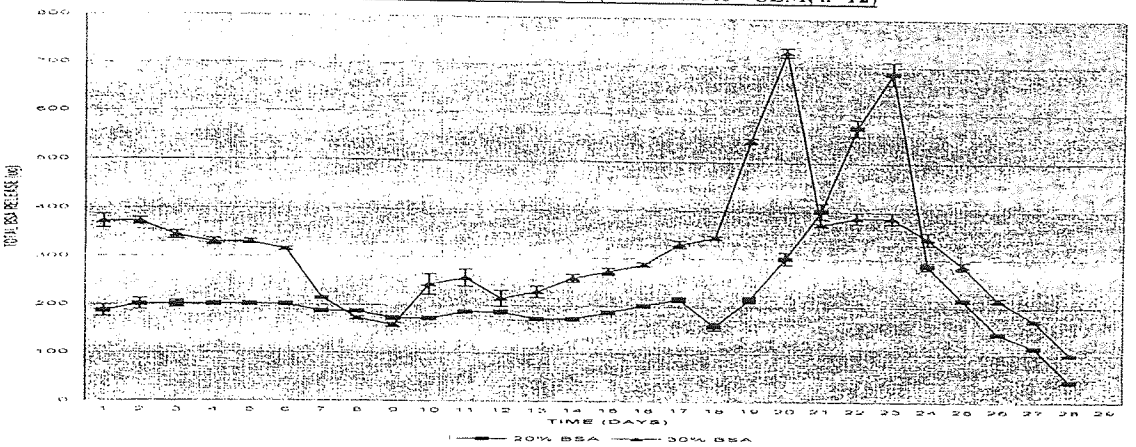

FIGURE 2 – DAILY BSA RELEASE PROFILE FOR THEORETICAL 20% AND 30% w/w BSA LOADED 3HB 3HC NANOSPHERES (mean values ± SEM, n=12)

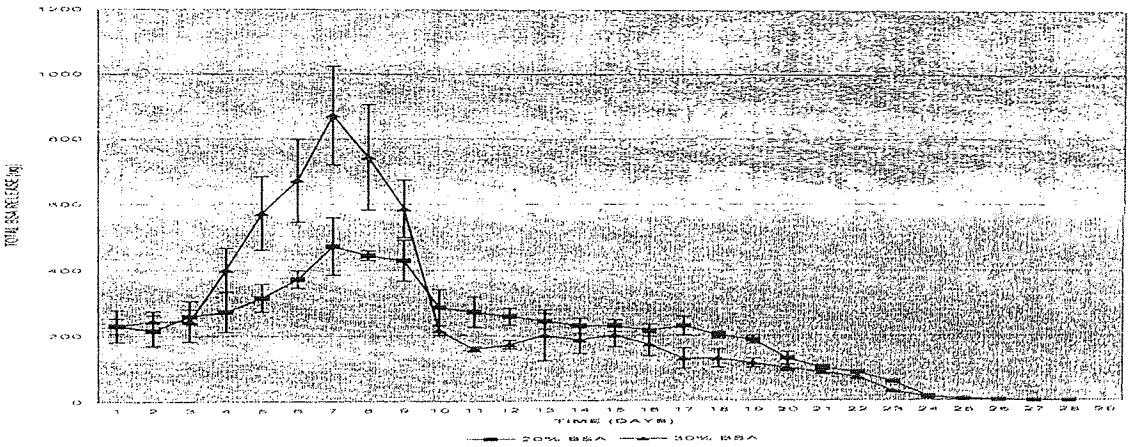

FIGURE 3 – DAILY BSA RELEASE PROFILE FOR THEORETICAL 20% AND 30% w/w BSA LOADED DIBLOCK NANOSPHERES (mean values ± SEM, n=12)

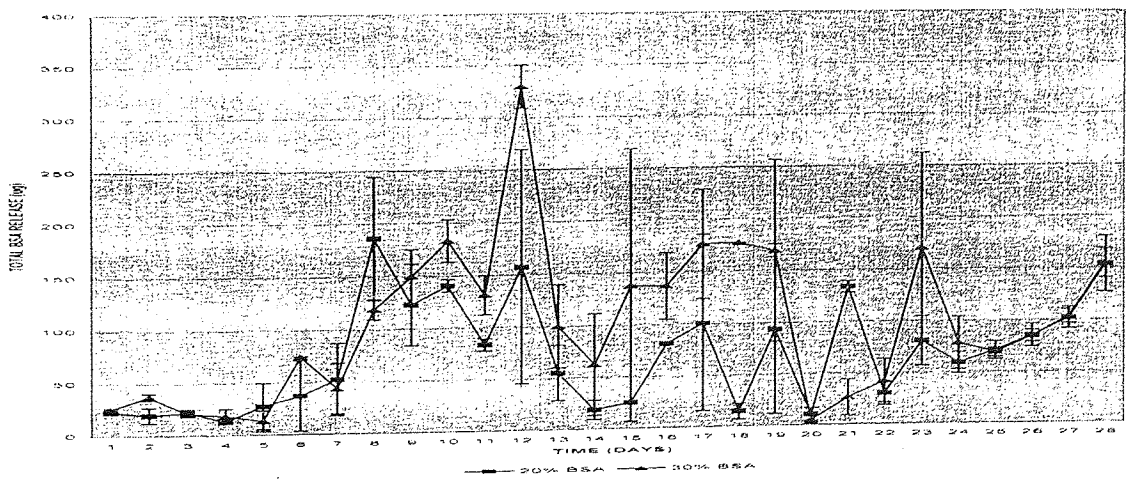

SECTION 2.3

TOTAL CUMULATIVE BSA RELEASE PROFILES

FIGURE 1 – TOTAL CUMULATIVE RELEASE PROFILE FOR THEORETICAL 20% AND 30% w/w BSA LOADED PHBHV-DIOL NANOSPHERES (mean values ± SEM, n=12)

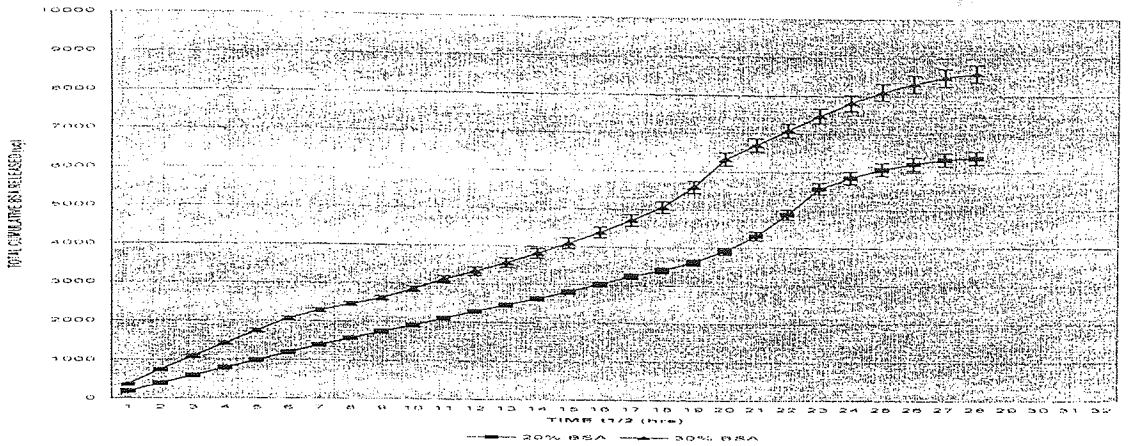

FIGURE 2 – TOTAL CUMULATIVE RELEASE PROFILE FOR THEORETICAL 20% AND 30% w/w BSA LOADED 3HB 3HC NANOSPHERES (mean values ± SEM, n=12)

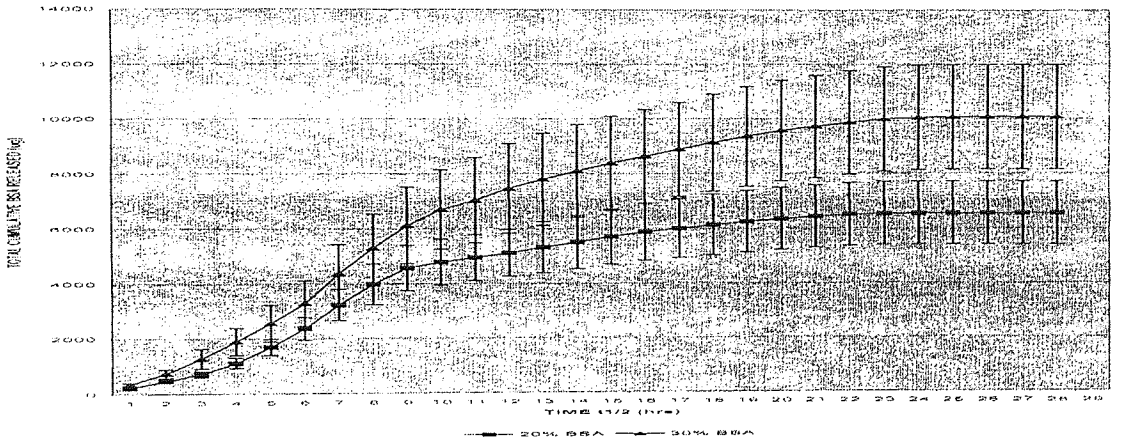

FIGURE 3 – TOTAL CUMULATIVE RELEASE PROFILE FOR THEORETICAL 20% AND 30% w/w BSA LOADED DIBLOCK NANOSPHERES (mean values ± SEM, n=12)

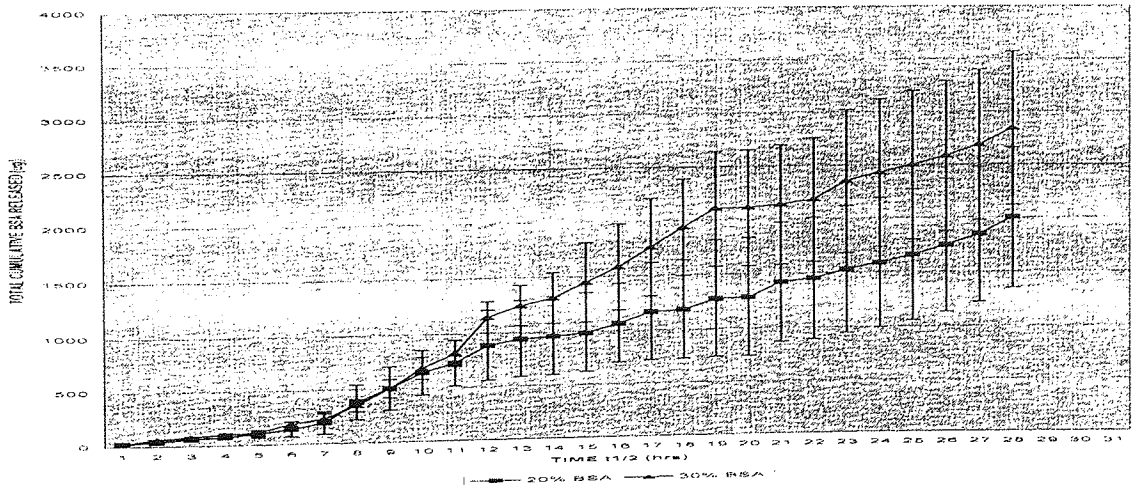

SECTION 3.1

MEAN TOTAL WEIGHT OF UNLOADED AND ADMIRE® LOADED NANOSPHERES PRODUCED DURING FABRICATION

THEORETICAL % LOADING	POLYMER	MEAN TOTAL WEIGHT (mg)
0	PHBHV-DIOL	179.4 ± 1.2
10	PHBHV-DIOL	170.93 ± 1.4
20	PHBHV-DIOL	165.58 ± 3.3
30	PHBHV-DIOL	161.25 ± 2.5
40	PHBHV-DIOL	152.75 ± 3.2
0	DIBLOCK	165.43 ± 2
10	DIBLOCK	142.75 ± 2.2
20	DIBLOCK	149.75 ± 7.8
30	DIBLOCK	123.25 ± 1.4
40	DIBLOCK	140.25 ± 4.8

SECTION 3.2

DAILY ADMIRE® RELEASE PROFILES

FIGURE 1 – DAILY ADMIRE RELEASE PROFILES FOR THEORETICAL 20% w/w ADMIRE LOADED PHBHV-DIOL NANOSPHERES INTO RURAL RAINWATER AT 4 DEGREES CELCIUS AND 23 DEGREES CELCIUS (mean values ± SEM, n=12)

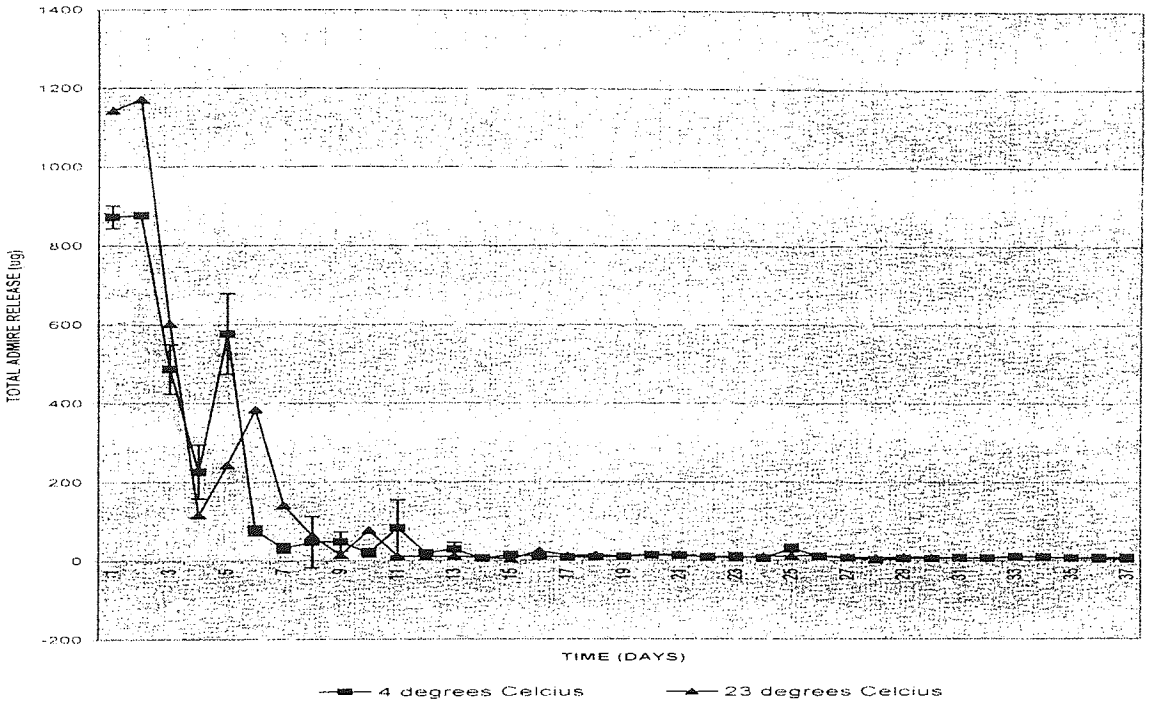

FIGURE 2 – DAILY ADMIRE RELEASE PROFILES FOR THEORETICAL 30% w/w ADMIRE LOADED PHBHV-DIOL NANOSPHERES INTO RURAL RAINWATER AT 4 DEGREES CELCIUS AND 23 DEGREES CELCIUS (mean values ± SEM, n=12)

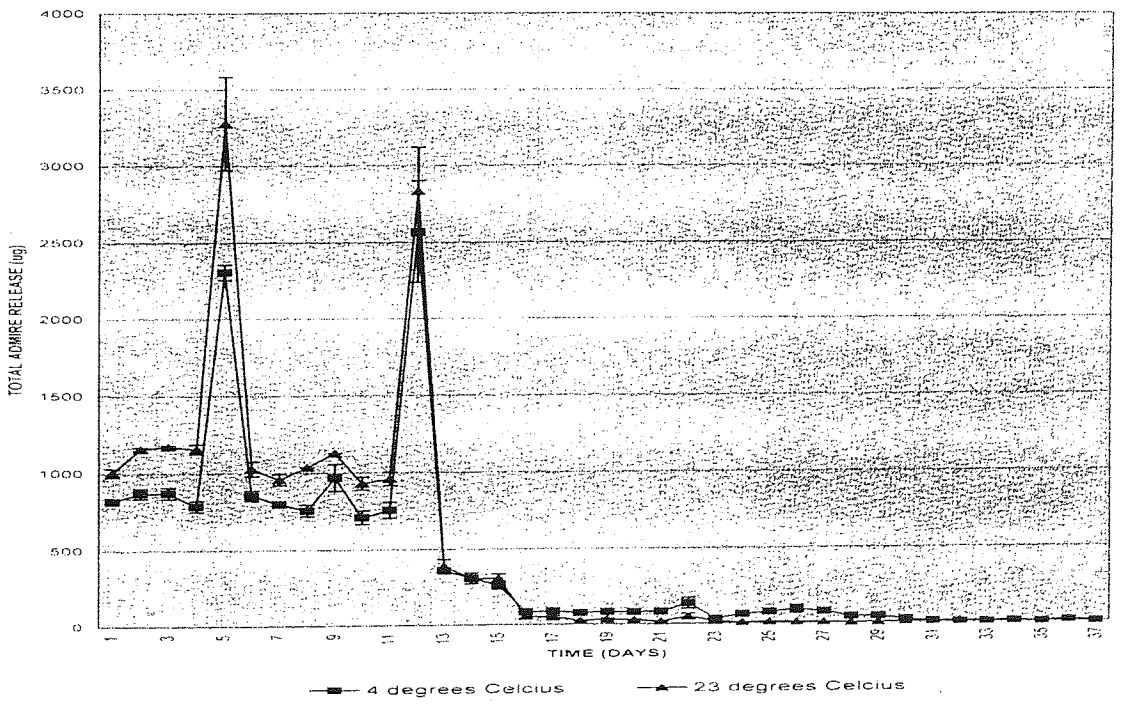

FIGURE 3 – DAILY ADMIRE RELEASE PROFILES FOR THEORETICAL 20% w/w ADMIRE LOADED DIBLOCK NANOSPHERES INTO RURAL RAINWATER AT 4 DEGREES CELCIUS AND 23 DEGREES CELCIUS (mean values ± SEM, n=12)

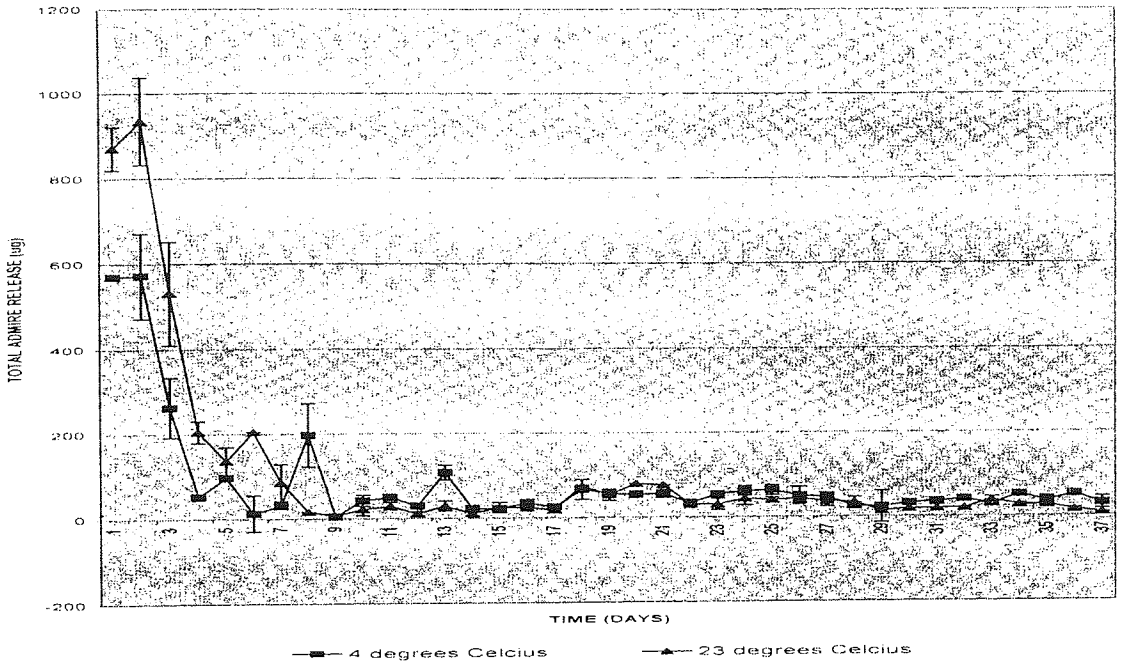

FIGURE 4 – DAILY ADMIRE RELEASE PROFILES FOR THEORETICAL 30% w/w ADMIRE LOADED DIBLOCK NANOSPHERES INTO RURAL RAINWATER AT 4 DEGREES CELCIUS AND 23 DEGREES CELCIUS (mean values ± SEM, n=12)

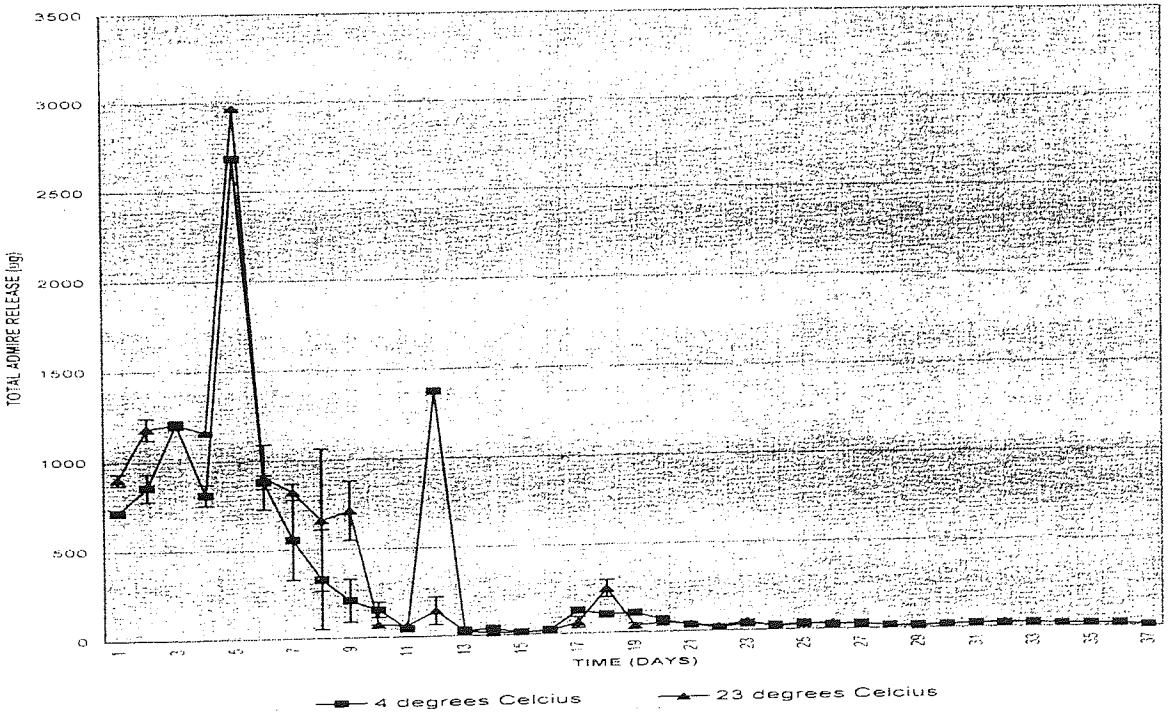

SECTION 3.3

TOTAL CUMULATIVE ADMIRE® RELEASE PROFILES

FIGURE 1 – TOTAL CUMULATIVE RELEASE PROFILES FOR THEORETICAL 20% w/w ADMIRE LOADED PHBHV-DIOL NANOSPHERES INTO RURAL RAINWATER AT 4 DEGREES CELCIUS AND 23 DEGREES CELCIUS (mean values ± SEM, n=12)

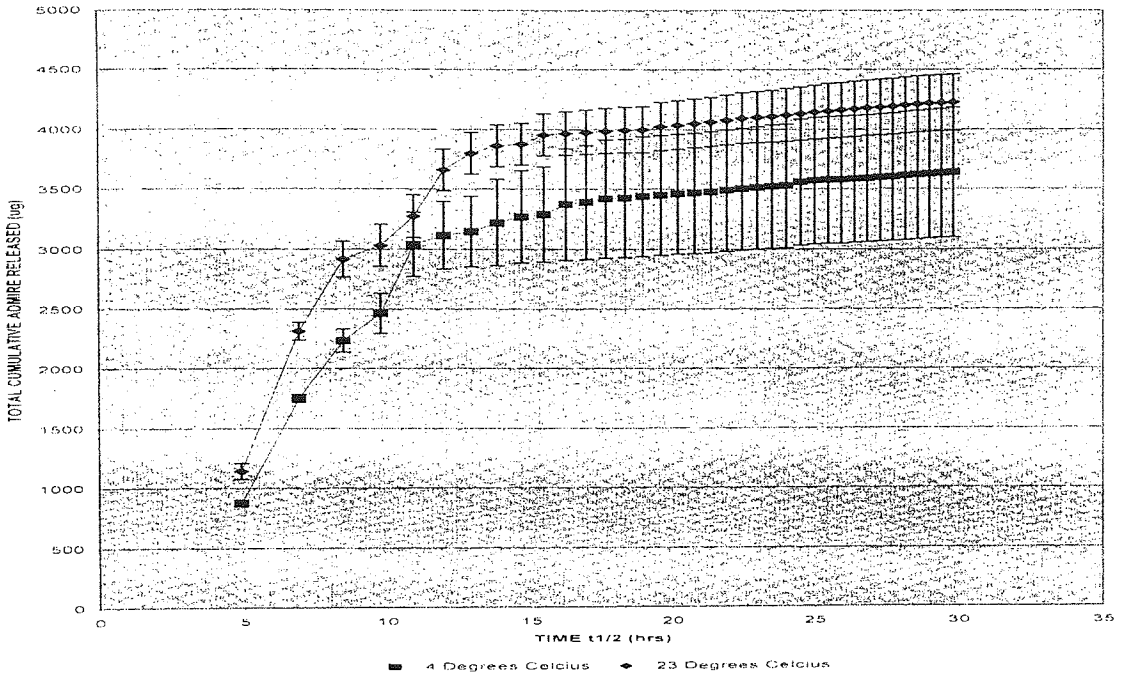

FIGURE 2 – TOTAL CUMULATIVE RELEASE PROFILES FOR THEORETICAL 30% w/w ADMIRE LOADED PHBHV-DIOL NANOSPHERES INTO RURAL RAINWATER AT 4 DEGREES CELCIUS AND 23 DEGREES CELCIUS (mean values ± SEM, n=12)

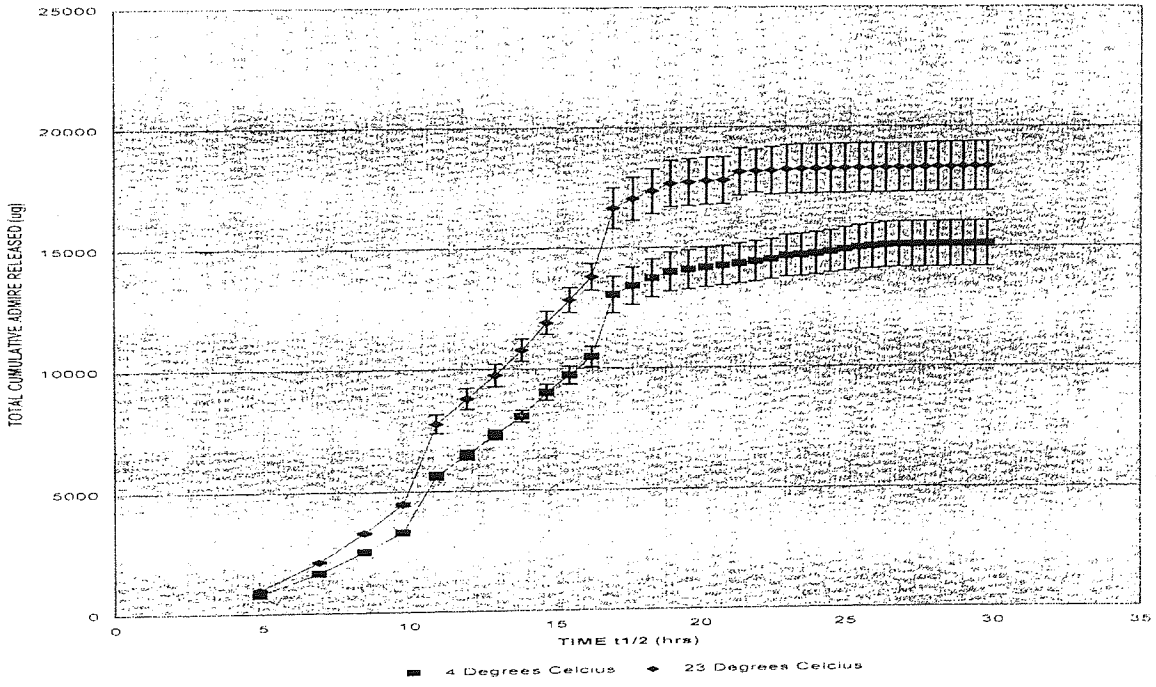

FIGURE 3 – TOTAL CUMULATIVE RELEASE PROFILES FOR THEORETICAL 20% w/w ADMIRE LOADED DIBLOCK NANOSPHERES INTO RURAL RAINWATER AT 4 DEGREES CELCIUS AND 23 DEGREES CELCIUS (mean values ± SEM, n=12)

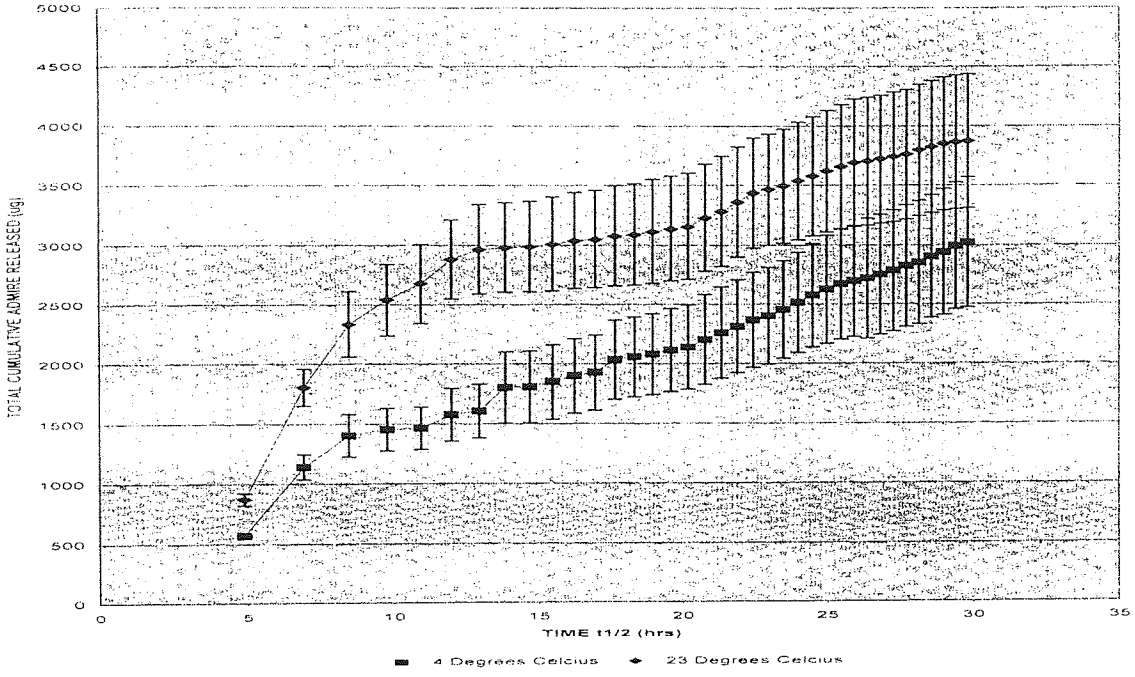

FIGURE 4 – TOTAL CUMULATIVE RELEASE PROFILES FOR THEORETICAL 20% w/w ADMIRE LOADED DIBLOCK NANOSPHERES INTO RURAL RAINWATER AT 4 DEGREES CELCIUS AND 23 DEGREES CELCIUS (mean values ± SEM, n=12)

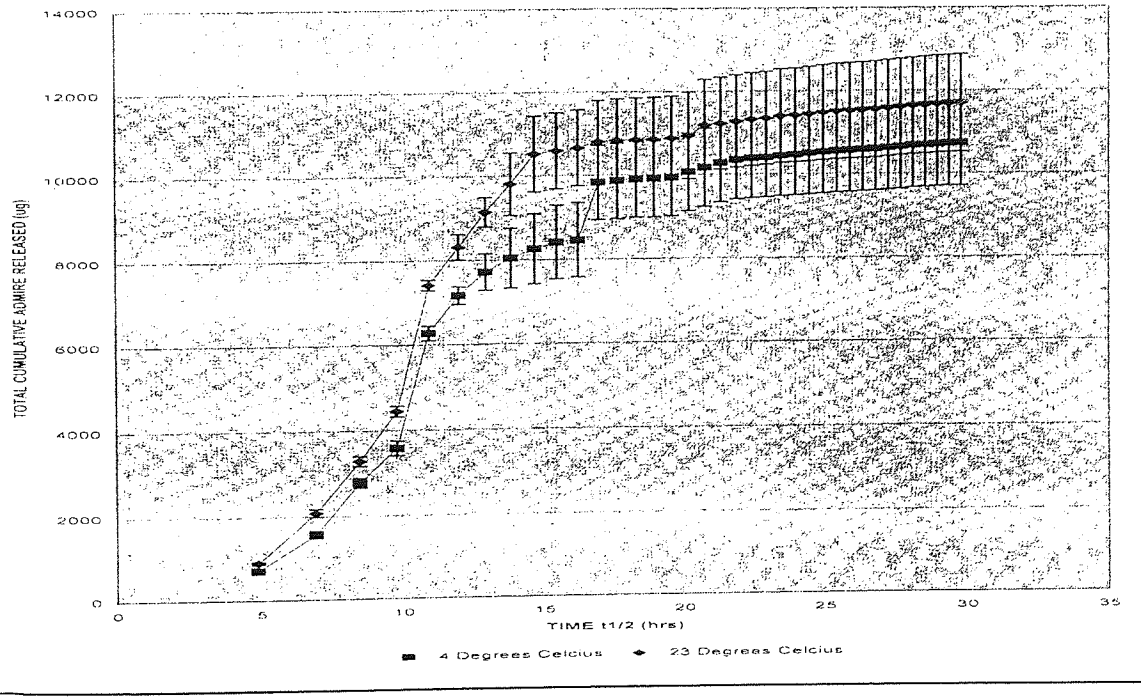

SECTION 4.1

MEAN TOTAL WEIGHT OF UNLOADED AND GA_3K LOADED NANOSPHERES PRODUCED DURING FABRICATION

THEORETICAL % LOADING	POLYMER	MEAN TOTAL WEIGHT (mg)
0	PHBHV-DIOL	179.4 ± 1.2
10	PHBHV-DIOL	188.25 ± 1
20	PHBHV-DIOL	169.75 ± 2.6
30	PHBHV-DIOL	152.25 ± 0.88
40	PHBHV-DIOL	119.75 ± 2.2
0	DIBLOCK	165.43 ± 2
10	DIBLOCK	153.18 ± 4.9
20	DIBLOCK	142.75 ± 1.3
30	DIBLOCK	128.75 ± 0.78
40	DIBLOCK	106.25 ± 0.95

SECTION 4.2

DAILY GA_3K RELEASE PROFILES

FIGURE 1 – DAILY GA_3K RELEASE PROFILES FOR THEORETICAL 20% w/w GA_3K LOADED PHBHV-DIOL NANOSPHERES INTO RURAL RAINWATER AT 4 DEGREES CELCIUS AND 23 DEGREES CELCIUS (mean values ± SEM, n=3)

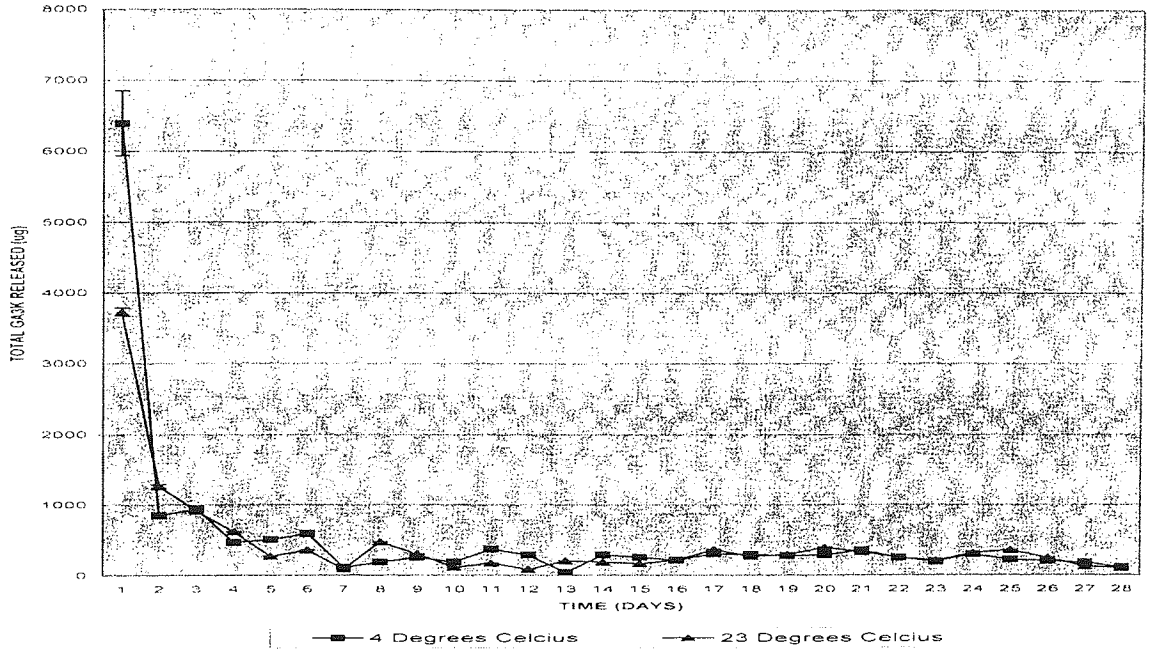

FIGURE 2 – DAILY GA_3K RELEASE PROFILES FOR THEORETICAL 30% w/w GA_3K LOADED PHBHV-DIOL NANOSPHERES INTO RURAL RAINWATER AT 4 DEGREES CELCIUS AND 23 DEGREES CELCIUS (mean values ± SEM, n=3)

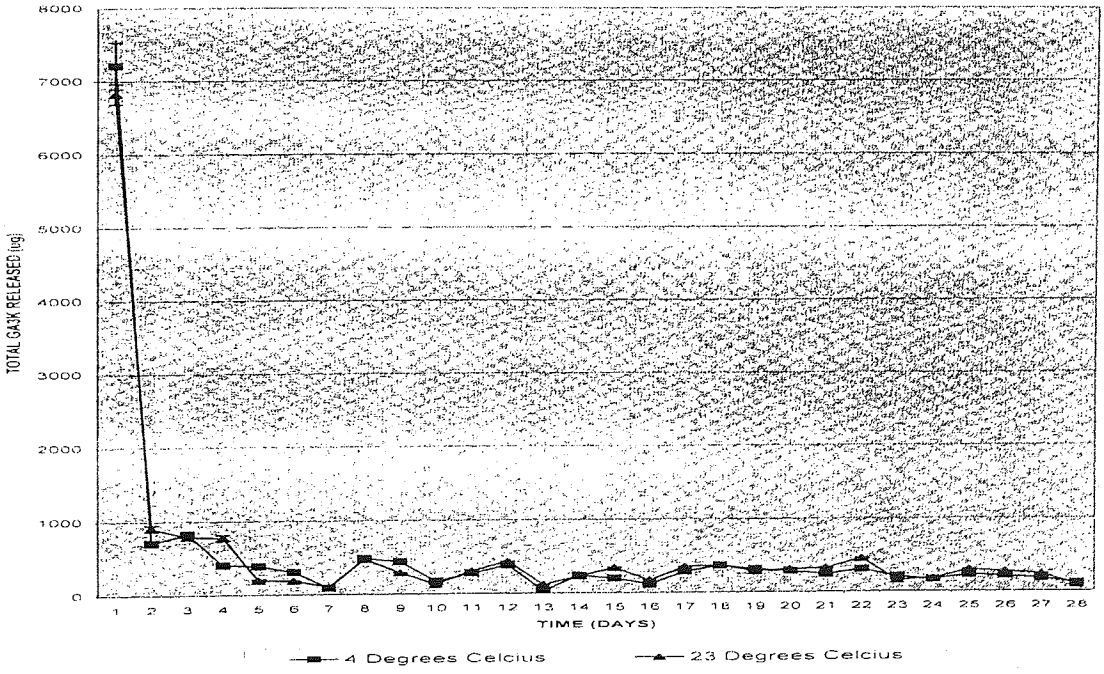

FIGURE 3 – DAILY GA_3K RELEASE PROFILES FOR THEORETICAL 20% w/w GA_3K LOADED DIBLOCK NANOSPHERES INTO RURAL RAINWATER AT 4 DEGREES CELCIUS AND 23 DEGREES CELCIUS (mean values ± SEM, n=3)

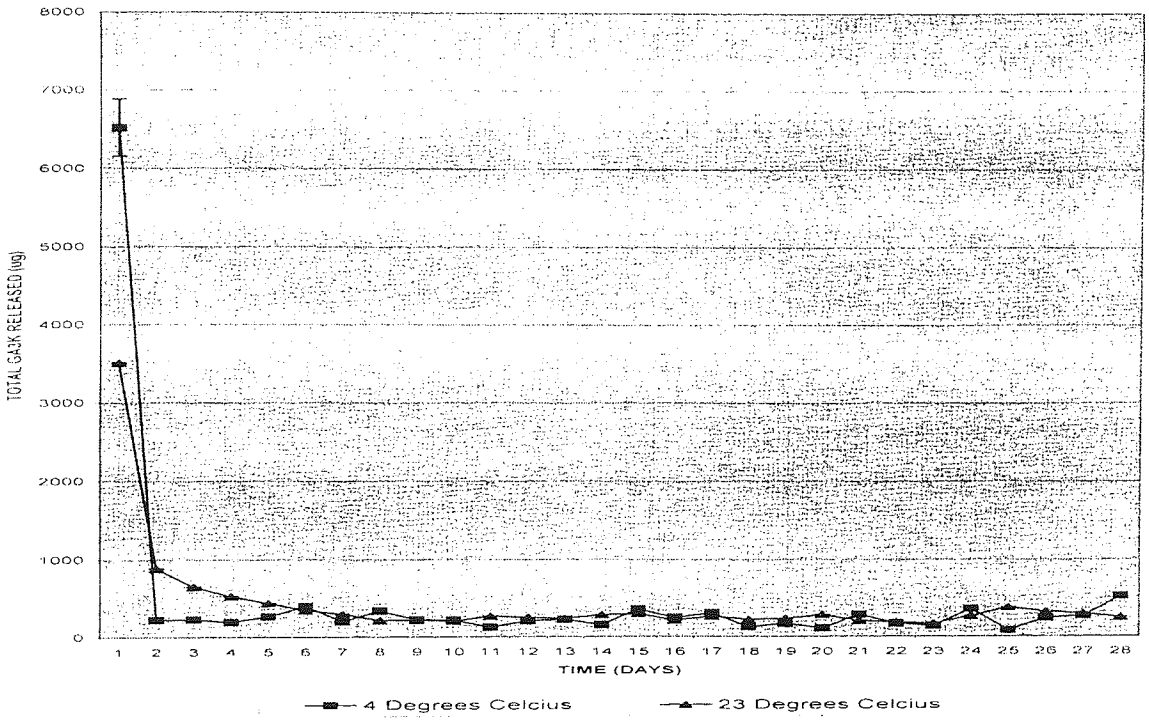

FIGURE 4 – DAILY GA_3K RELEASE PROFILES FOR THEORETICAL 30% w/w GA_3K LOADED DIBLOCK NANOSPHERES INTO RURAL RAINWATER AT 4 DEGREES CELCIUS AND 23 DEGREES CELCIUS (mean values ± SEM, n=3)

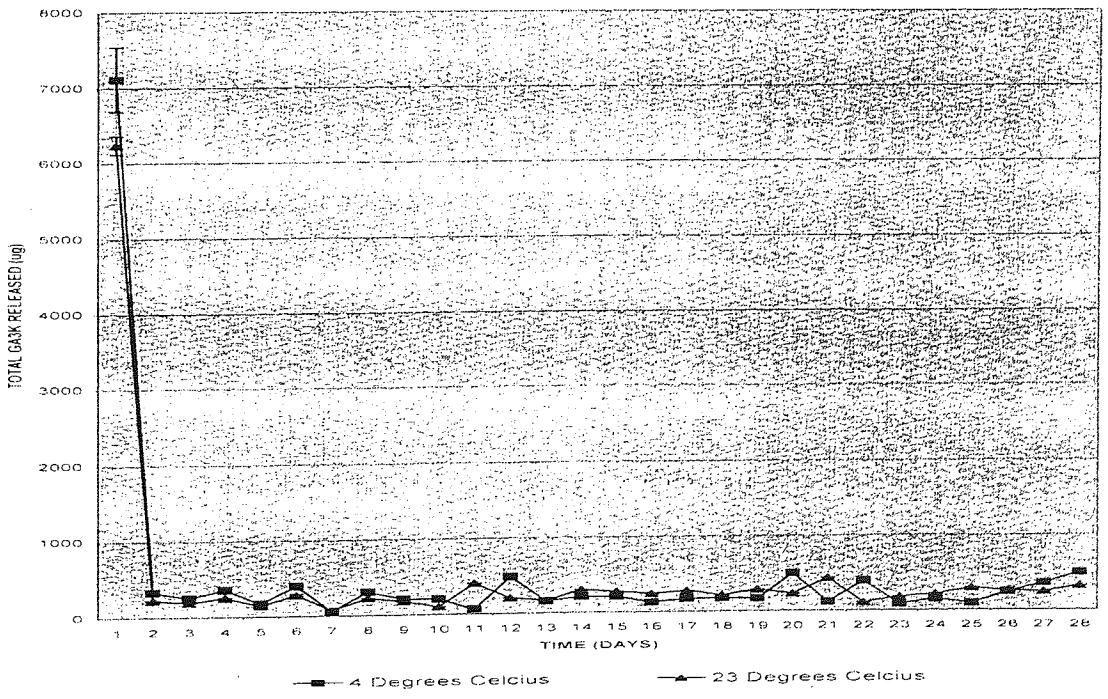

SECTION 4.3

TOTAL CUMULATIVE GA_3K RELEASE PROFILES

FIGURE 1 – TOTAL CUMULATIVE RELEASE PROFILES FOR THEORETICAL 20% w/w GA_3K LOADED PHBHV-DIOL NANOSPHERES INTO RURAL RAINWATER AT 4 DEGREES CELCIUS AND 23 DEGREES CELCIUS (mean values ± SEM, n=3)

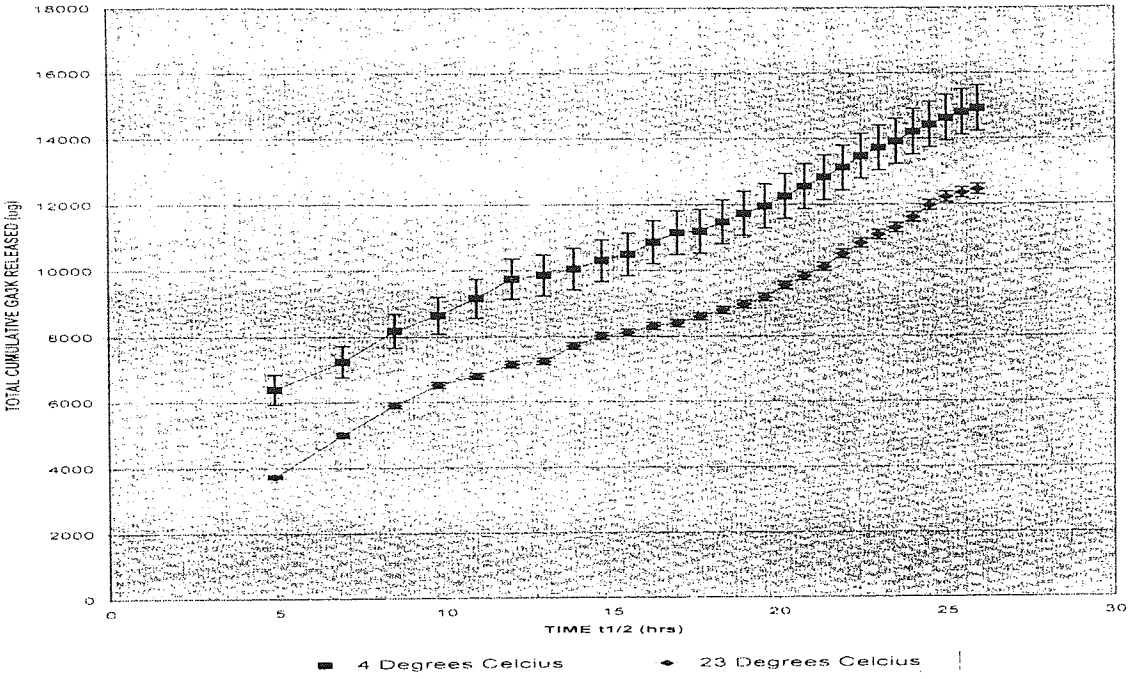

FIGURE 2 – TOTAL CUMULATIVE RELEASE PROFILES FOR THEORETICAL 30% w/w GA_3K LOADED PHBHV-DIOL NANOSPHERES INTO RURAL RAINWATER AT 4 DEGREES CELCIUS AND 23 DEGREES CELCIUS (mean values ± SEM, n=3)

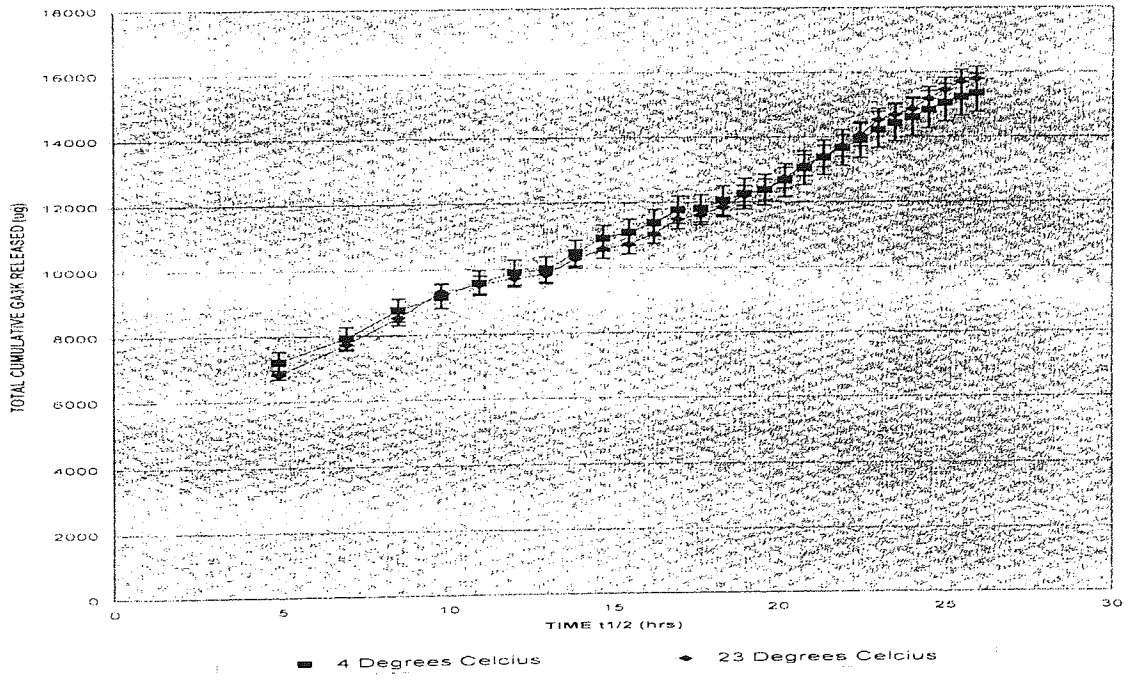

FIGURE 3 – TOTAL CUMULATIVE RELEASE PROFILES FOR THEORETICAL 20% w/w GA_3K LOADED DIBLOCK NANOSPHERES INTO RURAL RAINWATER AT 4 DEGREES CELCIUS AND 23 DEGREES CELCIUS (mean values ± SEM, n=3)

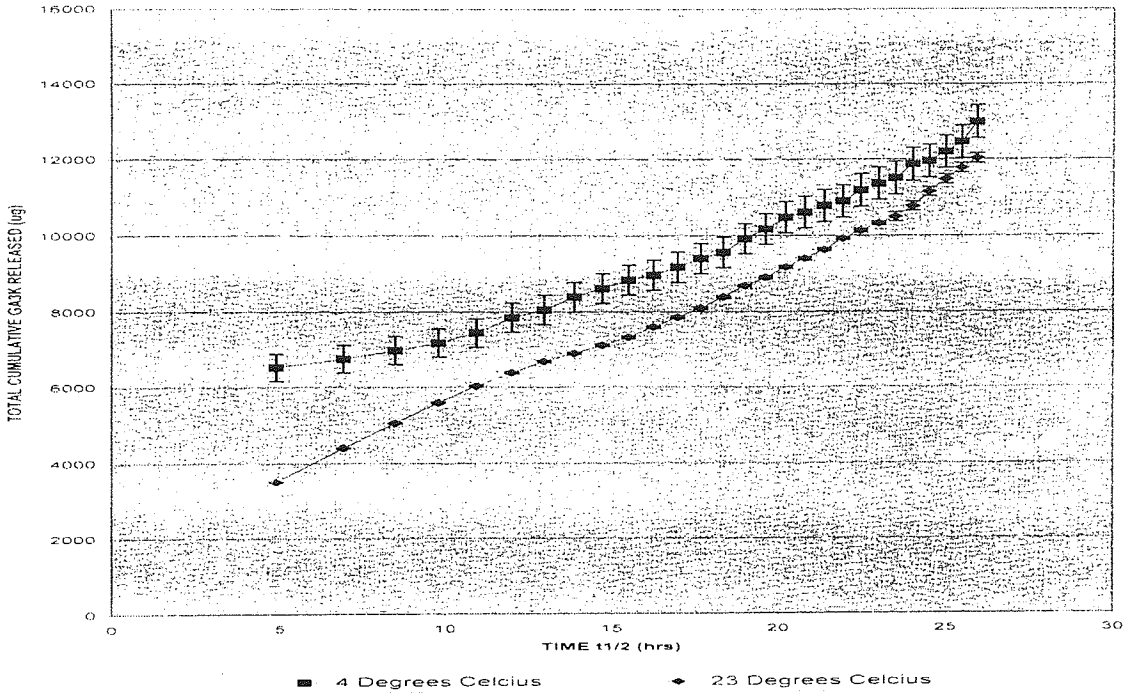

FIGURE 4 – TOTAL CUMULATIVE RELEASE PROFILES FOR THEORETICAL 30% w/w GA_3K LOADED DIBLOCK NANOSPHERES INTO RURAL RAINWATER AT 4 DEGREES CELCIUS AND 23 DEGREES CELCIUS (mean values ± SEM, n=3)

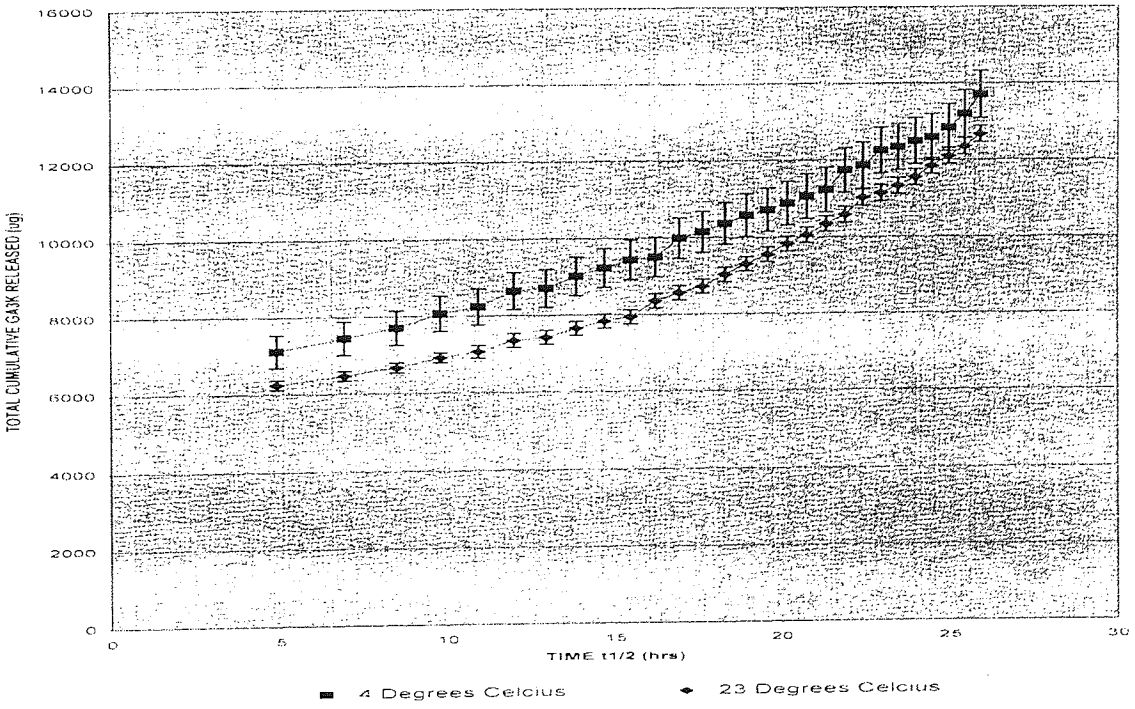

SECTION 5.1

CHEMICAL ANALYSIS OF M602 COMPOST OVER 75 DAY BIODEGRADATION PERIOD

WEEKLY CHEMICAL ANALYSIS OF M602 GREEN GARDEN WASTE COMPOST IN EACH REACTION VESSEL FROM WEEK ONE TO WEEK ELEVEN OF THE BIODEGRADATION PERIOD

WEEK	SAMPLE	pH	% NITROGEN	% WATER	% CARBON	% VOLATILE SOLIDS
1	BLANK	7.8	0.62	52.86	21.26	37.00
1	PHBHV-DIOL 1	7.8	0.66	51.57	23.68	41.20
1	PHBHV-DIOL 2	7.7	0.61	54.30	24.83	43.20
1	CELLULOSE 1	7.6	0.57	48.69	25.63	44.60
1	CELLULOSE 2	7.7	0.60	54.49	24.54	42.70
1	PHB	7.8	0.55	53.82	24.90	43.40
2	BLANK	7.8	0.58	51.55	21.32	37.10
2	PHBHV-DIOL 1	7.7	0.66	50.86	23.68	41.20
2	PHBHV-DIOL 2	7.8	0.57	52.33	23.68	41.20
2	CELLULOSE 1	7.4	0.55	50.31	24.37	42.40
2	CELLULOSE 2	7.8	0.58	52.30	24.77	43.10
2	PHB	7.9	0.51	51.60	24.83	43.20
3	BLANK	7.8	0.55	53.41	19.60	34.10
3	PHBHV-DIOL 1	7.8	0.62	51.60	23.10	40.20
3	PHBHV-DIOL 2	7.8	0.55	52.30	23.39	40.70
3	CELLULOSE 1	7.7	0.57	50.47	23.91	41.60
3	CELLULOSE 2	7.8	0.55	51.30	24.02	41.80
3	PHB	7.9	0.43	52.60	23.10	40.20
4	BLANK	7.9	0.51	53.31	18.05	31.40
4	PHBHV-DIOL 1	8.1	0.63	52.30	23.05	40.10
4	PHBHV-DIOL 2	7.9	0.43	51.60	21.61	37.60
4	CELLULOSE 1	7.8	0.51	53.60	21.95	38.20

WEEK	SAMPLE	pH	% NITROGEN	% WATER	% CARBON	% VOLATILE SOLIDS
4	CELLULOSE 2	7.9	0.43	52.70	21.49	37.40
4	PHB	8.0	0.47	51.30	22.53	39.20
5	BLANK	7.9	0.46	54.97	17.53	30.50
5	PHBHV-DIOL 1	8.0	0.60	53.60	22.20	38.70
5	PHBHV-DIOL 2	8.0	0.40	52.10	21.84	38.00
5	CELLULOSE 1	7.9	0.42	49.80	20.92	36.40
5	CELLULOSE 2	8.0	0.41	49.80	21.32	37.10
5	PHB	7.9	0.41	51.30	20.80	36.20
6	BLANK	8.1	0.39	54.52	16.55	28.80
6	PHBHV-DIOL 1	8.2	0.52	54.20	20.75	36.10
6	PHBHV-DIOL 2	8.1	0.37	52.40	20.23	35.20
6	CELLULOSE 1	8.0	0.38	45.70	19.89	34.60
6	CELLULOSE 2	7.9	0.29	50.30	20.80	36.20
6	PHB	8.0	0.42	51.60	20.00	34.80
7	BLANK	8.1	0.36	54.81	16.49	28.70
7	PHBHV-DIOL 1	8.1	0.45	52.60	19.66	34.20
7	PHBHV-DIOL 2	8.0	0.33	56.20	19.60	34.10
7	CELLULOSE 1	8.2	0.32	48.60	19.25	33.50
7	CELLULOSE 2	8.1	0.27	52.30	19.66	34.20
7	PHB	8.1	0.36	53.30	19.31	33.60
8	BLANK	8.4	0.35	58.62	16.00	27.90
8	PHBHV-DIOL 1	8.0	0.42	52.60	19.31	33.60
8	PHBHV-DIOL 2	8.2	0.31	61.30	19.60	34.10
8	CELLULOSE 1	8.0	0.27	50.60	18.05	31.40
8	CELLULOSE 2	8.3	0.23	51.30	19.37	33.70
8	PHB	8.2	0.35	52.60	19.02	33.10
9	BLANK	8.4	0.22	54.93	15.17	26.40
9	PHBHV-DIOL 1	8.1	0.41	54.30	16.90	29.40

WEEK	SAMPLE	pH	% NITROGEN	% WATER	% CARBON	% VOLATILE SOLIDS
9	PHBHV-DIOL 2	8.1	0.23	66.40	18.16	31.60
9	CELLULOSE 1	8.2	0.23	52.20	17.70	30.80
9	CELLULOSE 2	8.2	0.16	55.30	18.05	31.40
9	PHB	8.2	0.27	54.60	18.79	32.70
10	BLANK	8.4	0.16	50.73	14.43	25.10
10	PHBHV-DIOL 1	8.4	0.31	55.20	15.06	26.20
10	PHBHV-DIOL 2	8.3	0.18	51.40	16.49	28.70
10	CELLULOSE 1	8.1	0.17	53.60	16.26	28.30
10	CELLULOSE 2	8.2	0.11	54.40	17.30	30.10
10	PHB	8.4	0.20	51.30	17.00	29.60
11	BLANK	8.6	0.09	51.22	14.00	24.40
11	PHBHV-DIOL 1	8.4	0.18	53.60	14.48	25.20
11	PHBHV-DIOL 2	8.3	0.14	50.90	15.12	26.30
11	CELLULOSE 1	8.2	0.11	52.70	15.12	26.30
11	CELLULOSE 2	8.3	0.06	54.60	16.44	28.60
11	PHB	8.4	0.16	52.30	14.54	25.30

SECTION 5.2

THE RATE OF BIODEGRADATION OF CELLULOSE, PHBHV-DIOL AND PHB IN TERMS OF CARBON DIOXIDE EVOLUTION OVER 75 DAYS OF COMPOSTING.

CUMULATIVE DAILY PERCENTAGE BIODEGRADATION OF CELLULOSE, PHBHV-DIOL AND PHB POLYMERS IN TERMS OF THE EVOLUTION OF CARBON DIOXIDE OVER 75 DAYS COMPOSTING IN M602 GREEN GARDEN WASTE COMPOST

DAY	CELLULOSE 1	CELLULOSE 2	MEAN CELLULOSE	PHBHV -DIOL 1	PHBHV -DIOL 2	MEAN PHBHV -DIOL	PHB
0	0	0	0	0	0	0	0
1	0.1620	0.1944	0.1782	2.5500	1.6500	2.1000	0.4128
2	0.5508	1.1016	0.8262	4.7750	3.2750	4.0250	0.7740
3	1.0692	2.2356	1.6524	6.8000	4.4500	5.6250	1.0578
4	2.3328	3.8232	3.0780	8.4000	5.2000	6.8000	1.4964
5	3.4992	4.9572	4.2282	10.0250	5.5750	7.8000	1.9350
6	4.1796	5.5728	4.8762	11.5500	6.2250	8.8880	2.3478
7	4.9572	6.1884	5.5728	13.3250	6.7000	10.0130	2.6574
8	5.7024	6.8040	6.2532	14.9750	7.5250	11.2500	3.4572
9	6.3828	7.5816	6.9822	16.5000	8.1750	12.3375	4.6698
10	7.1928	8.5536	7.8732	17.9750	9.0250	13.5000	6.0888
11	8.0028	9.8820	8.9424	19.3250	9.9750	14.6500	7.4820
12	9.1692	10.7892	9.9792	20.5750	10.7750	15.6750	9.1590
13	10.1088	11.6964	10.9026	21.7750	11.5000	16.6375	10.7328
14	11.0484	12.4416	11.7450	23.1000	12.4500	17.7750	12.1002
15	12.0204	13.1544	12.5874	24.1500	13.1000	18.6250	13.1838
16	12.8952	13.8024	13.3488	25.100	13.7500	19.4250	14.0610
17	13.6404	14.3532	13.9968	25.9500	14.3000	20.1250	14.8608
18	14.3208	14.8716	14.5962	26.7500	14.8000	20.7750	15.6090
19	15.3252	15.6168	15.4710	27.7000	15.6500	21.6750	16.6668
20	16.3296	16.5888	16.4592	28.7500	16.7250	22.7375	18.0600
21	17.3340	17.5932	17.4636	29.9250	17.8750	23.9000	18.9630
22	18.1440	18.5004	18.3222	31.1500	18.8750	25.0125	20.5110
23	19.0836	19.5696	19.3266	32.3750	19.6250	26.0000	21.6462
24	20.0556	20.4768	20.2662	33.7750	20.4000	27.0875	22.8072
25	21.0276	21.5460	21.2868	35.2750	21.2250	28.2500	23.8908

DAY	CELLULOSE 1	CELLULOSE 2	MEAN CELLULOSE	PHBHV -DIOL 1	PHBHV -DIOL 2	MEAN PHBHV -DIOL	PHB
26	22.0320	22.5828	22.3074	36.8500	22.1000	29.4750	25.0260
27	23.1660	23.3604	23.2632	38.0000	22.8250	30.41250	26.0580
28	23.9436	24.2352	24.0894	39.1750	23.6250	31.4000	27.0900
29	25.1424	25.0776	25.1100	41.5500	24.4000	32.9750	28.1220
30	26.3088	25.9848	26.1468	43.1500	25.1500	34.1500	29.2056
31	27.4104	27.1188	27.2646	44.4250	25.9500	35.1875	30.2118
32	28.3176	28.1880	28.2528	45.3750	26.7000	36.0375	31.2180
33	29.1600	29.0628	29.1114	46.4750	27.6250	37.0500	32.5596
34	30.0672	29.8728	29.9700	47.6250	28.5250	38.0750	33.5916
35	30.8124	30.6828	30.7476	48.9000	29.400	39.1500	34.4946
36	32.6916	33.1776	32.9346	51.7250	32.1500	41.9375	36.3264
37	33.696	34.0848	33.8904	52.8750	33.0000	42.9375	37.6422
38	34.7328	34.9920	34.8624	54.5000	33.9500	44.2250	39.0096
39	35.7372	35.8020	35.7696	56.3000	34.9250	45.6125	40.0416
40	36.7740	36.7740	36.7740	58.1500	35.7750	46.9625	41.1768
41	37.9728	37.7460	37.8594	60.1250	36.6250	48.3750	42.2346
42	39.1392	38.9448	39.0420	61.7750	37.4250	49.6000	43.3956
43	40.2084	39.8844	40.0464	62.7750	38.5000	50.6375	44.6598
44	41.4396	41.1804	41.3100	63.9250	39.6250	51.7750	46.0014
45	42.7356	42.7032	42.7194	65.1750	40.8000	52.9875	47.4462
46	44.1612	44.3556	44.2584	66.4000	41.9250	54.1625	48.8652
47	45.4572	45.6516	45.5544	67.4000	42.9500	55.1750	50.0520
48	46.5588	47.0124	46.7856	68.6250	43.9000	56.2625	51.2130
49	47.6928	48.0492	47.8710	69.3750	44.9250	57.1500	52.2192
50	48.6324	49.0212	48.8268	70.0250	46.0750	58.0500	53.4318
51	49.7340	49.7988	49.7664	70.7250	46.9250	58.8250	54.7476
52	50.7384	50.7384	50.7384	71.3750	48.2500	59.81250	56.0118
53	51.8400	51.7752	51.8076	72.1250	49.8000	60.96250	57.4308
54	53.2656	53.0712	53.1684	72.9750	51.5750	62.2750	58.7724
55	54.0756	53.9784	54.0270	73.5000	53.0000	63.2500	59.7786
56	55.0800	55.0476	55.0638	74.1000	54.2500	64.1750	61.1976
57	56.0844	56.0196	56.0520	74.5250	55.4500	64.9875	62.3070
58	57.1536	56.9916	57.0726	74.9500	56.6750	65.8125	63.5970
59	58.1904	57.9960	58.0932	75.4500	57.7000	66.5750	64.9644
60	59.2272	58.9032	59.0652	75.8000	58.7500	67.2750	66.1512
61	60.3288	59.8104	60.0696	76.0500	60.1250	68.0875	67.2090

DAY	CELLULOSE 1	CELLULOSE 2	MEAN CELLULOSE	PHBHV -DIOL 1	PHBHV -DIOL 2	MEAN PHBHV -DIOL	PHB
62	61.2360	60.5880	60.9120	76.3000	60.9750	68.6375	68.2668
63	62.1432	61.3656	61.7544	76.6500	61.8500	69.2500	69.3762
64	62.9532	62.1756	62.5644	76.9250	62.6750	69.8000	70.6920
65	63.8280	63.2124	63.5202	77.3000	63.6000	70.4500	71.9304
66	64.7352	64.4760	64.6056	77.7750	64.4750	71.1250	73.1946
67	65.4804	65.6100	65.5452	78.1500	65.4500	71.8000	74.5362
68	66.3876	66.8412	66.6144	78.5000	66.3750	72.4375	75.9036
69	67.3920	68.2344	67.8132	78.8750	67.3500	73.1125	77.1936
70	68.3316	69.5628	68.9472	79.2750	68.3750	73.8250	78.4836
71	69.4656	70.9884	70.2270	79.6000	69.2000	74.4000	79.6962
72	70.3728	71.7660	71.0694	79.8500	69.8000	74.8250	80.9088
73	71.3772	72.7056	72.0414	80.0250	70.3000	75.1625	82.0956
74	72.4140	73.7424	73.0782	80.1000	70.7250	75.4125	83.1276
75	**73.5804**	**74.7792**	**74.1798**	**80.1250**	**71.0750**	**75.6000**	**84.0306**